

THE MINOR PLANET BULLETIN

BULLETIN OF THE MINOR PLANETS SECTION OF THE ASSOCIATION OF LUNAR AND PLANETARY OBSERVERS

VOLUME 51, NUMBER 1, A.D. 2024 JANUARY-MARCH

1.

SPACE-ROCKY ROAD TO OBSERVATORY AUTOMATION AND LIGHTCURVES

Dr Paula Fekete

US Military Academy, Department of Physics and Nuclear
Engineering, Bartlett Hall Science Center, 753 Cullum Road,
West Point, NY 10996-1790
paula.fekete@westpoint.edu

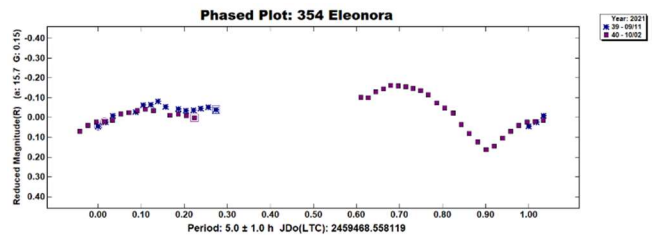
2LT Jaxon J Porter, 2LT Jacob P Willis
recent graduates of the US Military Academy
West Point, NY, USA

(Received: 2023 September 18 Revised: 2023 September 20)

We report six lightcurve analyses based on observations obtained at the West Point Observatory over the interval 2021 September through 2023 February. One notable result is finding a previously unreported rotation period for 4482 Frèrebasile; $P = 3.043 \pm 0.001$ hours with an amplitude of 0.12 magnitudes. Since these are the first asteroid photometry results reported from our Observatory, we also detail some aspects in developing our program and some unique challenges for meshing astronomical projects with the cadet lifestyle.

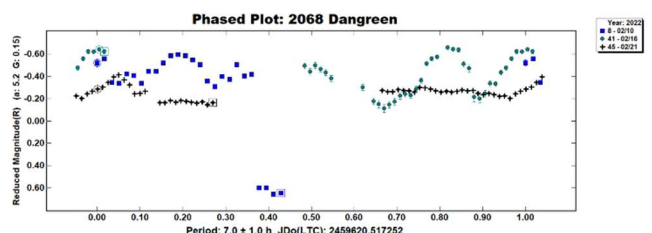
The West Point Observatory is situated atop the Bartlett Hall of Science on the campus of the US Military Academy. The Observatory features a 16.5-foot dome and houses a 16-inch Meade LX200 ACF $f/8$ Schmidt-Cassegrain telescope equipped with an SBIG STX-16803 CCD camera. Over the past three academic years (2021-2023) we sought to determine the rotational periods of six asteroids: starting with the “calibration” run for a known asteroid rotation 354 Eleonora, followed by 2068 Dangreen, 2427 Kobzar, 4482 Frèrebasile, 15304 Wikberg, and (16556) 1991 VQ1. At the start of image collection, all asteroids, except Eleonora, had unknown rotational periods. Subsequently, other teams determined the rotational period of two of our targets, (100085) 1992 UY4 and (16556) 1991 VQ1. We present our findings for Eleonora, Kobzar, Dangreen, Frèrebasile, and 1991 VQ1. Cloudy skies impeded imaging of the remaining targets for multiple nights, leading to inconclusive results. A particular challenge of an 11:30 PM curfew also limited the duration of our observing sessions.

354 Eleonora. We observed Eleonora during September-October, 2021. Following Zappala et al. (1979), we initially imaged (354) Eleonora to validate its established rotational period and refine our techniques. A shorter set of 300-second exposures were captured on 2021 September 10 and a more extensive dataset was acquired on 2021 October 1 after persistent cloudy conditions.

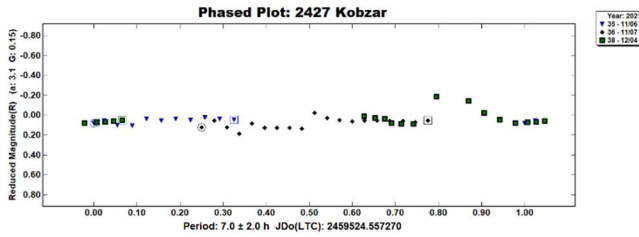


Data collection involved manual guiding due to our observatory dome not tracking the telescope’s movement. This experiment taught us two key lessons: using *MPO Canopus* effectively and selecting optimal target asteroids. Eleonora, chosen for its absolute magnitude ($H = 6.14$), served as an equipment capability test. However, its poor visibility, limited to a few hours post-sunset at low altitudes (below 30°) made it a suboptimal choice. Despite plans to revisit Eleonora when favorable, Ferrais et al. (2022) already published a lightcurve with a 4.28-hour rotational period.

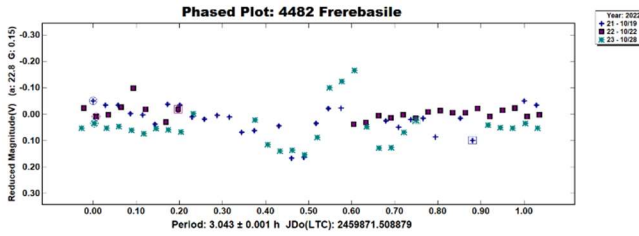
2068 Dangreen. We observed this asteroid in February 2022. Over the course of our observing nights, we adjusted our exposure times to minimize elongation of the asteroid images and learned to adjust focus of our telescope in response to changing outdoor temperatures. With Dangreen being the second asteroid measured at our observatory, we noted significant enhancement in our imaging procedures, which now included incorporating bias, dark, and flat frames, a lesson learned promptly. Similarly, we worked through the challenges of observing during full moon and the climb in our learning curve using *MPO Canopus* over the course of ten nights. Ultimately, Dangreen’s rotational period was determined only approximately as 7 hours, with a one-hour uncertainty.



2427 Kobzar. This asteroid was our third target attempted, observed over 2021 November to 2022 January. We spent six nights imaging Kobzar and accumulated more than twenty-five hours of data. Due to factors such as poor focus, unfavorable skies, limited comparison stars, and meridian shifts, only a subset of the images were analyzed. It became evident that Kobzar’s magnitude ($V \sim 16$) exceeded our own and our equipment’s capabilities, even with prolonged exposures of 12-14 minutes. Analysis yielded a 7-hour period, marred by a substantial absolute uncertainty of 2 hours. Consequently, we made the decision to dismiss Kobzar as a viable candidate, even though its predicted magnitude should have been within our equipment limits. While we cannot rule out some limiting systematic errors that could imply our Kobzar results are spurious, this experience underscored the importance of selecting brighter magnitude targets.



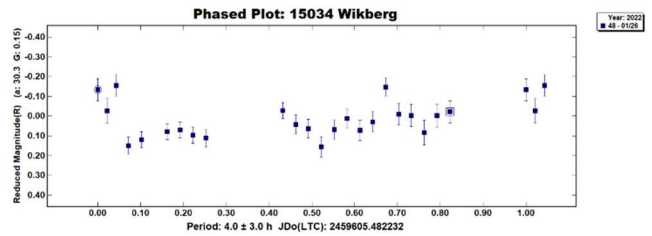
4482 Frèrebasile. We performed our observations of Frèrebasile in 2022 October when its V magnitude was near 15. We imaged it over three nights and obtained over one hundred images. On the second night, the asteroid’s path was intersecting several other asteroids or very faint stars.



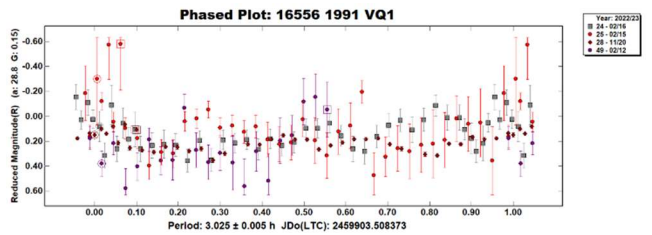
To address this, we utilized the “Star-B-gone” function in *MPO Canopus* to eliminate their effects. We achieved a breakthrough by processing images with a meridian flip within one session. This involved measuring post-flip data, containing fewer images, first and continuing with pre-flip images which comprised the bulk. On the third night, Frèrebasile’s path overlapped with a bright star causing a conspicuous spike in the lightcurve. Valuable insights were gained from Pilcher (2005), indicating two ALPO observers imaging Frèrebasile in 2004. Each took three image sets of the asteroid. The telescopes used were 8 and 30 inches in diameter, respectively. No lightcurve of Frèrebasile emerged from the 2004

observations. According to the LCDB database, our report is the first to establish a rotational period for Frèrebasile. Our data indicates a distinctive, brief rotational period of $P = 3.043 \pm 0.001$ hours with an amplitude of 0.12 magnitudes.

15304 Wikberg (1992 UX4). Despite the lack of success with imaging dim targets, we attempted imaging Wikberg for a single night in 2022 January when it had a predicted V magnitude near 19. In the thirty-seven images collected, the asteroid is often indiscernible by eye against the background. Nevertheless, the lightcurve wizard was able to locate it in twenty-three images, although with significant error bars denoting image quality issues. All selected comparison stars exhibited an identical scatter pattern in images where the asteroid was undetectable, aligning otherwise on a flat line. The asteroid’s 4-hour period, determined with an absolute uncertainty of 3 hours, lacks reliability. The lesson learned is to look for brighter targets.



(16556) 1991 VQ1. We initially observed asteroid 6556 (1991 VQ1) in mid-November 2022, yielding one of our best lightcurves. Subsequently, persistent winter cloud cover limited our imaging opportunities. In 2023 February, we managed a brief three-night imaging session, including our first trial of two-by-two binning. The suboptimal February sky conditions are evident from error bars in the plot.



While we narrowly missed the distinction of being the first to report this asteroid’s rotational period, which Benishek (2023) achieved using data from three nights in early 2022 October, our findings corroborate its relatively short rotational period of 2.653 hours. Our plot suggests a slightly longer duration, around 3.025 hours.

Number	Name	20yy/mm/dd	Phase	L_{PAB}	B_{PAB}	Period(h)	P.E.	Amp	A.E.	Grp
354	Eleonora	21/09/11-10/02	16.9, 18.2	300	5	5	1	0.30	0.03	MB-O
2068	Dangreen	22/02/10-02/21	*5.2, 7.9	138	11	7	1	0.35	0.10	MB-O
2427	Kobzar	21/11/05-12/04	*3.1, 15.4	38	0	7	2	0.10	0.03	513
4482	Frèrebasile	22/10/09-10/28	22.6, 23.4	26	31	3.043	0.001	0.12	0.03	701
15304	Wikberg	22/01/25-01/25	30.3	51	-2	3.044	0.001	0.10	0.03	MB-O
16556	1991 VQ1	22/10/20-23/02/16	*8.8, 28.8	36	-7	3.006	0.001	0.15	0.05	MB-I

Table I. Observing circumstances and results. The phase angle is given for the first and last date. If preceded by an asterisk, the phase angle reached an extremum during the period. L_{PAB} and B_{PAB} are the approximate phase angle bisector longitude/latitude at mid-date range (see Harris et al., 1984). Grps: 513: Merxia; 701: Phocaea; MB-I: Inner main-belt; MB-O: Outer main-belt; NEA: Near-Earth asteroid.

Conclusions

We determined the rotational period of Frèrebasilie, although the value's certainty is limited due to faint background stars intersecting its path on one imaging night, and a bright star crossing its path on another. Our three-year engagement with asteroid lightcurve analysis has been instructive, poised to benefit the future of West Point astronomy research. Our initial foray lacked familiarity with software, image acquisition, and we relied on manual dome-telescope adjustments. We also note that the predicted magnitude instead of the absolute magnitude (H) is a better means of selecting targets since the prediction includes allowances for the target's Earth/Sun distances and the phase angle. For example, at a phase angle of 0 deg, an asteroid with $H = 25$ at one lunar distance will be $V \sim 12.05$ while an asteroid with $H = 18$ at 2 au from Earth would be $V \sim 19.51$.

Presently, our observatory is almost fully autonomous, we have gained calibration experience for flat field and dark frames, we know how to use the software, and we have built institutional knowledge for meshing the unique cadet lifestyle with astronomical projects. We are confident these initial lessons learned will lead toward publications by future generations of cadets interested in astronomy.

Acknowledgements

The authors express their sincere gratitude to all those who contributed to the success of this research. We are especially thankful to Caroline Odden of the Phillips Academy in Andover, MA, whose support and guidance were invaluable during the initial phase of this study, helping us master the use of our observatory, software, and camera for asteroid imaging. Additionally, our heartfelt appreciation goes to CPT Basilio Yniguez from the US Military Academy at West Point, NY, whose insightful suggestions on the creation and implementation of reduction groups in image processing significantly enhanced our analysis. Their expertise was instrumental in shaping the results presented in this paper.

References

- Benishek, V. (2023). "Photometry of 10 Asteroids at Sopot Astronomical Observatory: 2022 May - October." *Minor Planet Bull.* **50**, 62-64.
- Ferrais, M.; Vernazza, P.; Jorda, L.; Jehin, E.; Pozuelos, F.J.; Manfroid, J.; Moulane, Y.; Barkaoui, K.; Benkhaldoun, Z. (2022). "Photometry of 25 Large Main-Belt Asteroids with Trappist-North and -South." *Minor Planet Bull.* **49**, 307-314.
- Harris, A.W.; Young, J.W.; Scaltriti, F.; Zappala, V. (1984). "Lightcurves and phase relations of the asteroids 82 Alkmene and 444 Gyptis." *Icarus* **57**, 251-258.
- Pilcher, F. (2005). "General Report of Position Observations by the ALPO (Association of Lunar and Planetary Observers) Minor Planets Section for the year 2004." *Minor Planet Bull.* **32**, 58-62.
- Zappala, V.; Van Houten-Groenveld, I.; Van Houten, C.J. (1979). "Rotation period and phase curve of the asteroids 349 Dembowska and 354 Eleonora." *Astrophys. Suppl.* **35**, 213-221.

LIGHTCURVES AND ROTATION PERIODS OF 1292 LUCE, 1340 YVETTE, 2738 VIRACOCHA, 2841 PUIJO, 4362 CARLISLE, AND 9911 QUANTZ

Geoffrey Stone
First Light Observatory Systems
17908 NE 391st St.
Amboy, WA 98601
geoff@first-light-systems.com

(Received: 2023 September 17)

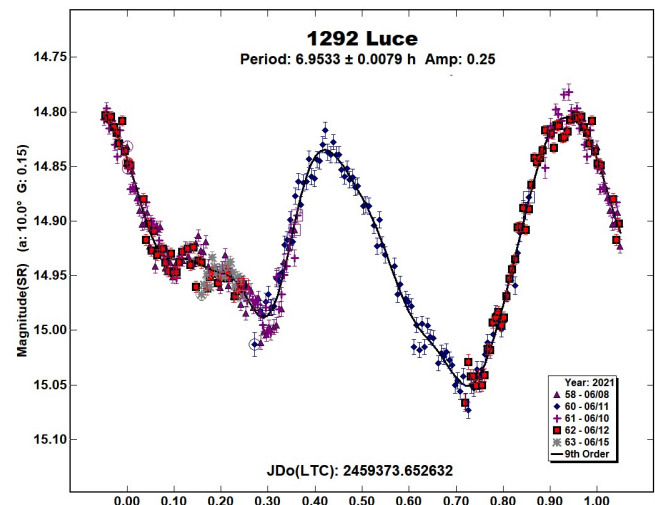
Lightcurves and rotation periods were found for six asteroids observed from 2021 April to May.

Photometric observations of six main-belt asteroids were obtained at Dimension Point Observatory located near Mayhill, NM.

Images were obtained using a 0.43-m $f/6.8$ Corrected Dall-Kirkham telescope and FLI Kepler KL400 back-illuminated CMOS camera. The equipment was operated remotely using *ACP Expert* (Denny, 2020) and *MaximDL* (George, 2020). Images were made unfiltered in HDR mode, utilizing camera internal stacking every 30 seconds. Exposure duration varied based on the target brightness and apparent motion. Images were calibrated with master dark and flat frames using *CCDStack* (Moore, 2019) and the authors own Python scripts.

Measurement and period analysis were performed using *MPO Canopus* (Warner, 2021), incorporating the Fourier analysis algorithm developed by Harris (Harris et al., 1989). Comp stars of near solar color were chosen from the ATLAS star catalog (Tonry et al., 2018) using the Comp Star Selector feature of *MPO Canopus*. ATLAS r' (SR) magnitudes were used.

1292 Luce. A search of the LCDB database showed a consensus period of 6.9541. Analysis of data from five observing sessions resulted in a period solution of 6.9533 ± 0.0079 h, with an amplitude of 0.25 ± 0.03 mag, in close agreement with the LCDB information.

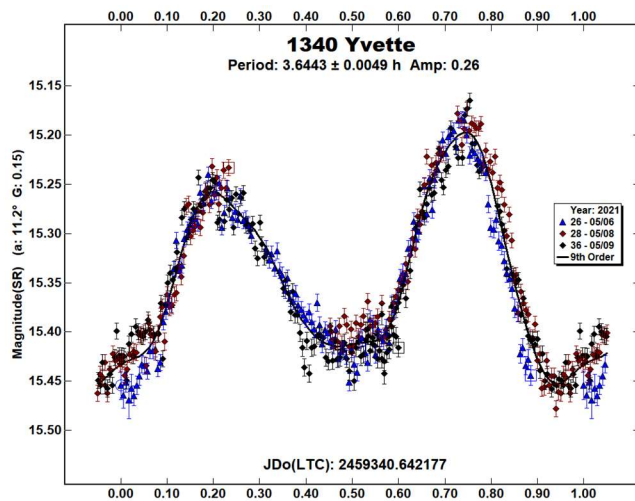


Number	Name	yyyy mm/dd	Phase	L _{PAB}	B _{PAB}	Period(h)	P.E.	Amp	A.E.	Grp
1292	Luce	2021 06/08-06/15	10.0, 12.7	237	-1	6.9533	0.008	0.25	0.02	MB
1340	Yvette	2021 05/06-05/09	4.4	205	1	3.644	0.005	0.26	0.02	THEM
2738	Viracocha	2021 04/20-05/02	1.0, 6.5	209	-1	2.639	0.001	0.19	0.03	MB-O
2841	Puijo	2021 04/08-05/08	4.4, 16.1	200	6	3.630	0.001	0.03	0.02	FLOR
4362	Carlisle	2021 04/22-05/07	4.4, 12.87	205	1	2.633	0.001	0.13	0.03	MB-I
9911	Quantz	2021 05/11-05/21	4.4, 12.87	205	1	2.633	0.001	0.13	0.03	FL

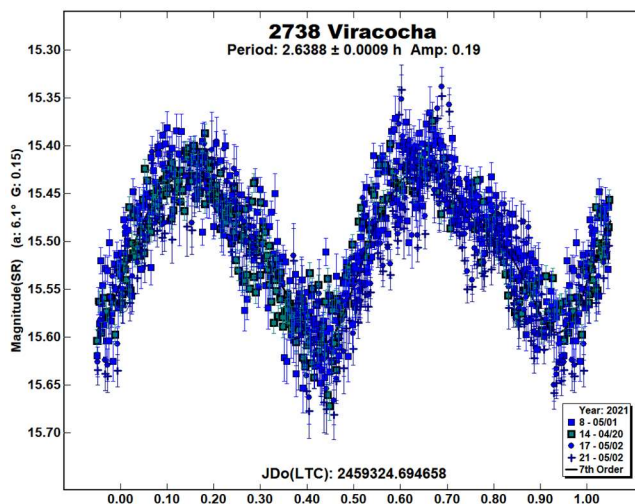
Table I. Observing circumstances and results. The phase angle is given for the first and last date. If preceded by an asterisk, the phase angle reached an extrema during the period. L_{PAB} and B_{PAB} are the approximate phase angle bisector longitude/latitude at mid-date range (see Harris et al., 1984). Grp is the asteroid family/group (Warner et al., 2009).

1340 Yvette is a member of the Themis group. Two prior synodic periods were listed in the Asteroid Lightcurve Database (LCDB; Warner et al., 2009), 3.525 ± 0.001 h from Alvarez-Candal et al. (2004) and 3.388 ± 0.001 h from Erasmus et al. (2020).

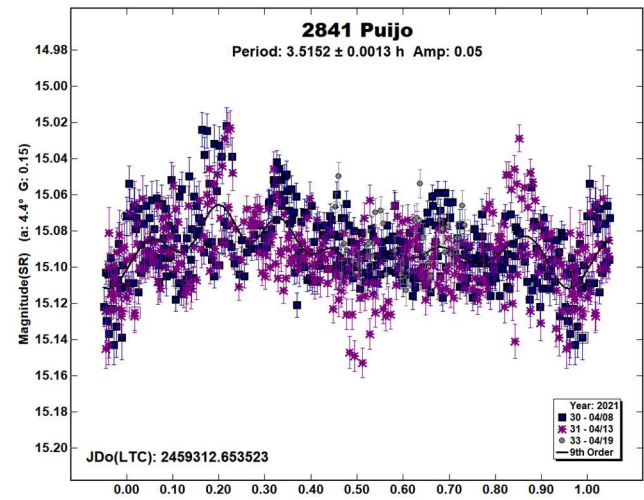
Analysis of the 484 data points led to a well-defined period solution of 3.64433 ± 0.0049 h, with an amplitude of 0.26 ± 0.02 mag, in close agreement with the prior reports.



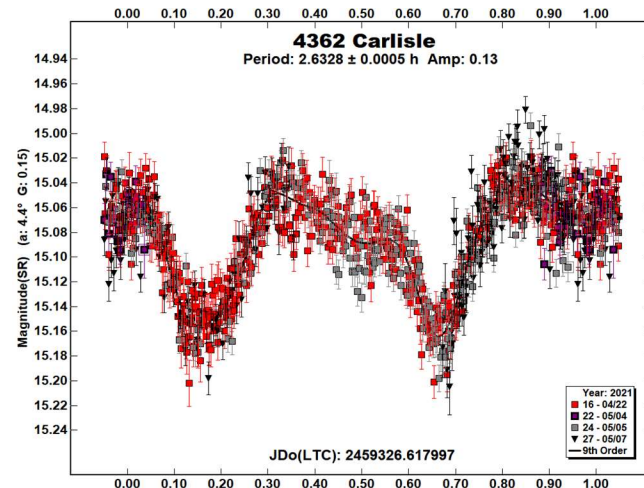
2738 Viracocha. A search of the LCDB and the JPL Solar System Dynamics website (JPL, 2021) did not find any previously reported results. Four observing sessions resulted in a total of 482 data points. Analysis led to a well-defined period solution of 2.6388 ± 0.0009 h, with an amplitude of 0.19 ± 0.03 mag.



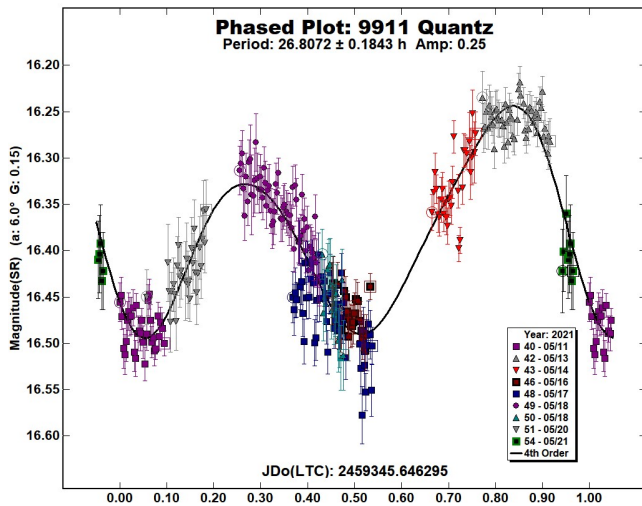
2841 Puijo is a member of the Flora group. It has a published period of 3.545 ± 0.0059 h (Warner, 2004). Analysis identified a period of 3.515 ± 0.0033 h, with an amplitude of 0.05 ± 0.02 mag in agreement with Warner. Short term events of approximately 0.75 h and 0.04 mag, like those reported by Warner, were observed. These may indicate the presence of a satellite. As mentioned by Warner, Pravec suggested a possible satellite orbital period near 24 h. Attempts were made to identify a second period, but the results were inconclusive, likely due to insufficient coverage.



4362 Carlisle. In the LCDB we found data from 4/28/2021 (Benishek et al., 2021) giving a period of 2.63289 ± 0.00007 h. A total of 983 data points were obtained in four observing sessions. Analysis led to a secure period solution of 2.6328 ± 0.0005 h, with an amplitude of 0.13 ± 0.02 mag in agreement with Benishek.



9911 Quantz is a member of the Flora group. A search of the LCDB database found no previous light curve entries for this asteroid. A total of 584 data points were obtained in nine observing sessions. Analysis led to a period solution of 26.8072 ± 0.1843 h, with an amplitude of 0.25 ± 0.04 mag. There are gaps in the period coverage so this solution could be wrong.



Acknowledgements

The author gratefully acknowledges the ongoing support of Dr. Richard Post who has graciously hosted the authors telescope equipment at his observatory in Mayhill, NM.

This work utilized data from the Asteroid Terrestrial-impact Last Alert System (ATLAS) project. ATLAS is primarily funded to search for near earth asteroids through NASA grants NN12AR55G, 80NSSC18K0284, and 80NSSC18K1575; byproducts of the NEO search include images and catalogs from the survey area. The ATLAS science products have been made possible through the contributions of the University of Hawaii Institute for Astronomy, the Queen's University Belfast, the Space Telescope Science Institute, and the South African Astronomical Observatory.

This work used data obtained from the Asteroid Lightcurve Data Exchange Format (ALCDEF) database, which is supported by funding from NASA grant 80NSSC18K0851.

Funding for PDS observations, analysis, and publication was provided by NASA grant NNX13AP56G. Work on the asteroid lightcurve database (LCDB) was also funded in part by National Science Foundation grants AST-1210099 and AST-1507535.

References

- Alvarez-Candal, A.; Duffard R.; Angeli C.A.; Lazzaro D.; Fernández S. (2004). "Rotational lightcurves of asteroids belonging to families." *Icarus* **172**, 388-401.
- Benishek, V.; Pravec, P.; Marchini, A.; Papini, R.; Durkee, R.; Chiofalo, V.; Montaigne, R.; Leroy, A.; Deldem, M. "(4362) Carlisle." IAU Central Bureau for Astronomical Telegrams, #4987, June 2021.
- Denny, R. (2020). *ACP Expert* software, version 8.3. DC-3 Dreams. <https://acpx.dc3.com>
- Erasmus, N.; Navarro-Meza, S.; McNeill, A.; Trilling, D.E.; Sickapoose, A.A.; Denneau, L.; Flewelling, H.; Heinze, A.; Tonry, J.L. (2020), "Investigating Taxonomic Diversity withing Asteroid Families through ATLAS Dual-Band Photometry" *ApJS* **247**, 13E.
- George, D. (2020). *MaximDL* software, version 6.26. Diffraction Limited. <https://diffractionlimited.com>
- Harris, A.W.; Young, J.W.; Scaltriti, F.; Zappala, V. (1984). "Lightcurves and phase relations of the asteroids 82 Alkmene and 444 Gyptis." *Icarus* **57(2)**, 251-258.
- Harris, A.W.; Young, J.W.; Bowell, E.; Martin, L.J.; Millis, R.L.; Poutanen, M.; Scaltriti, F.; Zappala, V.; Schoberm H.J.; Debehogne, H.; Zeigler, K.W. (1989). "Photoelectric observations of asteroids 3, 24, 60, 261, and 863." *Icarus* **77(1)**, 171-186.
- JPL (2021). JPL Solar System Dynamics website. <http://ssd.jpl.nasa.gov>
- Moore, S. (2019). CCDStack software version 2.95. CCDWare.com. <https://ccdware.com>
- Tonry, J.L.; Denneau, L.; Flewelling, H.; Heinze, A.N.; Onken, C.A.; Smartt, S.J.; Stalder, B.; Weiland, H.J.; Wolf, C. (2018). "The ATLAS All-Sky Stellar Reference Catalog." *Astrophys. J.* **867**, A105, 1-16.
- Warner, B.D. (2004). "Lightcurve analysis for numbered asteroids 863, 903, 907, 928, 977, 1386, 2841, and 7547." *Minor Planet Bulletin* **31**, 85-88.
- Warner, B.D.; Harris, A.W.; Pravec, P. (2009). "The asteroid lightcurve database." *Icarus* **202**, 134-146. Updated 2020 Oct. 22. <http://www.MinorPlanet.info/lightcurvedatabase.html>
- Warner, B.D. (2021). *MPO Canopus* software, version 10.8.4.2. BDW Publishing. <http://www.bdwpublishing.com>

LIGHTCURVES AND DERIVED RESULTS FOR KORONIS FAMILY MEMBER (5139) RUMOI, INCLUDING A DISCUSSION OF MEASUREMENTS FOR EPOCHS ANALYSIS

Stephen M. Slivan, Kaylee Barrera, Abigail M. Colclasure, Erin M. Cusson, Skylar S. Larsen, Claire J. McLellan-Cassivi, Summer A. Moulder, Prajna R. Nair, Paola D. Namphy, Orisvaldo S. Neto, Maurielle I. Noto, Maya S. Redden, Spencer J. Rhodes, Sandra A. Youssef
 Massachusetts Institute of Technology,
 Dept. of Earth, Atmospheric, and Planetary Sciences,
 77 Mass. Ave. Rm. 54-424, Cambridge, MA 02139
 slivan@mit.edu

(Received: 2023 October 2)

Lightcurves of (5139) Rumoi recorded during three apparitions are presented, with derived results for synodic rotation period, solar phase coefficients, color index, and absolute magnitude, along with an analysis for spin direction and sidereal rotation period in combination with previously published data. An approach for measuring lightcurves for epochs analyses also is described.

Introduction

Koronis family member (5139) Rumoi has been observed as a smaller target of opportunity during the study of larger Koronis members described by Slivan et al. (2008; 2023). Cooney et al. (2007) reported lightcurves of Rumoi and derived a rotation period of 3.257 h from data two nights apart, and ATLAS sky survey data sparsely-sampled in time have been analyzed by Erasmus et al. (2020) and by Ďurech et al. (2020). The present paper reports new lightcurve observations with derived results for a synodic period from data spanning three lunations, $V-R$ color, and solar phase coefficients, as well as a combined analysis with previous data to determine the sidereal rotation period and direction of spin. An approach for measurement of epochs from the lightcurves also is detailed here, in the context of using the epochs analysis sieve algorithm described by Slivan (2013).

Observations and single-apparition results

Lightcurves of Rumoi were recorded at Whittin Observatory (WhO) in Wellesley, MA, and at the George R. Wallace Astrophysical Observatory (WAO) in Westford, MA, during a total of three apparitions. The observing circumstances are presented in Table I, and information about the telescopes and cameras appears in Table II. Observing and data reduction procedures were as previously described by Slivan et al. (2008) using synthetic aperture sizes informed by Howell (1989). The lightcurves were reduced for light-time, and standard-calibrated brightnesses were reduced to unit distances. The composite lightcurves are shown in Fig. 1, where nights of uncalibrated relative photometry have been shifted in brightness for best fit to their respective composites.

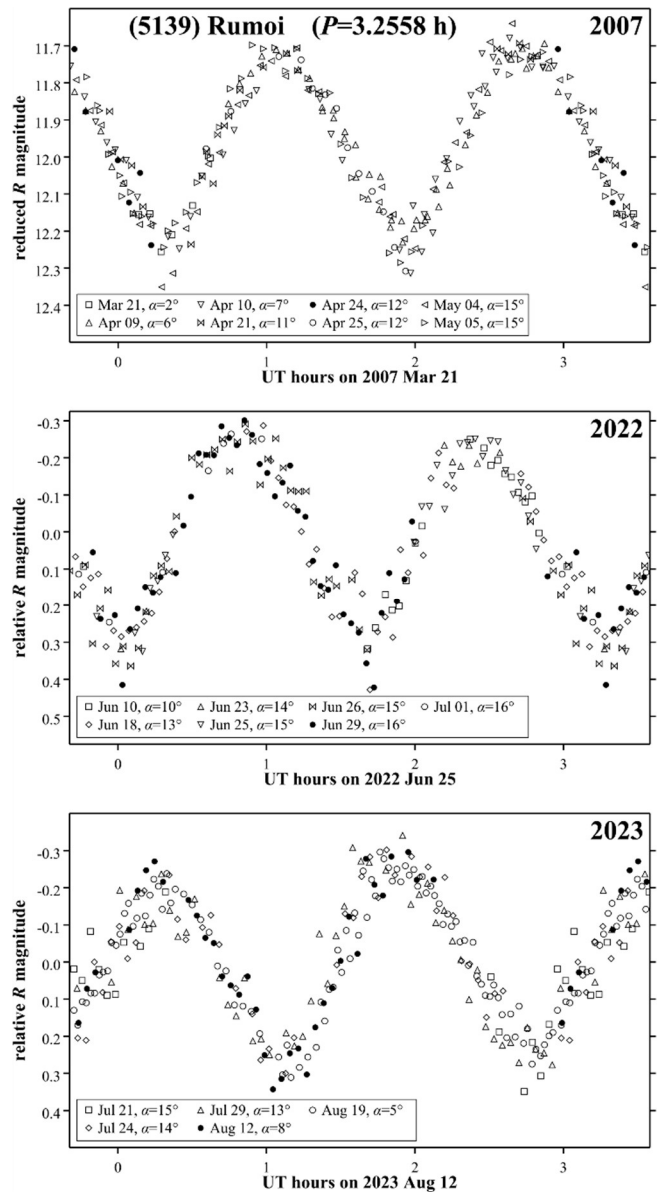


Figure 1. Folded composite lightcurves during apparitions in 2007 (top), 2022 (center), and 2023 (bottom), light-time corrected with the earliest and latest 10% of rotation repeated. Legends give UT dates of observations and solar phase angles α .

2007 apparition: (Fig. 1, top) The data span an interval of 46 nights during three lunations, making it the longest available time span of single-apparition data for synodic rotation period analysis, and yielding a period result of 3.2558 ± 0.0002 h. Observations of Landolt (1983) standard stars SA103-526 and SA104-337 were used to calibrate the lightcurves to standard system R and V , making it possible to determine R -band solar phase coefficients $H_R = 11.69 \pm 0.06$ and $G_R = 0.19 \pm 0.03$ (Fig. 2), and a color index $V-R = 0.49 \pm 0.04$, for a corresponding derived absolute magnitude of $H = 12.18 \pm 0.07$. A search of the literature did not find any previously reported solar phase results for Rumoi that are based on dedicated lightcurves, but our derived H is consistent with the (not-truncated) value 12.19 found in the Minor Planet Center (MPC) Orbit Database MPCORB, referencing MPC Daily Orbit Update MPEC 2023-Q164 (2023).

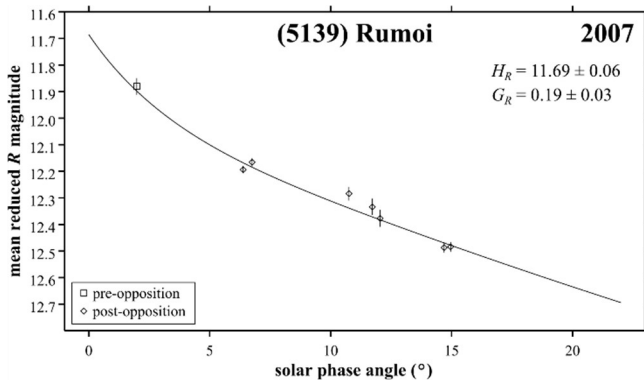


Figure 2. Lumme-Bowell solar phase model (Bowell et al., 1989).

2022 apparition: (Fig. 1, center) The data span an interval of 21 nights, at a viewing aspect about 50 degrees different in ecliptic longitude from that in 2007.

2023 apparition: (Fig. 1, bottom) The data span an interval of 29 nights, at a viewing aspect about 30 degrees different in ecliptic longitude from that in 2004.

All of the lightcurves reported here are consistent with the rotation period of 3.257 ± 0.003 h derived by Cooney et al. (2007) from data two nights apart. The Erasmus et al. (2020) 3.048 h result corresponds to an alias period that counts an extra 0.5 rotation per day.

Sidereal rotation counting

The dedicated lightcurves reported here, together with those recorded in 2004 (Cooney et al., 2007), define epochs from a total of four apparitions (Table III, Part A). The lightcurves are doubly-periodic with plenty of amplitude and only modest asymmetry in time, making the epoch data set well-suited for counting sidereal rotations.

Measurement of epochs and error estimates: A rotation-counting sieve algorithm to constrain an asteroid's sidereal rotation period has been described by Slivan (2013); that work noted the importance of supplying the algorithm with appropriate estimates of epochs and their uncertainties, but left for the future a more detailed discussion of the actual measuring of epochs from lightcurves. Here a further-developed approach for measuring epochs by modeling the lightcurve shape as a Fourier series is described, using a filtering strategy to disentangle systematic shifts related to lightcurves' shapes, and also relating the epoch error estimate to the brightness measurement errors.

The model lightcurve magnitude m calculated for time t since the compositing zero-time is

$$m(t) = c_0 + \sum_{k=1}^n \left[c_{(2k-1)} \cos\left(2\pi \frac{kt}{P}\right) + c_{(2k)} \sin\left(2\pi \frac{kt}{P}\right) \right] \quad (\text{Eq. 1})$$

where P is the rotation period, the $c_0 \dots c_{(2n)}$ are the fitted Fourier series coefficients being determined from the observed lightcurve data, and the summation limit n is chosen to specify the highest-order harmonic to include. An appropriate choice of n will be large enough to model the underlying lightcurve shape, but not so large as to be also modeling statistical noise in the data as signal. Harris and Lupishko (1989) have noted that ten harmonics seems in practice to be sufficient to define an asteroid lightcurve to better

than 0.01 mag. They also discuss considerations related to the time sampling of the data, which are pertinent in the present context of filtering to isolate the contribution of low-order shape, because the longest gap Δt_{\max} between data points in the folded lightcurve sets a formal upper bound on the choice of n :

$$n \leq P/2 \Delta t_{\max} \quad (\text{Eq. 2})$$

For a fixed period P the model is linear in the fitted coefficients which permits a least-squares fit to be calculated in closed form; for example, see Press et al. (1986, Sec. 14.3 General Linear Least Squares). The epochs are then measured from the dominant harmonic representing the low-order shape; for an object that is elongated enough to exhibit a doubly-periodic lightcurve this filtered magnitude m_f will be the second harmonic:

$$m_f(t) = c_3 \cos(2\pi \cdot 2t/P) + c_4 \sin(2\pi \cdot 2t/P) \quad (\text{Eq. 3})$$

Each epoch in Table III corresponds to a filtered maximum (where the slope is zero and the second derivative in magnitude is positive) on its composite date. The tabulated error for the epoch is estimated by first adopting the RMS residual of the Fourier series fit to represent the lightcurve brightness error, then dividing that by the maximum slope of the filtered model lightcurve (determined for a point midway between any pair of consecutive extrema) to calculate the corresponding error in time.

Example measurement of epoch and error: Measurement from the two nights of data recorded during the August lunation of the 2023 apparition, for a compositing zero-time of 0 h UT on 2023 Aug 12. The maximum time gap between data points in the folded composite is 0.057 h, plenty small enough for an $n = 10$ initial trial model (Eq. 2). The highest-order fitted harmonic in that trial model having a coefficient at least as large as half of the RMS fit residual is the fourth harmonic, and additional trials confirmed that the filtered epochs are insensitive to including higher-order harmonics, which informs the choice of $n = 4$ for the final model (Fig. 3, left). The filtered model used to measure the epoch in Table III is comprised of only the second harmonic (Fig. 3, right).

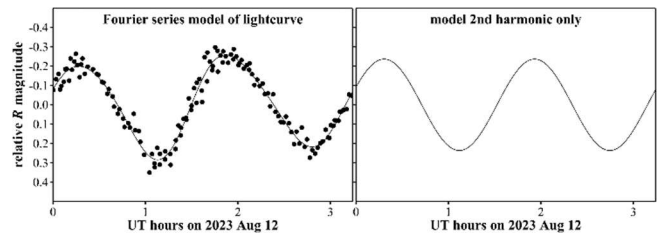


Figure 3. (left) $n = 4$ Fourier series model fit to the observations from the 2023 August lunation; the RMS fit residual is 0.037 mag. (right) The second harmonic from the same model shown at left; its fitted coefficients for Eq. 3 are $c_3 = -0.085$ and $c_4 = -0.220$, and the maximum slope is 0.91 mag/h.

Rotation counting for Rumoi: The single-apparition synodic period from 2007 is precise enough to narrow the rotation count between the consecutive apparitions in 2022 and 2023 to three possibilities, whose errors in the corresponding candidate sidereal periods are in turn small enough to count rotations across the next-longer interval, between epochs two apparitions apart from 2004 to 2007. The constraint from that interval improves the three candidate periods but not enough to count rotations across the next-longer interval of 12 apparitions from 2007 to 2022, and the existing 3-way count ambiguity remained not definitively resolved.

The MPC Orbits/Observations Database was checked for suitable photometry to supply an epoch for a time interval to fill the gap in the rotation counting progression. ATLAS sky survey data (Tonry et al., 2018) recorded during the 2017 apparition provides an epoch 5 apparitions away from the 2023 epoch, for an interval length close to the geometric mean between the 2- and 12-apparition intervals that bracket the progression gap. The 2017 data are given in the database to only 0.1 mag precision, but even so, the lightcurve amplitude of ~ 0.5 mag (Fig. 4) is sufficient to locate an epoch (Table III, Part B). Including this epoch for rotation counting provides intervals of 4 and 5 apparitions and resolves the 3-way period alias (Fig. 5).

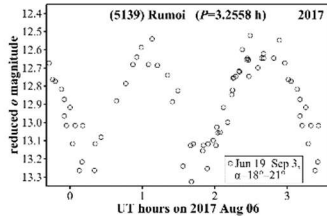


Figure 4. Photometry from the ATLAS sky survey (Tonry et al., 2018) during the 2017 apparition, composited to the median date of the data. The slope parameter $G = 0.23$ for S-type objects (Lagerkvist and Magnusson, 1990) was used to reduce for changing solar phase angle.

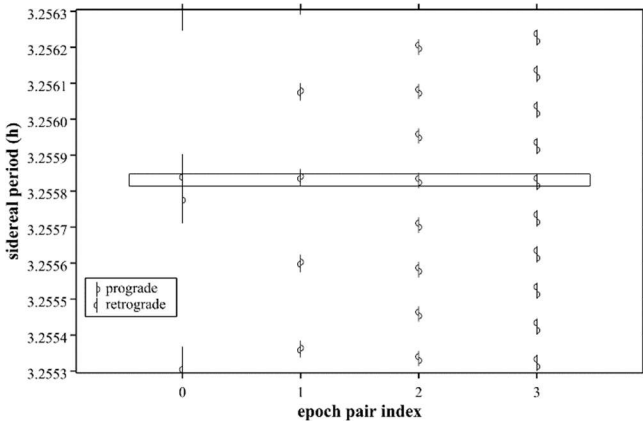


Figure 5. Sieve algorithm output showing that only a single range of sidereal rotation periods (thin horizontal rectangle) is allowed by the first four epoch intervals in Table IV. Candidate ranges of periods for each epoch interval were calculated using epoch range half-widths of 2.5 times the epoch errors.

Applying the sieve algorithm to all ten available intervals identifies an unambiguous count of sidereal rotations across the entire data set, and also distinguishes that the direction of spin is retrograde (Fig. 6). The period range constraint shown in Fig. 6 is 3.2558333 to 3.2558382 h; adopting its half-width as an estimate of a 2.5σ error gives a derived sidereal period of 3.255836 ± 0.000002 h, corresponding to 50737.08 rotations for the maximum interval.

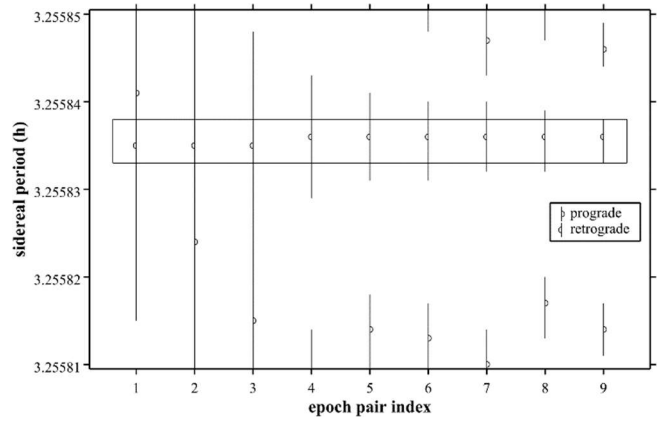


Figure 6. Similar to Fig. 5 but including all available intervals in the sieve calculations, and with the period axis range narrowed to the constraint result from the shortest four epoch intervals.

Our results from the combined analysis are consistent with the retrograde spin and sidereal period of 3.255841 ± 0.000004 h reported by Durech et al. (2020).

UT date	α ($^\circ$)	Tel. ID	Filter	Integration time (s)
2007 Mar 21.2	2.0	WhO	R	120,240
2007 Mar 26.1	1.3	WhO	V	240
2007 Apr 09.2	6.4	WhO	R	240
2007 Apr 10.1	6.8	WhO	R	240
2007 Apr 21.2	10.8	WhO	R	240
2007 Apr 24.1	11.7	WhO	R	240
2007 Apr 25.1	12.0	WhO	R	240
2007 May 04.1	14.7	WhO	R	240
2007 May 05.1	15.0	WhO	R	240
2022 Jun 10.2	10.0	WAO-3	R	165
2022 Jun 18.1	12.7	WAO-4	R	180
2022 Jun 23.1	14.2	WAO-P24	R	180,600
2022 Jun 25.1	14.8	WAO-4	R	180
2022 Jun 26.1	15.1	WAO-4	R	180
2022 Jun 29.1	15.8	WAO-4	R	180
2022 Jul 01.1	16.3	WAO-4	R	180
2023 Jul 21.3	15.1	WAO-1	R	200
2023 Jul 24.3	14.3	WAO-1	R	200
2023 Jul 29.2	12.8	WAO-1	R	200
2023 Aug 12.2	7.9	WAO-2	R	200
2023 Aug 19.2	5.2	WAO-4	R	200

Table I: Nightly observing information, grouped by lunation. Columns are: UT date at lightcurve mid-time, solar phase angle α , telescope ID (Table II), filter used (R, Cousins R; V, Johnson V), and image integration time(s).

Tel. ID	Dia. (m)	CCD camera	FOV (')	Bin	Scale ("/pix)
WhO	0.61	Photometrics TK 1K	16×16	2×2	1.84
WAO-1	0.36	FLI ML1001	22×22	1×1	1.29
WAO-2	0.36	SBIG STL-1001	21×21	1×1	1.21
WAO-3	0.36	FLI ML1001	20×20	1×1	1.18
WAO-4	0.36	SBIG STL-1001	21×21	1×1	1.25
WAO-P24	0.61	FLI PL16803	32×32	1×1	0.46

Table II: Telescopes and cameras information. Columns are: telescope ID (WhO, Sawyer Boller & Chivens 24-in; WAO-1 and WAO-2, shed piers #1 and #2 Celestron C14 Edge HD; WAO-3 and WAO-4, shed piers #3 and #4 Celestron Classic C14; WAO-P24, Elliot PlaneWave 24-in CDK), telescope diameter, CCD camera, detector field of view, image binning used, and binned image scale.

UT date	Epoch (UT h)	PAB λ, β (°)	Data ref.
Part A: Dedicated lightcurves			
2004 Oct 07	0.71 ± 0.02	6.1, -2.8	a
2007 Apr 21	1.06 ± 0.05	183.9, +2.6	b
2022 Jun 25	0.82 ± 0.06	236.3, -0.4	b
2023 Aug 12	0.31 ± 0.05	337.0, -3.6	b
Part B: Sky survey lightcurves sparse-in-time			
2017 Aug 06	1.04 ± 0.06	228.4, -0.1	c, d

Table III: Summary of lightcurve epochs, in each case locating a maximum from the second harmonic of a Fourier series model fit to the lightcurves. PAB λ, β are the J2000.0 ecliptic longitude and latitude of the phase angle bisector. Data references are a, Cooney et al. (2007); b, this work; c, ATLAS-MLO α -band; d, ATLAS-HKO α -band.

Epoch pair index	Interval (d)	Interval (app.)	Epochs source apparitions
0	413.0	1	2022, 2023
1	926.0	2	2004, 2007
2	1784.0	4	2017, 2022
3	2197.0	5	2017, 2023
4	3760.0	8	2007, 2017
5	4686.0	10	2004, 2017
6	5544.0	12	2007, 2022
7	5957.0	13	2007, 2023
8	6470.0	14	2004, 2022
9	6883.0	15	2004, 2023

Table IV: Time intervals between lightcurve epochs. Columns are: epoch pair index label, interval length rounded to 0.1 d, the corresponding integer count of elapsed apparitions, and the apparitions from which the defining epochs were measured.

Number	Name	yyyy mm/dd	Phase	L_{PAB}	B_{PAB}	Period(h)	P.E.	Amp	A.E.
5139	Rumoi	2007 03/21-05/05	*2.0, 15.0	184	3	3.2558	0.0002	0.56	0.05
5139	Rumoi	2022 06/10-07/01	10.0, 16.3	236	0			0.55	0.08
5139	Rumoi	2023 07/21-08/19	15.1, 5.2	337	-4			0.54	0.05

Table V. Observing circumstances and results. Phase angles are given for the first and last dates; the asterisk indicates that the phase angle reached a minimum during the interval. L_{PAB} and B_{PAB} are the approximate phase angle bisector longitude/latitude at mid-date range.

Acknowledgments

We thank the corps of loyal observers who recorded data at Whitin Observatory: Kathryn Neugent, Tim Smith, Alessondra Springmann, Amanda Zangari, Rebekah Dawson, Kirsten Levandowski, and Katherine Lonergan. At Wallace Observatory we thank Dr. Michael Person and Timothy Brothers for allocation of telescope time, and for observer instruction and support. We also thank Walter Cooney for providing to us his data from 2004, and Alan Chamberlin for clarifying pedigrees of catalog H values.

Student service observers at Whitin Observatory were supported in part by grants from the Massachusetts Space Grant Consortium. The student observers at Wallace were supported by grants from MIT's Undergraduate Research Opportunities Program. This work has made use of data and services provided by the International Astronomical Union's Minor Planet Center; specifically, the brightnesses accompanying astrometry from the Asteroid Terrestrial-impact Last Alert System (ATLAS) survey observing program.

References

- Bowell, E.; Hapke, B.; Domingue, D.; Lumme, K.; Peltoniemi, J.; Harris, A.W. (1989). "Application of Photometric Models to Asteroids." In *Asteroids II* (R.P. Binzel, T. Gehrels, M.S. Matthews, eds.) pp. 524-556. Univ. Arizona Press, Tucson.
- Cooney, W.R.Jr.; Gross, J.; Terrell, D.; Reddy, V.; Dyvig, R. (2007). "Lightcurve Results for 486 Cremona, 855 Newcombina, 942 Romilda, 3908 Nyx, 5139 Rumoi, 5653 Camarillo, (102866) 1999 WA5." *Minor Planet Bull.* **34**, 47-49.
- Đurech, J.; Tonry, J.; Erasmus, N.; Denneau, L.; Heinze, A.N.; Flewelling, H.; Vančo, R. (2020). "Asteroid models reconstructed from ATLAS photometry." *Astron. Astrophys.* **643**, A59.
- Erasmus, N.; Navarro-Meza, S.; McNeill, A.; Trilling, D.E.; Sickafoose, A.A.; Denneau, L.; Flewelling, H.; Heinze, A.; Tonry, J.L. (2020). "Investigating Taxonomic Diversity within Asteroid Families through ATLAS Dual-band Photometry." *Astrophys. J. Suppl. Ser.* **247**, A13.
- Harris, A.W.; Lupishko, D.F. (1989). "Photometric Lightcurve Observations and Reduction Techniques." In *Asteroids II* (R.P. Binzel, T. Gehrels, M.S. Matthews, eds.) pp. 39-53. Univ. Arizona Press, Tucson.
- Howell, S.B. (1989). "Two-dimensional Aperture Photometry: Signal-to-noise Ratio of Point-source Observations and Optimal Data-extraction Techniques." *PASP* **101**, 616-622.

Lagerkvist, C.I.; Magnusson, P. (1990). "Analysis of asteroid lightcurves. II. Phase curves in a Generalized HG-system." *Astron. Astrophys. Suppl. Ser.* **86**, 119-165.

Landolt, A.U. (1983). "UBVRI Photometric Standard Stars Around the Celestial Equator." *Astron. J.* **88**, 439-460.

Minor Planet Center (2023). "Minor Planet Electronic Circular 2023-Q164: Daily Orbit Update (2023 August 30)." <https://www.minorplanetcenter.net/mpec/K23/K23QG4.html>

Press, W.H.; Flannery, B.P.; Teukolsky, S.A., Vetterling, W.T. (1986). *Numerical Recipes*. Cambridge University Press, Cambridge.

Slivan, S.M.; Binzel, R.P.; Boroumand, S.C.; Pan, M.W.; Simpson, C.M.; Tanabe, J.T.; Villastrigo, R.M.; Yen, L.L.; Ditteon, R.P.; Pray, D.P.; Stephens, R.D. (2008). "Rotation rates in the Koronis family, complete to $H \approx 11.2$." *Icarus* **195**, 226-276.

Slivan, S.M. (2013). "Epoch Data in Sidereal Period Determination. II. Combining Epochs from Different Apparitions." *Minor Planet Bull.* **40**, 45-48.

Slivan, S.M.; Hosek Jr., M.; Kurzner, M.; Sokol, A.; Maynard, S.; Payne, A.V.; Radford, A.; Springmann, A.; Binzel, R.P.; Wilkin, F.P.; Mailhot, E.A.; Midkiff, A.H.; Russell, A.; Stephens, R.D.; Gardiner, V.; and 5 colleagues (2023). "Spin vectors in the Koronis family: IV. Completing the sample of its largest members after 35 years of study." *Icarus* **394**, A115397.

Tonry, J.L.; Denneau, L.; Heinze, A.N.; Stalder, B.; Smith, K.W.; Smartt, S.J.; Stubbs, C.W.; Weiland, H.J.; Rest, A. (2018). "ATLAS: A High-cadence All-sky Survey System." *PASP* **130**, 064505.

LIGHTCURVE ANALYSIS OF 5780 LAFONTAINE

Rafael González Farfán (Z55)
Observatorio Uraniborg
Écija (Sevilla, SPAIN)
uraniborg16@gmail.com

Faustino García de la Cuesta (J38)
La Vara, Valdés, (Asturias, SPAIN)

Juan-Luis González Carballo (I84)
Observatorio Cerro del Viento
(Badajoz, SPAIN)

José María Fernández (Z77)
Observatorio Inmaculada del Molino
(Sevilla, SPAIN)

Javier Ruiz Fernández (J96)
Observatorio de Cantabria
(Cantabria, SPAIN)

Esteban Reina (232)
Observatorio Masquefa l'Anoia
(Barcelona, SPAIN)

Edyta Podlewska-Gaca
Astronomical Observatory Institute
Adam Mickiewicz University
Poznan (POLAND)

Javier de Elias Cantalapiedra (L46)
Observatorio Majadahonda
(Madrid, SPAIN)

(Received: 2023 August 1)

CCD photometric observations of minor planet 5780 Lafontaine were made in 2023 July and August by a group of observers from Spain and Poland. Analysis of the data could not find a definitive solution for a synodic rotation period.

Our studies on 5780 Lafontaine began at the end of 2023 July and extended into August with amateur telescopes of between 0.25 to 0.30 m aperture along with the 1.23-m telescope of the Calar Alto Observatory in Almería. The campaign was a project of the Europlanet network that had the objective of determining the synodic rotation period and lightcurve of the asteroid.

All observations were unfiltered, except those from Calar Alto Observatory where a Johnson V filter was used. The images were calibrated in the standard way (bias, darks and flats) and then measured using *FotoDif* (2021) software. Period analysis was done using the *Periodos* (2020) package. All data were light-time corrected. The results are summarized below.

5780 Lafontaine is a main-belt asteroid that was discovered by Eric Walter Elst on 1990 March 2 at La Silla Observatory (Chile). Its orbit is characterized by a semi-major axis of 3.34 au, an eccentricity of 0.13, and an inclination of 8.67° to the ecliptic. It belongs to the 9106 (outer Main-Belt) orbital group; its spectral class is type C.

Due to its relatively recent discovery and its small size (about 23 km in diameter), the lightcurve, rotation period, and 3-D model had yet to be published. For this reason, not only telescopes of a certain aperture, but also skies with little light pollution and good seeing were necessary for the study. These characteristics are not always within the reach of the amateur astronomer. Thus, we decided to submit an observing project to the Europlanet network to use the 1.23-m telescope of the Calar Alto Observatory (Almería, Spain) on the nights of August 7 to 10; unfortunately, the weather was not as good as expected for those summer dates. As a result, additional observations by amateur observatories using telescopes with apertures of 0.25 m were required.

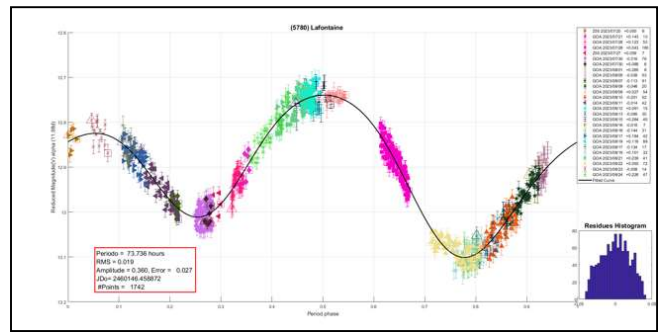
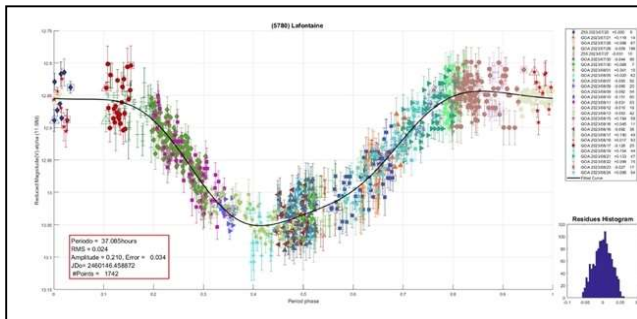
In total, 30 reports were obtained from 6 different observatories between 2023 July 20 (phase angle 11.7° , elongation 144.1°) and August 24 (phase angle 4.6° , elongation 166.5°). The final data set contained 1742 observations. Most of our data were uploaded to ALCDEF (<https://alcdef.org>).

After a preliminary analysis of the data, several proposed solutions for the rotation period were considered, although we already suspected that it should be longer than 12 hours and of low amplitude.

Our main problem was that, sometimes, the dispersion of the data obtained from semi-urban skies was confused with the low amplitude of the asteroid rotation. This forced us to repeat the observations until two or more series of data, from different observers, coincided in the same phase and with the same curve tracing.

With all data we got, it was possible to give only a hypothesis about the period: the issues being the data dispersion and the low amplitude. However, there was another factor to take into account, and that was that series with the same phase should have the same slope. When the dispersion of the series is smaller than the amplitude of the curve, both things go together, and the slopes are usually the same when the dispersion is minimal.

With Lafontaine, however, minimizing the dispersion did not guarantee that the slopes coincided. In this case, slopes should take precedence over dispersion.



Two of our series very clearly defined a minimum, which was the interesting part. Between 1 and 3 days, there was only one period in which that minimum appears framed by both series; better yet, with that period, the slopes of all the series were coherent, that is that ups and downs coincided with ups and downs based on the suggested period. This made us think that the period of 1.54 days might be the correct one.

We started to consider the period of 1.536 days, but we could not rule out the first harmonic, with two maxima and minima (3.072 days), which is the one we favor, given that it is already bimodal.

This study was only one step towards determining the asteroid's rotation period. The next opposition, 2024 November, may offer another opportunity to follow on this search. We encourage to other observers to get new lightcurve data and to report their results.

Acknowledgments

Europlanet 2024 RI has received funding from the European Union's Horizon 2020 research and innovation programme under grant agreement No 871149.

Based on observations collected at the Centro Astronómico Hispano en Andalucía (CAHA) at Calar Alto, operated jointly by Junta de Andalucía and Consejo Superior de Investigaciones Científicas (IAA-CSIC).

References.

ALCDEF (2022), Asteroid Photometry Database.
<http://alcdef.org/>

Europlanet.
<https://www.europlanet-society.org/>

FotoDif (2021).
<http://astrosurf.com/orodeno/fotodif/index.htm>

Minor Planet Center (MPC).
<https://minorplanetcenter.net/>

Periodos (2020).
<http://www.astrosurf.com/salvador/Programas.html>

LIGHTCURVES AND ROTATION PERIOD DETERMINATION OF SEVEN MAIN-BELT ASTEROIDS OBSERVED FROM MALTA AND SLOVAKIA

Stephen M. Brincat
Flarestar Observatory (MPC: 171)
Fl.5 George Tayar Street,
San Gwann SGN 3160, MALTA
stephenbrincat@gmail.com

Marek Bucek PhD
Luckystar Observatory (MPC: M55)
Dr. Lučanského 547, Važec, 032 61, SLOVAKIA
marbucek@hotmail.com

Charles Galdies PhD
Znith Observatory
Armonie, E. Bradford Street,
Naxxar NXR 2217, MALTA
charles.galdies@um.edu.mt

Martin Mifsud
Manikata Observatory
51, Penthouse 7, Sky Blue Court
Dun Manwel Grima Street,
Manikata MLH 5013, MALTA
mifsudm0@gmail.com

Winston Grech
Antares Observatory
76/3, Kent Street,
Fgura FGR 1555, MALTA
win.grech@gmail.com

(Received: 2023 August 17)

We present the results of our photometric observations of seven main-belt asteroids from five observatories in Malta and Slovakia. We have managed to derive the lightcurves for the following asteroids that can assist future analysis of these objects at different oppositions: (1400) Tirela; (1850) Kohoutek; (2591) Dworetsky; (5163) Vollmayr-Lee; (5606) Muramatsu; (23080) 1999 XH100 and (66875) 1999 VY52.

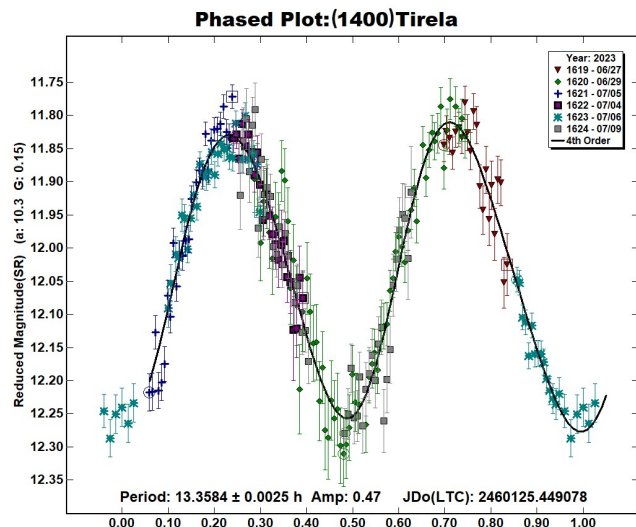
Photometric observations of seven asteroids were carried out from four observatories located on the Maltese mainland and another located at Važec, Slovakia. Observations of asteroids for (1400) Tirela; (1850) Kohoutek; (2591) Dworetsky; (5163) Vollmayr-Lee; (5606) Muramatsu; (23080) XH100; and (66875) 1999 VY52 were obtained from the observatories shown in Table 1. All of our images were taken through a clear filter (unfiltered) with R (Cousins) zero point with a calibrated through dark and flat-field subtraction. The asteroids: (1850) Kohoutek; (5163) Vollmayr-Lee; (5606) Muramatsu and (23080) 1999 XH100 were taken through a clear filter (unfiltered) with R (Cousins) zero point. A clear to V (Johnson) zero point was adopted for (5163) Vollmayr-Lee and (66875) 1999 VY52, while the images for (1400) Tirela were based on a clear to SR (Sloan R) zero point. This divergence of zero points is attributed to photometric databases quality of the sky areas concerned and preference by observers to mitigate scatter in the light curves.

All of our equipment were either controlled remotely over the internet or from a location near each telescope. Image acquisition was conducted via *Sequence Generator Pro* (Binary Star Software) by all Maltese Observatories. Luckystar Observatory employed the *NINA* image acquisition software (Berg, 2023). For our image analysis, we used *MPO Canopus* software (Warner, 2017), to gather differential aperture photometry and for light curve construction. Table I shows details of the instrumentation used and Observation Runs for each respective target. We used the Comparison Star Selector (CSS) feature of *MPO Canopus* to choose near-solar color comparison stars. All brightness measurements were based on the Asteroid Terrestrial-impact Last Alert System (ATLAS) catalogue (Tonry et al., 2018).

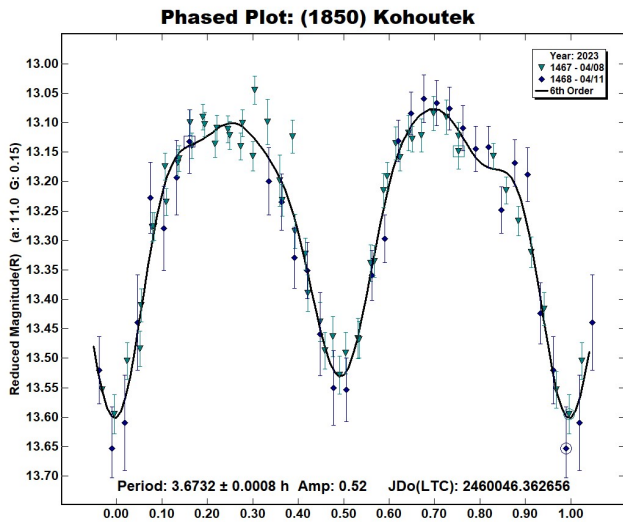
Observatory	Tel. and Type	Camera	Observed Asteroids (#Runs)
Antares obs.	0.28-m SCT	SBIG ST-11	1850 (1)
Flarestar Obs. (MPC: 171)	0.25-m SCT	Moravian G2-1600	1850 (1); 2458 (4); 23080 (3)
Luckystar Obs. (MPC: M55)	0.25-m SCT	Atik 460EX	5163 (5) 66875 (4)
Manikata Obs.	0.2-m SCT	SBIG ST-9	1400 (6)
Znith Obs.	0.2-m SCT	Moravian G2-1600	5606 (5)

Table I – Instrumentation and Observation Runs. SCT: Schmidt-Cassegrain

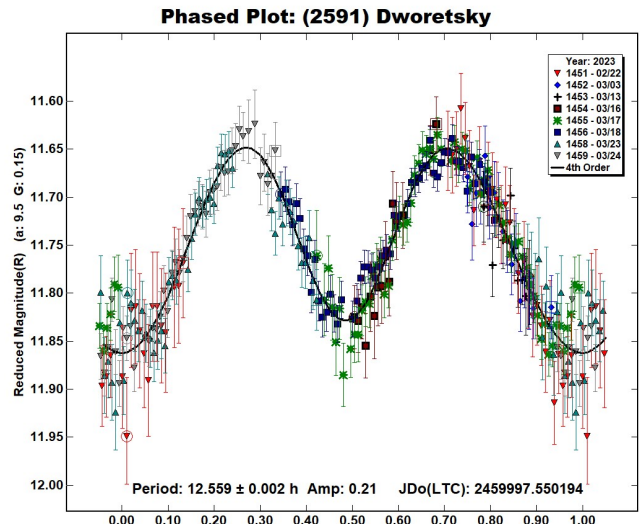
(1400) Tirela is main-belt asteroid that was discovered on 1936 November 17 by Boyer, L. at Algiers. This asteroid was named in honor of Charles Tirel, a friend of the discoverer (Schmadel, 2012). Asteroid (1400) Tirela has an estimated diameter of 15.697 ± 0.285 km, based on H of 11.45. It orbits the sun with a semi-major axis of 3.125 AU with an eccentricity of 0.232 and period of 5.524 years (JPL, 2023). This asteroid was previously observed by Székely et al. (2005) and Ďurech et al. (2016) with a period of 13.356 h and 13.35384 h respectively, having a U2 quality for both of these entries. This target was reobserved by Manikata Observatory over 6 nights from 2023 June 27 to 2023 July 09, where we derived its synodic rotation period as 13.3584 ± 0.0025 h with an amplitude of 0.47 ± 0.04 mag.



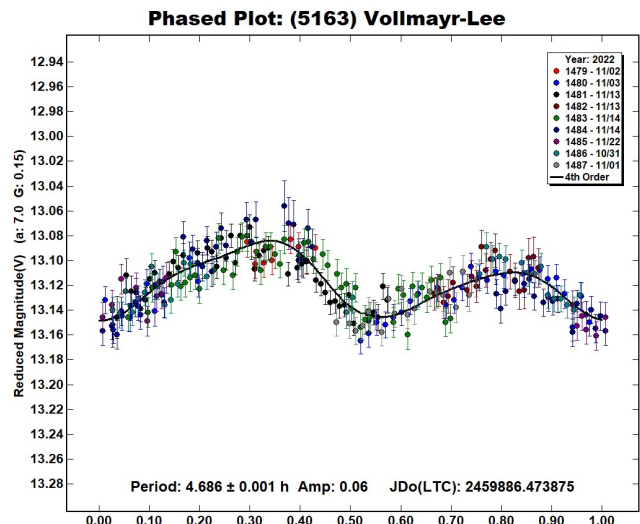
(1850) Kohoutek is a stony main-belt asteroid that was discovered on 1942 March 23 by K. Reinmuth at Heidelberg. This asteroid was named after Luboš Kohoutek, a Czech astronomer who has contributed knowledge on planetary nebulae and emission-line stars. He is also widely known as a discoverer of comets and minor planets and has been on the staff of the observatory at Hamburg-Bergedorf since 1969 (Schmadel, 2012). The estimated diameter was derived to be 7.642 ± 0.086 km, based on an absolute magnitude H of 12.85 and orbits the sun with a semi-major axis of 2.251 AU. Its orbit has an eccentricity of 0.126 and a period of 3.377 years (JPL, 2023). The asteroid Kohoutek, was observed from Flarestar Observatory and Antares Observatory respectively on 2023 April 8 and 11. Our results yielded a synodic period of 3.6732 ± 0.0008 h with an amplitude of 0.52 ± 0.05 mag. Our derived period is consistent with Āurech et al. (2020) and Erasmus et al. (2020).



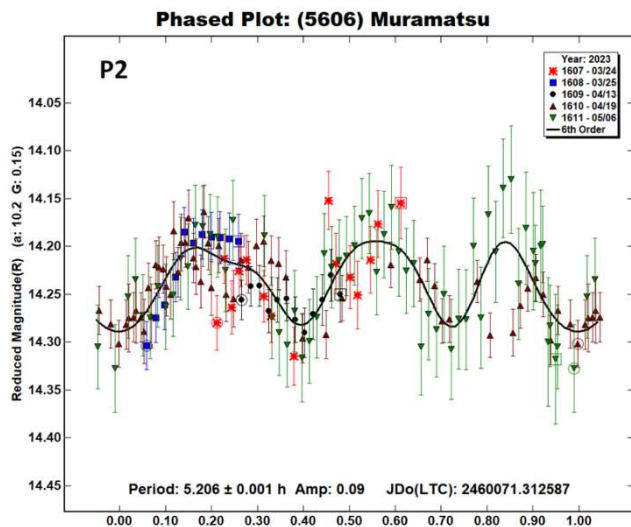
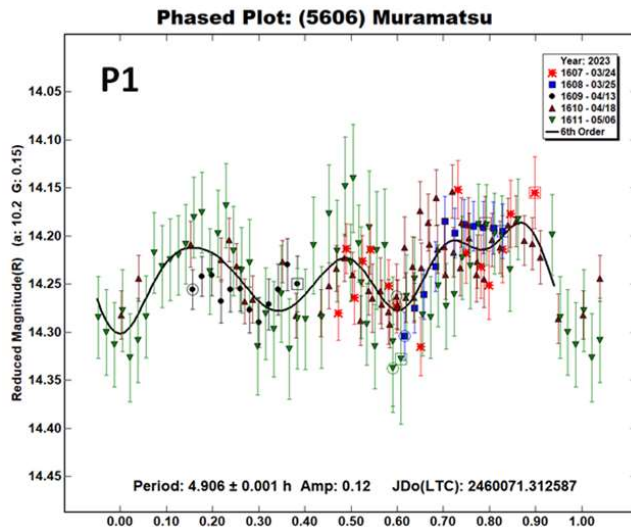
(2591) Dworetsky is a main-belt asteroid belonging to the Koronis family. It was discovered by K. Reinmuth at Heidelberg on 1949 August 02. This asteroid was named after Michael M. Dworetsky, a University of London, senior lecturer that mainly researched stellar abundances of the mercury group of elements. He was also instrumental for the development of the undergraduate astronomy degree program. This minor planet orbits the sun with a semi-major axis of 2.94 AU, eccentricity 0.04, and orbital period of 5.04 years (JPL, 2023). The JPL Small-Bodies Database Browser lists the diameter of 2591 Dworetsky as 12.925 ± 0.141 km based on an absolute magnitude $H = 11.62$. The asteroid (2591) Dworetsky was observed over 8 nights from 2023 February 02 to March 24. Our results yielded a synodic rotation period of 12.559 ± 0.002 h and amplitude of 0.21 ± 0.05 mag. Our derived period is consistent with Erasmus et al. (2020).



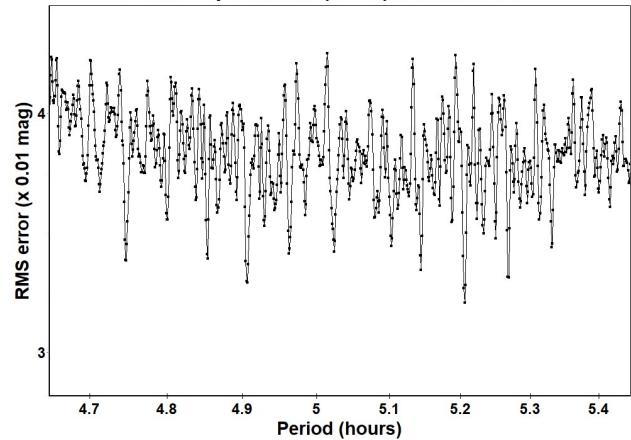
(5163) Vollmayr-Lee is a main-belt asteroid that was discovered by J. Wagner at the Anderson Mesa Station of the Lowell Observatory on 1983 October 09. The asteroid was named after Katharina Vollmayr-Lee (b. 1967), who is a Professor in the Department of Physics and Astronomy at Bucknell University. She investigates the behavior of structural glasses and granular media with computer simulations. She has earned praise for her inspiring and effective education. The estimated diameter of the asteroid Vollmayr-Lee was derived to be 6.869 ± 0.102 km, based on an absolute magnitude H of 12.95. This minor planet orbits the sun with a semi-major axis of 2.467AU. Its orbit has an eccentricity of 0.201, and a period of 3.88 years (JPL, 2023). Observations were conducted from Luckystar Observatory over 5 nights from 2022 October 31 to 2022 November 14 with the aim to improve the quality of the published period. Our results indicate a synodic period of 4.686 ± 0.001 h and shallow amplitude of 0.06 ± 0.04 mag. This is consistent with the published period of 4.728 ± 0.001 h (Behrend, 2010web).



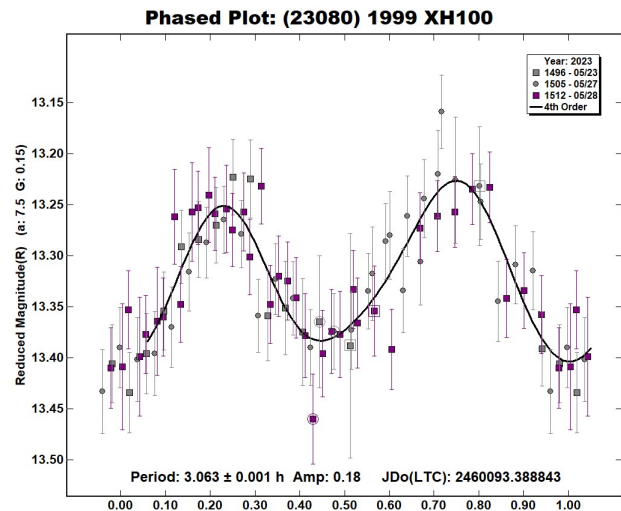
(5606) *Muramatsu* is an inner main-belt asteroid that was discovered on 1993 Mar. 1 by S. Otomo at Kiyosato. It has been named in honor of Osamu Muramatsu (b. 1949), who works at the planetarium in Shibuya, Japan and who has discovered a number of minor planets and comets since 1986. The estimated diameter was derived to be 4.811 ± 0.054 km based on an absolute magnitude H of 13.73 and orbits the sun with a semi-major axis of 2.225 AU. Its orbit has an eccentricity of 0.129, and orbits the sun every 3.32 years (JPL, 2023). We observed (5606) *Muramatsu* from Zniith Observatory on five nights between 2023 March 24 and 2023 May 06. We searched for the best period solution and found two possible periods, both having trimodal light curves. The first one had a period of 5.206 ± 0.001 h (P2) and an amplitude of 0.09 ± 0.06 mag, having a lower RMS residual than the preferred one. The second one, which is our preferred solution, had a period of 4.906 ± 0.001 h and an amplitude of 0.12 ± 0.06 mag. This solution also matched better the shape of the light curve as all observation runs are consistent with the fit contrary to the 5.206 h solution where one of the runs deviates from the rest at phase 0.85. Therefore, we believe that 4.906 h period is the correct period for (5606) *Muramatsu*. This is also consistent with the period of 4.90991 h reported by Warner et al. (2009) in the Light Curve Data Base (LCDB, Rev. 2023 February), which was based on partial coverage (U2).



Period Spectrum: (5606) Muramatsu



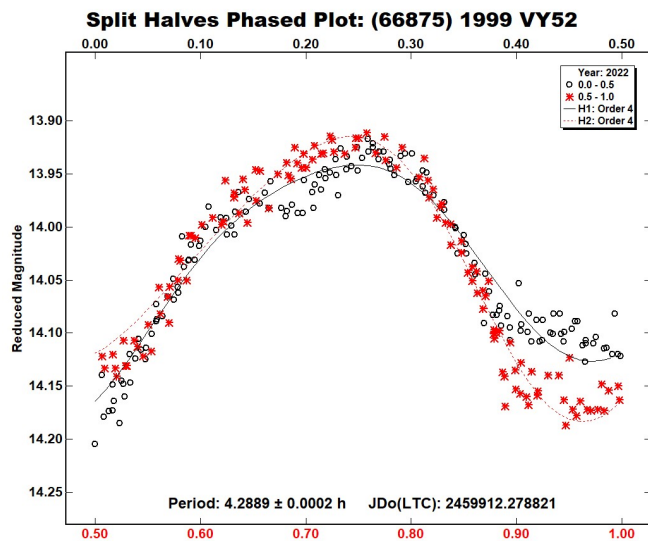
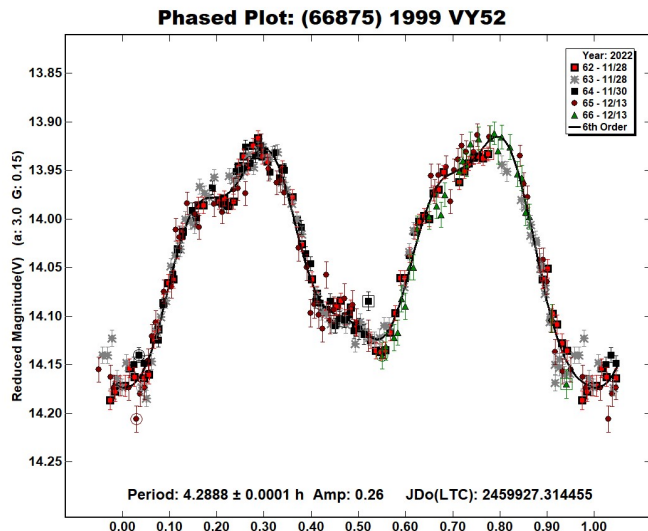
(23080) 1999 *XH100* is a middle main-belt asteroid that was discovered on 1999 December 07 by LINEAR at Socorro. The diameter of this asteroid is estimated to be 6.624 ± 0.162 km based on $H=13.18$. The asteroid orbits at a semi-major axis of 2.667 AU with an eccentricity of 0.167. The orbital period of this asteroid is 4.35 years (JPL, 2023). (23080) was observed on 3 nights from Flarestar Observatory, and derived the synodic period to be 3.063 ± 0.001 h with an amplitude of 0.18 ± 0.05 mag. Our data is consistent with that published by Pál et al. (2020) as available through the Asteroid Lightcurve Database (LCDB) (Warner, 2021).



(66875) 1999 *VY52* is a main-belt asteroid that does not pertain to any membership to a known family. This asteroid was discovered on 1999 November 03 by the LINEAR survey at Socorro, New Mexico, USA. The estimated diameter of (66875) was derived to be 4.636 ± 0.708 km based on an absolute magnitude H of 13.95 and orbits the sun with a semi-major axis of 2.774 AU. Its orbit has an eccentricity of 0.377, and orbits the sun every 3.82 years (JPL, 2023). (66875) 1999 *VY52*, was observed from Luckystar Observatory on four nights from 2022 November 28 to 2022 December 13, from which we derived the synodic period to be 4.2888 ± 0.0001 h having an amplitude of 0.26 ± 0.02 mag. Our results deviate from the published period by Pál et al. (2020) that listed a period of 2.148 h that is half of our period. Our split-halves does show some deviation among the phases and hence our lower residual values substantiate our derived period.

Number	Name	yyyy mm/dd	Phase	L _{PAB}	B _{PAB}	Period(h)	P.E.	Amp	A.E.	Grp
1400	Tirela	2023 06/27-07/09	10.3,10.0	283.7	19.9	13.3584	0.0025	0.47	0.04	MB
1850	Kohoutek	2023 04/08-04/11	10.9,12.4	180.8	5.0	3.6732	0.0008	0.52	0.05	Flora
2591	Dworetzky	2023 02/22-03/24	9.3,2.5	177.6	0.0	12.559	0.002	0.21	0.05	Koronis
5163	Vollmayr-Lee	2022 10/31-11/22	7.9,9.0	48.3	-0.9	4.686	0.001	0.06	0.04	MB
5606	Muramatsu	2023 03/24-04/19	27.1,23.7	90.4	-7.2	4.906	0.001	0.12	0.06	MB
						5.206	0.001	0.09	0.06	
23080	1999 XH100	2023 05/23-05/28	7.8,9.8	231.4	8.1	3.063	0.001	0.18	0.05	MB
66875	1999 VY52	2022 11/28-12/13	3.0,7.7	70.5	0.7	4.2888	0.0001	0.26	0.02	MB

Table I. Observing circumstances and results. The phase angle is given for the first and last date. LPAB and BPAB are the approximate phase angle bisector longitude and latitude at mid-date range (see Harris et al., 1984). Grp is the asteroid family/group (Warner et al., 2009).



Acknowledgements

We would like to thank Brian Warner for his work in the development of *MPO Canopus* and for his efforts in maintaining the CALL website (Warner, 2016; 2017). This research has made use of the JPL's Small-Body Database (JPL, 2023).

References

Behrend, R. (2010web). Observatoire de Geneve web site. http://obswww.unige.ch/~behrend/page_cou.html

Berg, S. (2023). Nighttime Imaging 'N' Astronomy (NINA) web site. Last accessed: 29 June 2023. <https://nighttime-imaging.eu/>

Đurech, J.; Hanuš, J.; Oszkiewicz, D.; Vančo, R. (2016). "Asteroid models from the Lowell photometric database." *Astronomy & Astrophysics* **587**, A48.

Đurech, J.; Tonry, J.; Erasmus, N.; Denneau, L.; Heinze, A.N.; Flewelling, H.; Vančo, R. (2020). "Asteroid models reconstructed from ATLAS photometry." *Astronomy & Astrophysics* **643**, A59.

Erasmus, N.; Navarro-Meza, S.; McNeill, A.; Trilling, D.E.; Sickafoose, A.A.; Denneau, L.; Flewelling, H.; Heinze, A.; Tonry, J.L. (2020). "Investigating taxonomic diversity within asteroid families through ATLAS dual-band photometry." *The Astrophysical Journal Supplement Series* **247(1)**, 13.

Harris, A.W.; Young, J.W.; Scaltriti, F.; Zappala, V. (1984). "Lightcurves and phase relations of asteroids 82 Alkmene and 444 Ggyptis." *Icarus* **57**, 251-258.

JPL (2023). Small-Body Database Browser - JPL Solar System Dynamics web site. Last accessed: 11 July 2023. <http://ssd.jpl.nasa.gov/sbdb.cgi>

Pál, A.; Szakáts, R.; Kiss, C.; Bódi, A.; Bognár, Z.; Kalup, C.; Kiss, L.L.; Marton, G.; Molnár, L.; Plachy, E.; Sárneczky, K.; Szabó, G.M.; Szabó, R. (2020). "Solar System Objects Observed with TESS - First Data Release: Bright Main-belt and Trojan Asteroids from the Southern Survey." *Ap. J. Suppl. Ser.* **247**, id. 26.

Schmadel, L.D. (2012). Catalogue of Minor Planet Names and Discovery Circumstances. In Dictionary of Minor Planet Names (pp. 11-1309). Springer, Berlin, Heidelberg.

Székely, P.; Kiss, L.L.; Szabó, G.M.; Sárneczky, K.; Csák, B.; Váradi, M.; Mészáros, S. (2005). "CCD photometry of 23 minor planets." *Planetary and Space Science* **53(9)**, 925-936.

Tonry, J.L.; Denneau, L.; Flewelling, H.; Heinze, A.N.; Onken, C.A.; Smartt, S.J.; Stalder, B.; Weiland, H.J.; Wolf, C. (2018). "The ATLAS All-Sky Stellar Reference Catalog." *Astrophys. J.* **867**, A105.

Warner, B.D.; Harris, A.W.; Pravec, P. (2009). "The Asteroid Lightcurve Database." *Icarus* **202**, 134-146. Updated 2016 Sep. <http://www.minorplanet.info/lightcurvedatabase.html>

Warner, B.D. (2016). Collaborative Asteroid Lightcurve Link website. Last accessed: 26 September 2018. <http://www.minorplanet.info/call.html>

Warner, B.D. (2017). MPO Software, *MPO Canopus* version 10.7.10.0. Bdw Publishing. <http://www.minorplanetobserver.com/>

Warner, B.D. (2021). Asteroid Lightcurve Photometry Database (ALCDEF). <https://minplanobs.org/alcdef/index.php>

**PHOTOMETRIC OBSERVATIONS OF MAIN-BELT
ASTEROIDS 784 PICKERINGIA, 1465 AUTONOMA,
1477 BONSDORFFIA, 3057 MALAREN,
5708 MELANCHOLIA, AND 8548 SUMIZIHARA**

Charles Galdies, PhD
Znith Observatory
Armonie, E. Bradford Street,
Naxxar NXR 2217, MALTA
charles.galdies@um.edu.mt

Stephen M. Brincat
Flarestar Observatory (MPC code: 171)
Fl.5 George Tayar Street,
San Gwann SGN 3160, MALTA
stephenbrincat@gmail.com

Marek Buček, PhD
Luckystar Observatory (MPC code: M55)
Dr. Lučanského 547, Važec, 032 61, SLOVAKIA
marbucek@hotmail.com

Martin Mifsud
Manikata Observatory
Manikata, MLH 5013, MALTA
mifsudm0@gmail.com

(Received: 2023 August 17)

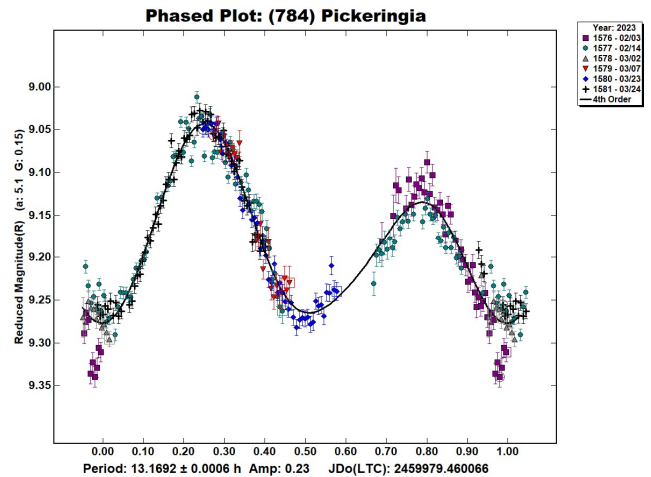
Photometric observations of selected asteroids were done from Znith Observatory, Flarestar Observatory (MPC-171), Luckystar Observatory (MPC-M55), and Manikata Observatory in 2023. The observations were made during a favorable apparition for each asteroid. Some of these targets were never studied in the past and thus their rotation periods were unknown.

In between the months of April 2022 and June 2023, photometric observations of 6 main-belt asteroids were carried out from five observatories located in Malta (Europe) and Slovakia. Observations of 784 Pickeringia and 8548 Sumizihara were obtained from Znith Observatory through a 0.20-m $f/6.3$ Schmidt-Cassegrain telescope (SCT) equipped with a Moravian G2-1600 CCD camera. Observations of 5708 Melancholia and 3057 Malaren were obtained from Luckystar Observatory through a 0.25-m $f/8$ Schmidt-Cassegrain telescope (SCT) equipped with an Atik460Exm CCD camera at 1×1 binning mode with a resultant pixel scale of $0.66''$ per pixel. 1477 Bonsdorffia was observed by Flarestar Observatory through a 0.25-m $f/6.3$ Schmidt-Cassegrain telescope (SCT) using a Moravian G2-1600 camera at 1×1 binning mode with a resultant pixel scale of $0.99''$ per pixel. 1465 Autonoma was jointly observed by Manikata Observatory, through a 0.20-m $f/10$ Schmidt-Cassegrain telescope (SCT) equipped with an SBIG ST-9 CCD camera and by Znith Observatory. All cameras were operated at sensor temperature of -15°C and images were dark subtracted and flat-fielded.

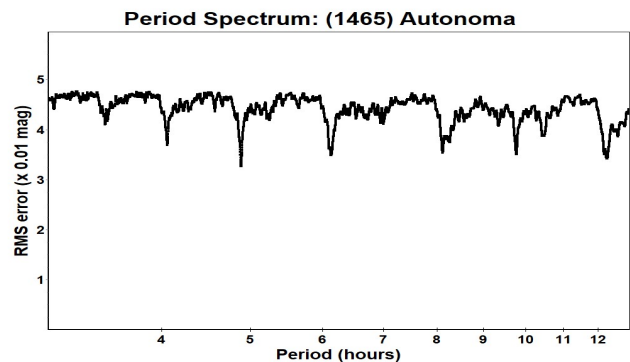
Telescopes and cameras were controlled remotely from a nearby location via *Sequence Generator Pro* (Binary Star Software) and *Nighttime Imaging 'N' Astronomy* (Berg, 2023). Photometric reduction, lightcurve construction and analyses were derived through *MPO Canopus* software (Warner, 2017). Differential aperture photometry was utilized and photometric measurements were derived through the use of *MPO Canopus*, Comparison Star Selector (CSS) that utilized comparison stars of near-solar color.

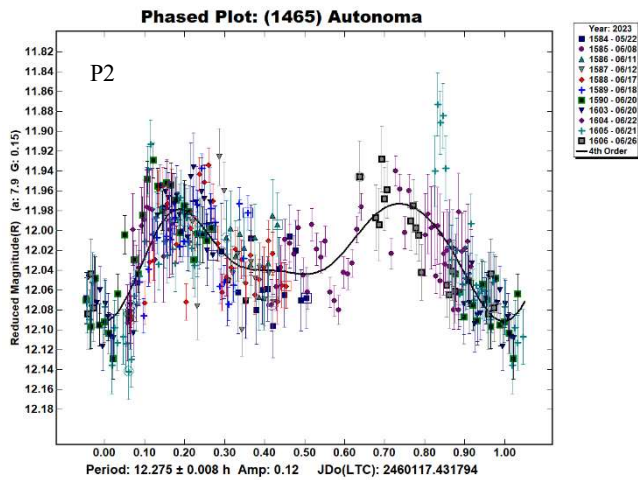
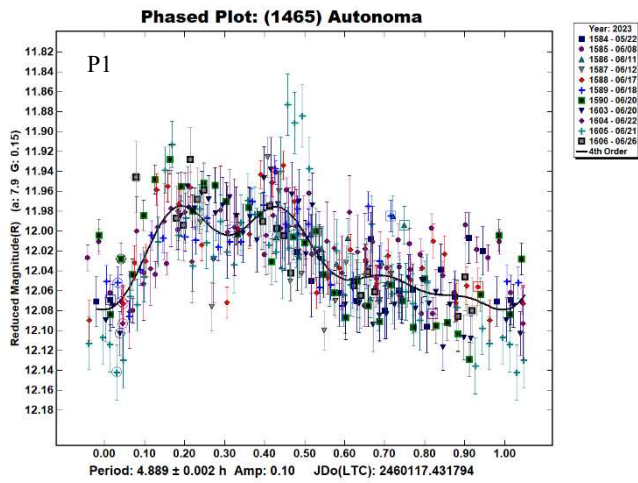
All measurements were taken from the MPOSC3 Catalog that is based on the 2MASS catalog (<http://www.ipac.caltech.edu/2mass>) with magnitudes converted from J-K to BVRI (Warner, 2007). The 6 asteroids for this research have been selected through the CALL website as maintained by Warner (2016).

784 Pickeringia is a main-belt asteroid that was discovered in 1914 March 20 by J.H. Metcalf at Winchester, UK. The asteroid orbits the sun with a semi-major axis of 3.099 AU, eccentricity 0.2411, and a period of 5.46 years (JPL, 2023). The JPL Small-Bodies Database Browser (JPL, 2023) lists the diameter of this asteroid as $75.596 \text{ km} \pm 0.311 \text{ km}$ based on an absolute magnitude $H = 13.2$. 784 Pickeringia was observed from Znith Observatory on 6 nights starting on the night of 2023 February 14/15 and ending on the night of 2023 March 24. Our results yielded a synodic period of $13.1692 \pm 0.0006 \text{ h}$ and amplitude of $0.23 \pm 0.03 \text{ mag}$. This is in line with the results published in the LCDB by Pilcher (2022) and Dose (2023).

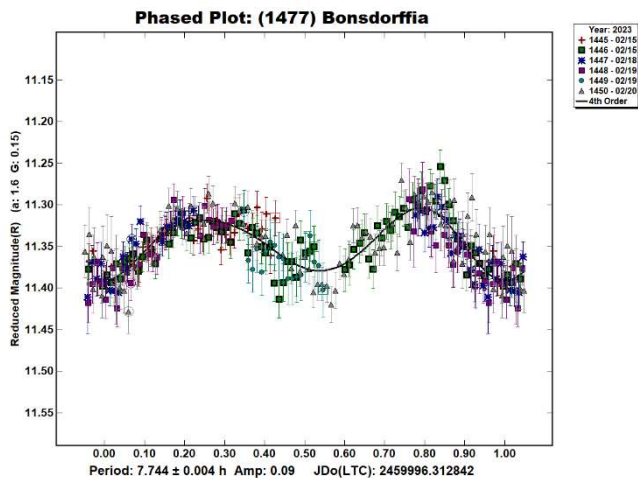


(1465) Autonoma is a main-belt asteroid that was discovered in 1938 March 20 by A. Wachmann at Bergerdorf. The asteroid orbits the sun with a semi-major axis of 3.027 AU, eccentricity 0.178, and a period of 5.27 years (JPL, 2023). The JPL Small-Bodies Database Browser (JPL, 2023) lists the diameter of 1465 Autonoma as $18.111 \text{ km} \pm 0.276 \text{ km}$ based on an absolute magnitude $H = 11.8$. Asteroid (1465) was observed from Znith Observatory on three nights from 2023 June 20 to June 22, and by Manikata Observatory on seven nights from 2023 May 22 to June 20. The derived lightcurves indicate a possible synodic period of $4.889 \pm 0.002 \text{ h}$ and amplitude of $0.10 \pm 0.005 \text{ mag}$ (“P1 figure”) with an RMS of 3.2672. Another period spectrum (“P2 figure”), shows a higher period than that of the other derived period of $12.275 \pm 0.008 \text{ h}$ and amplitude of $0.12 \pm 0.005 \text{ mag}$ but with a slightly higher RMS of 3.4158.

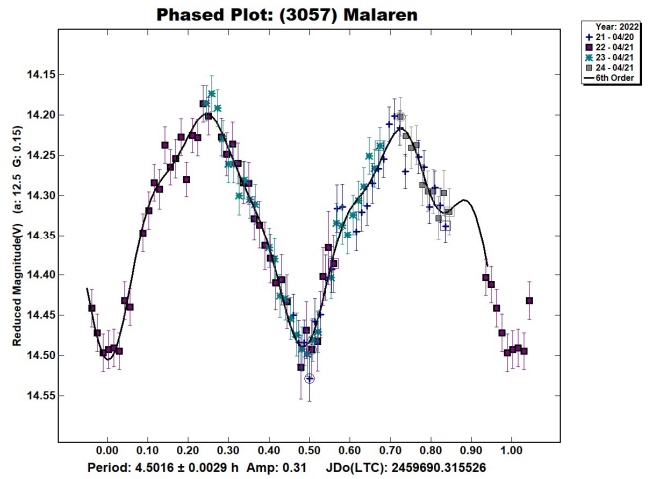




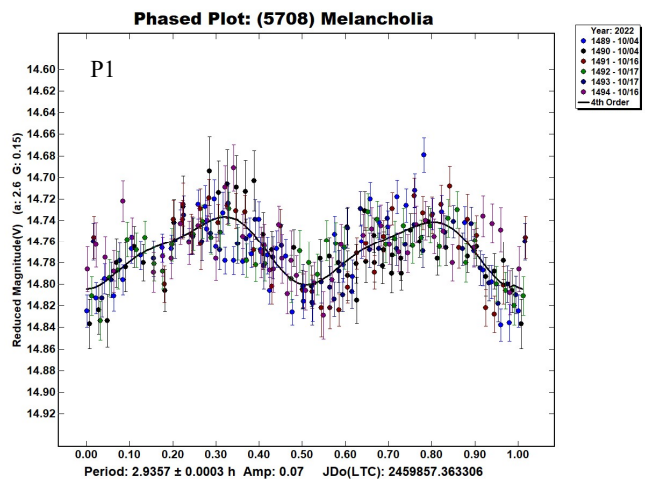
(1477) Bonsdorffia is a main-belt asteroid that was discovered in 1938 February 06 by Y. Vaisala at Turku. The asteroid orbits the sun with a semi-major axis of 3.208 AU, eccentricity 0.266, and a period of 5.74 years (JPL, 2023). The JPL Small-Bodies Database Browser (JPL, 2023) lists the diameter of 1477 Bonsdorffia as 25.851 ± 0.390 km based on an absolute magnitude $H = 11.5$. Bonsdorffia was observed from Flarestar Observatory on 2023 February 15 to February 20. The derived lightcurve indicates a synodic period of 7.744 ± 0.004 h and amplitude of 0.09 ± 0.04 mag. This is close to the U2 LCDB published value of 7.8 ± 0.1 h by Aznar (2011web; LCDB, 2023).



(3057) Malaren is a main-belt asteroid that was discovered on 1981 March 9 by E. Bowell at Flagstaff. This asteroid has an absolute magnitude (H) of 13.7 and orbits the sun with a semi-major axis of 2.260 AU, eccentricity 0.075, and a period of 3.397 years (JPL, 2023). Observations were conducted from Luckystar Observatory on 2 nights from 2022 April 20 until April 21. The derived lightcurve, which is based on an almost coverage, indicates a synodic period of 4.5016 ± 0.00029 h and amplitude of 0.31 ± 0.02 mag.

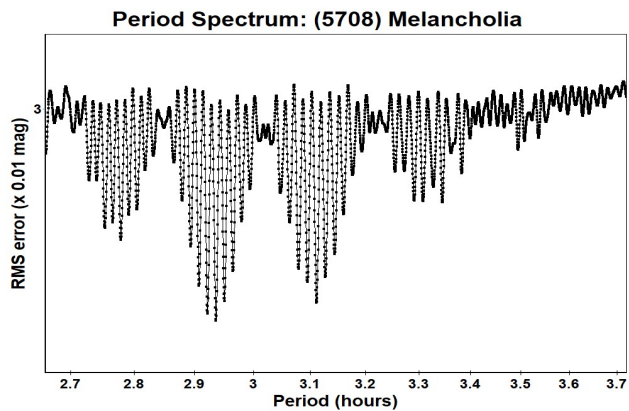
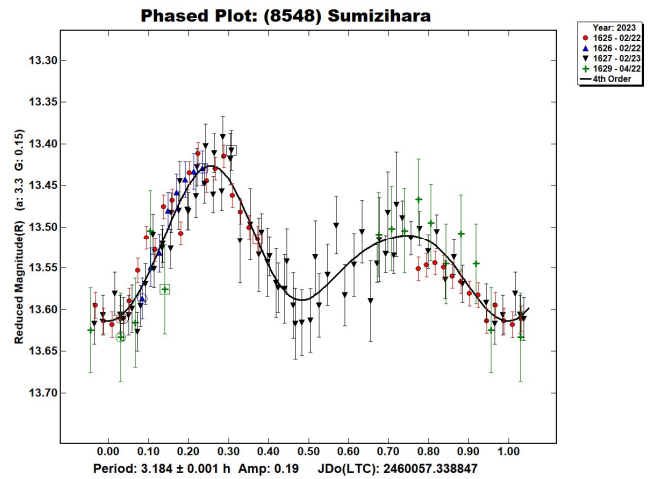
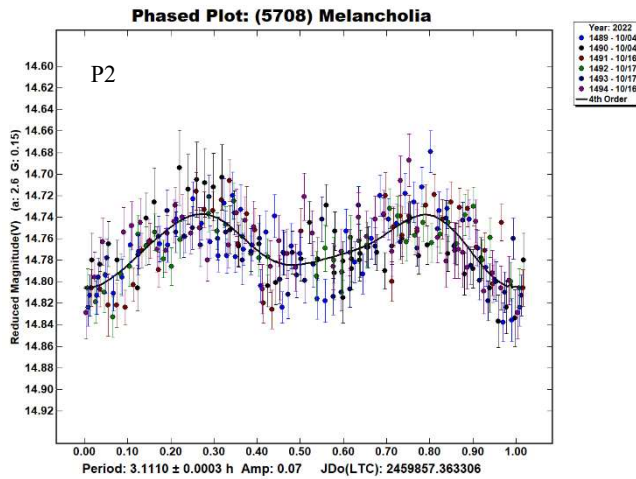


(5708) Melancholia is a main-belt asteroid that was discovered on 1977 October 12 by P. Wild at Zimmerwald. The asteroid orbits the sun with a semi-major axis of 2.179 AU, eccentricity 0.212, and a period of 3.216 years (JPL, 2023). The JPL Small-Bodies Database Browser does not list the diameter of this asteroid. Its absolute magnitude $H = 14.6$. Observations were conducted from Luckystar Observatory on 3 nights from the night of 2022 October 4 and ending on the night of October 16. Results following period spectrum analysis show two possible periods for this target, one with a synodic period of 2.9357 ± 0.0003 h and amplitude of 0.07 ± 0.04 mag (“P1 figure”; RMS 2.2135) and 3.1110 ± 0.0003 h and amplitude of 0.07 ± 0.04 mag (“P2 figure”; RMS 2.2801). The LCBD did not display any published periods of this asteroid.



Number	Name	yyyy mm/dd	Pts	Phase	L _{PAB}	B _{PAB}	Period(h)	P.E.	Amp	A.E.	Grp
784	Pickeringia	2023 02/14-03/24	299	4.5, 6.4	142	12	13.1692	0.0006	0.23	0.03	MB
1465	Autonoma	2023 05/22-06/22	312	7.9, 10.6	252	13	4.889	0.002	0.10	0.005	MB
1477	Bonsdorffia	2023 02/15-02/20	323	1.9, 4.0	142	-1	7.744	0.004	0.09	0.04	MB
3057	Malaren	2022 04/20-04/21	109	12.4, 12.9	192	9	4.5016	0.00029	0.31	0.02	MB
5708	Melancholia	2022 10/04-10/16	272	2.6, 7.0	14	3	2.9357	0.0003	0.07	0.04	MB
8548	Sumizihara	2023 02/22-02/23	117	3.8, 4.4	148	2	3.1110	0.0003	0.07	0.04	MB
							3.184	0.001	0.19	0.05	MB

Table I. Observing circumstances and results. Pts is the number of data points. The phase angle is given for the first and last date. If preceded by an asterisk, the phase angle reached an extrema during the period. L_{PAB} and B_{PAB} are the approximate phase angle bisector longitude/latitude at mid-date range (see Harris et al., 1984). Grp is the asteroid family/group (Warner et al., 2009).



(8548) Sumizihara is a main-belt asteroid that was discovered in 1994 March 14 by K. Endate and K. Watanab at Kitami. The asteroid orbits the sun with a semi-major axis of 2.587 AU, eccentricity 0.260, and a period of 4.16 years (JPL, 2023). The JPL Small-Bodies Database Browser (JPL, 2023) lists the diameter of 8548 Sumizihara as $5.286 \text{ km} \pm 0.090 \text{ km}$ based on an absolute magnitude $H = 13.5$. Sumizihara was observed from Znith Observatory on 2 nights from the night of 2023 February 22 until February 23. The derived lightcurve indicates a synodic period of $3.184 \pm 0.001 \text{ h}$ and amplitude of $0.19 \pm 0.05 \text{ mag}$.

Acknowledgements

We would like to thank Brian Warner for his work in the development of *MPO Canopus* and for his efforts in maintaining the CALL website. This research has made use of the JPL's Small-Body Database.

References

- Aznar, A. (2011web) Rotation period 7.8 ± 0.1 hours with a brightness amplitude of 0.32 mag. Last accessed: 7 November 2023. https://en.wikipedia.org/wiki/1477_Bonsdorffia
- Berg, S. (2023). Nighttime Imaging 'N' Astronomy (NINA) web site. Last accessed: 29 June 2023. <https://nighttime-imaging.eu/>
- Dose, E.V. (2023). "Lightcurves of Nine Asteroids." *Minor Planet Bull.* **50(3)**, 223-227.
- Harris, A.W.; Young, J.W.; Scaltriti, F.; Zappala, V. (1984). "Lightcurves and phase relations of asteroids 82 Alkmene and 444 Gytis." *Icarus* **57**, 251-258.
- JPL (2023). Small-Body Database Browser - JPL Solar System Dynamics web site. Last accessed: 17 may 2017. <http://ssd.jpl.nasa.gov/sbdb.cgi>
- LCDB (2023). (1477) Bonsdorffia Last accessed: 7 Nov. 2023. <https://www.minorplanet.info/PHP/generateoneasteroidinfo.php>
- Pilcher, F. (2022). "Lightcurves and Rotation Periods of 330 Adalberta, 494 Virtus, 530 Turandot, 784 Pickeringia, and 1009 Sirene." *Minor Planet Bull.* **49(2)**, 122-124.

Warner, B.D. (2007). "Initial Results of a Dedicated H-G Program." *Minor Planet Bull.* **34**, 113-119.

Warner, B.D.; Harris, A.W.; Pravec, P. (2009). "The Asteroid Lightcurve Database." *Icarus* **202**, 134-146. Updated 2023 June. <http://www.minorplanet.info/lightcurvedatabase.html>

Warner, B.D. (2016). Collaborative Asteroid Lightcurve Link website. Last accessed: 19 May 2017. <http://www.minorplanet.info/call.html>

Warner, B.D. (2017). MPO Software, *MPO Canopus* version 10.7.10.0. Bdw Publishing. <http://www.minorplanetobserver.com/>

LIGHTCURVES AND ROTATION PERIODS OF 903 NEALLEY, 1051 MEROPE, AND 1187 AFRA

Frederick Pilcher
Organ Mesa Observatory (G50)
4438 Organ Mesa Loop
Las Cruces, NM 88011 USA
fpilcher35@gmail.com

(Received: 2023 September 19)

Synodic rotation periods and amplitudes at their year 2023 oppositions are found for 903 Nealley 29.063 ± 0.006 hours, 0.06 ± 0.01 magnitudes with one maximum and minimum per rotational cycle; 1051 Merope 13.712 ± 0.001 hours, 0.17 ± 0.01 magnitudes with one maximum and minimum per rotational cycle; 1187 Afra 14.071 ± 0.001 hours, 0.68 ± 0.05 magnitudes.

The new observations to produce the results reported in this paper were made at the Organ Mesa Observatory with a Meade 35-cm LX200 GPS Schmidt-Cassegrain, SBIG STL-1001E CCD, 60 to 120 second exposures, unguided, clear filter. Image measurement and lightcurve construction were with *MPO Canopus* software with calibration star magnitudes for solar colored stars from the CMC15 catalog reduced to the Cousins R band. Zero-point adjustments of a few $\times 0.01$ magnitude were made for best fit. To reduce the number of data points on the lightcurves and make them easier to read, data points have been binned in sets of 3 with maximum time difference 5 minutes.

903 Nealley. Several different rotation periods of have been published previously. Warner (2004), near celestial longitude 150° , found 21.60 h, revised in Warner (2012) to 19.58 h. Also, in Warner (2012), additional data near celestial longitude 312° showed 19.72 h. Behrend (2020web) obtained 16.2 h near celestial longitude 140° . Pál et al (2020) found a longer period of 28.9882 h near celestial longitude 60° and based on a lightcurve with three unequal maxima and minima. Dose (2022) published a bimodal lightcurve with several gaps phased to a period 58.032 h near celestial longitude 195° .

New observations on 13 nights 2023 July 17 - Aug. 27, near celestial longitude 338° , provide a fit to a lightcurve with period 29.063 ± 0.006 hours, amplitude 0.06 ± 0.01 magnitudes with one maximum and minimum per rotational cycle (Fig. 1). This period is consistent with Pál et al. (2020), and also with Dose (2022) if his data were replotted to 29.016 h with a monomodal lightcurve analogous to the one found from this study and with half of his published period.

A period spectrum of the year 2023 data (Fig. 2) shows minima near 29 hours and the double period 58 hours to be much deeper than any minimum near 20 hours. The three maxima and minima per 28.9882-hour cycle in the study by Pál et al. (2020) make the double period with six maxima and minima per cycle highly unlikely. An attempt to draw a lightcurve phased to near 20 hours from the data of the current study shows a complete misfit, with segments from separate sessions overlapping in the form of an X. This failed lightcurve is not published here but is available from the author upon request. The periods by Warner (2004), Warner (2012), and Behrend (2020web) may be safely rejected.

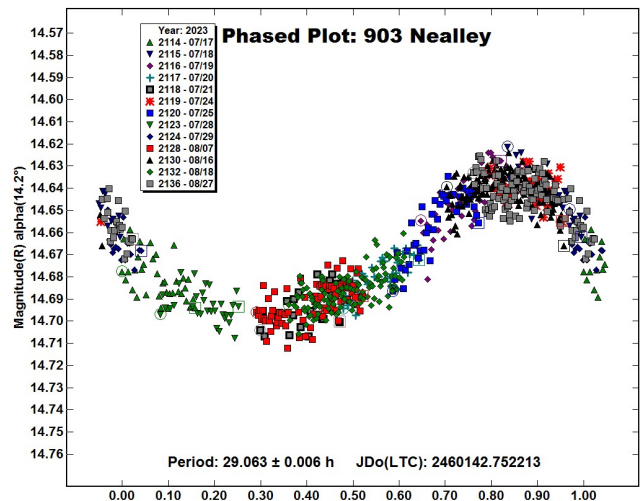


Figure 1. The lightcurve of 903 Nealley from year 2023 data (this study) phased to 29.063 hours.

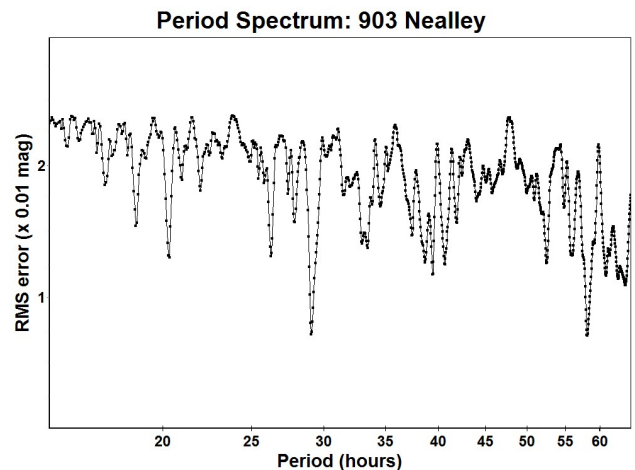


Figure 2. Period spectrum of 903 Nealley from year 2023 data (this study).

The data by Pál et al. (2020) are a by-product of the TESS (Transiting Exoplanet Satellite Survey) mission. The satellite was fixed to a single field for an interval of about three weeks and a data point for any asteroid passing through the field was obtained every half hour for this interval. The data set for each asteroid was subdivided into separate 24-hour sessions and posted on the Asteroid Lightcurve Data Exchange Format website. https://alcdex.org/php/alcdex_credits.html. This author downloaded the Pál et al. (2020) data for 903 Nealley from the year 2018. *MPO Canopus* software was used to plot the data into a lightcurve with the same *MPO Canopus* format as has been used for all the other lightcurves presented in this paper. A small number of highly discordant single data points were removed. This lightcurve shows three unequal maxima and minima per rotational cycle with period 29.038 ± 0.005 hours, amplitude 0.14 ± 0.01 magnitudes (Fig. 3). The original study by Pál et al. (2020) presented a slightly smaller period than was found for the same dataset by *MPO Canopus* software. With an amplitude much greater than the scatter of all but a very few outlying data points and a complex lightcurve, the period of 29.038 hours can be considered secure and is compatible with the 29.063 hours of the current study.

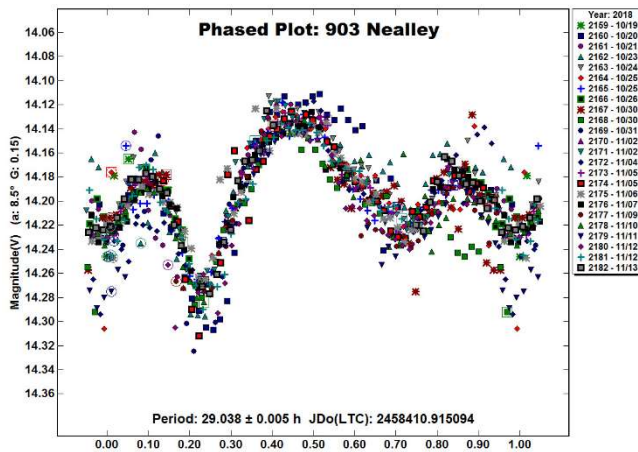


Figure 3. The lightcurve of 903 Nealley from year 2018 data (Pál et al., 2020) phased to 29.038 hours.

All of the lightcurves in the study by Pál et al. (2020) are downloadable, but not able to be manipulated, from the website https://archive.konkoly.hu/pub/tssys/dr1/object_plots/.

1051 Merope. Previously published periods are by Carbo et al. (2009), 27.2 h with an incomplete bimodal lightcurve; Waszczak et al. (2015), 13.717 h; Pál et al. (2020), 6.85563 h with a monomodal lightcurve; and Dose (2023), 13.71 h.

New observations on 8 nights 2023 July 26 - Sept. 8 provide a good fit to a lightcurve with period 13.712 ± 0.001 hours, amplitude 0.17 ± 0.01 magnitudes with one maximum and minimum per rotational cycle (Fig. 4). A split halves plot of the double period (Fig. 5) shows that the two halves are almost identical and very strongly supports the monomodal lightcurve interpretation with period 13.712 hours.

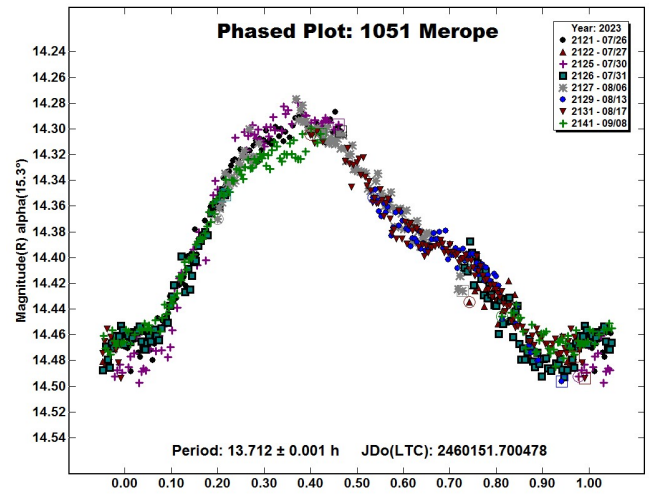


Figure 4. The lightcurve of 1051 Merope from year 2023 data (this study) phased to 13.712 hours.

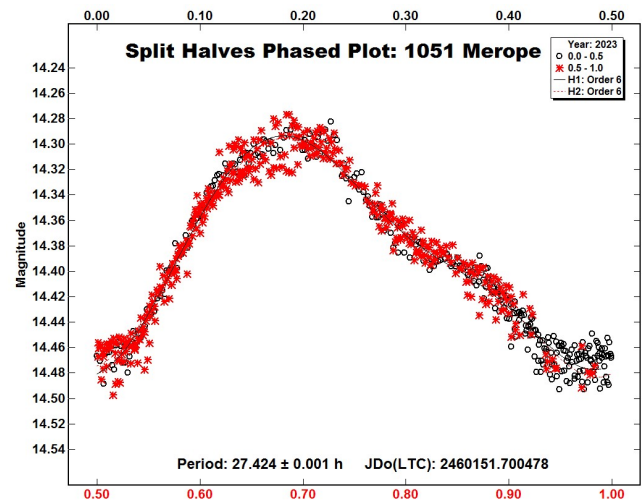


Figure 5. Split halves lightcurve of 1051 Merope from year 2023 data (this study).

Inspection of the incomplete bimodal 27.2 h lightcurve by Carbo et al. (2009) shows that it could be replotted with just as good fit to a monomodal 13.6-hour lightcurve analogous to the lightcurve in this study. The dataset for the monomodal 6.85563 h lightcurve by Pál et al. (2020) has been downloaded from www.ALCDEF.org in the manner as described above for 903 Nealley. *MPO Canopus* software shows an unsymmetric bimodal lightcurve with period 13.707 ± 0.001 hours, amplitude 0.14 ± 0.01 magnitudes (Fig. 6). A period near 6.85563 hours is definitively ruled out. With revised interpretations, all previously reported periods are consistent with a rotation period very near 13.712 hours.

Number	Name	yyyy/mm/dd	Phase	LPAB	BPAB	Period(h)	P.E	Amp	A.E.
903	Nealley	2023/07/17-2023/08/27	14.2 - 1.6	338	1	29.063	0.006	0.06	0.01
1051	Merope	2023/07/26-2023/09/08	15.3 - 4.0	343	11	13.712	0.001	0.17	0.01
1187	Afra	2023/08/19-2023/09/09	14.3 - 10.6	352	5	14.071	0.001	0.68	0.05

Table I. Observing circumstances and results. The phase angle is given for the first and last date, where in all cases minimum phase angle was reached on the last date. LPAB and BPAB are the approximate phase angle bisector longitude and latitude at mid-date range (see Harris et al., 1984).

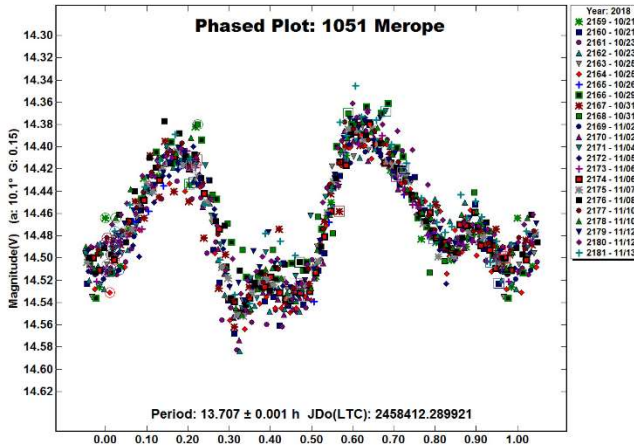


Figure 6. The lightcurve of 1051 Merope from year 2018 data (Pál et al., 2020) phased to 13.707 hours.

1187 Afra. The only previously published lightcurves are by three independent studies all made near the 2006 October favorable opposition: Behrend (2006web), 14.0701 h; Clark (2019), 14.645 h; and Menke et al. (2008), 14.09 h. New observations on 5 nights 2023 Aug. 19 - Sept. 9 provide a good fit to a lightcurve with period 14.071 ± 0.001 hours, maximum amplitude 0.68 ± 0.05 magnitudes (Fig. 7). This period is consistent with Behrend (2006web) and with Menke et al. (2008), and differs significantly from Clark (2019).

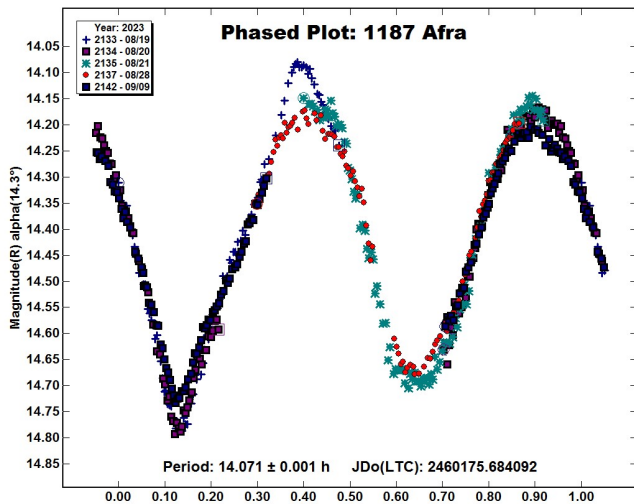


Figure 7. The lightcurve of 1187 Afra from year 2023 data (this study) phased to 14.071 hours.

References

- Asteroid Lightcurve Data Exchange Format website.
https://alcdex.org/php/alcdex_credits.html
- Behrend, R. (2006web, 2020web). Observatoire de Geneve web site. http://obswww.unige.ch/~behrend/page_cou.html
- Carbo, L.; Green, D.; Kragh, K.; Krotz, J.; Meiers, A.; Patino, B.; Pligge, Z.; Shaffer, N.; Ditteon, R. (2009). "Asteroid lightcurve analysis at the Oakley Southern Sky Observatory: 2008 October thru 2009 March." *Minor Planet Bull.* **36**, 152-157.
- Clark, M. (2019). "Asteroid photometry from the Preston Gott Observatory." *Minor Planet Bull.* **46**, 346-349.
- Dose, E.V. (2022). "Lightcurves of several asteroids." *Minor Planet Bull.* **49**, 44-47.
- Dose, E.V. (2023). "Lightcurves of nineteen asteroids." *Minor Planet Bull.* **50**, 65-73.
- Harris, A.W.; Young, J. W.; Scaltriti, F.; Zappala, V. (1984). "Lightcurves and phase relations of the asteroids 82 Alkmene and 444 Gyptis." *Icarus* **57**, 251-258.
- Menke, J.; Cooney, W.; Gross, J.; Terrell, D.; Higgins, D. (2008). "Asteroid lightcurve analysis at Menke Observatory." *Minor Planet Bulletin* **35**, 155-160.
- Pál, A.; Szakáts, R.; Kiss, C.; Bódi, A.; Bognár, Z.; Kalup, C.; Kiss, L.L.; Marton, G.; Molnár, L.; Plachy, E.; Sárneczky, K.; Szabó, G. M.; Szabó, R. (2020). "Solar System Objects Observed with TESS - First Data Release: Bright Main-belt and Trojan Asteroids from the Southern Survey." *Ap. J.* **247**, A26.
- Warner, B.D. (2004). "Lightcurve analysis for numbered asteroids 863, 903, 907, 928, 977, 1386, 2841, and 75747." *Minor Planet Bull.* **31**, 81-85.
- Warner, B.D.; Harris, A.W.; Pravec, P. (2009). "The Asteroid Lightcurve Database." *Icarus* **202**, 134-146. Updated 2023 April. <http://www.minorplanet.info/lightcurvedatabase.html>
- Warner, B.D. (2012). "Asteroid lightcurve analysis at the Palmer Divide Observatory: 2011 June - Sept." *Minor Planet Bull.* **39**, 16-21.
- Waszczak, A.; Chang, C.-K.; Ofek, E.O.; Laher, R.; Masci, F.; Levitan, D.; Surace, J.; Cheng, Y.-C.; Ip, W.-H.; Kinoshita, D.; Helou, G.; Prince, T.A.; Kulkarni, S. (2015). "Asteroid Light Curves from the Palomar Transient Factory Survey: Rotation Periods and Phase Functions from Sparse Photometry." *Astron. J.* **150**, 75.

**ASTEROID LIGHTCURVE ANALYSIS
AT THE CENTER FOR SOLAR SYSTEM STUDIES
PALMER DIVIDE STATION:
2023 JULY-OCTOBER**

Brian D. Warner
Center for Solar System Studies (CS3)
446 Sycamore Ave.
Eaton, CO 80615 USA
brian@MinPlanObs.org

(Received: 2023 October 12)

CCD photometric observations of 22 asteroids were made at the Center for Solar System Studies Palmer Divide Station during 2023 July to October. Data analysis found four likely binary asteroids: 7187 Isobe, 20037 Duke, 21149 Kenmitchell, and (53453) 1999 XX135. A review of data from 2018 for 17405 McAdams found a period somewhat near half that found using 2023 data. As standalone solutions, both would seem to be valid.

CCD photometric observations of 22 asteroids were carried out at the Center for Solar System Studies Palmer Divide Station (CS3-PDS) during 2023 July to October as part of an ongoing general study of asteroid rotation periods with a concentration on near-Earth, Hungaria, and Hilda group/family asteroids.

Telescope	Camera
0.30-m f/6.3 SCT	SBIG STL-1001E
0.35-m f/9.1 SCT (x3)	FLI Microline 1001E
0.50-m f/8.1 Ritchey-Chrétien	FLI Proline 1001E

Table I. List of available telescopes and CCD cameras at CS3-PDS. The exact combination for each telescope/camera pair can vary due to maintenance or specific needs.

Table I lists the three telescope/CCD cameras pairs used at CS3-PDS. All the cameras use CCD chips from the KAF 1001 blue-enhanced family and so have essentially the same response. The pixel scales ranged from 1.24-1.60 arcsec/pixel. All lightcurve observations were made with no or a clear filter. The exposures varied depending on the asteroid's brightness.

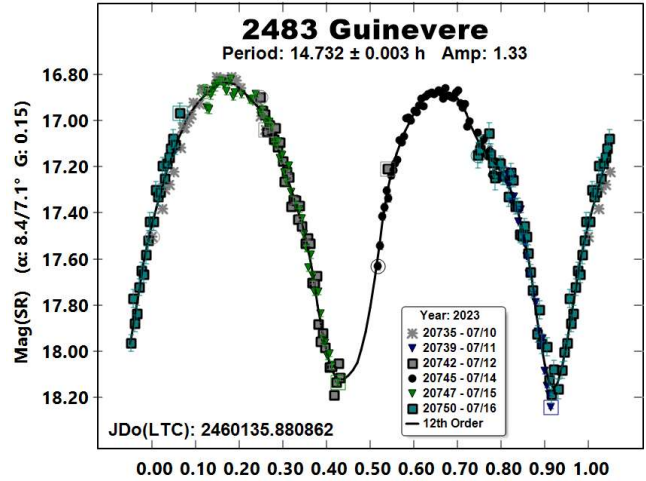
To reduce the number of times and amounts of adjusting nightly zero-points, the ATLAS catalog r' (SR) magnitudes (Tonry et al., 2018) are used. Those adjustments are usually $\leq \pm 0.03$ mag. The rare larger corrections may have been related in part to using unfiltered observations, poor centroiding of the reference stars, and not correcting for second-order extinction. Another cause may be selecting what appears to be a single star but is actually an unresolved pair.

The Y-axis values are ATLAS SR "sky" (catalog) magnitudes. The values in the parentheses give the phase angle(s), a , along with the value of G used to normalize the data to the comparison stars and asteroid phase angle used in the earliest session. This, in effect, adjusts all the observations so that they seem to have been made at a single fixed date/time and phase angle. Presumably, any remaining variations are due only to the asteroid's rotation and/or albedo changes.

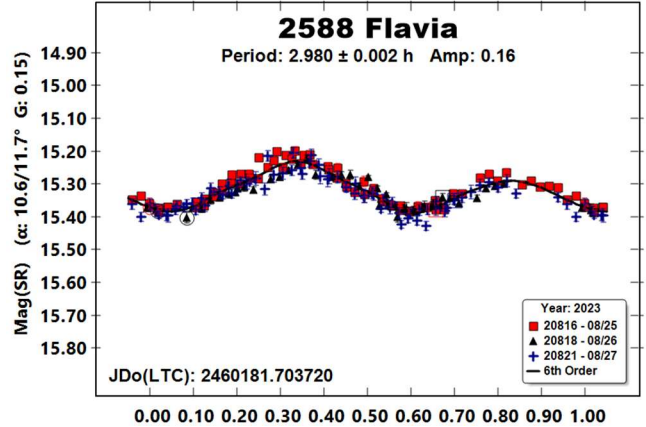
There can be up to three phase angles. If two, the values are for the first and last night of observations. If three, the middle value is the extrema (maximum or minimum) reached between the first and last observing runs. The X-axis shows rotational phase from -0.05 to 1.05. If the plot includes the amplitude, e.g., "Amp: 0.65," this is the amplitude of the Fourier model curve and *not necessarily the adopted amplitude for the lightcurve*.

For brevity, only some of the previous results are referenced. A more complete listing is in the asteroid lightcurve database (Warner et al, 2009; "LCDB" from here on).

2483 Guinevere. There are numerous solutions near 14.73 h in the LCDB for this member of the Hungaria group, i.e., not part of the collisional family (Nesvorný, 2015; Nesvorný et al., 2015). This was the third apparition observed by the author, the others being Warner et al. (2017b) and Warner et al. (2018).

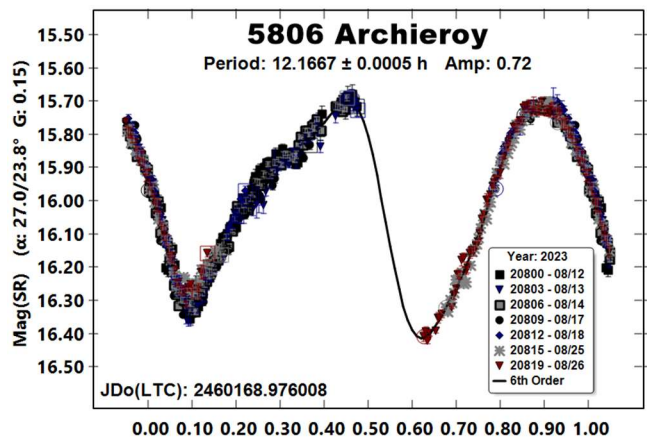
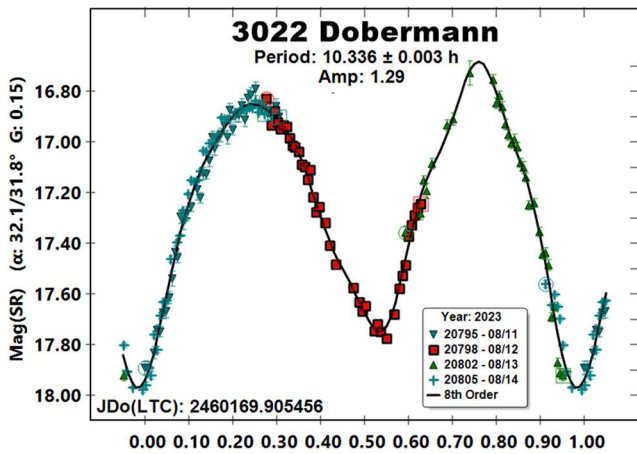


2588 Flavia. There were no previously reported rotation periods in the LCDB. The asteroid was observed on behalf of Vladimir Benishek, who will publish information in greater detail in the near future.

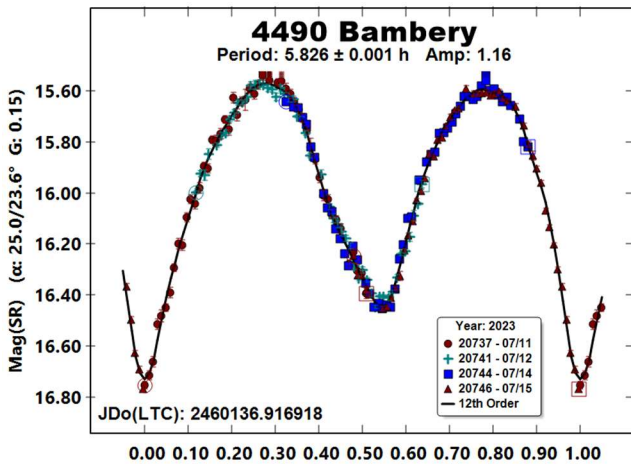


3022 Dobermann. The 2023 observations were at the seventh apparition made by the author since 2004. In every case, the period was found close to 10.33 h.

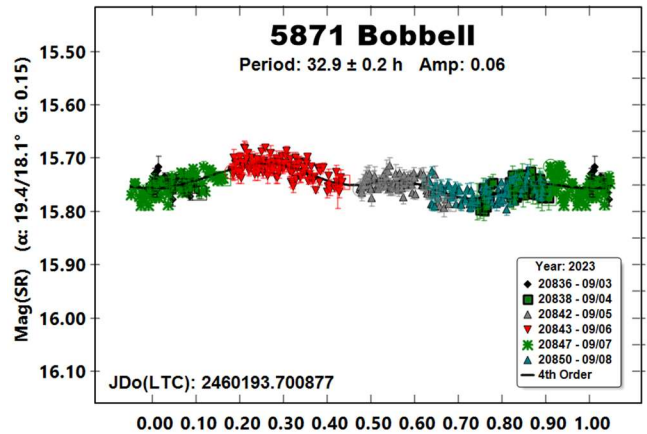
Based on observations from 2004 through 2014, which included 20 dense lightcurves and 170 sparse data points from the Catalina Sky Survey (CSS), a preliminary pole solution was found. The preferred solution is $(\lambda, \beta, P) = (275^\circ, -54^\circ, 10.331693 \text{ h})$. The alternate solution is $(\lambda, \beta, P) = (329^\circ, -71^\circ, 10.331690 \text{ h})$. Given the significant southerly latitude, it's good to assume that the asteroid has a retrograde rotation. An improved model that includes observations from 2017, 2021, and 2023 will be found. The existing model is available at <https://minorplanetobserver.com/Hungarias/>.



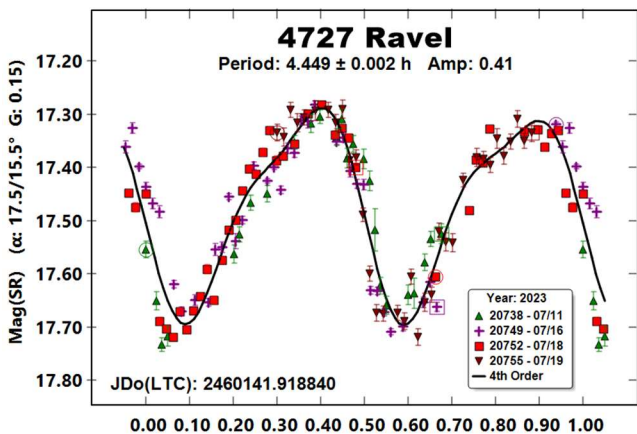
4490 Bambery. The results by the author for seven previous apparitions all had a period of about 5.82 h. A preliminary pole model based on 15 dense lightcurve and 115 sparse data from CSS covering 2006–2014, gives $(\lambda, \beta, P) = (57^\circ, 56^\circ, 5.82345 \text{ h})$. Hanuš et al. (2016) found $(\lambda, \beta, P) = (53^\circ, 59^\circ, 5.82345 \text{ h})$.



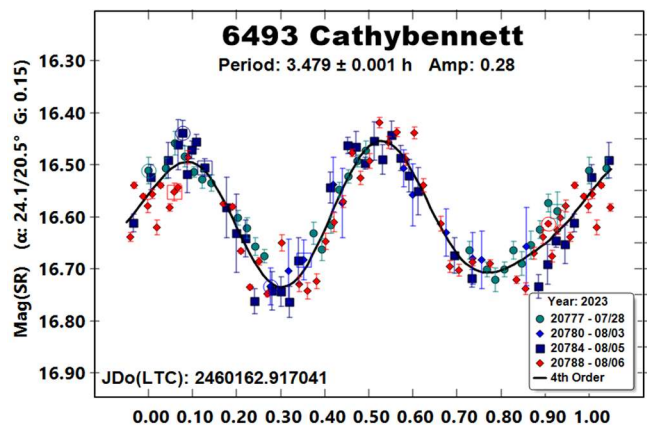
5871 Bobbell. The true period for this Hungaria group member is uncertain, i.e., Warner (2009, 30.21 h) and Warner (2014, 29.3 h). The amplitude at those apparitions exceeded 0.25 mag. The $A = 0.06$ mag in 2023 suggests that the view was nearly pole-on.



4727 Ravel. There were only two reported periods in the LCDB: Ergashev et al. (2014, 4.44 h) and Erasmus et al. (2020, 4.448 h). According to Nesvorný (2015), Ravel is a member of the Koronis collisional family.

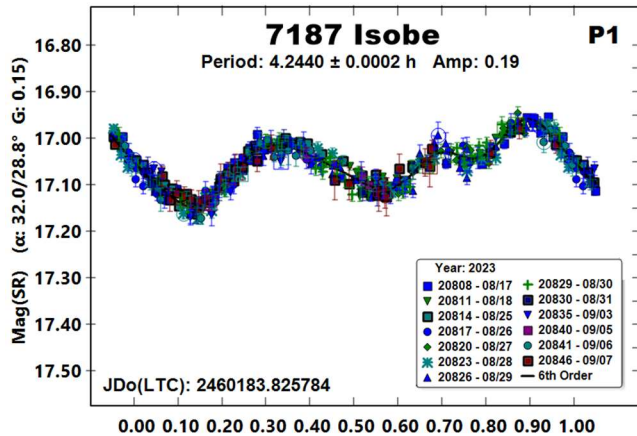
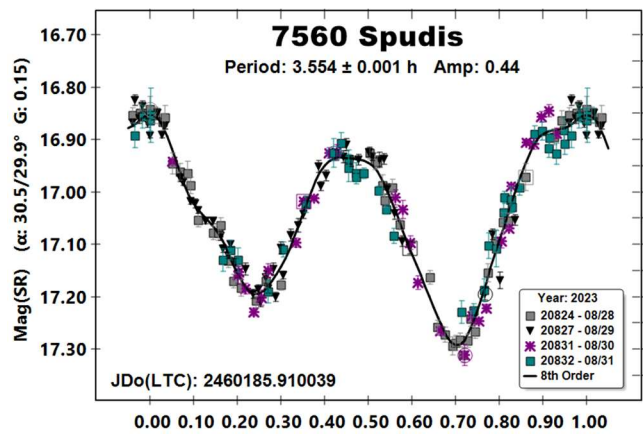
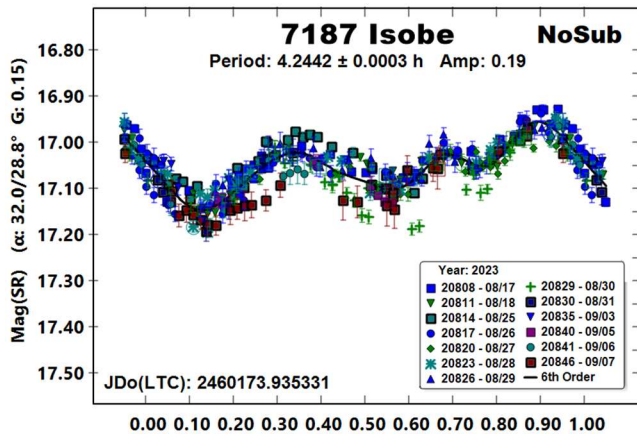


6493 Cathybennett. Analysis of data obtained by the author from four previous apparitions gave a period near 3.47 h. The period derived from 2023 data is consistent with those earlier results.

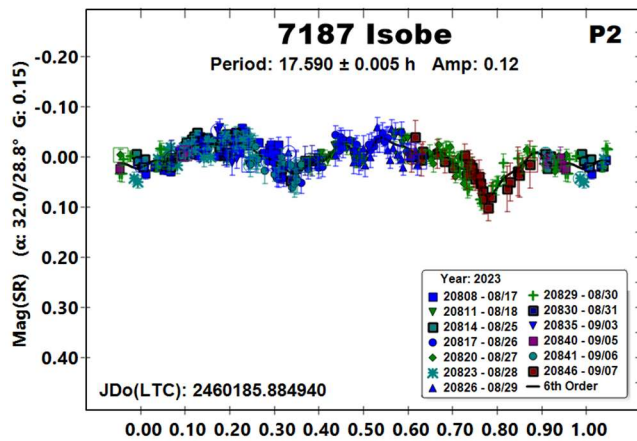
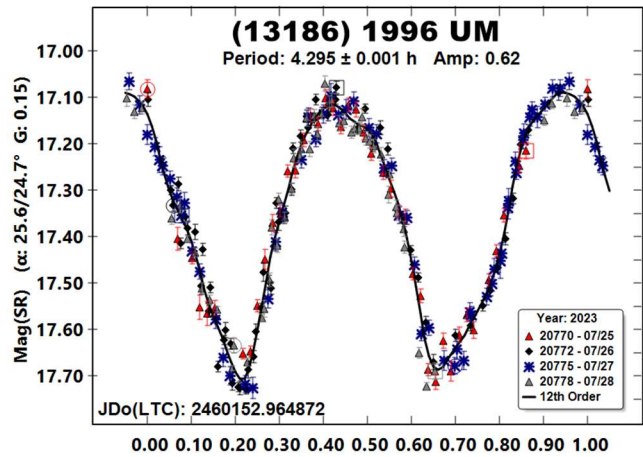


5806 Archieroy. Behrend (2020web) found a period of 12.144 h. This is in good agreement with the 2023 result of 12.1667 h and three previous results reported by the author.

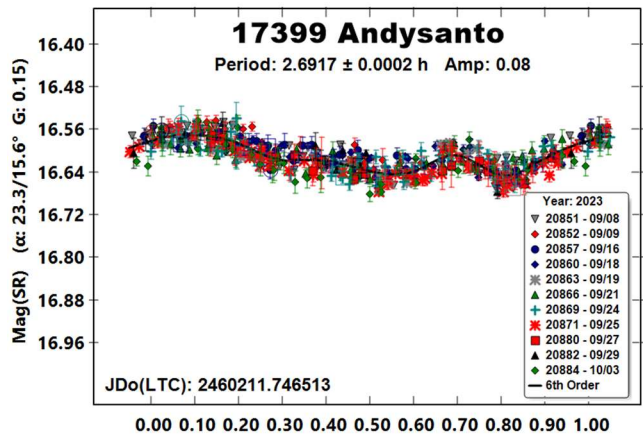
7187 Isobe. This is a Hungaria group member and very likely a binary asteroid. Data from 2004 and 2007 (Warner, 2013b) made a stronger argument over those from 2011 and 2012 (Warner, 2013b). The initial analysis for those four apparitions led to an orbital period of about 33.6 h. However, the 2023 data said otherwise: $P_{ORB} = 17.589 \text{ h}$, which is not close to the half-period from before.



(13186) 1996 UM. Several previous results in the LCDB are all near 4.30 h. This is the third largest amplitude for the asteroid, suggesting a near equatorial view. The smallest amplitude (0.34 mag; Stephens, 2017) was at $L_{PAB} = 221^\circ$, suggesting that the spin axis pole longitude is near that or the diametric opposite of 41° .



17399 Andysanto. A period of 2.692 h (Stephens, 2016) was the only previous result in the LCDB. His and the 2023 observations were at nearly the same L_{PAB} , so the low amplitude was expected.

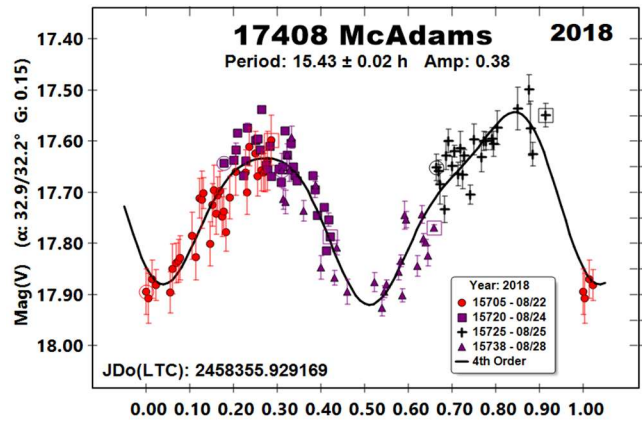
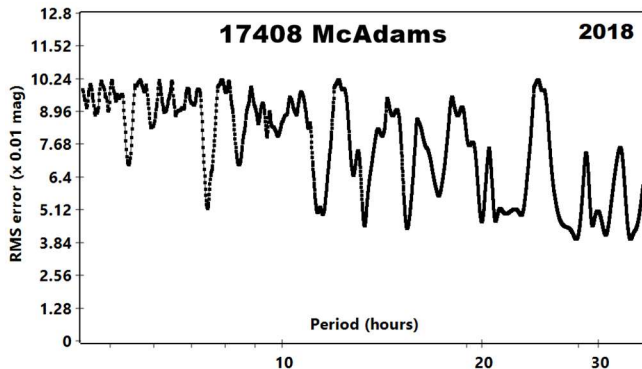
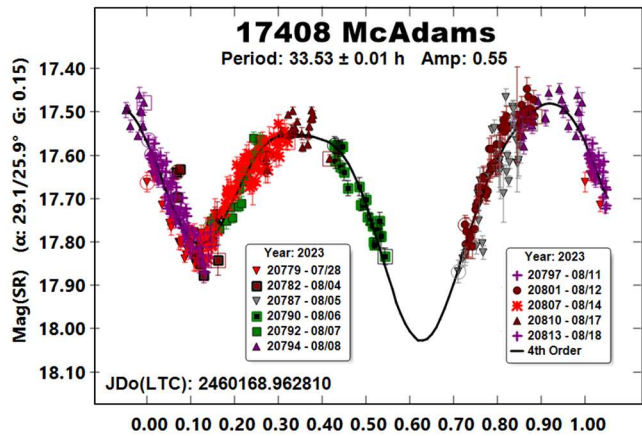
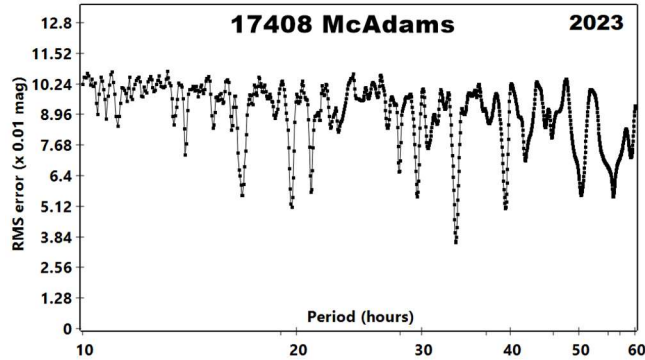


The quality of the four previous data sets leaves much to be desired, which made it difficult to see if they could be forced to match the 2023 orbital period. Only those from 2017 provided something above an improbable lightcurve with a period of 15.91 h. This asteroid should be carefully observed at future apparitions.

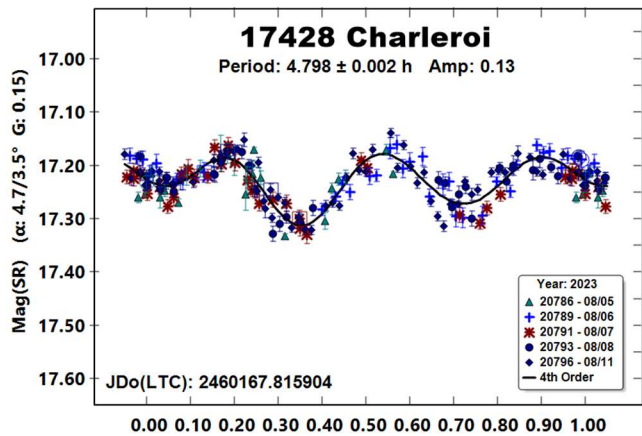
7560 Spudis. Many times, an asteroid has been said to resemble a spinning potato, with “spud” being a slang term for the vegetable. However, in this case the name is of a much more distinguished nature, that of Paul Spudis, an American geologist and lunar scientist. In addition to the asteroid, a crater on the Moon bears his name.

The rotation period was first said to be 5.402 h (Warner, 2005). However, that was revised to 3.544 h (Warner, 2013c). Other results obtained by the author are all in close agreement with the shorter period.

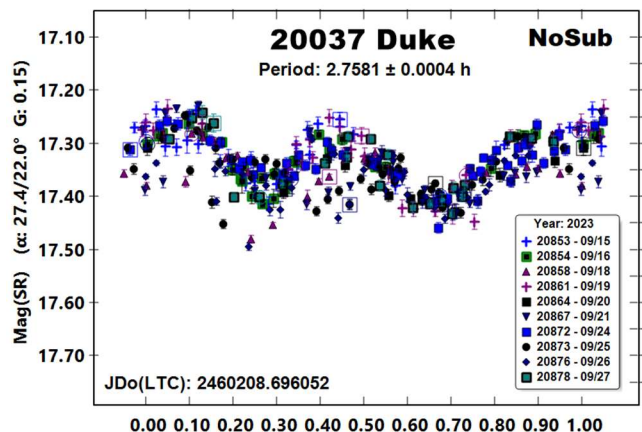
17408 McAdams. To paraphrase an old saying, “A person with one good asteroid lightcurve knows the rotation period. A person with two good lightcurves can’t be sure.” The 2023 data led to a period of 33.53 h. While the lightcurve is incomplete, the shape and amplitude of existing data and implied amplitude of the complete curve strongly favor the 33.53 h period being correct (Harris et al., 2014). However, the same argument can be made for a period nearly half as long: 15.43 h (Warner, 2019). Observations during future apparitions that involve observers at significantly different longitudes are recommended.

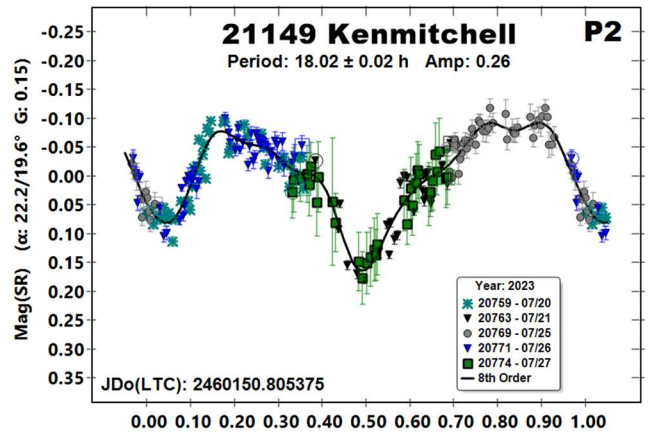
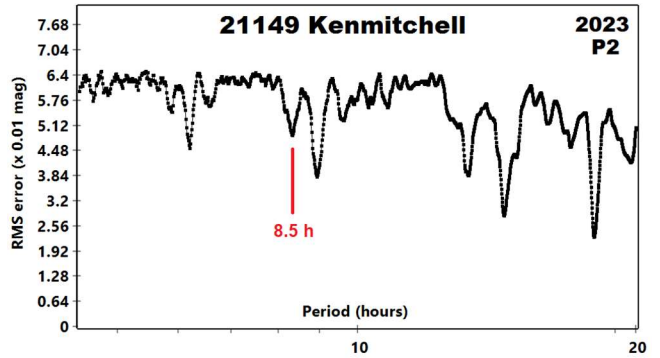
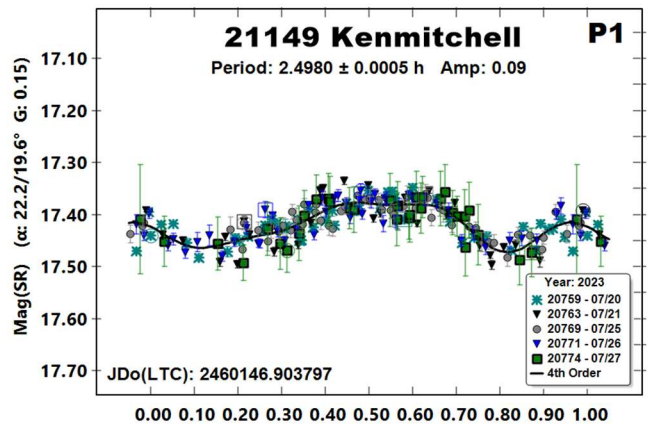
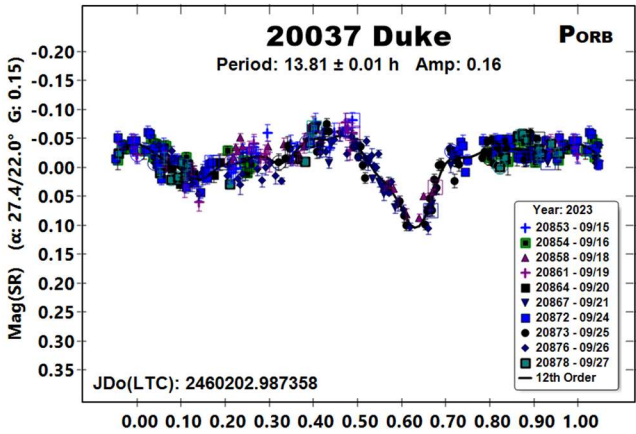
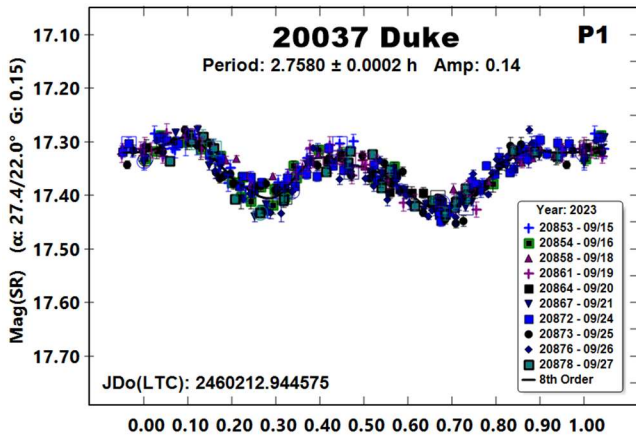


17428 Charleroi. Previous results by the author include 5.990 h (Warner et al., 2017a), 6.034 h (Warner et al., 2018), and 5.335 h (Stephens and Warner, 2020). The 2023 data led to yet another result, $P = 4.798$ h. In each case, the amplitude was small enough to allow for other than bimodal solutions, which can confuse matters even more.



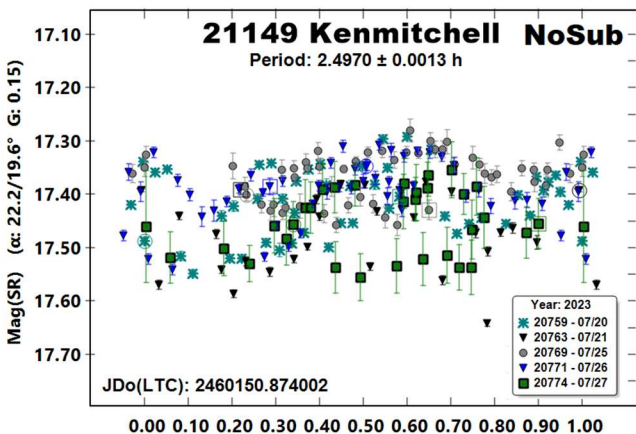
20037 Duke. A member of the Hungaria group, this asteroid has been observed several times before, e.g., Stephens and Warner (2020), who reported new and revised periods of 13.935 h (2020), 13.078 h (2010), and 13.078 (2015, rated U = 1). It now appears that a satellite was producing the 13-hour solution and the rotation of the primary had gone unnoticed or signs of it dismissed. The 2023 data clearly show the expected primary lightcurve with $P = 2.7581$ h (“NoSub”).





The dual-period search utility of *MPO Canopus* was used to separate the periods of primary rotation and the (apparent) orbital period of the satellite (“PORB”, $P_{ORB} = 13.81$ h), which is close to the previous single-period results. Based on the putative mutual evens of 0.04-0.10 mag, the secondary-to-primary ratio of the effective diameters is $D_s/D_p \geq 0.19 \pm 0.02$.

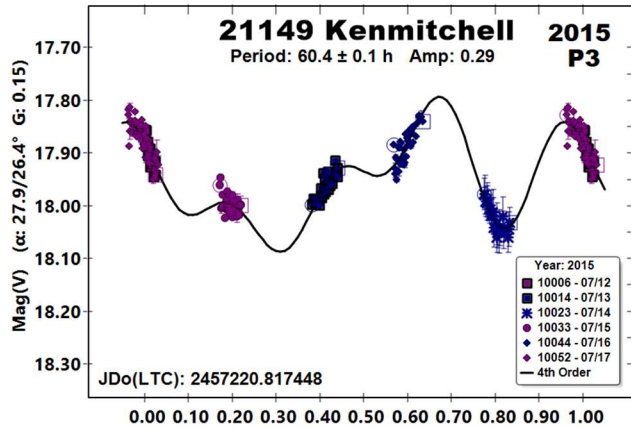
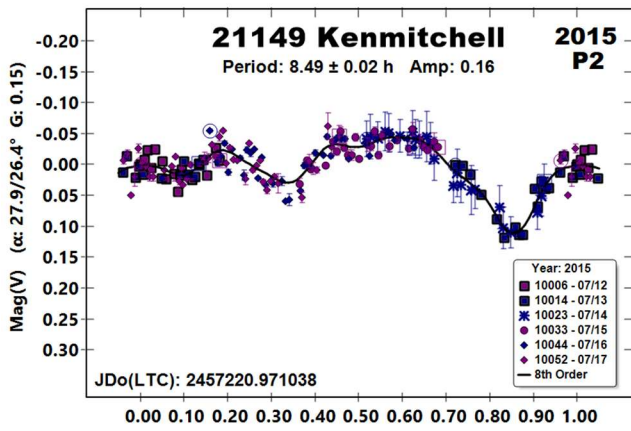
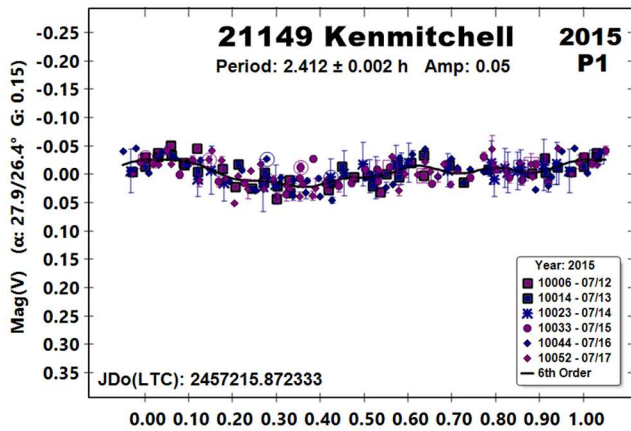
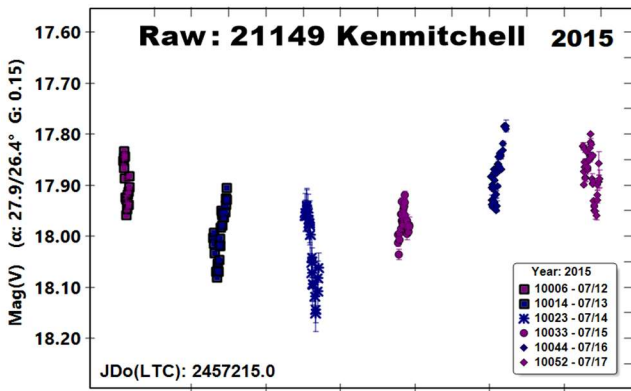
21149 Kenmitchell. First observed by the author in 2015 (Warner, 2016), a period of 7.22 h was found. The 2023 data did not support that result. Instead, it appears that the asteroid is binary with a primary rotation period of 2.4980 h and the orbital period of a significantly elongated satellite to be 18.02 h with mutual events of 0.08-0.14 mag ($D_s/D_p \geq 0.28 \pm 0.02$). This led to a re-examination of the data from the 2015 apparition and created a difficult conundrum.



An unexpected long period of about 60 h seemed to be superimposed on any primary and/or satellite periods. Once removed (“P3”), the search for the primary and satellites began.

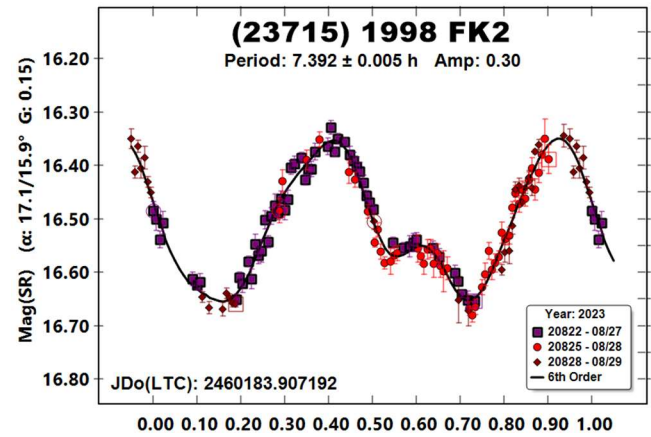
The first part of the puzzle is the significant difference in the primary periods: $PI_{2023} = 2.4980$ h and $PI_{2015} = 2.412$ h. The sparser data set of 2015, its higher noise, and the low amplitude may account for a good deal of the difference.

The second part of the puzzle is not so easily explained. In 2023, the amplitude of 0.26 mag for the secondary lightcurve virtually assures that it should be bimodal and so the period of 18.02 h. On the other hand, the lightcurve for 2015 ($P_{ORB} = 8.49$ h) is very reminiscent of that for an elongated satellite locked to its orbital period with mutual events (occultations/eclipses). There is little reason to suspect that the lightcurve should be other than bimodal. Those events lead to $(D_s/D_p \geq 0.29 \pm 0.02)$, which is in good agreement with the 2023 result.

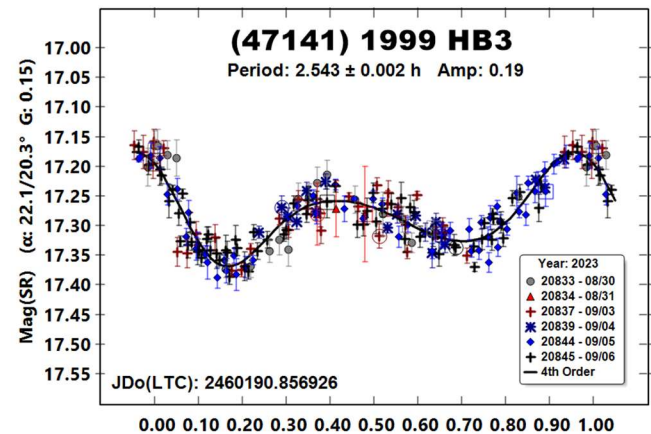


The period spectrum in 2023 for the secondary period shows a weak solution at 8.5 h, which makes sense since the two periods are close to a 2:1 ratio (17/8). While the differences in lightcurve shape and amplitude might be the result of different viewing aspects, the radically different orbital periods, and the superimposed long period will need to be resolved with future observations.

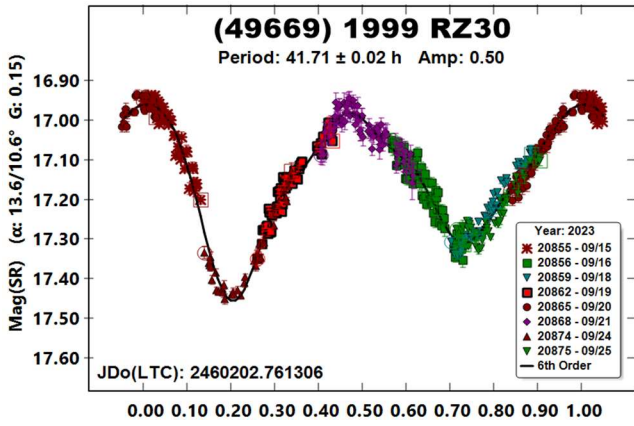
(23715) 1998 FK2. This member of the Hungaria collisional family (Nesvorny, 2015; Nesvorny et al., 2015) was first observed by the author in 2012 (Warner, 2013a, 7.436 h). Stephens (2016) found 7.434 h based on observations in 2015. The data led to a slightly shorter period of 7.392 h, which is outside the stated errors but not enough to affect rotation period statistics.



(47141) 1999 HB3. While the period might cause speculation about the asteroid being a binary, no signs of a satellite were found, unlike observations in 2015 (Warner, 2016), which hinted at one with an orbital period of 10.56 h. The difference in L_{PAB} angles (308° vs. 353°) is sufficient to offer an explanation for the difference.



(49669) 1999 RZ30. Here is another case where having more than one lightcurve can make a period solution uncertain.

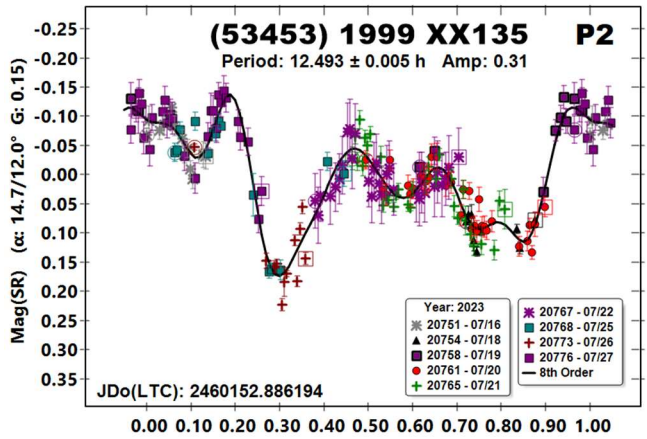
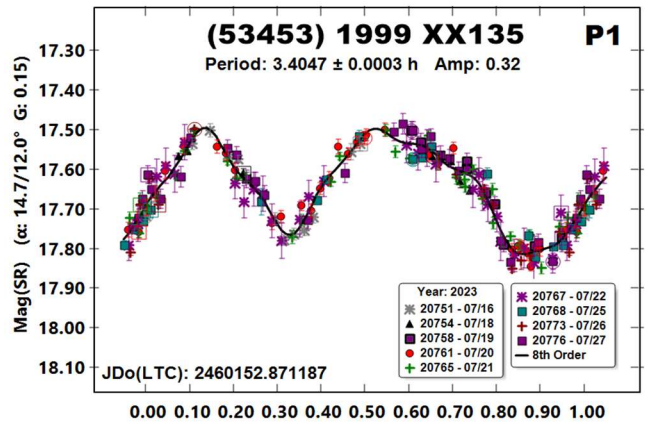
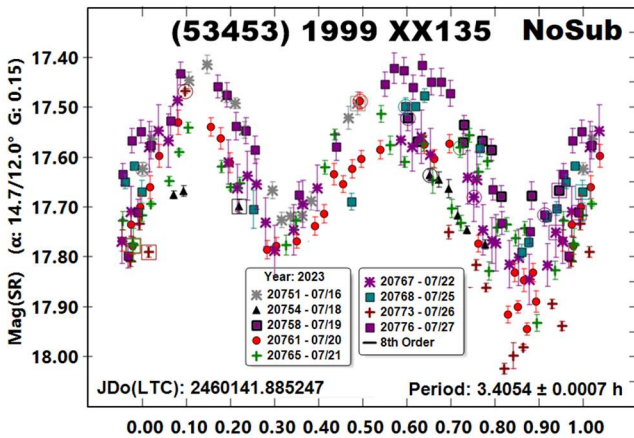


Observations in 2022 (Warner and Stephens, 2022) show a long period of $P \sim 50.6$ h, $A = 0.36$ mag. Superimposed on that was a weak period of $P_2 = 3.136$ h, $A_2 = 0.05$ mag. The main lightcurve had significant gaps and so both periods remained uncertain, especially the shorter one.

New observations 18 months later (2023 September) led to a dominant period of $P = 41.71$ h. A very weak secondary signal was found at $P_2 = 3.140$ h, but there were numerous others in the range of 2 to 5 hours. A dual-period search was also tried by keeping the two possible periods in the range of 40-60 h. P_2 always gave a noisy, nearly flat-line plot.

Due to the diameter and period, tumbling cannot be fully discounted (Pravec et al., 2005; 2014) but given the lack of a viable secondary signal, this seems more unlikely than not.

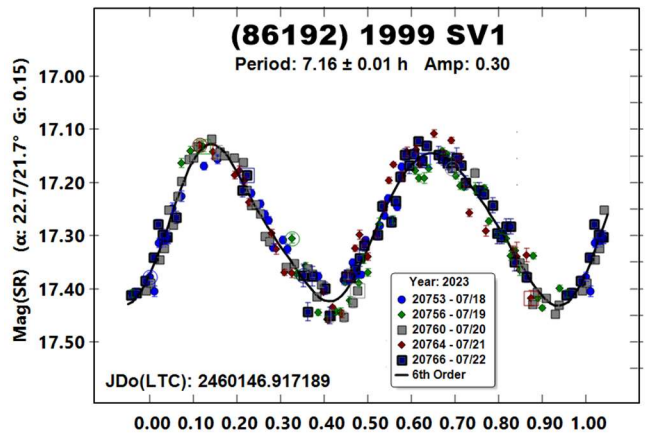
(53453) 1999 XX135. Stephens (2016) found a single period solution of 3.407 h using data from 2015 ($L_{PAB} \sim 344^\circ$). The data from 2023 clearly show that a single period solution would not work (“NoSub”). The *MPO Canopus* dual-period search found one period essentially identical to that from Stephens (2016), $P = 3.4047$ h.



The secondary period lightcurve is more than somewhat unusual. It seems to reveal a satellite with an orbital period of 12.493 h. What seem to be mutual events of 0.13-0.22 mag led to $D_s/D_p \geq 0.36 \pm 0.03$. If the shallower event (0.8 rotation phase) is to be taken as a total eclipse, then the diameter ratio is the actual value, not a minimum.

Given the unusual solution, the asteroid (a Hungaria collisional member) is a “likely binary”, i.e., not firmly confirmed, and should be carefully observed at future apparitions.

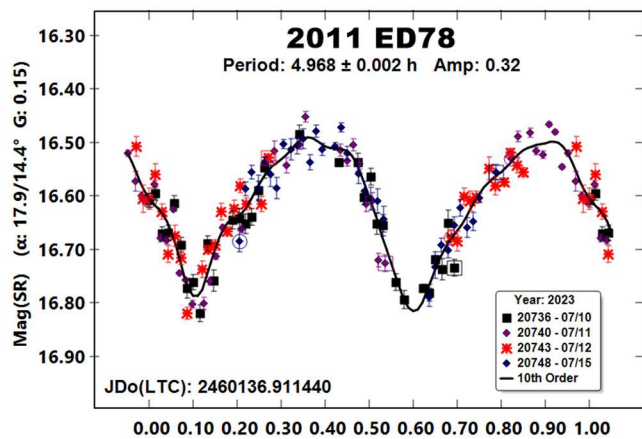
(86192) 1999 SV1. This is the fourth set of results by the author for 1999 SV, which is a member of the Hungaria collisional family (Nesvorny, 2015). All results have a period of about 7.16 h and an amplitude range of 0.23-0.30 mag.



Number	Name	2023/mm/dd	Phase	L _{PAB}	B _{PAB}	Period(h)	P.E.	Amp	A.E.	Grp Ds/Dp
2483	Guinevere	07/10-07/16	8.4, 7.1	320	5	14.732	0.003	1.33	0.05	HIL
2588	Flavia	08/25-08/27	10.7, 11.8	316	3	2.98	0.002	0.16	0.01	MB-I
3022	Dobermann	08/11-08/12	32.1, 32.0	17	0	10.336	0.003	1.39	0.03	H
4490	Bambery	07/11-07/15	25.0, 23.6	329	-1	5.826	0.001	1.16	0.03	H
4727	Ravel	07/11-07/19	17.5, 15.5	333	-1	4.449	0.002	0.41	0.03	KOR
5806	Archieroy	08/12-08/26	26.9, 23.8	2	23	12.1667	0.0005	0.72	0.03	H
5871	Bobbell	09/03-09/06	19.3, 18.5	359	18	32.9	0.2	0.06	0.01	H
6493	Cathybennett	07/28-08/06	24.1, 20.5	341	-6	3.479	0.001	0.28	0.02	H
7187	Isobe	08/18-09/06	31.9, 29.0	19	23	^B 4.244 17.590	0.0002 0.005	0.19 0.12	0.02 0.01	H 0.19
7560	Spudis	08/28-08/30	30.5, 30.1	17	23	3.554	0.001	0.44	0.03	H
13186	1996 UM	07/25-07/28	25.5, 24.7	336	23	4.295	0.001	0.62	0.03	H
17399	Andysanto	09/08-10/03	23.2, 15.6	15	15	2.6917	0.0002	0.08	0.01	H
17408	McAdams	07/28-08/18 ²⁰¹⁸ 08/22-08/28	29.1, 25.9 32.9, 32.3	350 27	32 19	33.53 15.43	0.01 0.02	0.5 0.38	0.1 0.03	H
17428	Charleroi	08/05-08/11	4.7, 3.4	326	9	4.793	0.004	0.13	0.02	HIL
20037	Duke	09/15-09/27	*27.3, 21.9	38	18	^B 2.758 13.81	0.0002 0.01	0.14 0.16	0.01 0.01	H 0.19
21149	Kenmitchell	07/20-07/27 ²⁰¹⁵ 07/12-07/17	22.2, 19.6 28.0, 26.5	322 332	22 18	^B 2.498 18.02 ^B 2.412 8.49 60.4	0.0005 0.02 0.002 0.02 0.1	0.09 0.26 0.05 0.16 0.29	0.01 0.01 0.01 0.01 0.03	H 0.24 0.16
23715	1998 FK2	08/27-08/29	17.1, 15.9	354	10	7.392	0.005	0.3	0.03	H
47141	1999 HB3	08/30-09/06	22.0, 20.3	353	27	2.543	0.002	0.19	0.02	H
49669	1999 RZ30	09/15-09/25	13.5, 10.5	8	14	41.71	0.02	0.5	0.04	H
53453	1999 XX135	07/16-07/27	14.7, 12.0	311	16	3.4047 12.493	0.0003 0.005	0.32 0.31	0.03 0.03	H 0.47
86192	1999 SV1	07/18-07/22	*22.7, 21.6	301	16	7.15	0.01	0.3	0.03	H
	2011 ED78	07/10-07/15	18.0, 14.5	301	6	4.968	0.002	0.32	0.03	NEA

Table II. Observing circumstances and results. ^BPeriod of primary with one or more confirmed or suspected satellites. If a confirmed or suspected binary with mutual events, the second line gives the secondary (or orbital) period and the effective diameter ratio (*D_s/D_p*). The phase angle is given for the first and last date. If preceded by an asterisk, the phase angle reached an extremum during the period. L_{PAB} and B_{PAB} are the approximate phase angle bisector longitude/latitude at mid-date range (see Harris et al., 1984).

2011 ED78. The rotation period from the 2023 observations is very close to the only other period in the LCDB, 4.976 h (Warner, 2017).



Acknowledgements

This work includes data from the Asteroid Terrestrial-impact Last Alert System (ATLAS) project. ATLAS is primarily funded to search for near earth asteroids through NASA grants NN12AR55G, 80NSSC18K0284, and 80NSSC18K1575; byproducts of the NEO search include images and catalogs from the survey area. The ATLAS science products have been made possible through the contributions of the University of Hawaii Institute for Astronomy, the Queen's University Belfast, the Space Telescope Science Institute, and the South African Astronomical Observatory.

The author gratefully acknowledges a Shoemaker NEO Grants from the Planetary Society (2007). This was used to purchase some of the equipment used in this research.

References

- Behrend, R. (2020web) Observatoire de Geneve web site. http://obswww.unige.ch/~behrend/page_cou.html.
- Erasmus, N.; Navarro-Meza, S.; McNeill, A.; Trilling, D.E.; Sickafoose, A.A.; Denneau, L.; Flewelling, H.; Heinze, A.; Tonry, J.L. (2020). "Investigating Taxonomic Diversity within Asteroid Families through ATLAS Dual-band Photometry." *Ap. J. Suppl. Ser.* **247**, A13.
- Ergashev, K.E.; Ehgamberdiev, Sh.A.; Burkhonov, O.A.; Yoshida, F. (2014). "Rotation Period of Asteroid 4727 Ravel." *Minor Planet Bull.* **41**, 79.
- Hanuš, J.; Ďurech, J.; Oszkiewicz, D.A.; Behrend, R.; Carry, B.; Delbo, M.; Adam, O.; Afonina, V.; Anquetin, R.; Antonini, P. and 159 colleagues. (2016). "New and updated convex shape models of asteroids based on optical data from a large collaboration network." *Astron. Astrophys.* **586**, A108.
- Harris, A.W.; Young, J.W.; Scaltriti, F.; Zappala, V. (1984). "Lightcurves and phase relations of the asteroids 82 Alkeme and 444 Gypsis." *Icarus* **57**, 251-258.
- Harris, A.W.; Pravec, P.; Galad, A.; Skiff, B.A.; Warner, B.D.; Vilagi, J.; Gajdos, S.; Carbognani, A.; Hornoch, K.; Kusnirak, P.; Cooney, W.R.; Gross, J.; Terrell, D.; Higgins, D.; Bowell, E.; Koehn, B.W. (2014). "On the maximum amplitude of harmonics on an asteroid lightcurve." *Icarus* **235**, 55-59.
- Nesvorný, D. (2015). "Nesvorný HCM Asteroids Families V3.0." NASA Planetary Data Systems, id. EAR-A-VARGBET-5-NESVORNYFAM-V3.0.
- Nesvorný, D.; Broz, M.; Carruba, V. (2015). "Identification and Dynamical Properties of Asteroid Families." In *Asteroids IV* (P. Michel, F. DeMeo, W.F. Bottke, R. Binzel, Eds.). Univ. of Arizona Press, Tucson, also available on astro-ph.
- Pravec, P.; Harris, A.W.; Scheirich, P.; Kušnirák, P.; Šarounová, L.; Hergenrother, C.W.; Mottola, S.; Hicks, M.D.; Masi, G.; Krugly, Yu.N.; Shevchenko, V.G.; Nolan, M.C.; Howell, E.S.; Kaasalainen, M.; Galád, A.; Brown, P.; Degraff, D.R.; Lambert, J.V.; Cooney, W.R.; Foglia, S. (2005). "Tumbling asteroids." *Icarus* **173**, 108-131.
- Pravec, P.; Scheirich, P.; Ďurech, J.; Pollock, J.; Kusnirak, P.; Hornoch, K.; Galad, A.; Vokrouhlický, D.; Harris, A.W.; Jehin, E.; Manfroid, J.; Opitom, C.; Gillon, M.; Colas, F.; Oey, J.; Vrástil, J.; Reichart, D.; Ivarsen, K.; Haislip, J.; LaCluyze, A. (2014). "The tumbling state of (99942) Apophis." *Icarus* **233**, 48-60.
- Stephens, R.D. (2016). "Asteroids Observed from CS3: 2015 July - September." *Minor Planet Bull.* **43**, 52-56.
- Stephens R.D. (2017). "Asteroids Observed from CS3: 2017 April - June." *Minor Planet Bull.* **44**, 321-323.
- Stephens, R.D.; Warner, B.D. (2020). "Main-Belt Asteroids Observed from CS3: 2020 April to June." *Minor Planet Bull.* **47**, 275-284.
- Tonry, J.L.; Denneau, L.; Flewelling, H.; Heinze, A.N.; Onken, C.A.; Smartt, S.J.; Stalder, B.; Weiland, H.J.; Wolf, C. (2018). "The ATLAS All-Sky Stellar Reference Catalog." *Astrophys. J.* **867**, A105.
- Warner, B.D. (2005). "Asteroid Lightcurve Analysis at the Palmer Divide Observatory - Fall 2004." *Minor Planet Bull.* **32**, 29-32.
- Warner, B.D. (2009). "Asteroid Lightcurve Analysis at the Palmer Divide Observatory: 2008 September-December." *Minor Planet Bull.* **36**, 70-73.
- Warner, B.D. (2013a). "Asteroid Lightcurve Analysis at the Palmer Divide Observatory: 2012 June - September." *Minor Planet Bull.* **40**, 26-29.
- Warner, B.D. (2013b). "Rounding Up the Unusual Suspects." *Minor Planet Bull.* **40**, 36-42.
- Warner, B.D. (2013c). "Asteroid Lightcurve Analysis at the Palmer Divide Observatory: 2012 September - 2013 January." *Minor Planet Bull.* **40**, 71-80.
- Warner, B.D. (2014). "Asteroid Lightcurve Analysis at CS3-Palmer Divide Station: 2014 January-March." *Minor Planet Bull.* **41**, 144-155.
- Warner, B.D. (2016). "Asteroid Lightcurve Analysis at CS3-Palmer Divide Station: 2015 June-September." *Minor Planet Bull.* **43**, 57-65.
- Warner, B.D. (2017). "Near-Earth Asteroid Lightcurves at CS3-Palmer Divide Station: 2017 April thru June." *Minor Planet Bull.* **44**, 335-344.
- Warner, B.D. (2019). "Asteroid Lightcurve Analysis at CS3-Palmer Divide Station: 2018 July-September." *Minor Planet Bull.* **46**, 46-51.
- Warner, B.D.; Stephens, R.D. (2022). "On Confirmed and Suspected Binary Asteroids Observed at The Center for Solar System Studies: 2022 February and March." *Minor Planet Bull.* **49**, 223-226.
- Warner, B.D.; Harris, A.W.; Pravec, P. (2009). "The Asteroid Lightcurve Database." *Icarus* **202**, 134-146. Updated 2023 Oct. <http://www.minorplanet.info/lightcurvedatabase.html>
- Warner, B.D.; Stephens, R.D.; Coley, D.R. (2017a). "Lightcurve Analysis of Hilda Asteroids at the Center for Solar System Studies: 2016 June-September." *Minor Planet Bull.* **44**, 36-41.
- Warner, B.D.; Stephens, R.D.; Coley, D.R. (2017b). "Lightcurve Analysis of Hilda Asteroids at the Center for Solar System Studies: 2016 September-December." *Minor Planet Bull.* **44**, 130-137.
- Warner, B.D.; Stephens, R.D.; Coley, D.R. (2018). "Lightcurve Analysis of Hilda Asteroids at the Center for Solar System Studies: 2017 September-December." *Minor Planet Bull.* **45**, 147-161.

ASTEROID PHOTOMETRY FROM THE DUNWURKIN OBSERVATORY

Dr. Maurice Clark
Department of Physics and Chemistry
Ball State University
Muncie IN 47304
maurice.clark@bsu.edu

(Received: 2023 August 17)

Asteroid period and amplitude results obtained at the Dunwurkin Observatory in Koorda Western Australia during May and July 2023 are presented.

The May and July asteroid lightcurve results reported here correspond to a time window when the author was able to visit his observatory in Koorda, Western Australia. Located about 250km northeast of the capital, Perth, the main instrument used was a 14" *f*/11 Schmidt-Cassegrain telescope with an *f*/6.3 focal reducer, giving an effective focal length of *f*/7. An SBIG STL-1001E CCD, was used with this telescope. All images were unfiltered and were reduced with dark frames and twilight sky flats. Image analysis was accomplished using differential aperture photometry with *MPO Canopus*. Period analysis was also done in *Canopus*. Differential magnitudes were calculated using reference stars from the UCAC4 catalog.

The results are summarized in the table below, and the lightcurve plots are presented at the end of the paper. The data and lightcurves are presented without additional comment except where circumstances warrant.

3015 Candy. Observations of this asteroid were made on 7 nights as part of an ongoing project to model its shape. In addition, Clark (2016) speculated that the period of 3015 Candy seemed to be increasing slightly. The latest observations show that speculation to be incorrect. The derived rotation period of 4.62456h is in close agreement with that found in previous studies, with no apparent increase in the rotation period.

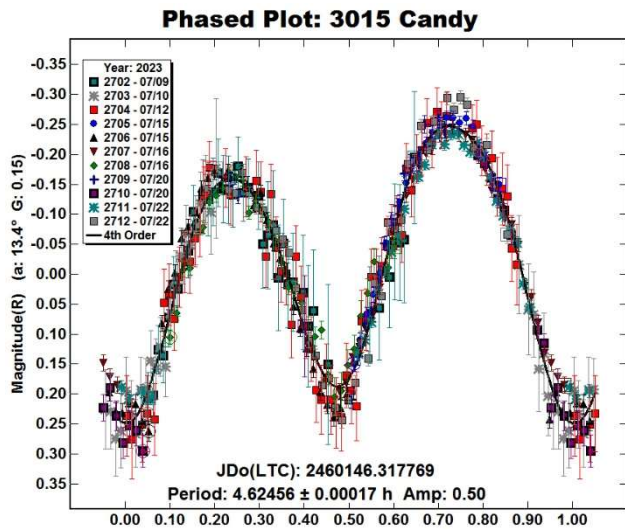


Figure 1: Lightcurve for 3015 Candy.

10423 Dajic. Observations were made over 4 nights. The resulting lightcurve was very asymmetric and is uncertain. A search of the Asteroid Lightcurve Database did not reveal any previously reported period for asteroid 10423 Dajic.

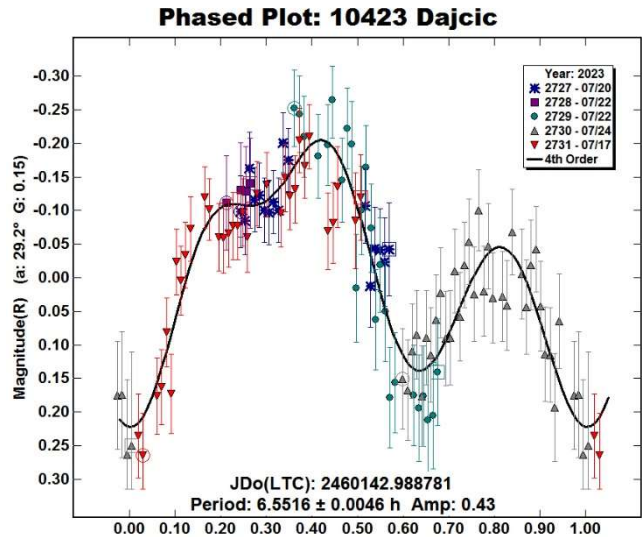


Figure 2: Lightcurve for 10423 Dajic.

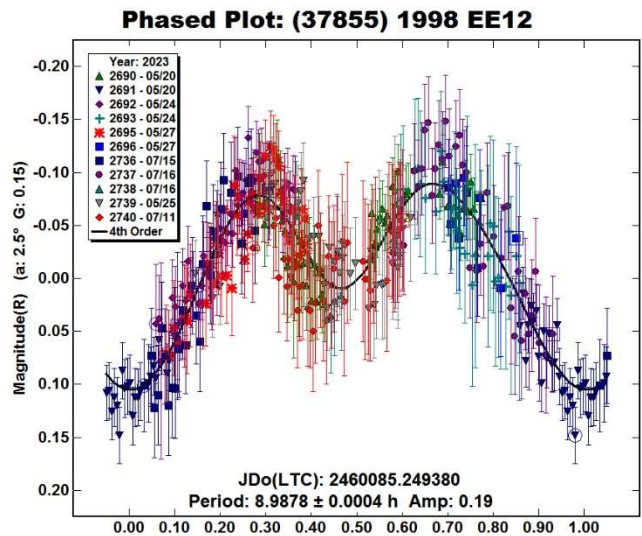


Figure 3: Lightcurve for (37855) 1998 EE12.

(56451) 2000 GN81. The asteroid was observed on one night when it was in the field of another asteroid being studied. Unfortunately, only a portion of the lightcurve was observed and the result published here is probably only half of the true period. A search of the Asteroid Lightcurve Database did not reveal any previously reported period for asteroid (56451) 2000 GN81.

Number	Name	2023 mm/dd	Phase	L _{PAB}	B _{PAB}	Period(h)	P.E.	Amp	A.E.	Grp
3015	Candy	07/09-07/22	12.0	314.1	-21.6	4.62456	0.00017	0.50	0.02	MBA
10423	Dajcic	07/17-07/24	29.1	242.3	-2.2	6.6516	0.0046	0.43	0.05	MBA
37855	1998 EE12	05/20-07/16	18.0	244.0	1.5	8.9878	0.0004	0.19	0.03	MBA
56451	2000 GN81	05/25	1.2	243.8	-2.3	2.74?	0.13	0.53	0.1	MBA
99676	2002 JR12	05/24-05/27	3.1	239.7	3.5	4.576	0.004	1.18	0.1	MBA
100584	1997 JJ14	05/24-05/27	3.6	240.0	3.5	9.2834	0.0082	1.53	0.1	MBA

Table I. Observing circumstances and results. The phase angle is given for the first and last date. L_{PAB} and B_{PAB} are the approximate phase angle bisector longitude and latitude at mid-date range (see Harris et al., 1984). Grp is the asteroid family/group (Warner et al., 2009).

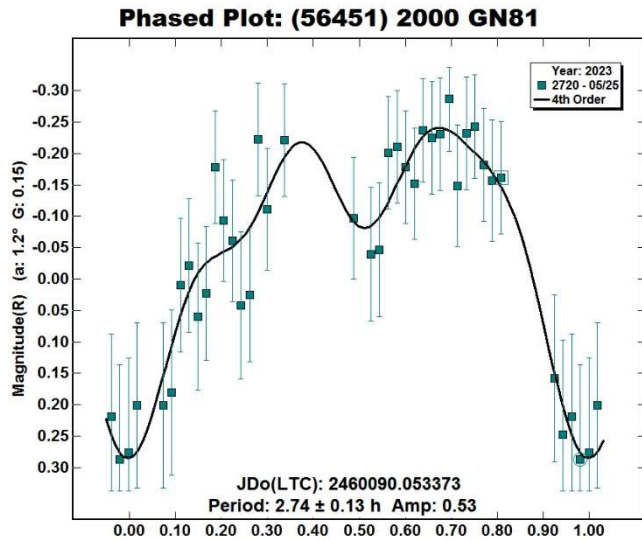


Figure 4: Lightcurve for (56451) 2000 GN81.

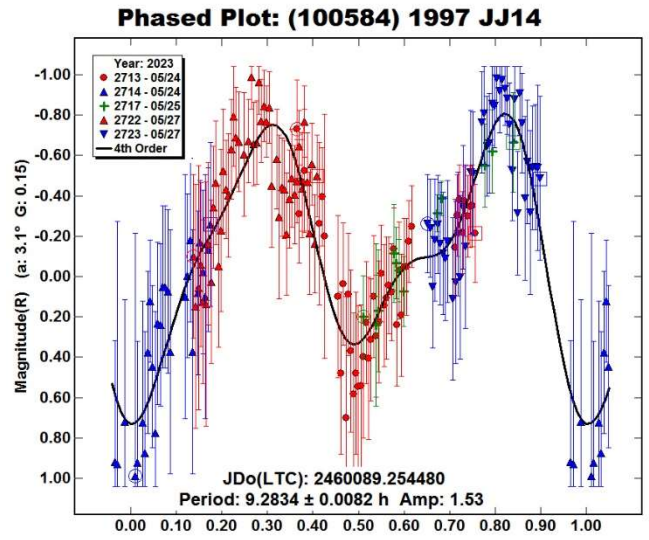


Figure 6: Lightcurve for (100584) 1997 JJ14.

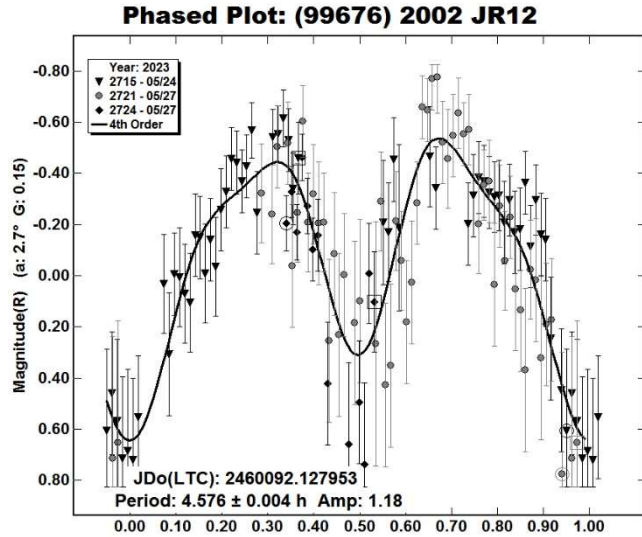


Figure 5: Lightcurve for (99676) 2002 JR12.

Acknowledgments

The author would like to thank Brian Warner for all of his work with the program *MPO Canopus* and for his efforts in maintaining the “CALL” website.

References

Clark, M.L. (2016). “Asteroid Photometry from the Preston Gott Observatory.” *Minor Planet Bull.* **43-1**, 2-5.

Harris, A.W.; Young, J.W.; Scaltriti, F.; Zappala, V. (1984). “Lightcurves and phase relations of asteroids 82 Alkmene and 444 Gytis.” *Icarus* **57**, 251-258.

Warner, B.D.; Harris, A.W.; Pravec, P. (2009). “The Asteroid Lightcurve Database.” *Icarus* **202**, 134-146. Updated 2023 Aug. <http://www.minorplanet.info/lightcurvedatabase.html>

LIGHTCURVE ANALYSIS FOR TWELVE MAIN-BELT AND ONE PHA ASTEROIDS

Gonzalo Fornas, AVA - J57, CAAT
Centro Astronómico del Alto Turia, SPAIN
gon@iicv.es

Fernando Huet, AVA - Z93

Rafael Barberá, AVA - J57, CAAT
Centro Astronómico del Alto Turia, SPAIN

Álvaro Fornas, AVA - J57, CAAT
Centro Astronómico del Alto Turia, SPAIN

Vicente Mas, AVA - J57, CAAT
Centro Astronómico del Alto Turia, SPAIN

(Received: 2023 September 11)

Photometric observations of twelve main-belt asteroids and one PHA were obtained between 2023/1/11 - 2023/7/17. We derived the following rotational synodic periods: 489 Comacina, 9.0250 ± 0.0012 h; 600 Musa, 5.88647 ± 0.00064 h; 716 Berkeley, 15.580657 ± 0.00048 h; 907 Rhoda, 22.4700 ± 0.0008 h; 1354 Botha, 8.3776 ± 0.0007 h; 3210 Lupishko, 14.247 ± 0.002 h; 3286 Anatoliya, 5.8103 ± 0.0009 h; 3379 Oishi, 19.2199 ± 0.019 h; 11736 Viktorfischl, 9.78407 ± 0.0012 h; 13653 Priscus, 6.7498 ± 0.0022 h; (23552) 1994 NB, 3.63175 ± 0.00052 ; (37638) 1993 VB, 3.529 ± 0.001 h; (76644) 2000 HY24, 9.6625 ± 0.012 h. And the following sidereal periods: 716 Berkeley, 15.57505 ± 0.00007 h; 11736 Viktorfischl, 9.78218 ± 0.00003 h; (23552) 1994 NB, 3.628683 ± 0.000004 ; (76644) 2000 HY24, 9.702441 ± 0.00005 h

We report on the photometric analysis results for twelve main-belt asteroids and one PHA by Asociación Valenciana de Astronomía (AVA). The data were obtained during the first months of 2023. We present graphic results of data analysis, mainly lightcurves, with the plot phased to a given period. We managed to obtain a number of accurate and complete lightcurves and calculating as accurately as possible their rotation periods.

Observatory	Telescope (meters)	CCD
C.A.A.T. J57	43 cm DK	QHY- 600
C.A.A.T. J57	106 mm Refr	ZWO ASI 1600
Z93	SC 8"	SBIG ST8300
J67	SC 10"	SBIG ST7

Table 1. List of instruments used for the observations.

We focused on asteroids with no reported period and those where the reported period was poorly established and needed confirmation. All the targets were selected from the Collaborative Asteroid Lightcurve (CALL) website (<http://www.minorplanet.info/call.html>) and the Minor Planet Center (<http://www.minorplanet.net>). The Asteroid Lightcurve Database (LCDB; Warner et al., 2009) was consulted to locate previously published results.

Images were measured using *MPO Canopus* (Bdw Publishing) with a differential photometry technique. The comparison stars were restricted to near solar-color to minimize color dependencies, especially at larger air masses. The lightcurves show the synodic rotation period. The amplitude (peak-to-peak) that is shown is that for the Fourier model curve and not necessarily the true amplitude.

If we have enough data in ALCDEF in addition to our own data, we can try a second step with the software *LC INVERT* (Bdw Publishing), which uses the inversion method described by Kaasalainen and Torppa (2001). This software uses the code written by J. Durech based on the original FORTRAN code written by Kaasalainen (2001): "Period Scan". The advantage of this method is that it allows the use of "dense" data such as the ones we have obtained in our measurements together with "sparse" data type, available in databases from Catalina, Usno, Atlas, Palomar, etc.

This is an iterative method that, based on an initial estimate of the period given by the lightcurve, finds the local minimum of χ^2 and gives the corresponding solution. The procedure starts with six initial poles for each trial period and selects the period that gives the lowest χ^2 . If there is a clear minimum in χ^2 when plotted as a function of the period, we can assume it as a correct solution. Not always we get a clear solution. We have referenced only those asteroids with an unambiguous calculation.

When calculating we use weighting coefficients to take into account the density of the data. We assign to "dense" data a value of 1 and to "sparse" data a value of 0.3 as an empiric rule. Error estimates for inversion method are no obvious. The smallest separation ΔP of local minima (Kaasalainen et al., 2001), in the period parameter space is roughly given by

$$\Delta P \approx 0.5 * P^2 / \Delta t$$

where Δt is the full epoch range of the data set. This derives from the fact that the maxima and minima of a double sinusoidal lightcurve for periods P and $P \pm \Delta P$ are at the same epochs after Δt time.

As we can read in Kaasalainen et al. (2001), "The period error is mostly governed by the epochs of the lightcurves. If the best local χ^2 minimum of the period spectrum is clearly lower than the others, one can obtain an error estimate of, say, a hundredth part of the smallest minimum width ΔP since the edge of a local minimum ravine always lies much higher than its bottom".

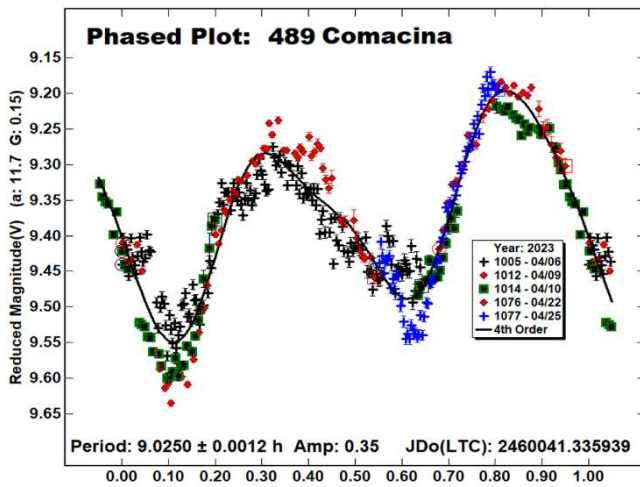
Durech (2006) proposes an estimate of error to be:

$$\Delta P \approx (1/10 * 0.5) * P^2 / \Delta t$$

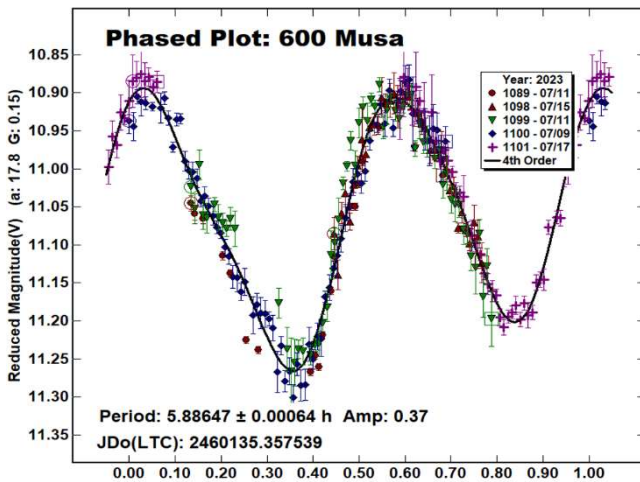
The factor 1/10 means that the period accuracy is 1/10 of the difference between local minima in the periodogram.

Results

489 Comacina. This outer main-belt asteroid was discovered on 1902 September 2 by L. Camera at Heidelberg in Germany. We made observations on 2023 April 6 to 25. We derived a rotation period of 9.0250 ± 0.0012 h and an amplitude of 0.39 mag. This is consistent with the previous result of 9 h from Weidenschilling et al. (1990) and Hawkins and Ditteon (2008), and 9.02 h from Stephens et al. (2001). Durech (2006) and Hanus et al. (2016) found a sidereal period of 9.0232 h with the inversion method.

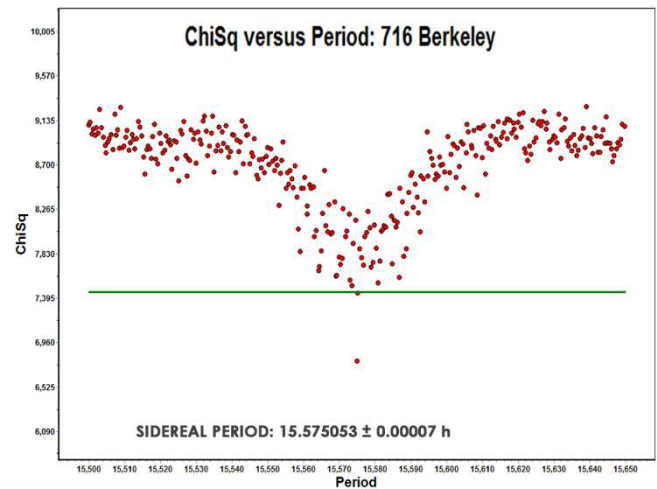
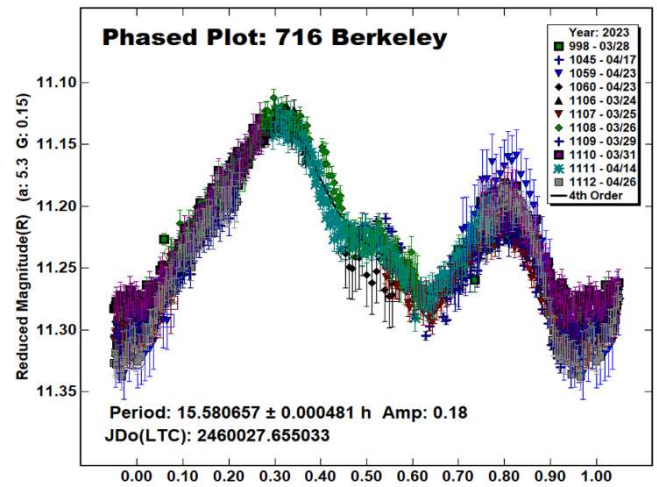


600 Musa. This middle main-belt asteroid was discovered on 1906 Jun 14 by J.H. Metcalf at Tauton. We made observations from 2023 Jul 11-17. From our data we derive a rotation period of 5.88647 ± 0.00064 h and an amplitude of 0.37 mag. Garcerán (2014web – no longer active) got 5.892 h, Behrend (2005web) got 5.8856 h and Binzel (1987) got 5.92 h. Hanus et al. (2013) found a sidereal period of 5.88638 h with the inversion method.

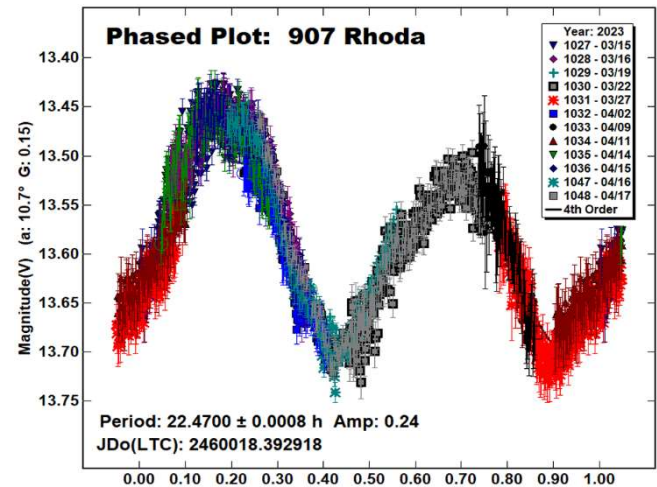


716 Berkeley. This middle main-belt asteroid was discovered on 1911 Jul 30 by J. Palisa at Vienna. We made observations on 2023 March 28 to April 23. In ALCDEF we found data from F. Pilcher on 2023 March 25 to April 26 with a very good quality. We have studied the rotation period of Berkeley using both sets of data. The period calculation is 15.580657 ± 0.00048 h and an amplitude of 0.18 mag. This is consistent with the previous result from Garlitz (2011web) with 15.55 h and Polakis (2021) with 15.46 h. Behrend (2018web) found 34.3 h, and Lagerkvist (1978) got 17 h. We can't agree with them.

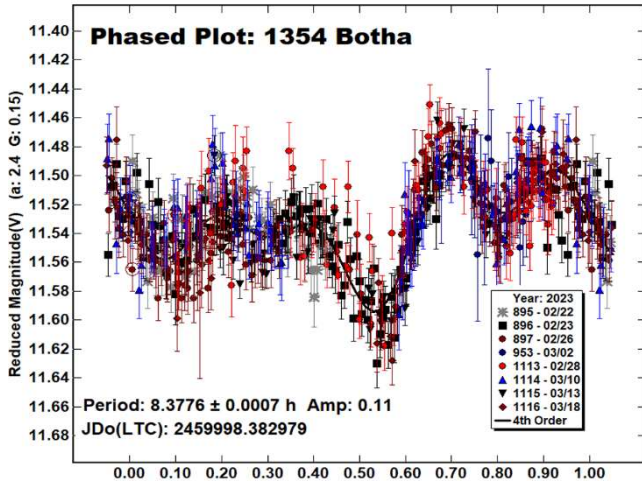
In ALCDEF we found good quality data from Garlitz (2011web), Polakis (2021), Benisheck (LCDB) and Pilcher (LCDB). We use this data in conjunction with our own dense data and sparse data from Catalina (414 points, 2003/11/15 - 2023/4/2), Palomar (146 points, 2018/2/16 - 2022/4/9) and USNO (146 points, 1998/11/27 - 2007/12/6). With the inversion method we calculate a sidereal rotation period of 15.575053 ± 0.00007 h. For the error estimation we have used the interval 2003-2023. In the lower graph we show the χ^2 value as a function of the period, which clearly shows the convergence of the iterative method used.



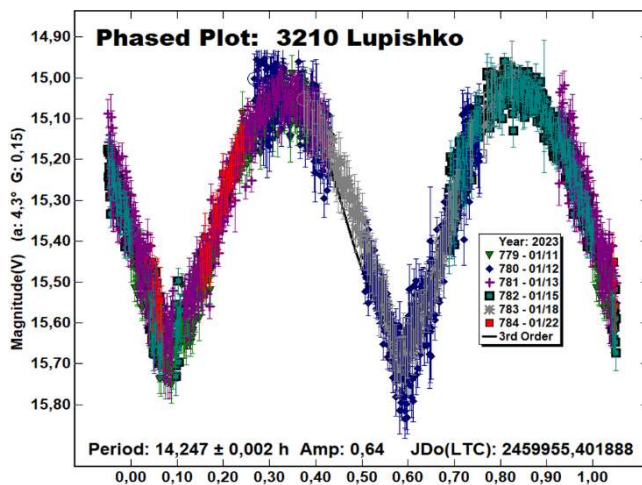
907 Rhoda. This middle main-belt asteroid was discovered on 1918 Nov 12 by M. Wolf at Heidelberg. We made observations on 2023 from March 15 to April 17. From our data, we derive a rotation period of 22.4700 ± 0.0008 h and an amplitude of 0.24 mag. This is consistent with Marciniak (ALCDEF) who got 22.46 h and Behrend (2018web) with 22.4 h. Warner (2004) got 22.44 h. We can't agree with Pal et al. (2020) with 42.6307 h.



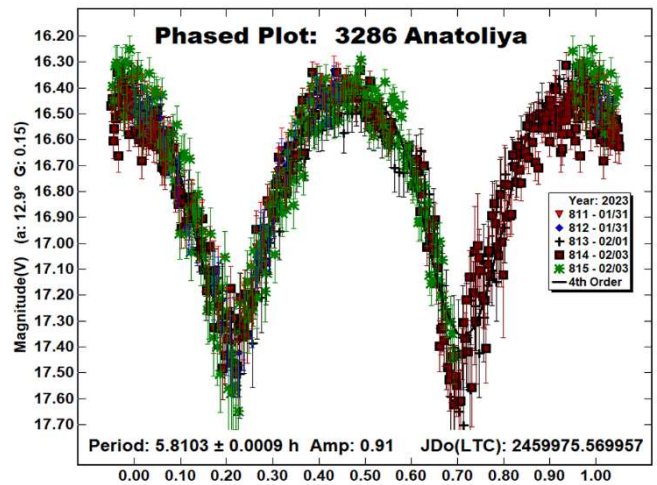
1354 Botha. This outer main-belt asteroid was discovered on 1935 April 3 by C. Jackson at Johannesburg. We made observations on 2023 Feb 22 to March 2. In ALCDF we found observations from Wiles (2023) for the same months in 2023 and we joined them to ours to improve the result. We derive a rotation period of 8.3776 ± 0.0007 h and an amplitude of 0.11 mag. In the LCDB we just find a previous calculation. Behrend (2003web) found 4 h.



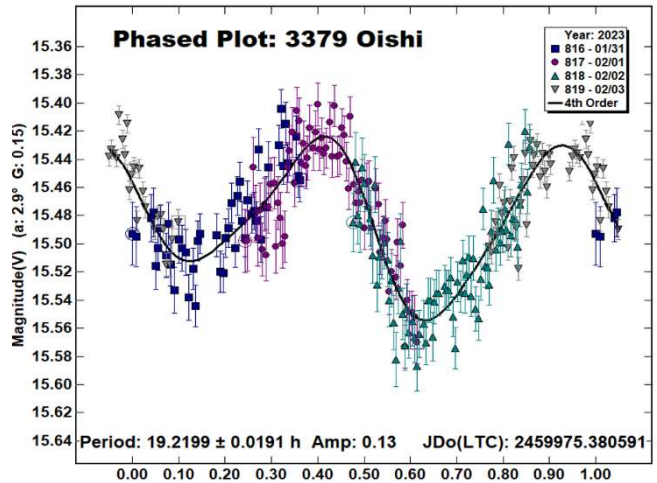
3210 Lupishko. This outer main-belt asteroid was discovered on 1983 Nov 29 by E. Bowell at Anderson Mesa. We made observations on 2023 Jan 11-22. From our data we derive a rotation period of 14.247 ± 0.002 h and an amplitude of 0.64 mag. There are several results in LCDB consistent with us: Waszczak et al. (2015) got 14.241 h and Montminy et al. (2018) found 14.255 h. Using the inversion method, Durech and Hanus (2018) found 14.2490 h, and Durech et al. (2020) got 14.24917 h.



3286 Anatoliya. This middle main-belt asteroid was discovered on 1980 Jan 23 by L.G. Karachkina at the Nauchnij observatory in Crimea. We made observations on 2023 Jan 31 to Feb 3. Data analysis found a rotation period of 5.8103 ± 0.0009 h and an amplitude of 0.91 mag. Durech et al. (2016) got a sidereal period of 5.81029 h with the inversion method.

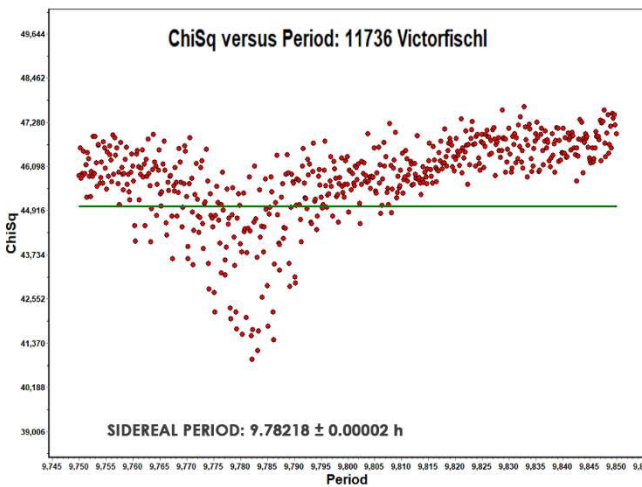
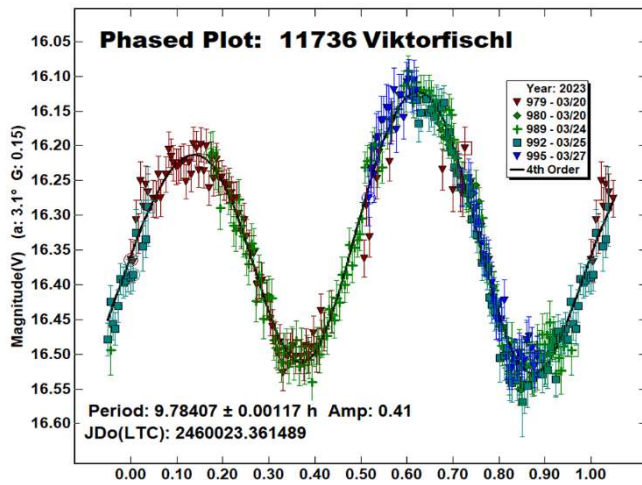


3379 Oishi. This inner main-belt asteroid was discovered on 1931 Oct 6 by K. Reinmuth at Heidelberg. We made observations on 2023 Jan 31 to Feb 3. From our data we derive a rotation period of 19.2199 ± 0.0191 h and an amplitude of 0.13 mag. We have not found previous information about its rotation period.

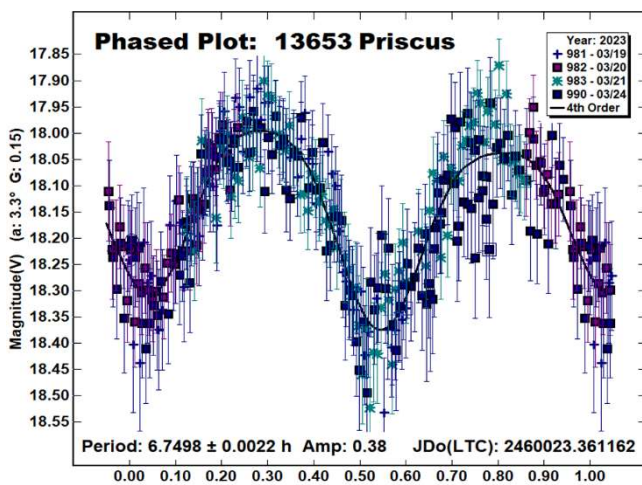


11736 Viktorfischl. This inner main-belt asteroid of the Nysa - Polana complex was discovered on 1998 Aug 18 at Ondřejov Observatory by L. Kotková. We made observations on 2023 March 20-27. From our data we derive a rotation period of 9.78407 ± 0.00117 h and an amplitude of 0.41 mag. Erasmus et al. (2020) found a period of 9.783 h which is consistent with us.

We use our dense data this data in conjunction with sparse data from Catalina (458 points, 2003/10/29 - 2023/6/21), Palomar (64 points, 2017/12/17 - 2022/4/6) and ATLAS (611 points, 2017/7/29 - 2023/3/25). With the inversion method we get a sidereal rotation period of 9.78218 ± 0.00002 h. For the error estimation we have used the interval 2003-2023. In the lower graph we show the χ^2 value as a function of the period, which clearly shows the convergence of the iterative method used.

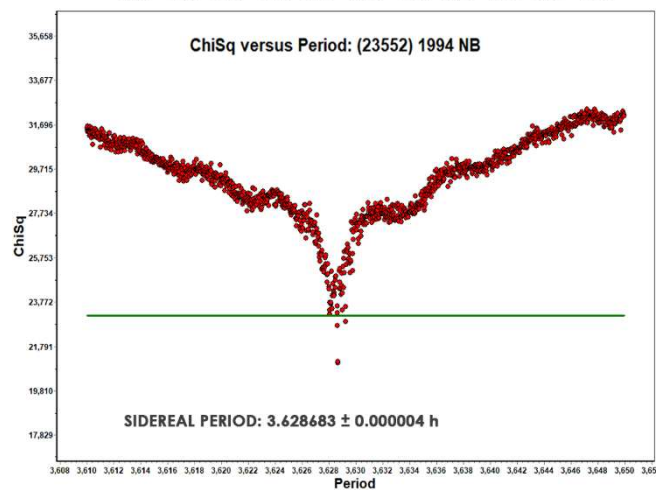
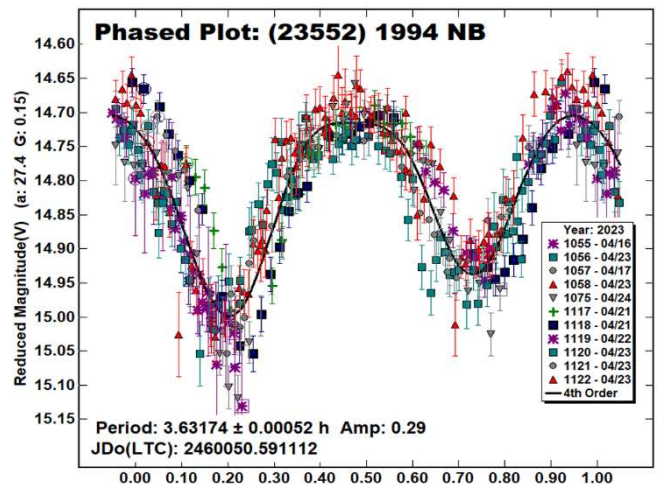


13653 Priscus. This inner main-belt asteroid was discovered on 1997 Feb 2 by V.S. Casulli at Coleverde observatory. We made observations 2023 March 19-24. From our data we derive a rotation period of 6.7498 ± 0.0022 h and an amplitude of 0.38 mag. We have not found previous information about its rotation period.



(23552) 1994 NB. This inner main-belt asteroid of the Phocaea family was discovered on 1994 Jul 3 by E.F. Helin at Palomar. We made observations on 2023 March 22-24. In ALCDEF we found data from Bucek (LCDB) on 2023 March 21-24 with a very good quality. We have studied the rotation period using both sets of data. Our period is 3.63175 ± 0.00052 h and an amplitude of 0.29 mag. Consistent with our results are those Waszczak et al. (2015) with 3.629 h and Skiff et al. (2023) with 3.630h. Pal et al. (2020) found a sidereal period of 3.62757 h with the inversion method.

In ALCDEF we found good quality data from Waszczak et al. (2015), Skiff et al. (2023), Pal et al. (2020), and Bucek (LCDB). We use these data in conjunction with our own dense data and sparse data from Catalina (454 points, 2003/12/5 - 2023/7/1), Palomar (42 points, 2018/12/13 - 2022/12/21) and ATLAS (671 points, 2015/9/17 - 2023/6/30). With the inversion method we get a sidereal rotation period of 3.628683 ± 0.000004 h. For the error estimation we have used the interval 2003-2023. In the lower graph we show the χ^2 value as a function of the period, which clearly shows the convergence of the iterative method used.



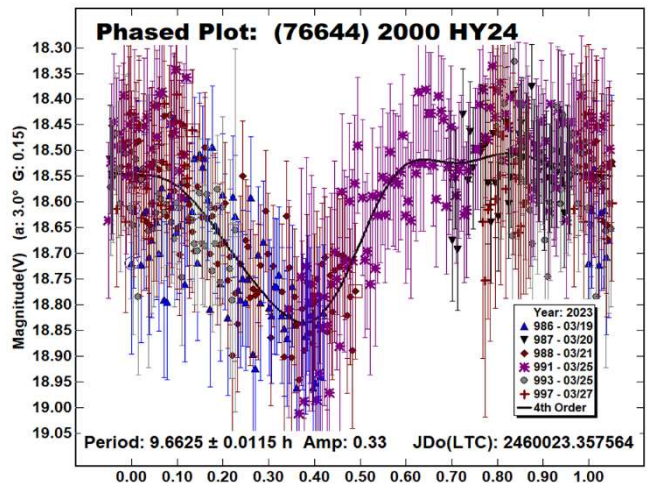
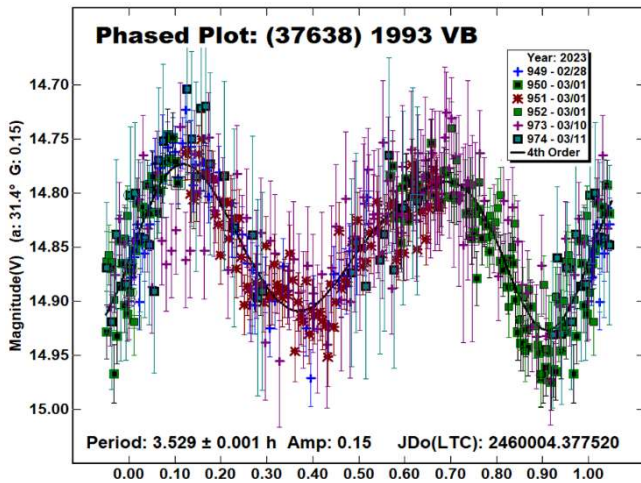
(37638) 1993 VB. This PHA was discovered on 1993 Nov 6 by R.H. McNaught at Siding Spring observatory. We made observations on 2023 Feb 28 to March 11. From our data we derive a rotation period of 3.529 ± 0.001 h and an amplitude of 0.158 mag. Pravec et al. (2022web) found 3.5301 h which is consistent with our data.

Number	Name	mm/dd	Phase	L _{PAB}	B _{PAB}	Period(h)	P.E.	Amp	A.E.	Grp
489	Comacina	2023/4/6-25	11.4, 16.1	165.4	1.5	9.0250	0.0012	0.39	0.05	MB-O
600	Musa	2023/7/11-17	17.5, 19	250.4	10.9	5.88647	0.00064	0.37	0.05	MB-M
716	Berkeley	2023/3/28-4/23	5.3, 23	201.5	8.3	15.580657	0.00048	0.18	0.03	MB-M
	(from Pilcher)	2023/3/25-4/26								
907	Rhoda	2023/3/15-4/17	10.3, 10.6	188.1	15.8	22.4700	0.0008	0.24	0.02	MB-M
1354	Botha	2023/2/22-3/2	2.3, 4.4	149.1	6.1	8.3776	0.0007	0.11	0.02	MB-O
3210	Lupishko	2023/1/11-12	4.3, 3.9	120.8	-2.7	14.247	0.002	0.64	0.05	MB-M
3286	Anatoliya	2023/1/31-3/2	15.6, 7.7	162.1	13.8	5.8103	0.0009	0.91	0.05	MB-M
3379	Oishi	2023/1/31-3/2	2.8, 1.1	135.2	-9	19.2199	0.0191	0.13	0.02	MB-I
11736	Viktorfischl	2023/3/20-27	3.2, 6.1	177.1	4.765	9.78407	0.00117	0.41	0.02	MB-I
13653	Priscus	2023/3/19-24	.1, 4.8	176.4	5.0	6.7498	0.0022	0.38	0.05	MB-I
23552	1994 NB	2023/3/22-24	23.6, 23.7	191.2	32.3	3.63175	0.00052	0.29	0.05	MB-I
37638	1993 VB	2023/2/28-3/11	34.1, 20.6	152.2	9.1	3.529	0.001	0.15	0.03	PHA
76644	2000 HY24	2023/3/19-27	2.4, 4.6	176.6	5.3	9.6625	0.012	0.18	0.05	MB-I

Table I. Sinodic Periods. Observing circumstances and results. The phase angle values are for the first and last date. L_{PAB} and B_{PAB} are the approximate phase angle bisector longitude and latitude at mid-date range (see Harris et al., 1984). Grp is the asteroid family/group (Warner et al., 2009). MB-I/O: Main-belt inner/outer; PHA: Potentially Hazardous Asteroid).

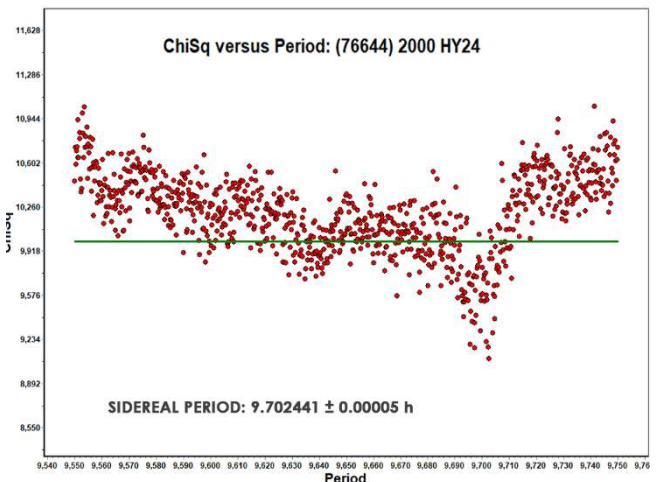
Number	Name	mm/dd	Phase	L _{PAB}	B _{PAB}	Period(h)	P.E.	Grp
716	Berkeley	2023/3/28-4/23	5.3, 23	201.5	8.3	15.57505	0.00007	MB-M
	(From Pilcher)	2023/3/25-4/26						
11736	Viktorfischl	2023/3/20-27	3.2, 6.1	177.1	4.7	9.78218	0.00003	MB-I
23552	1994 NB	2023/3/22-24	23.6, 23.7	191.2	32.3	3.628683	0.000004	MB-I
76644	2000 HY24	2023/3/19-27	2.4, 4.6	176.6	5.3	9.70244	0.00005	MB-I

Table II. Sidereal Periods. Observing circumstances and results. The phase angle values are for the first and last date. L_{PAB} and B_{PAB} are the approximate phase angle bisector longitude and latitude at mid-date range (see Harris et al., 1984). Grp is the asteroid family/group (Warner et al., 2009). MB-I/O: Main-belt inner/outer.



(76644) 2000 HY24. This middle main-belt asteroid was discovered on 2000 April 24 by LONEOS at Anderson Mesa. We made observations on 2023 March 19-27. From our data we derive a rotation period of 9.6625 ± 0.0115 h and an amplitude of 0.33 mag. We have not previous information about its rotation period.

We use our dense data this data in conjunction with sparse data from Catalina (184 points, 2004/3/26 - 2023/10), Palomar (48 points, 2018/2/7 - 2022/12/19) and ATLAS (204 points, 2017/12/30 - 2023/3/25). With the inversion method we get a sidereal rotation period of 9.702441 ± 0.00005 h. For the error estimation we have used the interval 2004-2023. In the lower graph we show the χ^2 value as a function of the period, which clearly shows the convergence of the iterative method used.



Acknowledgements

We would like to express our gratitude to Brian Warner for supporting the CALL web site and his suggestions, and to Dr. Stephen Slivan for his advice.

References

- Binzel, R.P. (1987). "A photoelectric survey of 130 asteroids". *Icarus* **72**, 135-208.
- Behrend, R. (2003web, 2005web, 2018web). Observatoire de Geneve web site. http://obswww.unige.ch/~behrend/page_cou.html
- Durech, J. (2006). IAU 2006, poster paper.
- Durech, J.; Hanus, J.; Oszkiewicz, D.; Vanco, R. (2016). "Asteroid models from the Lowell photometric database." *Astron. Astrophys.* **587**, A48.
- Durech, J.; Hanus, J. (2018). "Reconstruction of asteroid spin states from Gaia DR2 photometry." *Astron. Astrophys.* **620**, A91.
- Durech, J.; Tonry, J.; Erasmus, N.; Denneau, L.; Heinze, A.N.; Flewelling, H.; Vanco, R. (2020). "Asteroid models reconstructed from ATLAS photometry." *Astron. Astrophys.* **643**, A59.
- Erasmus, N.; Navarro-Meza, S.; McNeill, A.; Trilling, D.E.; Sickafoose, A.A.; Denneau, L.; Flewelling, H.; Heinze, A.; Tonry, J.L. (2020). "Investigating Taxonomic Diversity within Asteroid Families through ATLAS Dual-band Photometry." *Ap. J. Suppl. Ser.* **247**, A13.
- Garlitz, J. (2011web). <http://eoni.com/~garlitzj/Period.htm>
- Hanus, J.; Durech, J.; Broz, M.; Marciniak, A. and 116 colleagues (2013). "Asteroids' physical models from combined dense and sparse photometry and scaling of the YORP effect by the observed obliquity distribution." *Astron. Astrophys.* **551**, A67.
- Hanus, J.; Durech, J.; Oszkiewicz, D.A.; Behrend, R.; and 165 colleagues (2016). "New and updated convex shape models of asteroids based on optical data from a large collaboration network." *Astron. Astrophys.* **586**, A108.
- Harris, A.W.; Young, J.W.; Scaltriti, F.; Zappala, V. (1984). "Lightcurves and phase relations of the asteroids 82 Alkmene and 444 Gypsis." *Icarus* **57(2)**, 251-258.
- Hawkins, S.; Diteon, R. (2008). "Asteroid Lightcurve Analysis at the Oakley Observatory - May 2007." *Minor Planet Bull.* **35**, 1-4.
- Kaasalainen, M., (2001). "Interpretation of lightcurves of precessing Asteroids". *Astron. and Astrophysics* **376**, 302-309.
- Kaasalainen, M.; Torppa, J. (2001) "Optimization Methods for Asteroid Lightcurve Inversion. I Shape determination." *Icarus* **143**, 24-36.
- Kaasalainen, M.; Torppa, J.; Muinonen, K. (2001) "Optimization Methods for Asteroid Lightcurve Inversion. II The complete Inversion Problem." *Icarus* **153**, 37-51.
- Lagerkvist, C.-I. (1978). "Photographic Photometry of the Asteroids 716 Berkeley and 1245 Calvinia." *Astron. Astrophys. Suppl. Ser.* **34**, 203-205.
- Montminy, B.; McDonald, K.; Durkee, R.I. (2018). "Five Lightcurves from the Shed of Science: 2017 November - 2018 April." *Minor Planet Bull.* **45**, 331-333.
- Pal, A.; Szakáts, R.; Kiss, C.; Bódi, A.; Bognár, Z.; Kalup, C.; Kiss, L.L.; Marton, G.; Molnár, L.; Plachy, E.; Sárneczky, K.; Szabó, G.M.; Szabó, R. (2020). "Solar System Objects Observed with TESS - First Data Release: Bright Main-belt and Trojan Asteroids from the Southern Survey." *Ap. J. Suppl. Ser.* **247**, id. 26.
- Polakis, T. (2021). "Photometric Observations of Seven Minor Planets." *Minor Planet Bull.* **48**, 23-251.
- Pravec, P.; Wolf, M.; Sarounova, L. (2022web). <http://www.asu.cas.cz/~ppravec/neo.htm>
- Skiff, B.A.; McLelland, K.P.; Sanborn, J.J.; Koehn, B.W. (2023). "Lowell Observatory Near-Earth Asteroid Photometric Survey (NEAPS): Paper 5." *Minor Planet Bull.* **50**, 74-101.
- Stephens, R.D.; Brincat, S.M.; Koff, R.A. (2001) "Collaborative Photometry of 489 Comacina, March through May 2001." *Minor Planet Bull.* **28**, 73.
- Warner, B.D. (2004). "Lightcurve analysis for numbered asteroids 863, 903, 907, 928, 977, 1386 2841, and 75747." *Minor Planet Bull.* **41**, 54-57.
- Warner, B.D.; Harris, A.W.; Pravec, P. (2009). "The Asteroid Lightcurve Database." *Icarus* **202**, 134-146. 2023. <https://minplanobs.org/alcdef/index.php>
- Weidenschilling, S.J.; Chapman, C.R.; Davis, D.R.; Greenberg, R.; Levy, D.H.; Binzel, R.P.; Vail, S.M.; Magee, M.; Spaute, D. (1990). "Photometric geodesy of main-belt asteroids III. Additional lightcurves." *Icarus* **86(2)**, 402-447.
- Wiles, M. (2023). "Rotation Period and Lightcurve Determination for Fourteen Minor Planets." *Minor Planet Bull.* **50**, 290-294.
- Waszczak, A.; Chang, C.-K.; Ofeck, E.O.; Laher, R.; Masci, F.; Levitan, D.; Surace, J.; Cheng, Y.-Ch.; Ip, W.-H.; Kinoshita, D.; Helou, G.; Prince, T.A.; Kulkarni, S. (2015). "Asteroid Light Curves from the Palomar Transient Factory Survey: Rotation Periods and Phase Functions from Sparse Photometry." *Astron. J.* **150**, A75.

ASTEROID PHOTOMETRY AND LIGHTCURVES FOR TWELVE ASTEROIDS – SEPTEMBER 2023

Milagros Colazo

Instituto de Astronomía Teórica y Experimental
(IATE-CONICET), Argentina

Facultad de Matemática, Astronomía y Física, Universidad
Nacional de Córdoba, Argentina
Grupo de Observadores de Rotaciones de Asteroides (GORA),
Argentina, <https://aoacm.com.ar/gora/index.php>
milirita.colazovinovo@gmail.com

César Fornari

Grupo de Observadores de Rotaciones de Asteroides (GORA)
Argentina

Néstor Suárez

Observatorio Astronómico Giordano Bruno (MPC G05)
Piconcillo (Córdoba-España)

Mario Morales

Observatorio Astronómico El Gato Gris (MPC I19)
Tanti (Córdoba-Argentina)

Alberto Garcí

Observatorio de Sencelles (MPC K14)
Sencelles (Mallorca-Islas Baleares-España)

Damián Scotta

Osservatorio Astronomico "La Macchina del Tempo" (MPC M24)
Ardore Marina (Reggio Calabria-Italia)

Raúl Melia

Observatorio Los Cabezones (MPC X12)
Santa Rosa (La Pampa-Argentina)

Tiago Speranza

Observatorio Galileo Galilei (MPC X31)
Oro Verde (Entre Ríos-Argentina)

Ariel Stechina

Observatorio Antares (MPC X39)
Pilar (Buenos Aires-Argentina)

Bruno Monteleone

Observatorio Río Cofio (MPC Z03)
Robledo de Chavela (Madrid-España)

Giuseppe Cianci

Specola "Giuseppe Pustorino 3" (GORA GC3)
Palizzi Marina (Reggio Calabria-Italia)

Aldo Wilberge

Observatorio de Ariel Stechina 1 (GORA OAS)
Reconquista (Santa Fe-Argentina)

Matías Suligoy

Observatorio de Ariel Stechina 2 (GORA OA2)
Reconquista (Santa Fe-Argentina)

Axel Ortiz

Observatorio de Damián Scotta 1 (GORA ODS)
San Carlos Centro (Santa Fe-Argentina)

Francisco Santos

Observatorio Astronómico Municipal Reconquista (GORA OMR)
Reconquista (Santa Fe-Argentina)

Carlos Colazo

Observatorio de Raúl Melia Carlos Paz (GORA RMC)
Carlos Paz (Córdoba-Argentina)

(Received: 2023 September 8)

Synodic rotation periods and amplitudes are reported for:
830 Petropolitana, 931 Whittemora, 953 Painleva, 1064
Aethusa, 1199 Geldonia, 1465 Autonoma, 1937 Locarno,
4569 Baerbel.

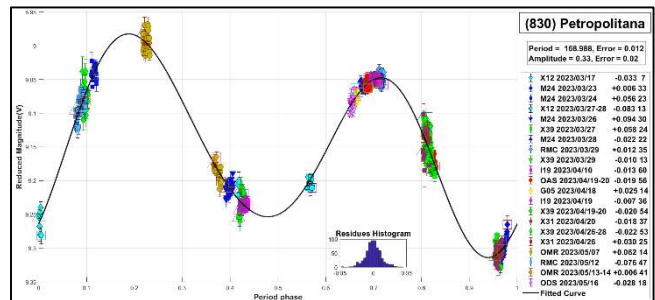
The periods and amplitudes of asteroid lightcurves presented in this paper are the product of collaborative work by the GORA (Grupo de Observadores de Rotaciones de Asteroides) group. In all the studies, we have applied relative photometry assigning V magnitudes to the calibration stars.

The image acquisition was performed without filters and with exposure times of a few minutes. All images used were corrected using dark frames and, in some cases, bias and flat-field corrections were also used. Photometry measurements were performed using *FotoDif* software and for the analysis, we employed *Periodos* software (Mazzone, 2012).

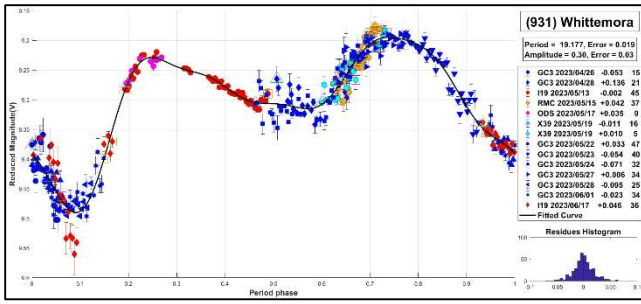
Below, we present the results for each asteroid studied. The lightcurve figures contain the following information: the estimated period and period error and the estimated amplitude and amplitude error. In the reference boxes, the columns represent, respectively, the marker, observatory MPC code, or - failing that - the GORA internal code, session date, session offset, and several data points.

Targets were selected based on the following criteria: 1) those asteroids with magnitudes accessible to the equipment of all participants, 2) those with favorable observation conditions from Argentina or Spain, i.e., with negative or positive declinations δ , respectively, and 3) objects with few periods reported in the literature and/or with Lightcurve Database (LCDB) (Warner et al., 2009) quality codes (U) of less than 3.

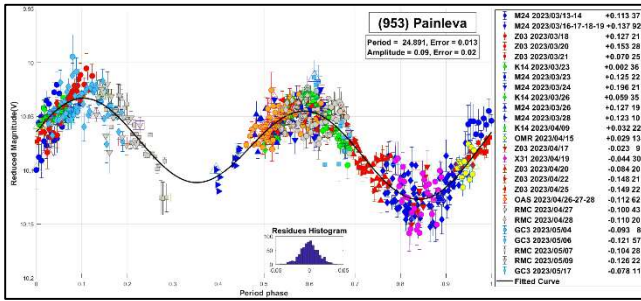
830 Petropolitana. It is an S-type asteroid, discovered in 1916 by G. Neujmin. The two more recent periods published in the literature correspond to $P = 39.0 \pm 0.5$ h (Behrend, 2005web) and $P = 37.347 \pm 0.005$ h (Hanus et al., 2016). In this work, we provide rather different results and propose a longer period of $P = 168.988 \pm 0.012$ h and $\Delta m = 0.33 \pm 0.02$ mag.



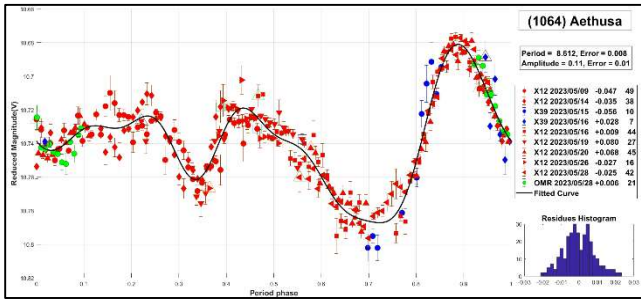
931 Whittemora. It is a M-type asteroid, discovered in 1920 by F. Gonnessiat. In the literature, we found only one reported period for this asteroid: $P = 19.20 \pm 0.01$ h with $\Delta m = 0.20 \pm 0.05$ mag (Menke, 2005). Our study supports the aforementioned period and yielded the following data: $P = 19.177 \pm 0.019$ h with $\Delta m = 0.30 \pm 0.03$ mag.



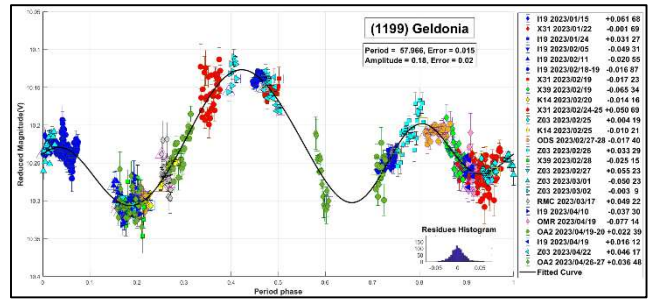
953 Painleva. It was discovered in 1921 by B. Jekhovsky. We found in the literature three rather different periods calculated for this object: $P = 10$ h (Behrend, 2006 web), $P = 7.389 \pm 0.004$ h (Schmidt, 2015), and $P = 24,884 \pm 0.002$ h (Dose, 2022). The results we obtained are $P = 24.891 \pm 0.013$ h and $\Delta m = 0.09 \pm 0.02$ mag. Our period well agrees with the one measured by Dose.



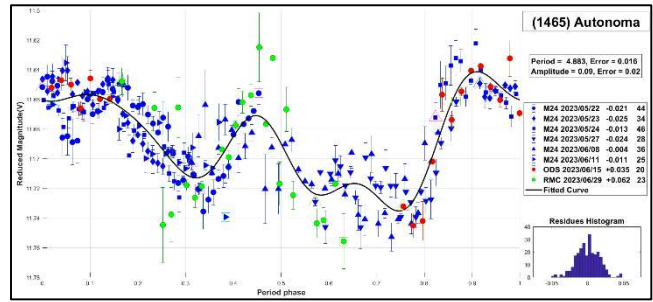
1064 Aethusa. It was discovered in 1926 by K. Reinmuth. We found in the literature two rather different periods calculated for this object: $P = 12.916 \pm .002$ h (Behrend, 2004web) and $P = 8.61275 \pm 0.00004$ h (Đurech et al., 2020). Our period $P = 8.612 \pm 0.008$ with $\Delta m = 0.11 \pm 0.01$ mag agrees with the one measured by Durech.



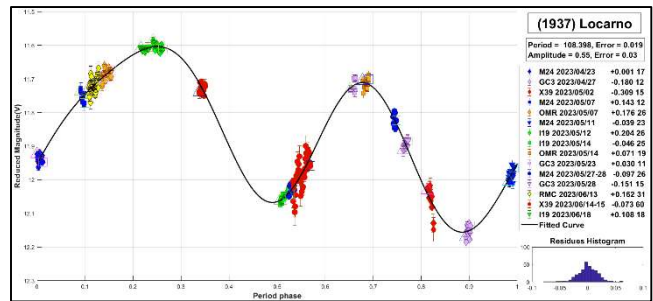
1199 Geldonia. It was discovered in 1931 by E. Delporte. Two different periods were reported in the literature. Behrend (2010web) found a period of 28.3 ± 0.2 h with $\Delta m = 0.11 \pm 0.03$ mag, whereas Polakis (2019) measured a period of $P = 57.82 \pm 0.21$ h with $\Delta m = 0.20$ mag. We have determined a period of 57.966 ± 0.015 h with $\Delta m = 0.18 \pm 0.02$ mag, which is consistent with the one proposed by Polakis.



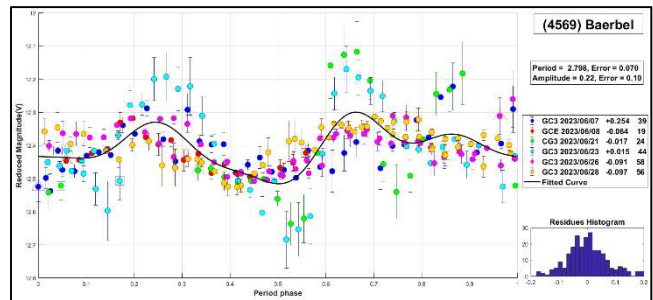
1465 Autonoma. This L-type Asteroid was discovered in 1938 by A. Wachmann. The period more recently reported in the literature is $P = 4.882$ h (Ditteon et al., 2018). The results we obtained are $P = 4.882 \pm 0.016$ h and $\Delta m = 0.09 \pm 0.02$ mag. Our period well agrees with the one measured by Ditteon.



1937 Locarno. It is an S-type asteroid, discovered in 1973 by P. Wild. In the literature, we found only one reported period for this asteroid: $P = 110$ h (Behrend, 2019 web). In this work, we propose a shorter period of $P = 108.398 \pm 0.019$ h with $\Delta m = 0.55 \pm 0.03$ mag.



4569 Baerbel. It was discovered in 1985 by C. S. Shoemaker. The more recent period published in the literature corresponds to $P = 2.790 \pm 0.002$ h with $\Delta m = 0.14$ mag (Stephens and Warner, 2020). In this work, we provide similar results and propose $P = 2.708 \pm 0.070$ h and $\Delta m = 0.22 \pm 0.10$ mag.



Number	Name	yy/ mm/dd- yy/ mm/dd	Phase	L _{PAB}	B _{PAB}	Period(h)	P.E.	Amp	A.E.	Grp
830	Petropolitana	23/03/17-23/05/17	*6.0,13.2	193	-3	168.988	0.012	0.33	0.02	MB-O
931	Whittemora	23/04/26-23/06/17	*7.9,07.7	241	10	19.177	0.019	0.30	0.03	MB-O
953	Painleva	23/03/13-23/05/17	*3.3,19.0	176	6	24.891	0.013	0.09	0.02	MB-O
1064	Aethusa	23/05/09-23/05/29	*6.7,08.1	235	-9	8.612	0.008	0.11	0.01	MB-I
1199	Geldonia	23/01/15-23/04/29	*11.5,19.8	144	-10	57.966	0.015	0.18	0.02	Eos
1465	Autonoma	23/05/22-23/06/30	*8.1,12.8	252	13	4.883	0.016	0.09	0.02	MB-O
1937	Locarno	23/04/23-23/06/18	*7.4,22,0	220	9	108.398	0.019	0.55	0.03	MB-I
4569	Baerbel	23/06/07-23/06/29	*11.4,09.3	271	17	2.798	0.070	0.22	0.10	Maria

Table I. Observing circumstances and results. The phase angle is given for the first and last date. If preceded by an asterisk, the phase angle reached an extremum during the period. L_{PAB} and B_{PAB} are the approximate phase angle bisector longitude/latitude at mid-date range (see Harris et al., 1984). Grp is the asteroid family/group (Warner et al., 2009). MB-O: main-belt outer; MB-I: main-belt inner; Eos: 221 Eos; Maria: 170 Maria.

Observatory	Telescope	Camera
G05 Obs.Astr.Giordano Bruno	SCT (D=203mm; f=6.3)	CCD Atik 420 m
I19 Obs.Astr.El Gato Gris	SCT (D=355mm; f=10.6)	CCD SBIG STF-8300M
K14 Obs.Astr.de Sencelles	Newtonian (D=250mm; f=4.0)	CCD SBIG ST-7XME
M24 Oss.Astr.La Macchina del Tempo	RCT (D250mm; f=8.0)	CMOS ZWO ASI 1600MM
X12 Obs.Astr.Los Cabezones	Newtonian (D=200mm; f=5.0)	CMOS QHY 174M
X31 Obs.Astr.Galileo Galilei	RCT ap (D=405mm; f=8.0)	CCD SBIG STF-8300M
X39 Obs.Astr.Antares	Newtonian (D=250mm; f=4.72)	CCD QHY9 Mono
Z03 Obs.Astr.Río Cofio	SCT (D=254mm; f=6.3)	CCD SBIG ST-8XME
GC3 Specola Giuseppe Pustorino 3	RCT (D=400mm; f=5.7)	CCD Atik 383L+Mono
OAS Obs.Astr.de Ariel Stechina 1	Newtonian (D=254mm; f=4.7)	CCD SBIG STF-402
OA2 Obs.Astr.de Ariel Stechina 2	Newtonian (D=305mm; f=5.0)	CMOS QHY 174M
ODS Obs.Astr.de Damián Scotta 1	Newtonian (D=300mm; f=4.0)	CMOS QHY 174M
OMR Obs.Astr.Municipal Reconquista	Newtonian (D=254mm; f=4.0)	Player One Ceres-M
RMC Obs.Astr.de Raúl Melia Carlos Paz	Newtonian (D=254mm; f=4.7)	CMOS QHY 174M

Table II. List of observatories and equipment.

Acknowledgements

We want to thank Julio Castellano as we used his *FotoDif* program for preliminary analyses, Fernando Mazzone for his *Periods* program, which was used in final analyses, and Matías Martini for his *CalculadorMDE v0.2* used for generating ephemerides used in the planning stage of the observations. This research has made use of the Small Bodies Data Ferret (<http://sbn.psi.edu/ferret/>), supported by the NASA Planetary System. This research has made use of data and/or services provided by the International Astronomical Union's Minor Planet Center.

References

- Behrend, R. (2004web, 2005web, 2006web, 2010web, 2019web). Observatoire de Geneve web site. http://obswww.unige.ch/~behrend/page_cou.html
- Castellano, J. FotoDif software. <http://www.astrosurf.com/orodeno/fotodif/>
- Ditton, R.; Adam, A.; Doyel, M.; Gibson, J.; Lee, S.; Linville, D.; Michalik, D.; Turner, R.; Washburn, K. (2018). "Lightcurve Analysis of Minor Planets Observed at the Oakley Southern Sky Observatory: 2016 October - 2017 March." *Minor Planet Bulletin* **45(1)**, 13-16.
- Dose, E.V. (2022). "Lightcurves of Eight Asteroids." *Minor Planet Bulletin* **49(3)**, 218-222.
- Đurech, J.; Tonry, J.; Erasmus, N.; Denneau, L.; Heinze, A.N.; Flewelling, H.; Vančo, R. (2020). "Asteroid models reconstructed from ATLAS photometry." *Astronomy & Astrophysics* **643**, A59.
- Harris, A.W.; Young, J.W.; Scaltriti, F.; Zappala, V. (1984). "Lightcurves and phase relations of the asteroids 82 Alkmene and 444 Gyptis." *Icarus* **57(2)**, 251-258.
- Martini, M. Calculador de magnitud diferencial estandarizada. <https://www.observatorioomega.com.ar/2020/11/calculador-de-magnitud-diferencial.html>
- Mazzone, F.D. (2012). Periodos software, version 1.0. <http://www.astrosurf.com/salvador/Programas.html>
- Menke, J. (2005). "Asteroid lightcurve results from Menke Observatory." *Minor Planet Bulletin* **32**, 85-88.
- Polakis, T. (2019). "Photometric Observations of Seventeen Minor Planets." *Minor Planet Bulletin* **46(4)**, 400-406.
- Schmidt, R.E. (2015). "NIR Minor Planet Photometry from Burleigh Observatory: 2014 February-June." *Minor Planet Bulletin* **42(1)**, 1-3.
- Stephens, R.D.; Warner, B.D. (2020). "Main-belt Asteroids Observed from CS3: 2019 July to September." *Minor Planet Bulletin* **47(1)**, 50.
- Warner, B.D., Harris, A.W., Pravec, P. (2009). "The asteroid lightcurve database." *Icarus* **202(1)**, 134-146. Updated 2023-07-01. <https://minplanobs.org/MPInfo/php/lcdb.php>

LIGHTCURVES OF EIGHTEEN ASTEROIDS

Eric V. Dose
3167 San Mateo Blvd NE #329
Albuquerque, NM 87110
mp@ericdose.com

(Received: 2023 October 15)

We present lightcurves and synodic rotation periods for eighteen asteroids observed July through October 2023.

We present asteroid lightcurves obtained via the workflow process described by Dose (2020) and later improved (Dose, 2021). This workflow applies to each image an ensemble of typically 25-100 nearby comparison (“comp”) stars selected from the ATLAS refcat2 catalog (Tonry, 2018). Custom diagnostic plots and the abundance of comp stars allow for rapid identification and removal of outlier, variable, and poorly measured comp stars.

The product of this custom workflow is one night’s time series of absolute magnitudes, on Sloan r' (SR) catalog basis, for one target asteroid. These absolute magnitudes are corrected for instrument transforms, sky extinction, and image-to-image (“cirrus”) fluctuations, and thus they represent magnitudes at the top of earth’s atmosphere. These magnitudes are imported directly into *MPO Canopus* software (Warner, 2021) where they are adjusted for distances and phase-angle dependence, fit by Fourier analysis including identifying and ruling out of aliases, and plotted.

Phase-angle corrections are made by applying a H-G model to the night’s phase angle, using the G value minimizing best-fit RMS error across all nights’ data. When we cannot estimate an asteroid’s G value, usually due to a campaign’s narrow range of phase angles, we apply the Minor Planet Center’s default value of 0.15. No nightly zero-point adjustments (Delta Comps in *MPO Canopus*) were made to any session herein, other than by estimating G .

Lightcurve Results

Eighteen asteroids were observed from New Mexico Skies observatory at 2310 meters elevation in southern New Mexico. Images were acquired without autoguiding, using: a 0.50-meter PlaneWave OTA on a PlaneWave L-500 mount and equatorial wedge, and a SBIG AC4040M CMOS camera cooled to -15 C and fitted with a GG495 yellow filter (Schott).

This equipment was operated remotely via *ACP Software* (DC-3 Dreams), running one-night plan files generated by python scripts (Dose, 2020). Exposure times targeted 2.5-5 millimagitudes uncertainty in asteroid instrumental magnitude, subject to a minimum exposure of 90 seconds to ensure suitable comp-star photometry, and to a maximum of 480 seconds.

FITS images were calibrated using temperature-matched, exposure-matched, median-averaged dark images and recent flat images of a flux-adjustable light panel. These calibrated images were plate-solved by *TheSkyX* (Software Bisque). Target asteroids were identified in *Astrometrica* (Herbert Raab). All photometric images were visually inspected; the author excluded images with poor tracking, excessive interference by cloud or moon, or having stars, satellite tracks, cosmic ray artifacts, residual image artifacts, or other apparent light sources within 12 arcseconds of the target asteroid’s signal centroid. Images passing these screens were submitted to the workflow.

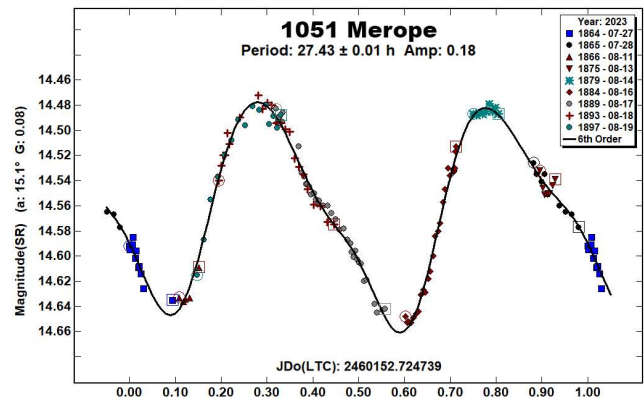
The GG495 yellow filter used here requires only modest first-order transforms to yield magnitudes in the standard Sloan r' (SR) passband. In our hands, using a light yellow filter (rather than a clear filter or no filter) improves night-to-night reproducibility to a degree outweighing loss of signal-to-noise ratio caused by ~15% loss of measured flux.

Comparison stars from the ATLAS refcat2 catalog were selected only if they had: distance of at least 15 arcseconds from image boundaries and from other catalogued flux sources, no catalog VARIABLE flag, SR magnitude within [-2, +1] of the target asteroid’s SR magnitude on that night (except that very faint asteroids used comp stars with magnitudes in the range 14 to 16), Sloan $r'-i'$ color value within [0.10, 0.34], and absence of variability as seen in session plots of each comp star’s instrumental magnitude vs time.

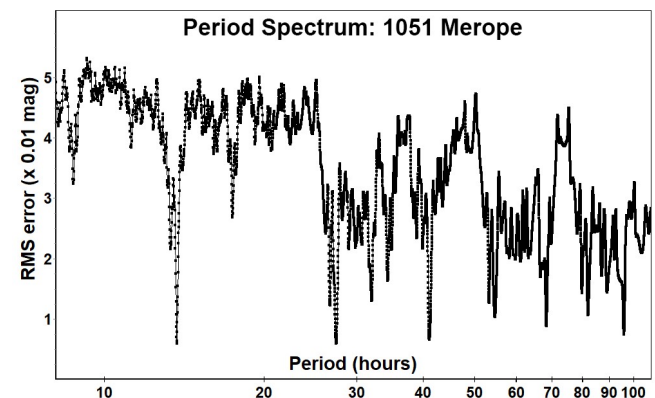
In this work, “period” refers to an asteroid’s synodic rotation period, “SR” denotes the Sloan r' passband, and “mmag” denotes millimagitudes (0.001 magnitude). G value given in the lightcurve plot is that which optimized the Fourier fit.

1051 Merope. For this Alauda-family, outer-main-belt asteroid, we estimate a synodic rotation period of 27.43 ± 0.01 h. This differs from the author’s previous estimate of 13.710 ± 0.001 h (Dose, 2023) from data taken May-June 2022 in the previous apparition. Viewed separately, the author’s two campaigns’ lightcurves and period spectra are convincing, yet they are hard to reconcile.

Our best G estimate is 0.08, and RMS error of Fourier fit is 6 mmag.



The current period spectrum has major signals only at multiples of half the current period estimate.

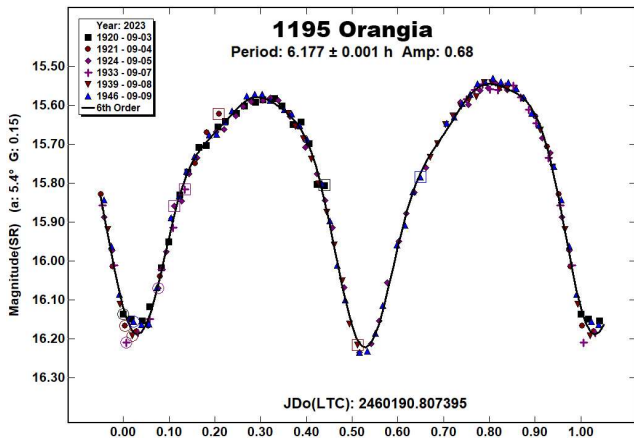


Number	Name	yyyy mm/dd	Phase	L _{PAB}	B _{PAB}	Period(h)	P.E.	Amp	A.E.	Grp
1051	Merope	2023 07/27-08/19	15.2, 8.5	343	12	27.430	0.010	0.18	0.02	ALA
1195	Orangia	2023 09/03-09/09	5.3, 6.7	339	8	6.177	0.001	0.68	0.05	MB-I
1337	Gerarda	2023 07/01-07/24	17.9, 11.5	323	9	12.474	0.001	0.40	0.04	MB-O
1525	Savonlinna	2023 08/18-09/20	*16.9, 6.0	352	8	22.701	0.002	0.24	0.04	MB-M
1796	Riga	2023 08/20-10/08	*9.1, 7.1	353	7	22.236	0.001	0.40	0.03	MB-O
1887	Virton	2023 08/30-10/09	16.6, 3.2	18	5	70.071	0.011	0.37	0.03	EOS
2466	Golson	2023 09/02-09/06	13.1, 14.8	317	2	3.583	0.002	0.14	0.03	MB-M
2697	Albina	2023 09/20-10/05	9.0, 4.3	23	4	16.638	0.005	0.12	0.02	MB-O
3042	Zelinsky	2023 08/28-10/03	*9.9, 13.5	348	6	2.662	0.001	0.05	0.02	FLO
3127	Bagration	2023 08/20-09/07	12.5, 4.2	347	5	15.667	0.003	0.18	0.04	MB-I
3811	Karma	2023 07/30-08/19	14.3, 6.0	335	-2	14.421	0.001	0.52	0.04	KRM
3819	Robinson	2023 10/10-10/14	11.8, 10.1	39	-3	3.069	0.001	0.15	0.02	MB-O
5468	Hamatonbetsu	2023 07/07-08/14	18.3, 23.6	253	11	42.045	0.008	0.40	0.06	MB-O
6147	Straub	2023 07/03-07/28	22.0, 14.6	316	15	10.301	0.001	0.54	0.04	EUN
7102	Neilbone	2023 08/06-08/18	*5.1, 6.0	318	8	6.178	0.001	0.42	0.04	MB-O
9628	Sendaiotsuna	2023 08/30-09/19	21.3, 15.1	13	17	2.664	0.001	0.08	0.02	EUN
14815	Rutberg	2023 07/01-08/17	*19.8, 10.5	307	5	154.350	0.052	1.16	0.10	MB-I
14835	Holdridge	2023 09/01-10/14	32.5, 16.4	28	22	164.401	0.029	0.76	0.06	PHO

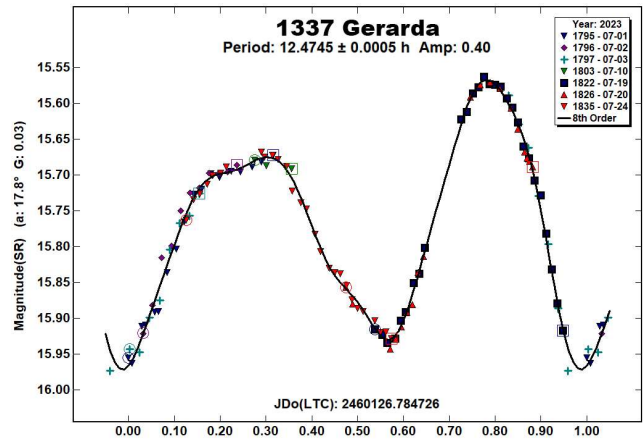
Table I. Observing circumstances and results. The phase angle is given for the first and last date. If preceded by an asterisk, the phase angle reached an extrema during the period. L_{PAB} and B_{PAB} are the approximate phase angle bisector longitude/latitude at mid-date range (see Harris, 1984). Grp is the asteroid family/group (Warner, 2009).

Other reported period estimates for Merope of 27.2 h (Carbo et al., 2009), 13.717 h (Waszczak et al., 2015), and 6.85563 h (Pál et al., 2020) follow the same factor-of-two pattern. We speculate that in recent apparitions this asteroid’s rotation axis has presented very different rotation-latitude viewing aspects, and that its northern and southern hemispheres differ markedly. These possibilities, together with the accessible brightnesses of the 2024 and 2026 apparitions, may render 1051 Merope an attractive candidate for future shape modeling.

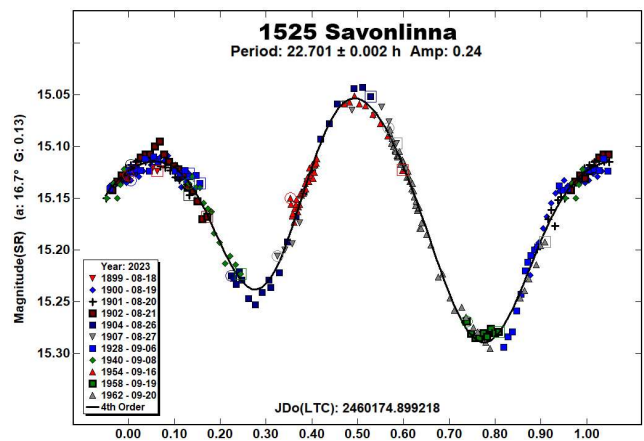
1195 Orangia. Our period estimate of 6.177 ± 0.001 h for this inner main-belt asteroid agrees with one known survey result of 6.167 h (Waszczak et al., 2015). The amplitude is high, and our phased lightcurve appears bimodal and unambiguous. Given our short campaign of less than a week, we could not confidently estimate a G value and so adopted MPC’s default value of 0.15. Fourier fit RMS error is 16 mmag.



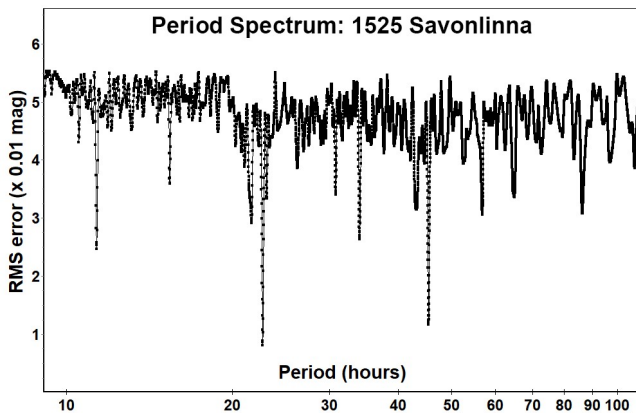
1337 Gerarda. For this outer main-belt asteroid, we estimate a rotation period of 12.4745 ± 0.0005 h, agreeing with all three known reports (12.52 h, Binzel, 1987; 12.462 h, Waszczak et al., 2015; 12.47036 h, Āurech et al., 2018). The phased lightcurve is bimodal. Our Fourier fit RMS error is 10 mmag.



1525 Savonlinna. For this middle main-belt asteroid, our period estimate of 22.701 ± 0.002 h agrees approximately with one survey result of 22.841 h (Waszczak et al., 2015), but it disagrees with another result of 14.634 h (Gartelle, 2012). Our best G-value estimate is 0.13, and our Fourier fit RMS error is 8 mmag.

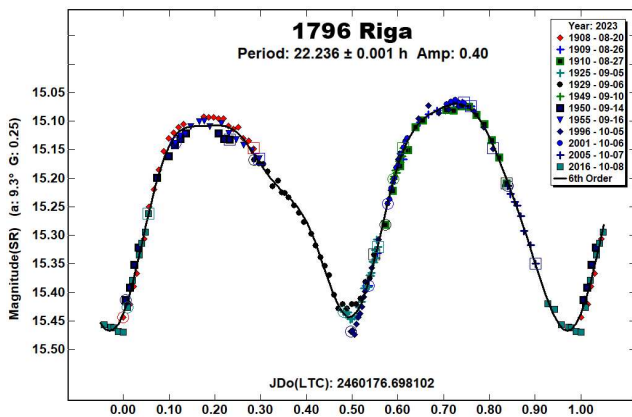


The period spectrum has major signals only at multiples of $\frac{1}{2}$ our period estimate. No period spectrum signal appears at the previously reported period of 14.634 h; the nearest minor signal appears at 15.38 h, an alias of our estimate by $\frac{1}{2}$ period per day.

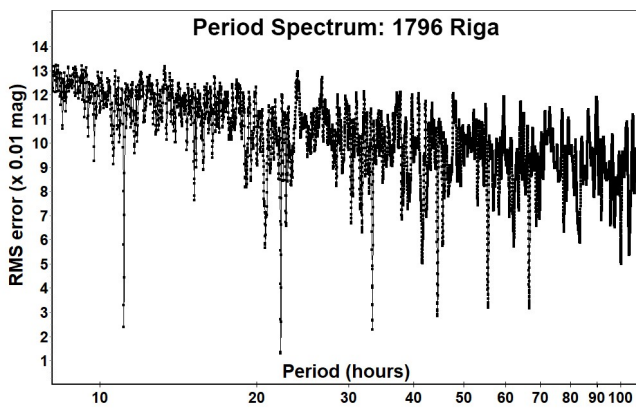


1796 Riga. Several diverse period estimates have been reported for this outer main-belt asteroid. We find a rotation period of 22.236 ± 0.001 h, agreeing with one report (22.226 h, Oey, 2016) and consistent with another (>16 h, Chiorny et al., 2007) but disagreeing with all others (11.00 h, Warner, 2004; 10.608 h, Warner, 2011; 44.2046 h, Pál et al., 2020; 10.16 h, Behrend, 2021web). The lightcurve is clearly bimodal. Our best G value is 0.25, and our Fourier fit RMS error is 10 mmag.

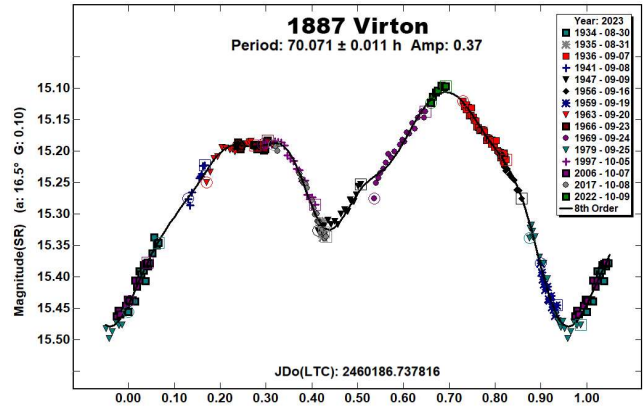
This asteroid's lightcurve amplitude is often reported to be 0.05-0.10 magnitude, much lower than ours. Indeed, the sole previous report with amplitude much higher (0.40 mag, Oey, 2016) and close to ours is the very report with period estimate close to our own.



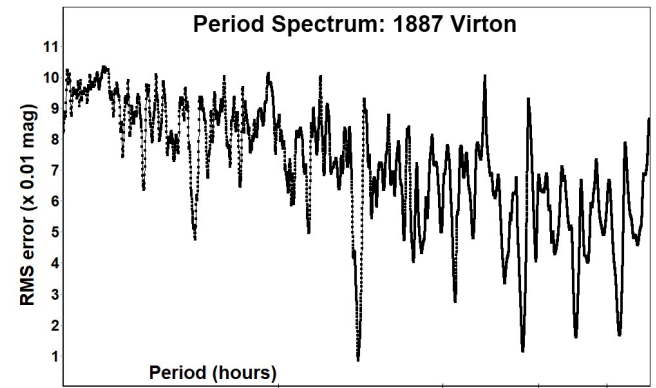
In our period spectrum, the 22.236 h signal is strongest, and other strong signals are limited to multiples of $\frac{1}{2}$ of our period estimate.



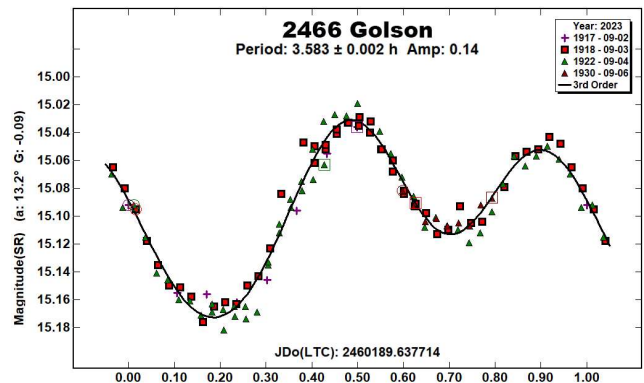
1887 Virton. Rotation period determination for this Eos-family asteroid has eluded both known previous attempts (Simpson et al., 2013; Ditteon and Trent, 2018). After the first few nights, we strove to maximize the length of our observing sessions in order to compensate for the period's proximity to 3 days and thus to afford complete phase coverage. From fifteen nights' observations we report a period of 70.071 ± 0.011 h and a distinctly bimodal lightcurve. Our G value estimate is 0.10, and our Fourier fit RMS error is 8 mmag.



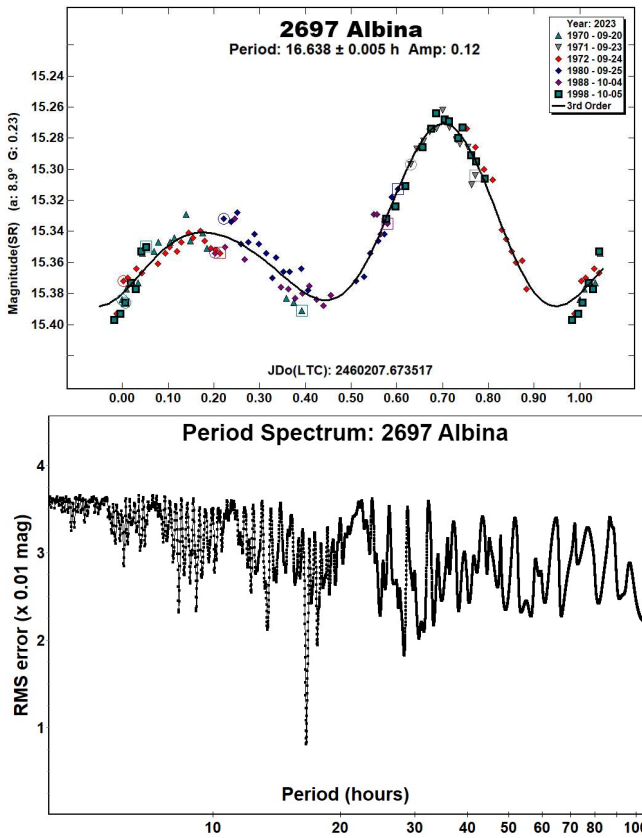
The period spectrum is dominated by our period estimate, and all major secondary signals fall at multiples of half that bimodal period.



2466 Golson. Our period estimate for this middle main-belt asteroid is 3.583 ± 0.002 h, agreeing with the sole known report of 3.583 h (Polakis, 2020). Our best G-value estimate of -0.09 is uncertain due to the short duration of our campaign and resulting narrow range of phase angles. Our Fourier fit RMS error is 8 mmag.

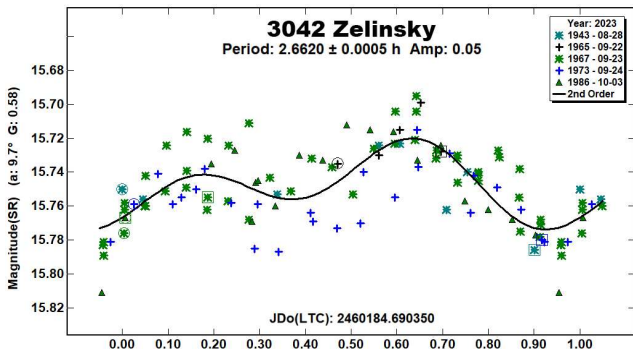


2697 Albina. For this outer main-belt asteroid, we find a rotation period of 16.638 ± 0.005 h, in fair agreement with one survey result (16.587 h, Waszczak et al., 2015) but disagreeing with another result (9.6 h, Behrend, 2006web) which is an alias of our result by one period per day. The lightcurve is clearly bimodal. Our best G value is 0.23, and our Fourier fit RMS error is 8 mmag.

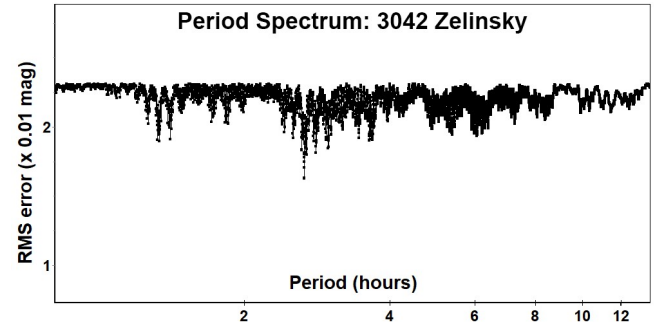


3042 Zelinsky. Despite the very low amplitude for this Flora-family asteroid, we determined a lightcurve and a rotation period of 2.6620 ± 0.0005 h. At MPC's default G value of 0.15, we could find no consistent periodicity, but by adopting a G value near 0.58 we found the lightcurve given here. Of our five nights' observations, four sessions extended over at least one period length. Our Fourier fit RMS error is 16 mmag.

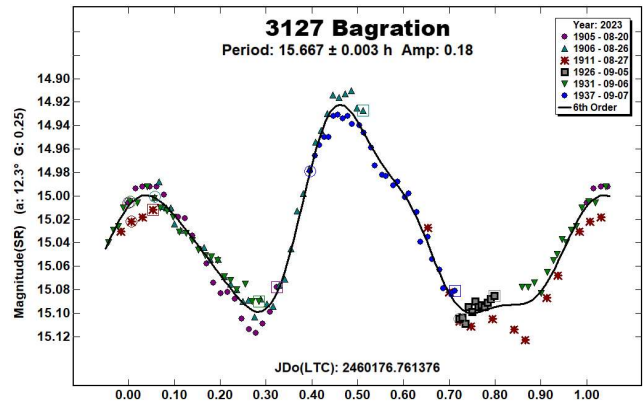
Our period estimate is at variance with three previously reported estimates, which themselves disagree (5.3248 h, Pravec et al., 2016web; 4.469 h, Aznar Macias et al., 2017; 32 h, Behrend, 2023web). The Pravec period estimate is close to twice ours; the Aznar Macias lightcurve is built from one night's observations, and its phase coverage is incomplete.



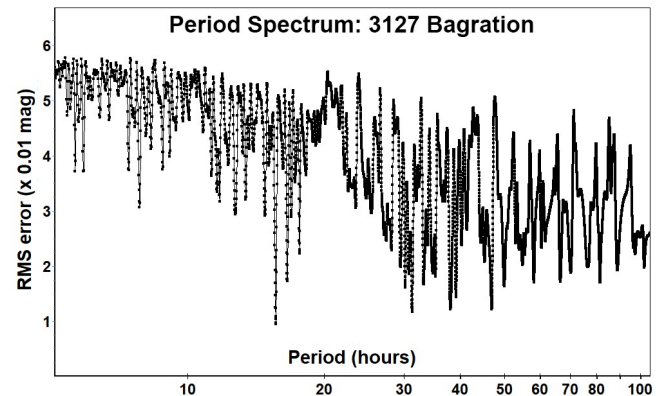
The period spectrum is clearer than the lightcurve might suggest. We favor a bimodal interpretation based on the lightcurve's own shape and on the dominance of the 2.662 h signal. We found no significant signals for periods longer than 10 h.



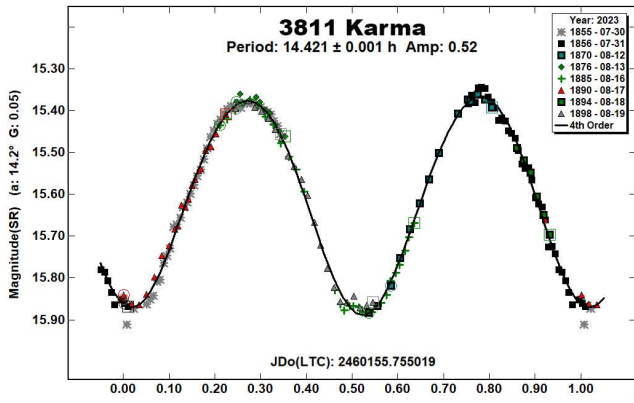
3127 Bagration. Our period estimate of 15.667 ± 0.003 h for this inner main-belt asteroid is consistent with one previously reported period limit (>12 h, Behrend, 2015web) but not with the other (>16 h, Behrend, 2019web). The phased lightcurve shape is distinctive and clearly bimodal. Our G-value estimate is 0.25, and our Fourier fit RMS error is 9 mmag.



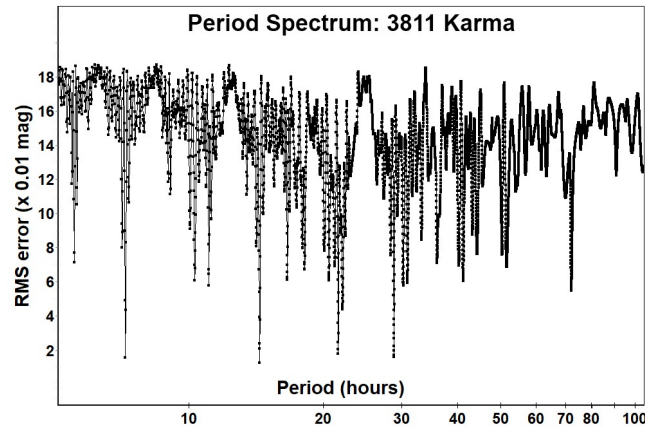
The period spectrum supports our period estimate. The lightcurve's strongly bimodal shape is reflected in suppression of period-spectrum signals at most odd multiples of $\frac{1}{2}$ our period estimate.



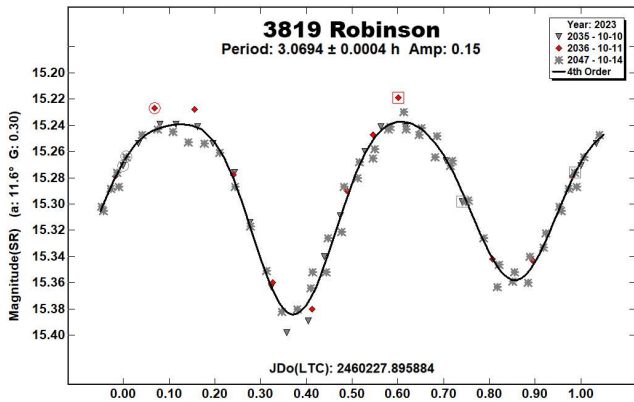
3811 Karma. For this namesake asteroid of the Karma family, we obtain a rotation period estimate of 14.421 ± 0.001 h, which agrees with two reported results (14.4234 h, Āurech et al., 2020; 14.41 h, Yeh et al., 2020) but which disagrees with two other reports (11.52 h, Behrend, 2007web; 13.23 h, Aznar Macias et al., 2016). Our G value estimate is 0.05, and our Fourier fit RMS error is 13 mmag.



The lightcurve's two halves are quite similar, which causes strong period-spectrum signals at multiples of $\frac{1}{2}$ period. The large amplitude supports a bimodal interpretation.

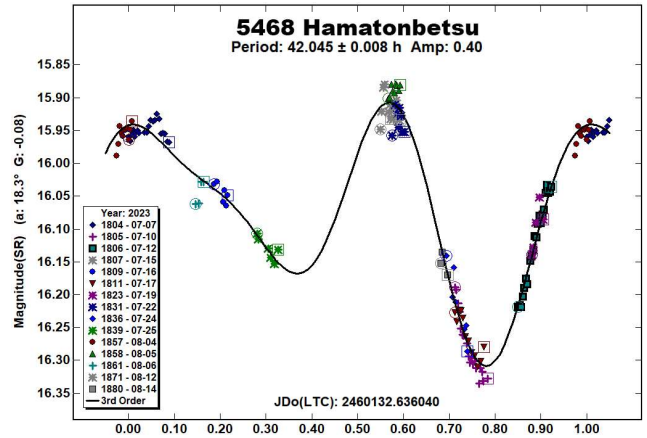


3819 Robinson. Our period estimate of 3.0694 ± 0.0004 h for this outer main-belt asteroid agrees with previous known estimates (3.070 h, Ferrero and Bonamico, 2020; 3.06886 h, Pál et al., 2020). The lightcurve is bimodal. Our Fourier fit RMS error is 8 mmag.

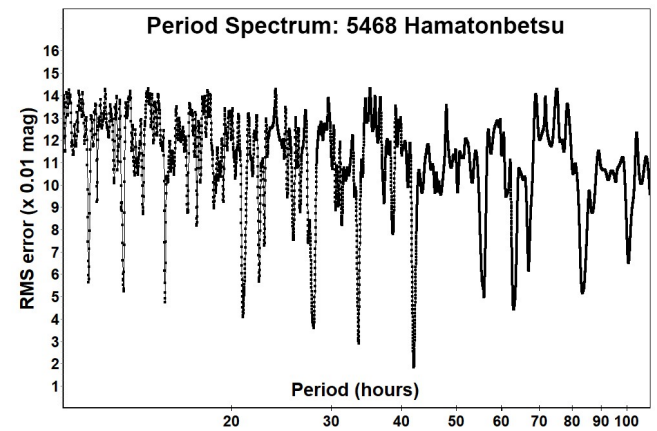


5468 Hamatonbetsu. Complete phase coverage remains elusive for this outer main-belt asteroid, even though its apparent period should make it readily achievable. Even though our period estimate of 42.045 ± 0.008 h is based on 15 nights of observation, considerable phase coverage remains missing from both sides of the brightness maximum. Our estimate confirms the 42.0 h estimate of Stephens and Warner (2003), which showed a similar lightcurve, but their lightcurves suffered phase coverage gaps similar to ours. We propose that 42.0 h is the likeliest rotational period; the amplitude

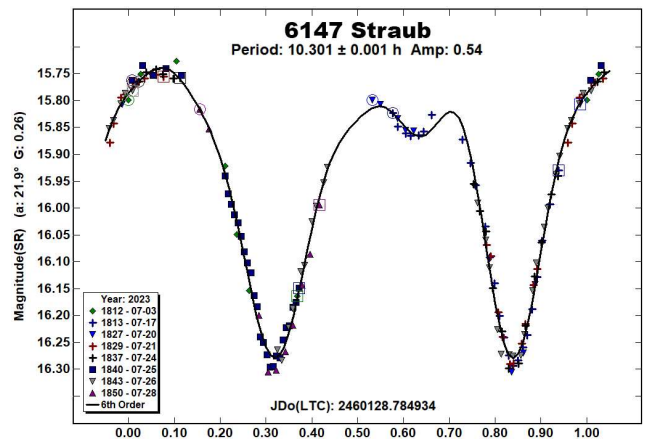
given in both reports indicates a bimodal interpretation. Our RMS error is 18 mmag.



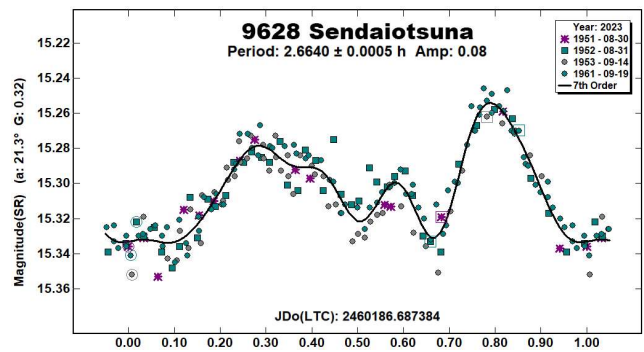
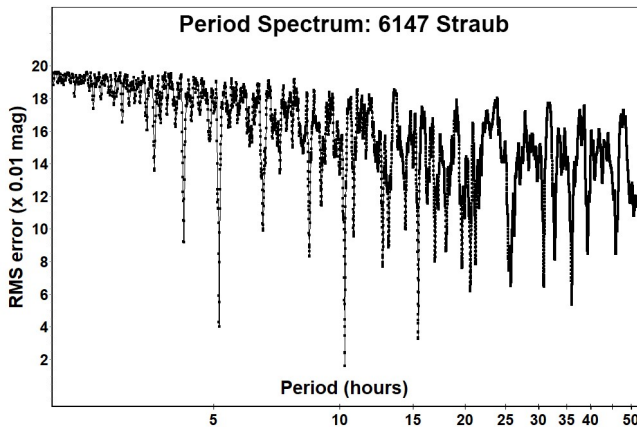
The period spectrum's primary signal occurs at 42.045 h. Secondary signals are numerous, which is probably caused by the uneven phase coverage, but most appear related to the primary signal. 5468 Hamatonbetsu merits another attempt at complete phase coverage; unfortunately, apparitions through 2025 are fainter.



6147 Straub. For this Eunomia-family asteroid, we report a period estimate of 10.301 ± 0.001 h. We know of no previous lightcurves or period estimates. Our Fourier fit RMS error is 16 mmag.

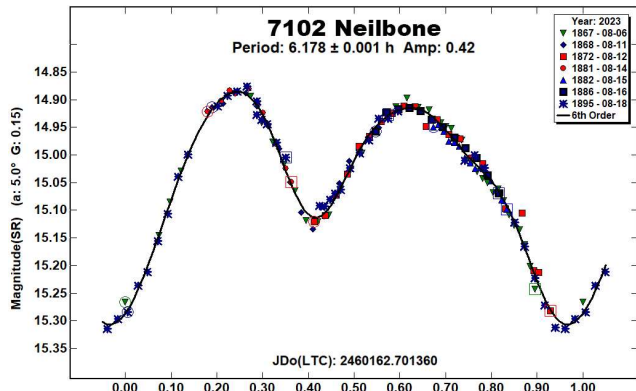
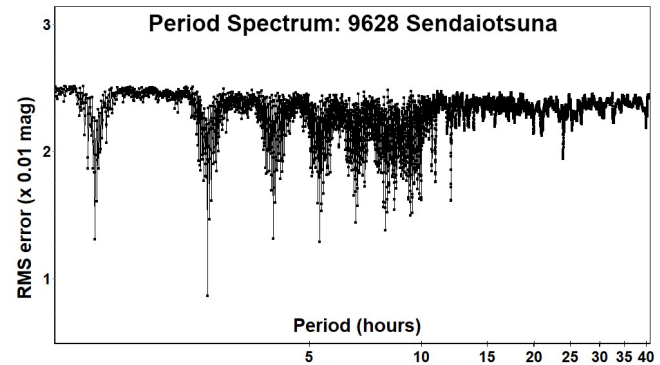


The large lightcurve amplitude and dominant period spectrum signal both support a bimodal interpretation.



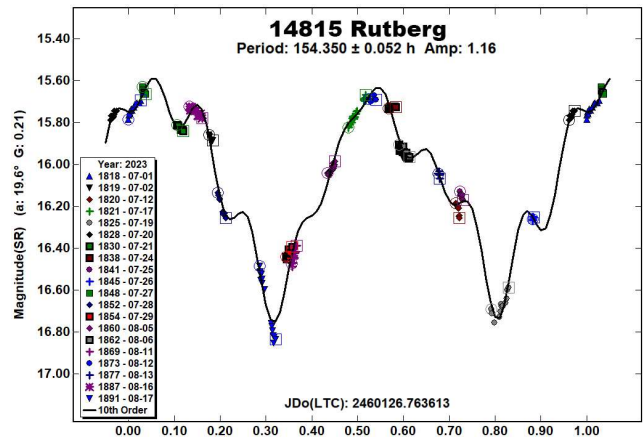
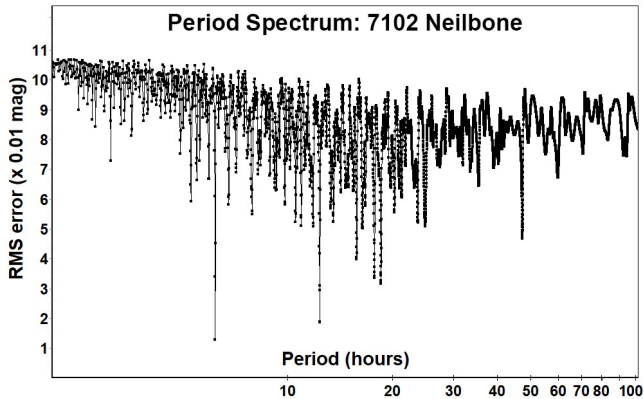
Despite the lightcurve's low amplitude, the period spectrum is unambiguous.

7102 Neilbone. We report a period estimate of $6.178 \text{ h} \pm 0.001 \text{ h}$ for this outer main-belt asteroid. We know of no previous lightcurves or period estimates. The lightcurve shape is bimodal but highly asymmetric with a shallow secondary minimum. Our Fourier fit RMS error is 11 mmag.



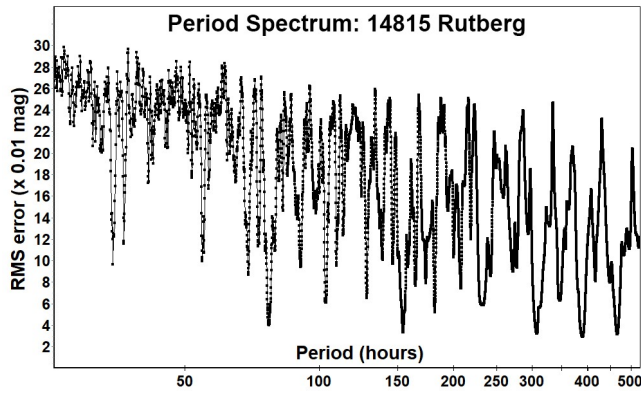
The period spectrum very strongly confirms the period estimate, and the lack of significant signal at half that estimate is consistent with the lightcurve's markedly bimodal shape.

14815 Rutberg. Thorough phase coverage for this inner main-belt asteroid required 21 nights of observation spanning 7 period cycles. Many of the sessions were long enough to capture significant brightness change within the session, and these together with the sharp lightcurve shape led to a very high-order Fourier fit. In the end, we estimate the rotation period to be $154.350 \pm 0.052 \text{ h}$, with a remarkable amplitude of 1.16 magnitudes. Our estimate is consistent with two previous reports: a lower limit of 10 h (Carbognani, 2011) and a broad central estimate of $150 \pm 10 \text{ h}$ (Higgins, 2011). Our Fourier fit RMS error is 33 mmag.



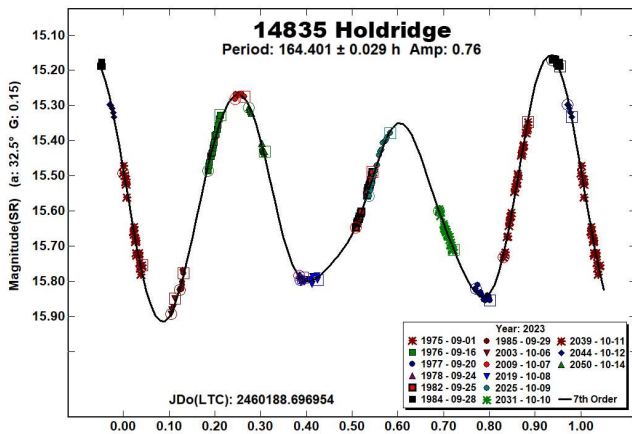
9628 Sendaiotsuna. For this Eunomia-family asteroid, our period estimate of $2.6640 \pm 0.0005 \text{ h}$ results from four nights of observation covering each well over a period's duration, with the last night covering 3 periods. We know of no previous lightcurves or period estimates. The RMS fit error is 9 mmag.

The period spectrum is littered with secondary signals, but the strongest signals are limited to multiples of $1/2$ our proposed period.

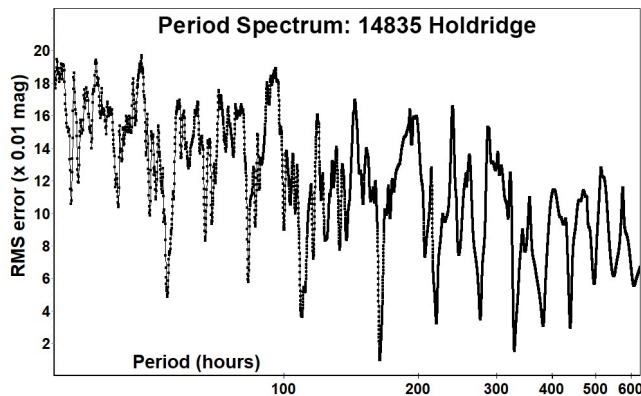


The unusual lightcurve shape warrants a call for confirming observations on 14815 Rutberg; unfortunately, apparitions through 2016 are fainter.

14835 Holdridge. Our rotation period estimate of 164.401 ± 0.029 h for this Phocaea-family asteroid is consistent with the only known previous limiting estimate ($P > 10$ h, Pravec et al., 2005web). The lightcurve is trimodal and of high amplitude, suggesting that the asteroid is non-convex in shape or markedly non-uniform in surface albedo. Our best G-value estimate was indistinguishable from MPC's default value of 0.15; Fourier fit RMS error is 10 mmag.



Our estimate's signal dominates the period spectrum and is significantly lower in RMS error than that of the second strongest signal (15 mmag) which corresponds to twice our estimate's duration but which represents an unrealistically complex lightcurve.



Acknowledgements

The author thanks all contributors to the ATLAS paper (Tonry et al 2018) for providing openly and without cost the ATLAS refcat2 catalog release. This current work also makes extensive use of the python language interpreter and of several supporting packages (notably: astropy, ccdproc, ephemeris, matplotlib, pandas, photutils, requests, skyfield, and statsmodels), all made available openly and without cost.

References

Aznar Macias, A.; Garcerán, A.C.; Mansego, E.A.; Rodriguez, P.B.; de Haro, J.L.; Silva, A.F.; Silva, G.F.; Martinez, V.M.; Chiner, O.R. (2016). "Twenty-Three Asteroids Lightcurves at Observadores de Asteroides (OBAS): 2015 October - December." *Minor Planet Bull.* **43**, 174-181.

Aznar Macias, A. (2017). "Lightcurve Analysis from APT Observatory Group for Nine Mainbelt Asteroids: 2016 July-September. Rotation Period and Physical Parameters." *Minor Planet Bull.* **44**, 60-63.

Behrend, R. (2006web, 2007web, 2015web, 2019web, 2021web, 2023web). Observatoire de Genève web site. http://obswww.unige.ch/~behrend/page_cou.html

Binzel, R.P. (1987). "A photoelectric survey of 130 asteroids." *Icarus* **72**, 135-208.

Carbo, L.; Green, D.; Kragh, K.; Krotz, J.; Meiers, A.; Patino, B.; Pligge, Z.; Shaffer, N.; Ditteon, R. (2009). "Asteroid Lightcurve Analysis at the Oakley Southern Sky Observatory: 2008 October thru 2009 March." *Minor Planet Bull.* **36**, 152-157.

Carbognani, A. (2011). "Lightcurves and Periods of Eighteen NEAs and MBAs." *Minor Planet Bull.* **38**, 57-63.

Chiorny, V.G.; Shevchenko, V.G.; Krugly, Y.N.; Velichko, F.P.; Gaftonyuk, N.M. (2007). "Photometry of asteroids: Lightcurves of 24 asteroids obtained in 1993-2005." *Planet. Space Sci.* **55**, 986-997.

Ditteon, R.; Trent, L. (2018). "Lightcurve Analysis of Minor Planets Observed at the Oakley Southern Sky Observatory: 2017 June-July." *Minor Planet Bull.* **45**, 328-329.

Dose, E.V. (2020). "A New Photometric Workflow and Lightcurves of Fifteen Asteroids." *Minor Planet Bull.* **47**, 324-330.

Dose, E.V. (2021). "Lightcurves of Nineteen Asteroids." *Minor Planet Bull.* **48**, 69-76.

Dose, E.V. (2023). "Lightcurves of Nineteen Asteroids." *Minor Planet Bull.* **50**, 65-73.

Đurech, J.; Hanuš, J.; Alí-Lagoa, V. (2018). "Asteroid models reconstructed from the Lowell Photometric Database and WISE data." *Astron. Astrophys.* **617**, A57.

Đurech, J.; Tonry, J.; Erasmus, N.; Denneau, L.; Heinze, A.N.; Flewelling, H.; Vančo, R. (2020). "Asteroid models reconstructed from ATLAS photometry." *Astron. Astrophys.* **643**, A59.

Ferrero, A.; Bonamico, R. (2020). "Lightcurves of Seven Main-Belt Asteroids." *Minor Planet Bull.* **47**, 147-149.

Gartrelle, G.M. (2012). "Lightcurve Results for Eleven Asteroids." *Minor Planet Bull.* **39**, 40-46.

Harris, A.W.; Young, J.W.; Scaltriti, F.; Zappala, V. (1984). "Lightcurves and phase relations of the asteroids 82 Alkeme and 444 Gyptis." *Icarus* **57**, 251-258.

Higgins, D. (2011). "Period Determination of Asteroid Targets Observed at Hunters Hill Observatory: May 2009 - September 2010." *Minor Planet Bull.* **38**, 41-46.

Oey, J. (2016). "Lightcurve Analysis of Asteroids from Blue Mountains Observatory in 2014." *Minor Planet Bull.* **43**, 45-51.

Pál, A.; Szakáts, R.; Kiss, C.; Bódi, A.; Bognár, Z.; Kalup, C.; Kiss, L.L.; Marton, G.; Molnár, L.; Plachy, E.; Sárneczky, K.; Szabó, G.M.; Szabó, R. (2020). "Solar System Objects Observed with TESS - First Data Release: Bright Main-belt and Trojan Asteroids from the Southern Survey." *Ap. J. Suppl. Ser.* **247**, id. 26.

Polakis, T. (2020). "Photometric Observations of Twenty-Three Minor Planets." *Minor Planet Bull.* **47**, 94-101.

Pravec, P.; Wolf, M.; Sarounova, L. (2005web, 2016web). Ondrejov Asteroid Photometry Project. <http://www.asu.cas.cz/~ppravec/neo.htm>

Simpson, G. and 10 colleagues (2013). "Asteroid Lightcurve Analysis at the Oakley Southern Sky Observatory: 2012 August-October." *Minor Planet Bull.* **40**, 146-151.

Stephens, R.D.; Warner, B.D. (2003). "Lightcurve Analysis for 5468 Hamatonbetsu: Insights into Merging Collaborative Data." *Minor Planet Bull.* **30**, 49-51.

Tonry, J.L.; Denneau, L.; Flewelling, H.; Heinze, A.N.; Onken, C.A.; Smartt, S.J.; Stalder, B.; Weiland, H.J.; Wolf, C. (2018). "The ATLAS All-Sky Stellar Reference Catalog." *Astrophys. J.* **867**, A105.

Warner, B.D. (2004). "Rotation Rates for Asteroids 875, 926, 1679, 1796, 3915, 4209, and 34817." *Minor Planet Bull.* **31**, 19-22.

Warner, B.D.; Harris, A.W.; Pravec, P. (2009). "The asteroid lightcurve database." *Icarus* **202**, 134-146. <https://minplanobs.org/MPInfo/php/lcdb.php>

Warner, B.D. (2011). "Upon Further Review: VI. An Examination of Previous Lightcurve Analysis from the Palmer Divide Observatory." *Minor Planet Bull.* **38**, 96-101.

Warner, B.D. (2021). *MPO Canopus* Software, version 10.8.4.11. BDW Publishing. <http://www.bdwpublishing.com>

Waszczak, A.; Chang, C.-K.; Ofeck, E.O.; Laher, R.; Masci, F.; Levitan, D.; Surace, J.; Cheng, Y.-Ch.; Ip, W.-H.; Kinoshita, D.; Helou, G.; Prince, T.A.; Kulkarni, S. (2015). "Asteroid Light Curves from the Palomar Transient Factory Survey: Rotation Periods and Phase Functions from Sparse Photometry." *Astron. J.* **150**, A75.

Yeh, T.-S.; Li, B.; Chang, C.-K.; Zhao, H.-B.; Ji, J.-H.; Lin, Z.-Y.; Ip, W.-H. (2020). "The Asteroid Rotation Period Survey Using the China Near-Earth Object Survey Telescope (CNEOST)." *Astron. J.* **160**, 73.

PHOTOMETRIC RESULTS FOR TEN MINOR PLANETS

Tom Polakis
Command Module Observatory
121 W. Alameda Dr.
Tempe, AZ 85282
tpolakis@cox.net

(Received: 2023 October 8 Revised: 2023 November 5)

Photometric measurements were made for 10 main-belt asteroids, based on CCD observations made from 2023 September through 2023 October. Phased lightcurves were created for all ten asteroids, and an orbital period was computed for one binary asteroid. All the data have been submitted to the ALCDEF database.

CCD photometric observations of 10 main-belt asteroids were performed at Command Module Observatory (MPC V02) in Tempe, AZ. Images were taken using a 0.32-m *f*/6.7 Modified Dall-Kirkham telescope, SBIG STXL-6303 CCD camera, and a 'clear' glass filter. Exposure time for all the images was 2 minutes. The image scale after 2×2 binning was 1.76 arcsec/pixel. Table I shows the observing circumstances and results. All of the images for these asteroids were obtained between 2023 September and 2023 October.

Images were calibrated using a dozen bias, dark, and flat frames. Flat-field images were made using an electroluminescent panel. Image calibration and alignment was performed using *MaxIm DL* software.

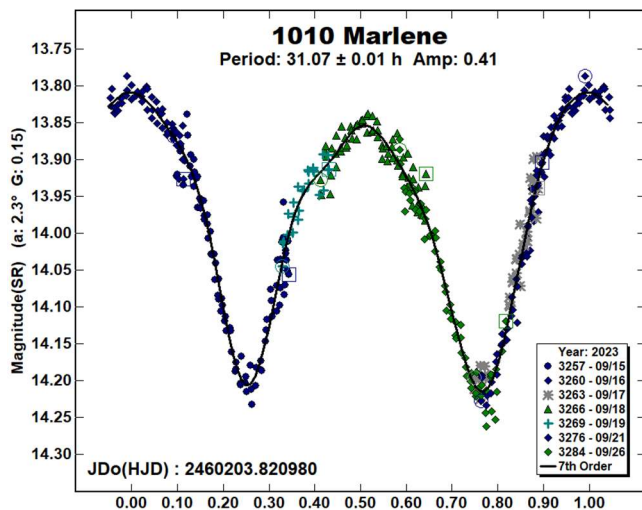
The data reduction and period analysis were done using *MPO Canopus* (Warner, 2023). The 45'×30' field of the CCD typically enables the use of the same field center for three consecutive nights. In these fields, the asteroid and three to five comparison stars were measured. Comparison stars were selected with colors within the range of $0.5 < B-V < 0.95$ to correspond with color ranges of asteroids. In order to reduce the internal scatter in the data, the brightest stars of appropriate color that had peak ADU counts below the range where chip response becomes nonlinear were selected. *MPO Canopus* plots instrumental vs. catalog magnitudes for solar-colored stars, which is useful for selecting comp stars of suitable color and brightness.

Since the sensitivity of the KAF-6303 chip peaks in the red, the clear-filtered images were reduced to Sloan *r'* to minimize error with respect to a color term. Comparison star magnitudes were obtained from the ATLAS catalog (Tonry et al., 2018), which is incorporated directly into *MPO Canopus*. The ATLAS catalog derives Sloan *griz* magnitudes using a number of available catalogs. The consistency of the ATLAS comp star magnitudes and color-indices allowed the separate nightly runs to be linked often with no zero-point offset required or shifts of only a few hundredths of a magnitude in a series.

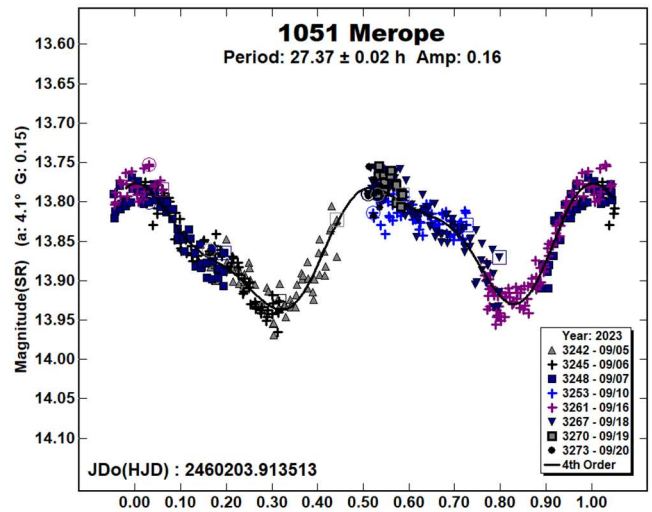
A 9-pixel (16 arcsec) diameter measuring aperture was used for asteroids and comp stars. It was typically necessary to employ star subtraction to remove contamination by field stars. For the asteroids described here, I note the RMS scatter on the phased lightcurves, which gives an indication of the overall data quality including errors from the calibration of the frames, measurement of the comp stars, the asteroid itself, and the period-fit. Period determination was done using the *MPO Canopus* Fourier-type FALC fitting method (cf. Harris et al., 1989). Phased lightcurves show the maximum at phase zero. Magnitudes in these plots are apparent and scaled by *MPO Canopus* to the first night.

Asteroids were selected from the CALL website (Warner, 2011), either for having uncertain periods or for needing more lightcurves for shape modeling. In this set of observations, 2 of the 10 asteroids had $U = 1$, and the remainder were rated as $U=2$. The Asteroid Lightcurve Database (LCDB; Warner et al., 2009) was consulted to locate previously published results. All the new data for these asteroids can be found in the ALCDEF database.

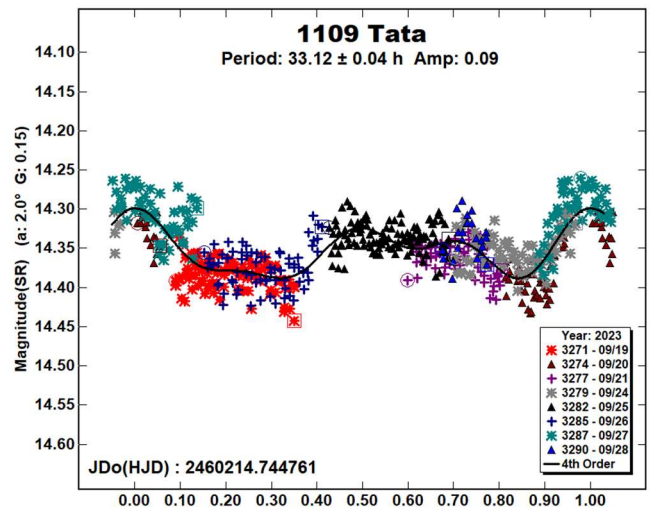
1010 Marlene was discovered in 1923 by Karl Reinmuth at Heidelberg. It lies in a highly eccentric and inclined orbit. Recent published rotation periods include Hanus et al. (2016) 31.0651 ± 0.0005 h and Pal et al. (2020) 31.0282 ± 0.0005 h. During seven nights, 403 images were used to determine a period of 31.07 ± 0.01 h, agreeing with previous values. The amplitude of the lightcurve is 0.41 ± 0.020 mag.



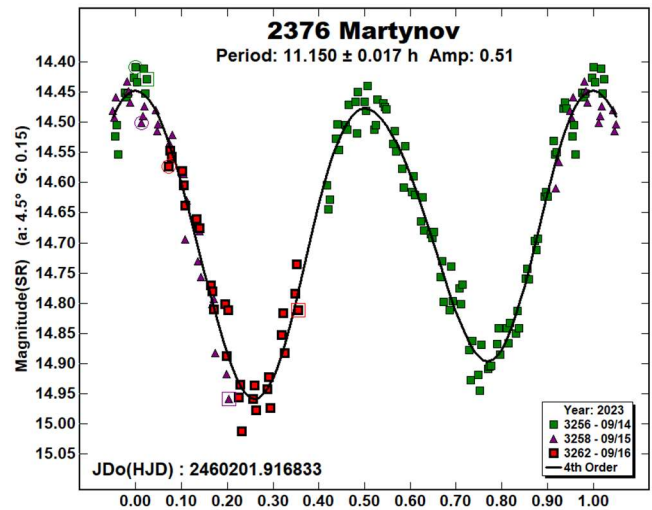
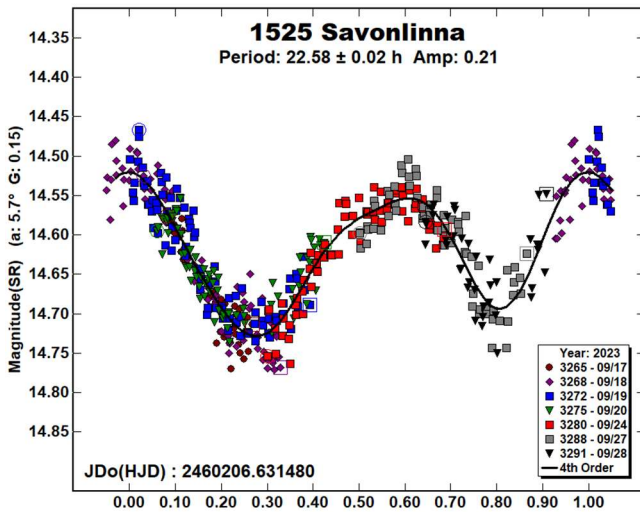
1051 Merope. This Alauda-family asteroid lies in an orbit that is inclined 23° to the ecliptic. It was discovered in 1925 by Karl Reinmuth at Heidelberg. Waszczak et al. (2015) found a rotation period of 13.717 ± 0.0164 h, while Pal et al. (2020) shows roughly half this value: 6.85563 ± 0.00005 h. Dose (2023) computed a period of 13.710 ± 0.001 h. A total of 491 images were taken over the course of eight nights, resulting in a period of 27.37 ± 0.02 h. This value is double that of Waszczak and Dose, and forcing their period solution results in a monomodal curve. The lightcurve has an amplitude of 0.16 mag, and an RMS error on the fit of 0.017 mag.



1109 Tata is another of Karl Reinmuth's discoveries from Heidelberg, in 1929. Behrend (2005web) computed a period of 8.277 ± 0.002 h, while Polakis (2020) shows 55.50 ± 0.12 h, with a poor curve fit. Eight nights and 586 data points were used to produce a period of 33.14 ± 0.04 h. Again, the fit is poor, with an RMS error of 0.025 mag on an amplitude of 0.09 mag. No significant signal could be found near the 55.50 h. Likewise, no signals near 33 h appeared in this author's 2020 dataset.

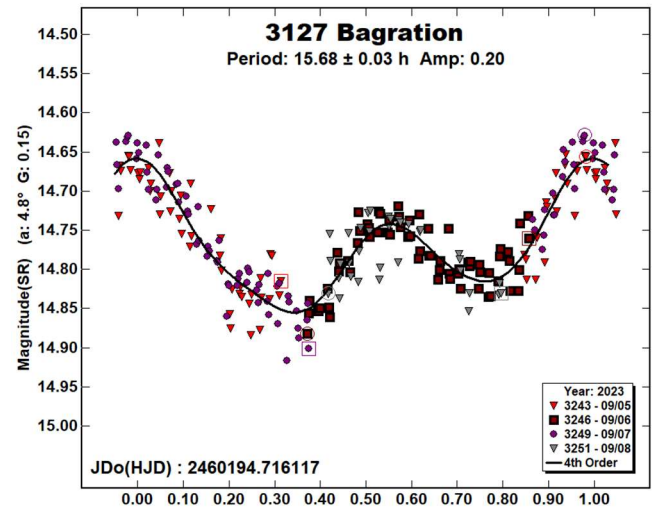
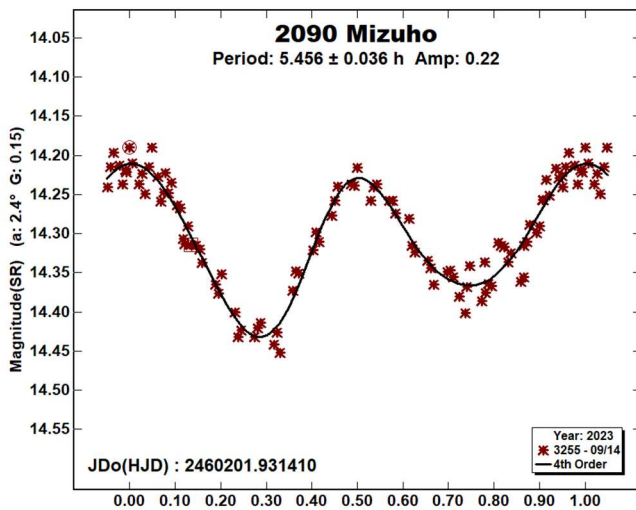


1525 Savonlinna. Yrjö Väisälä discovered this minor planet at Turku in 1939. Its high eccentricity of 0.26 resulted in a favorable 2023 opposition, during which 475 images were gathered in seven nights. The LCDB shows two period solutions: Gattelle (2012), 14.634 ± 0.002 h, and Waszczak et al. (2015), 22.841 ± 0.0296 h. This analysis produced a period of 22.58 ± 0.02 h, with an amplitude of 0.21 ± 0.03 mag, agreeing with Waszczak's value.



2090 Mizuho, an outer main-belt asteroid, was discovered in 1978 at Yakimo Station by Takeshi Urata. Brinsfield (2010) published a period of 5.47 ± 0.01 , and Durech et al. (2018) computed 5.4793 ± 0.0002 h. One night with 97 images was sufficient to calculate a similar period of 5.456 ± 0.036 h. The amplitude of the lightcurve is 0.22 ± 0.019 mag.

3127 Bagration is an inner main-belt asteroid. Its discovery was also made by Nikolai Chernykh at Nauchnyj, in 1973. No precise periods were found in the LCDB. After four nights during this favorable opposition, 233 data points were used to compute a synodic period of 15.68 ± 0.03 h, with an amplitude of 0.20 ± 0.026 mag.

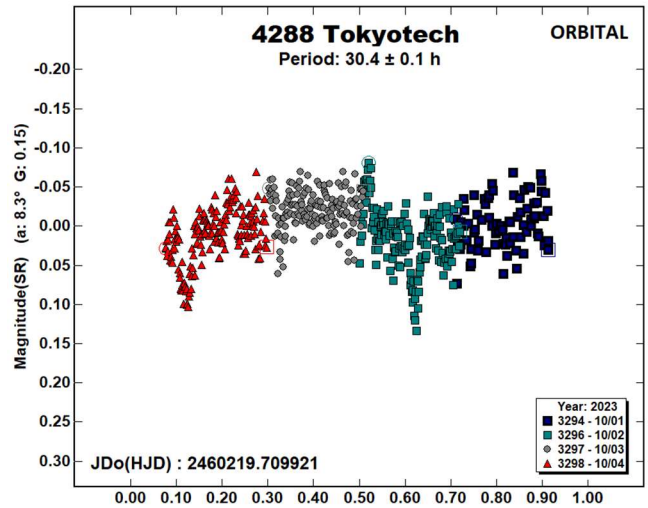
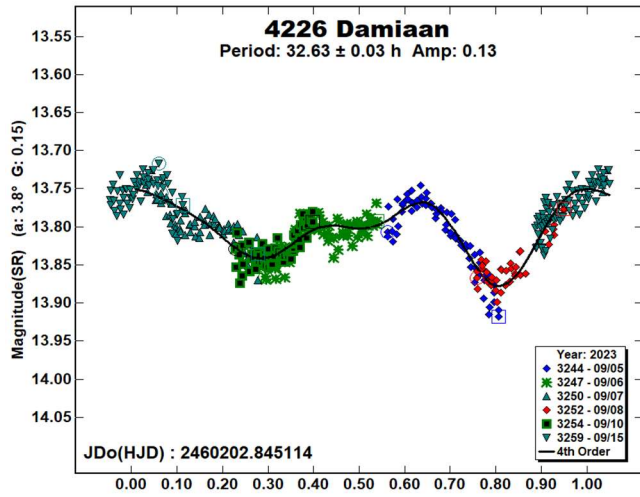


2376 Martynov. This asteroid was discovered in 1977 by Nikolai Chernykh at Nauchnyj. The only period solution in the LCDB belongs to Schmalz et al. (2022), 11.133 ± 0.005 h. One hundred and fifty points were taken during three nights, to arrive at a rotation period of 11.150 ± 0.017 h, agreeing with Schmalz's result. The lightcurve has an amplitude of 0.51 mag, with an RMS error of 0.032 mag.

4226 Damiaan. Eric Elst discovered this asteroid in 1989 at Haute Provence. The LCDB shows no precise period solutions. A total of 420 data points were acquired on six nights, resulting in a rotation period of 32.63 ± 0.03 h. The amplitude of the lightcurve is 0.13 mag, with an RMS error of 0.016 mag.

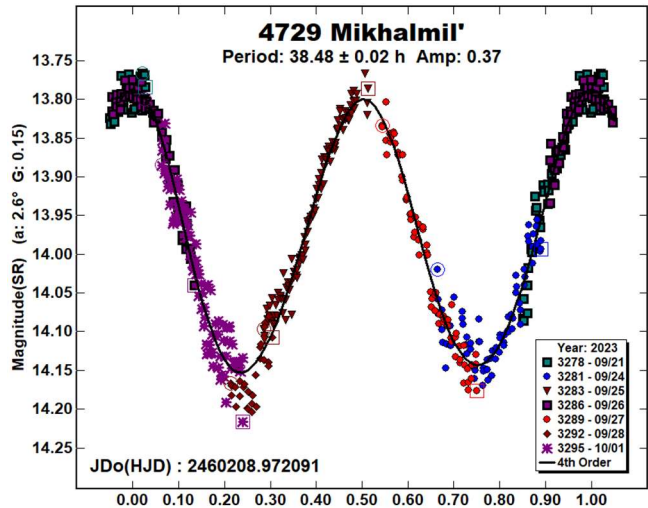
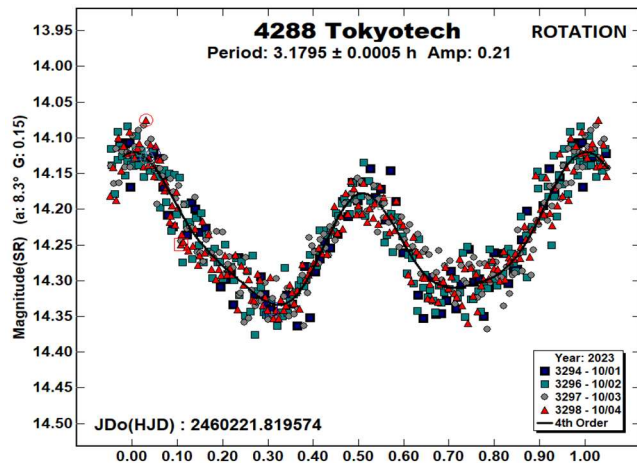
Number	Name	yy/mm/dd	Phase	L _{PAB}	B _{PAB}	Period(h)	P.E.	Amp	A.E.	Grp
1010	Marlene	23/09/15-09/26	2.5, 5.3	352	-5	31.07	0.01	0.41	0.02	MB-O
1051	Merope	23/09/05-09/20	4.0, 6.6	343	9	27.37	0.02	0.16	0.02	ALA
1109	Tata	23/09/19-09/28	*2.0, 3.3	357	5	33.14	0.04	0.09	0.03	PAL
1525	Savonlinna	23/09/17-09/28	5.7, 8.6	354	9	22.58	0.02	0.21	0.03	MB-M
2090	Mizuho	23/09/14-09/14	2.4, 2.5	346	2	5.456	0.036	0.22	0.02	MB-O
2376	Martynov	23/09/14-09/16	4.5, 5.2	342	-5	11.150	0.017	0.51	0.03	MB-O
3127	Bagration	23/09/05-09/08	4.8, 3.9	348	6	15.68	0.03	0.20	0.03	MB-I
4226	Damiaan	23/09/05-09/15	*3.7, 5.6	344	6	32.63	0.03	0.13	0.02	MB-O
4288	Tokyotech	23/10/01-10/04	8.3, 8.8	2	14	3.1795	0.0005	0.21	0.03	EUN
						30.4	0.1	0.10	0.02	
4729	Mikhailmil'	23/09/21-10/01	2.6, 6.8	358	3	38.48	0.02	0.37	0.02	MB-I

Table I. Observing circumstances and results. The phase angle is given for the first and last date. If preceded by an asterisk, the phase angle reached an extrema during the period. L_{PAB} and B_{PAB} are the approximate phase angle bisector longitude/latitude at mid-date range (see Harris et al., 1984). Grp is the asteroid family/group (Warner et al., 2009).



4288 Tokyotech was discovered in 1989 by Takuo Kojima at Chiyoda. Koff (2003) published a period of 3.181 ± 0.001 h. Augustin (2019) reported a rotation period of 3.1800 ± 0.0003 h, and made note of the discovery of a secondary body that orbits with a period of 30.264 ± 0.012 h. During four nights of dedicated observing on this single target, 585 images were gathered. Using several iterations with the dual-period search feature in *MPO Canopus*, the rotation period is 3.1795 ± 0.0005 h. Mutual events were apparent, showing a strong signal in the period spectrum, with two discrepant events overlaid at 15.2 h. Therefore, the orbital period was forced to be double this value, 30.4 h. Rotation and orbital lightcurves are provided.

4729 Mikhailmil'. Lyudmilla Zhuravleva discovered this inner main-belt asteroid in 1990 at Nauchnyj. The most recent period solutions in the LCDB are Durech et al. (2019), 38.4856 ± 0.0002 h, and Polakis (2021), 38.31 ± 0.03 h. During seven nights, 512 images were acquired, resulting in a period of 38.48 ± 0.02 h, and an amplitude of 0.37 ± 0.021 mag.



Acknowledgements

The author would like to express his gratitude to Brian Skiff for his indispensable mentoring in data acquisition and reduction. Thanks also go out to Brian Warner for support of his *MPO Canopus* software package.

References

- Augustin, D. and 8 colleagues (2019). “(4288) Tokyotech.” *CBET*, 4705.
- Behrend, R. (2005web). Observatoire de Geneve web site. http://obswww.unige.ch/~behrend/page_cou.html
- Brinsfield J. (2010). “Asteroid Lightcurve Analysis at the Via Capote Observatory: 2010 February - May.” *Minor Planet Bull.* **37**, 146-147.
- Dose, E. (2023). “Lightcurves of Nineteen Asteroids.” *Minor Planet Bull.* **50**, 65-73.
- Durech, J.; Hanus, J.; Ali-Lagoa, V. (2018). “Photometric Observations of Seventeen Minor Planets.” *Astron. Astrophys.* **617**, A57-A64.
- Durech, J.; Hanus, J.; Vanco, R. (2019). “Inversion of asteroid photometry from Gaia DR2 and the Lowell Observatory photometric database.” *Astron. Astrophys.* **631**, A2-A5.
- Gatelle, G. (2012). “Lightcurve Results for Eleven Asteroids.” *Minor Planet Bull.* **39**, 40-46.
- Hanus, J. and 19 colleagues (2016). “New and updated convex shape models of asteroids based on optical data from a large collaboration network.” *Astron. Astrophys.* **586**, 108-131.
- Harris, A.W.; Young, J.W.; Scaltriti, F.; Zappala, V. (1984). “Lightcurves and phase relations of the asteroids 82 Alkmene and 444 Gytis.” *Icarus* **57**(2), 251-258.
- Harris, A.W.; Young, J.W.; Bowell, E.; Martin, L.J.; Millis, R.L.; Poutanen, M.; Scaltriti, F.; Zappala, V.; Schober, H.J.; Debehogne, H.; Zeigler, K.W. (1989). “Photoelectric Observations of Asteroids 3, 24, 60, 261, and 863.” *Icarus* **77**, 171-186.
- Koff, R. (2003). “Lightcurve photometry of 2890 Vilyujsk, 3106 Morabito, (4288) 1989 TQ1.” *Minor Planet Bull.* **30**, 38-39.
- Pal, A.; Szakáts, R.; Kiss, C.; Bódi, A.; Bognár, Z.; Kalup, C.; Kiss, L.L.; Marton, G.; Molnár, L.; Plachy, E.; Sárneczky, K.; Szabó, G.M.; Szabó, R. (2020). “Solar System Objects Observed with TESS - First Data Release: Bright Main-belt and Trojan Asteroids from the Southern Survey.” *Ap. J. Suppl. Ser.* **247**, id. 26.
- Polakis, T. (2020). “Photometric Observations of Thirty Minor Planets.” *Minor Planet Bull.* **47**, 177-184.
- Polakis, T. (2021). “Period Determinations for Seventeen Minor Planets.” *Minor Planet Bull.* **48**, 158-163.
- Schmalz, S. and 19 colleagues (2022). “Photometric Observations and Rotation Periods of Asteroids 2376 Martynov, (7335) 1989 JA, 12923 Zephyr, and (85184) 1991 JG1.” *Minor Planet Bull.* **49**, 291-295.
- Tonry, J.L.; Denneau, L.; Flewelling, H.; Heinze, A.N.; Onken, C.A.; Smartt, S.J.; Stalder, B.; Weiland, H.J.; Wolf, C. (2018). “The ATLAS All-Sky Stellar Reference Catalog.” *Astrophys. J.* **867**, 105-120.
- Warner, B.D., Harris, A.W., Pravec, P. (2009). “The Asteroid Lightcurve Database.” *Icarus* **202**, 134-146. Updated 2023 Oct. <http://www.minorplanet.info/lightcurvedatabase.html>
- Warner, B.D. (2011). Collaborative Asteroid Lightcurve Link website. <http://www.minorplanet.info/call.html>
- Warner, B.D. (2023). MPO Canopus Software. <http://bdwpublishing.com>
- Waszczak, A.; Chang, C.-K.; Ofeck, E.O.; Laher, R.; Masci, F.; Levitan, D.; Surace, J.; Cheng, Y.-Ch.; Ip, W.-H.; Kinoshita, D.; Helou, G.; Prince, T.A.; Kulkarni, S. (2015). “Asteroid Light Curves from the Palomar Transient Factory Survey: Rotation Periods and Phase Functions from Sparse Photometry.” *Astron. J.* **150**, 75-109.

LIGHTCURVE AND ROTATION PERIOD ANALYSIS OF 4226 DAMIAAN AND (25242) 1998 UH15

W. Hawley
Old Orchard Observatory (Z09)
The Old Orchard House, Church Road
Fiddington, UK, TA5 1JG
hawley.wayne@gmail.com

R. Miles
British Astronomical Association

P. Wiggins
University of Utah
Tooele Observatory (718)

J. McCormick
Farm Cove Observatory (E85)
24 Rapallo Place, Farm Cove
Auckland 2012, New Zealand

M. Dawson
Longitude 16.5402 E
Latitude 38.7655 N
Height 132.0 m (247)

F. Pilcher
Organ Mesa Observatory (G50)
4438 Organ Mesa Loop
Las Cruces, NM 88011 USA

(Received: 2023 Oct 12 Revised: 2023 Oct 15)

Photometric observations of two main-belt asteroids were obtained between 2023 July 7 and 2021 October 3. The following rotational periods were determined: 4226 Damiaan, 32.639 ± 0.005 h; (25242) 1998 UH15, 7.869 ± 0.002 h. Images were obtained from observatories around the globe. Several of the co-authors used their own equipment while others used the Las Cumbres Observatory facilities.

Photometry and period determination were carried out using *TychoTracker Pro* Version 10.7.5. (TT), easily performing both functions. Photometric analysis was done using standard differential techniques on images. The TT software has the facility to allow the user to choose comparison stars, for which the default color range of $+0.50 < (B-V) < +0.90$ was employed. The Carlsberg Meridian Catalog (CMC15) catalog was used as the source of reference stars for 4226 Damiaan, whereas the UCAC4 magnitude database was used as the reference catalog for photometry of (25242) 1998 UH15. TT's period determination operates by finding model light curves - comprising a user-defined number of Fourier components which best fit the asteroid photometric data. The program lists the candidate periods found within a user-defined period range and sampling frequency, based on minimizing Root Mean Square Errors (RMSE), i.e., using the difference between modelled and photometric magnitudes. The candidate periods are listed in increasing RMSE value and the entire suite of RMSE values is plotted as a "periodogram" for quality control.

In these periodograms, both objects yielded clear 'best-fit' period solutions having well-defined 'stalactites' as shown in the following Figures. 4226 Damiaan (1989 RE) has a previously published rotation period of approximately 24 hours (Behrend, 2004web), but this value has been assigned an quality value of

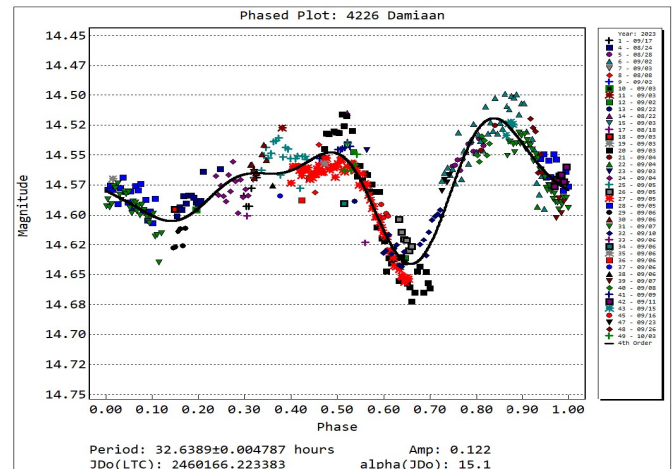
$U = 1$, i.e., it is unlikely to be correct. The period reported in this work is very different to that previously published online.

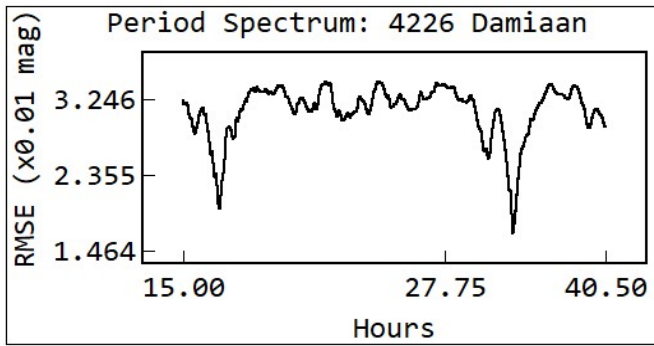
Periodograms often exhibit several possible candidate periods, in which case an examination of the rotational phase plot for each of these is then conducted looking for a credible lightcurve. Where the object shape is the dominant factor in producing the observed magnitude changes (typically having lightcurve amplitudes of >0.2 mag), the rotational phase plot often has two peaks and two troughs (bimodal) and this is usually chosen as the most likely for such asteroids.

In this paper, there is no attempt to find an absolute magnitude for any of the asteroids and a value of $G = 0.15$ has been used throughout the calculations. Time-series from different nights and observing locations using a variety of imaging equipment were offset in magnitude to bring them into alignment when producing the raw and rotational-phase plots. The same offset was used for each instance of an individual imaging setup. When this paper is accepted for publication all the observations will be loaded into the ALCDEF database. Some individual datapoints have been combined by stacking during period analysis to improve the signal-to-noise ratio.

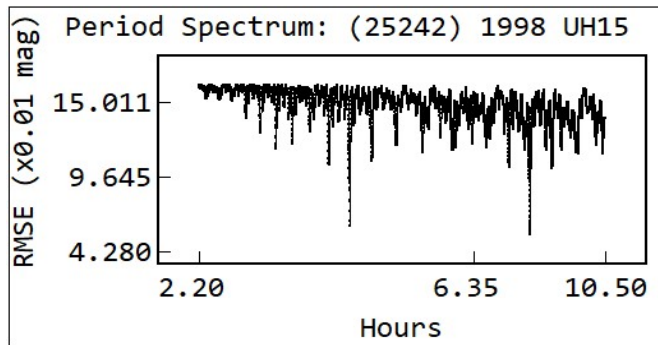
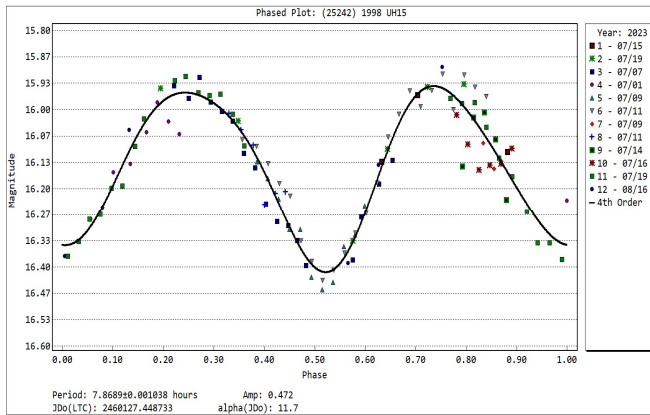
The results are summarized in Table I. Column 3 gives the span of dates over which the observations were made. Column 4 is the range of phase angles for each date range; if this is preceded by an asterisk, the asteroid passed through opposition during the observing period. Columns 5 and 6 give the range of values for the Phase Angle Bisector (PAB) longitude and latitude respectively. Column 7 gives the period and Column 8 the minimum possible formal error in hours given by *TychoTracker Pro*. Columns 9 and 10 give the amplitude and its associated uncertainty in magnitude. Dips in the results from the period analysis have been checked to see if they are monomodal or bimodal and bimodal periods have been chosen for the best-fit period for each asteroid. Information given below for each of the objects is taken from the JPL Small-Body Database Lookup webpage.

4226 Damiaan is an outer main-belt asteroid that was discovered on 1989 September 1 by Eric W. Elst at Haute Provence, France. It has approximate diameter of 31 km. Behrend (2004web) from observations by Laurent Bernasconi suggested a rotation period of 24 h based on a very fragmentary partial lightcurve. The lightcurve period and amplitude results reported here are based on 49 observing sessions (a total of 2451 exposures) during 2023 July - October (32.639 ± 0.005 h, 0.12 ± 0.02 mag).





(25242) 1998 UH15 is a member of the Eunomia family. It was discovered on 1998 October 20 by R.G. Davis from Granville, MA, USA. It is a relatively small object having an approximate diameter of 5 km. No previously published rotation period has been found. Lightcurve period and amplitude results from 12 sessions (529 exposures) are reported for 2023 July - August (7.869 ± 0.002 h, 0.47 ± 0.04 mag).



Acknowledgements

Our thanks are extended to Daniel Parrott, author of *TychoTracker Pro*.

References

Behrend, R. (2004web). Observatoire de Geneve web site. <https://obswww.unige.ch/~behrend/page4cou.html>

Harris, A.W.; Young, J.W.; Scaltriti, F.; Zappala, V. (1984). "Lightcurves and phase relations of the asteroids 82 Alkmene and 444 Ggyptis." *Icarus* **57**, 251-258.

JPL Small-Body Database Lookup. https://ssd.jpl.nasa.gov/tools/sbdb_lookup.html

Warner, B.D.; Harris, A.W.; Pravec, P. (2009). "The Asteroid Lightcurve Database." *Icarus* **202**, 134-146. Updated: 2023 Oct. 1. <https://minorplanet.info/php/lcdb.php>

Observatory	Telescope	CCD/CMOS	Filter	Asteroid (Sessions)
Old Orchard (Z09, Hawley)	0.25-m f/10 SCT	SX694 Trius Pro (2x2)	SG/SR	4226 (12) 25242 (5)
University of Utah, Tooele (718, Wiggins)	0.35-m f/5.5 SCT	ST-10XME (3x3)	C	4226 (11) 25242 (4)
Farm Cove (E85, McCormick)	0.35-m f/10 SCT	ST-8XME (2x2)	C	4226 (1)
Siding Spring LCO-A (Q63, Miles)	1.0-m f/8	Sinistro (1x1)	SR	4226 (11)
Siding Spring Faulkes Telescope South (E10, Miles)	2.0-m f/10	Spectral (2x2)	SR/V	4226 (18) 25242 (3)
Siding Spring LCO-B (Q64, Miles)	1.0-m f/8	Sinistro (1x1)	SR/V	4226 (5)
Sutherland LCO-A (K91, Miles)	1.0-m f/8	Sinistro (1x1)	SR	4226 (1)
Sutherland LCO-C (K93, Miles)	1.0-m f/8	Sinistro (1x1)	SR	4226 (1)
McDonald LCO-A (V37, Miles)	1.0-m f/8	Sinistro (1x1)	SR/V	4226 (3)
McDonald LCO Aqawan A #1 (V38, Miles)	0.4-m f/8	SBIG STL6303 (1x1)	SR	4226 (2)
16.5402 East 38.7655 North (247, Dawson)	0.5-m f/3.76 Newtonian	Apogee U9000 (1x1)	C	4226 (1)
Organ Mesa Las Cruces (G50, Pilcher)	0.35-m f/10 SCT	SBIG STL-1001E (1x1)	C	4226 (3)

Table II. The first three columns are the observers, equipment used, and filters (Sx = Sloan; C = clear or unfiltered). The fourth column is the number of the asteroid observed and, in parentheses, the number of sessions for that asteroid.

Number	Name	yyyy mm/dd	Phase	L _{PAB}	B _{PAB}	Period (h)	P.E.	Amp	A.E.	Grp
4226	Damiaan	2023 07/26-10/03	*3.6, 15.1	344	6	32.639	0.005	0.121	0.015	9106
25242	1998 UH15	2023 07/07-08/16	11.3, 20.6	286	19	7.869	0.002	0.470	0.044	502

Table I. Observing circumstances and results. The phase angle is given for the first and last date. If preceded by an asterisk, the phase angle reached a minimum during the period. L_{PAB} and B_{PAB} are the approximate phase angle bisector longitude/latitude at mid-date range (see Harris et al., 1984). Grp is the asteroid family/group (Warner et al., 2009).

COLLABORATIVE ASTEROID PHOTOMETRY FROM UAI: 2023 JULY-SEPTEMBER

Lorenzo Franco
Balzaretto Observatory (A81), Rome, ITALY
lor_franco@libero.it

Giulio Scarfi
Iota Scorpis Observatory (K78), La Spezia, ITALY

Giorgio Baj
M57 Observatory (K38), Saltrio, ITALY

Marco Iozzi
HOB Astronomical Observatory (L63)
Capraia Fiorentina, ITALY

Matteo Lombardo
Zen Observatory (M26), Scandicci, ITALY

Alessandro Marchini, Riccardo Papini
Astronomical Observatory, University of Siena (K54)
Via Roma 56, 53100 - Siena, ITALY

Carmelo Falco, Alessandro Nastasi
GAL Hassin, Centro Internazionale per le Scienze Astronomiche
(GRT2 - L34), Isnello, ITALY

Paolo Fini, Guido Betti, Julie Arangio
Blessed Hermann Observatory (L73), Impruneta, ITALY

Paolo Bacci, Martina Maestripieri
GAMP - San Marcello Pistoiese (104), Pistoia, ITALY

Nico Montigiani, Massimiliano Mannucci
Osservatorio Astronomico Margherita Hack (A57)
Florence, ITALY

Alessandro Coffano, Wladimiro Marinello
Osservatorio Serafino Zani (130), Lumezzane, ITALY

Pietro Aceti, Massimo Banfi
Osservatorio Liceo Iris Versari, Felizzano, ITALY

Gianni Galli
GiaGa Observatory (203), Pogliano Milanese, ITALY

Nello Ruocco
Osservatorio Astronomico Nastro Verde (C82)
Sorrento, ITALY

Luciano Tinelli
GAV (Gruppo Astrofili Villasanta), Villasanta, ITALY

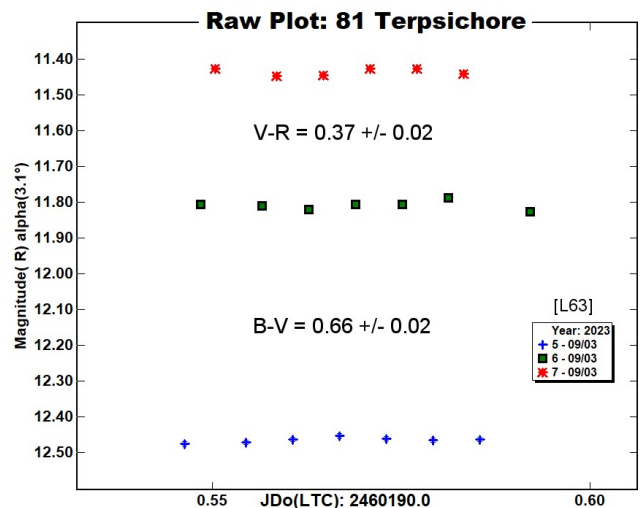
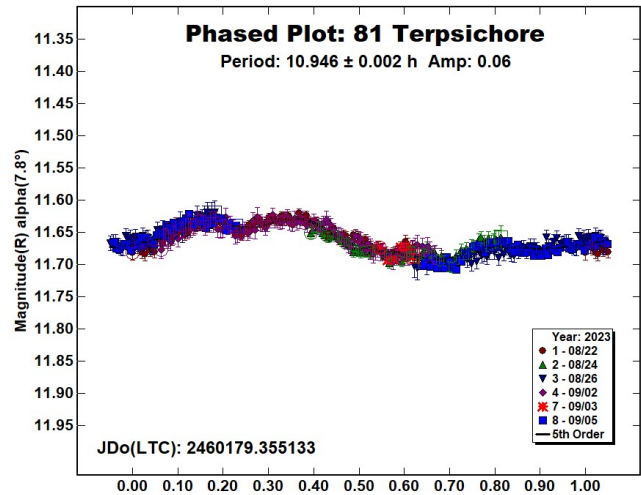
(Received: 2023 October 12)

Photometric observations of nine asteroids were made in order to acquire lightcurves for shape/spin axis modeling. Lightcurves were acquired for 81 Terpsichore, 238 Hypatia, 773 Irmintraud, 862 Franzia, 894 Erda, 914 Palisana, 2763 Jeans, 5766 Carmelofalco, and (458732) 2011 MD5.

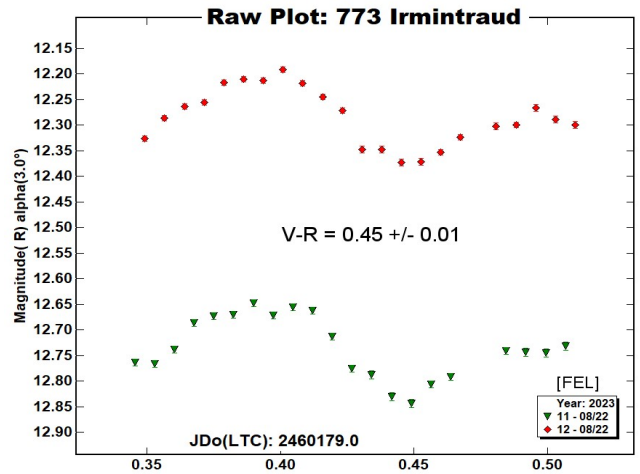
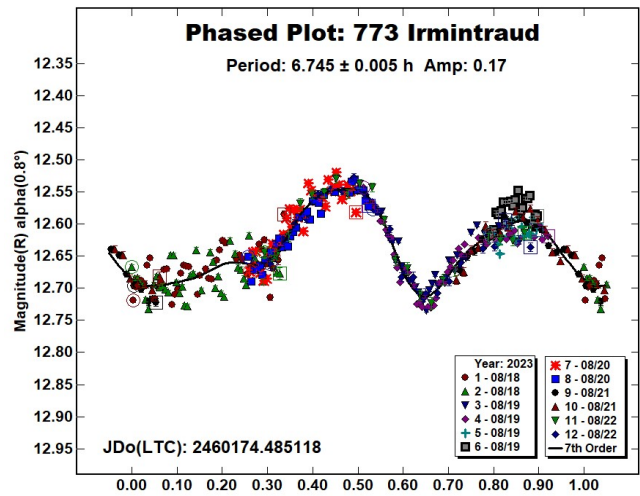
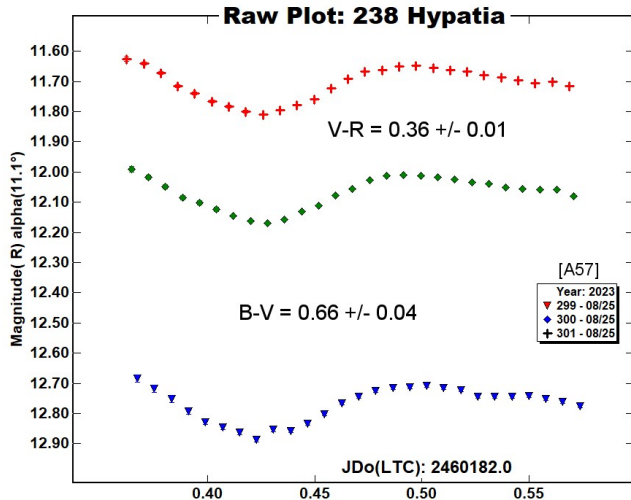
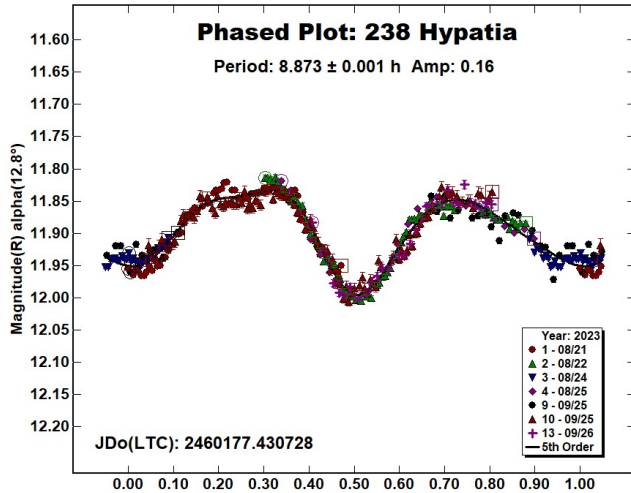
Collaborative asteroid photometry was done inside the Italian Amateur Astronomers Union (UAI; 2023) group. The targets were selected mainly in order to acquire lightcurves for shape/spin axis modeling. Table I shows the observing circumstances and results.

The CCD observations of nine asteroids were made in 2023 July - September using the instrumentation described in the Table II. Lightcurve analysis was performed at the Balzaretto Observatory with *MPO Canopus* (Warner, 2021). All the images were calibrated with dark and flat frames and converted to standard magnitudes using solar colored field stars from CMC15 and ATLAS catalogues, distributed with *MPO Canopus*. For brevity, the following citations to the asteroid lightcurve database (LCDB; Warner et al., 2009) will be summarized only as "LCDB".

81 Terpsichore is a Cb-type (Bus and Binzel, 2002) outer main-belt asteroid. Collaborative observations were made over five nights. The period analysis shows a synodic period of $P = 10.946 \pm 0.002$ h with an amplitude $A = 0.06 \pm 0.01$ mag. The period is close to the previously published results in the LCDB. Multiband photometry was made by M. Iozzi (L63) on 2023 September 3. We found $B-V = 0.66 \pm 0.02$ and $V-R = 0.37 \pm 0.02$, which are consistent with a C-type asteroid (Shevchenko and Lupishko, 1998).



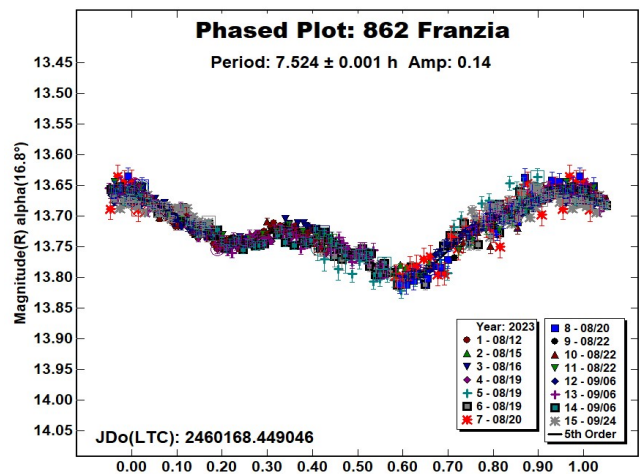
238 Hypatia is a Ch-type (Bus and Binzel, 2002) outer main-belt asteroid. Collaborative observations were made over six nights. The period analysis shows a synodic period of $P = 8.873 \pm 0.001$ h with an amplitude $A = 0.16 \pm 0.03$ mag. The period is close to the previously published results in the LCDB. Multiband photometry was made by N. Montigiani and M. Mannucci (A57) and by G. Baj (K38), respectively on 2023 August 25 and 2023 September 25-26. We found $B-V = 0.66 \pm 0.04$ and $V-R = 0.36 \pm 0.01$ as the average of three values. These color indices are consistent with a C-type asteroid (Shevchenko and Lupishko, 1998).

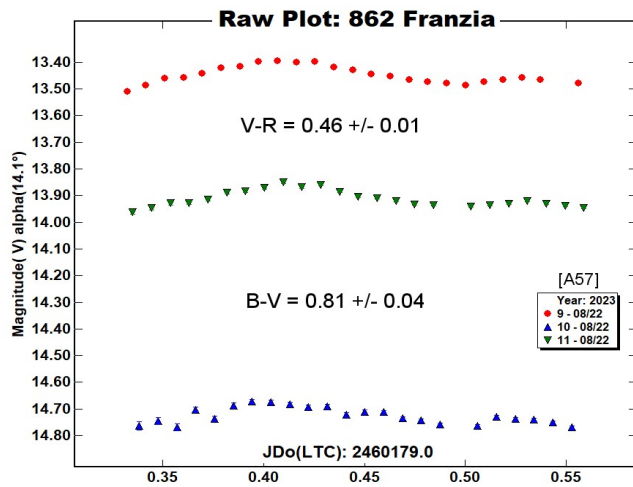


862 Franzia is a S-type (Bus and Binzel, 2002) middle main-belt asteroid. Collaborative observations were made over eight nights. The period analysis shows a synodic period of $P = 7.524 \pm 0.001$ h with an amplitude $A = 0.14 \pm 0.03$ mag.

773 Irmintraud is a T-type (Bus and Binzel, 2002) outer main-belt asteroid. Collaborative observations were made over six nights. The period analysis shows a synodic period of $P = 6.745 \pm 0.005$ h with an amplitude $A = 0.17 \pm 0.03$ mag. The period is close to the previously published results in the LCDB.

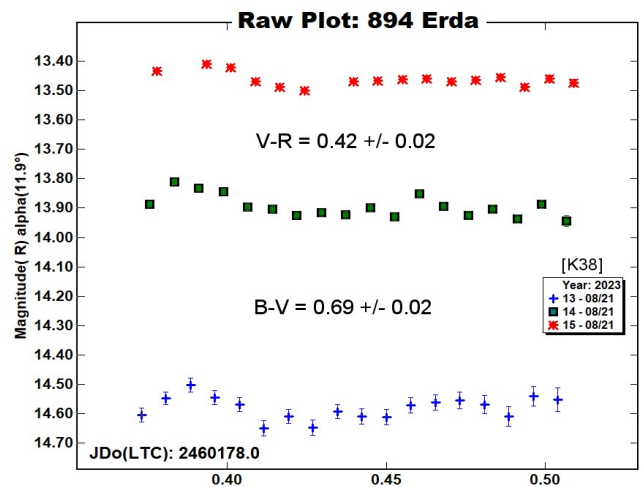
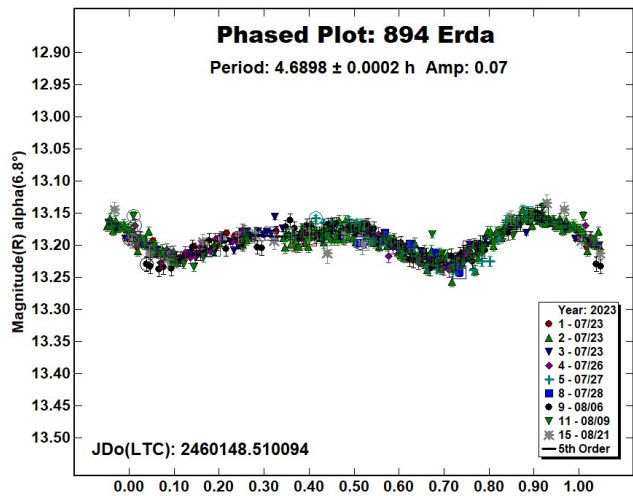
Multiband photometry was made by P. Fini and G. Betti (L73) and by P. Aceti and M. Banfi, respectively, on 2023 August 17-20 and 2023 August 21-22. We found $V-R = 0.45 \pm 0.01$ as the average of six values. This color index is consistent with T-type asteroid (Pravec, 2012).





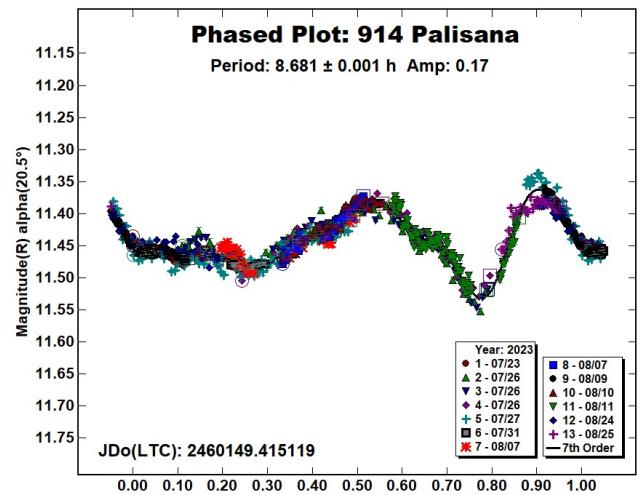
The period is close to the previously published results in the LCDB. Multiband photometry was made by N. Montigiani and M. Mannucci (A57) and by G. Baj (K38), respectively (BVR) on 2023 August 22 and (VR) 2023 August 19-20, September 7. We found $B-V = 0.81 \pm 0.04$ and $V-R = 0.46 \pm 0.01$, this last as the average of four values. These color indices are consistent with a S-type asteroid (Shevchenko and Lupishko, 1998).

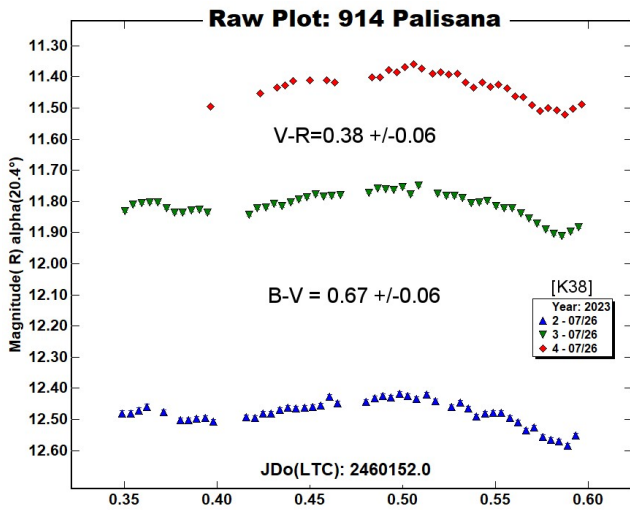
894 Erda is a low-medium albedo outer main-belt asteroid. Collaborative observations were made over seven nights. The period analysis shows a synodic period of $P = 4.6898 \pm 0.0002$ h with an amplitude $A = 0.07 \pm 0.02$ mag.



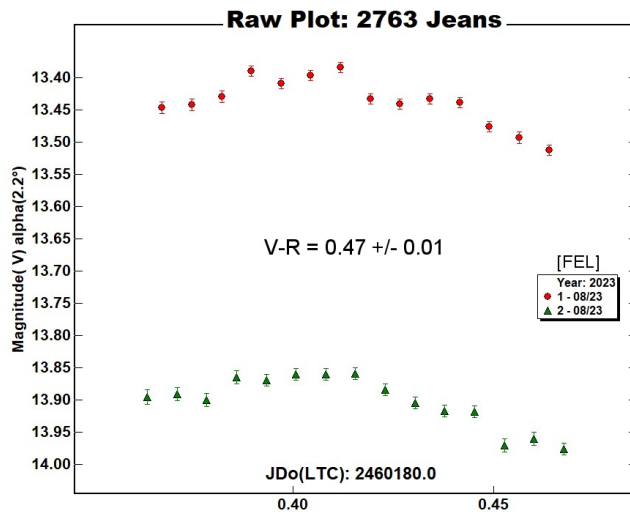
The period is close to the previously published results in the LCDB. Multiband photometry was made by M. Iozzi (L63) and by G. Baj (K38), respectively on 2023 July 28 and 2023 August 21. We found $B-V = 0.69 \pm 0.02$ and $V-R = 0.42 \pm 0.02$ as the average of a pair of two values. These color indices are close to M-type asteroid (Shevchenko and Lupishko, 1998).

914 Palisana is a CU-type (Tholen, 1984) inner main-belt asteroid. Collaborative observations were made over nine nights. The period analysis shows a synodic period of $P = 8.681 \pm 0.001$ h with an amplitude $A = 0.17 \pm 0.03$ mag. The period is close to the previously published results in the LCDB. Multiband photometry was made by G. Baj (K38) on 2023 July 26. We found $B-V = 0.67 \pm 0.06$ and $V-R = 0.38 \pm 0.05$, which are close to C-type asteroid (Shevchenko and Lupishko, 1998).

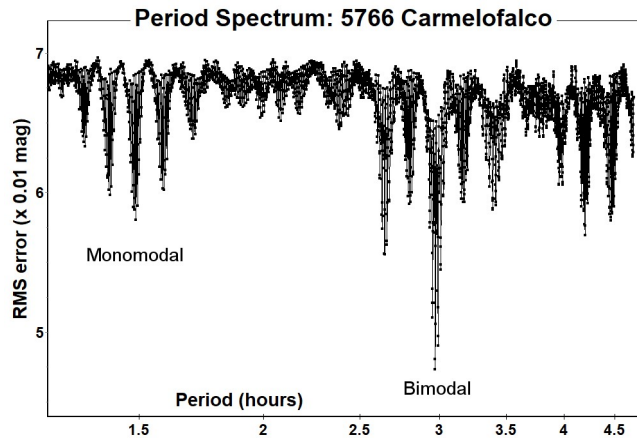
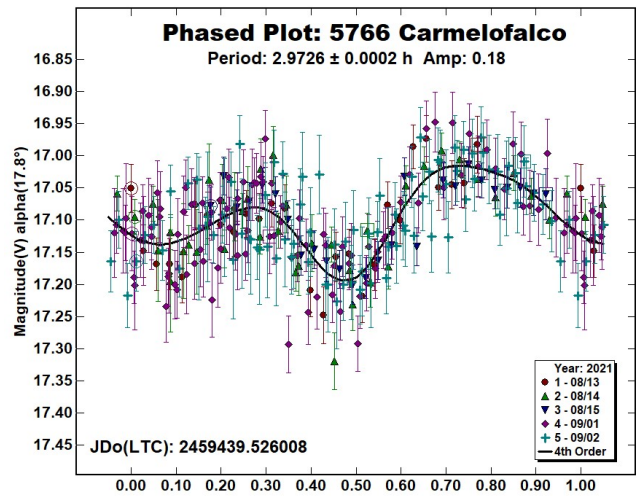




2763 Jeans is a V-type (Bus and Binzel, 2002) inner main-belt asteroid. Multiband photometry was made by P. Aceti and M. Banfi and M. Iozzi (L63), respectively on 2023 August 23 and 2023 September 3. We found $V-R = 0.47 \pm 0.01$ as the average of two values. This color index is consistent with V-type asteroid (Pravec, 2012).



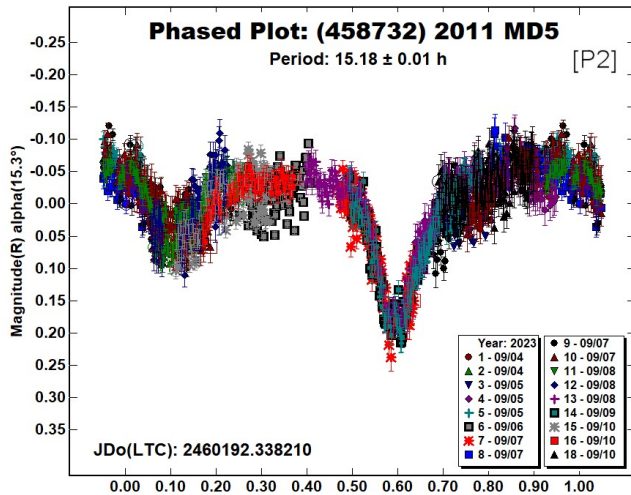
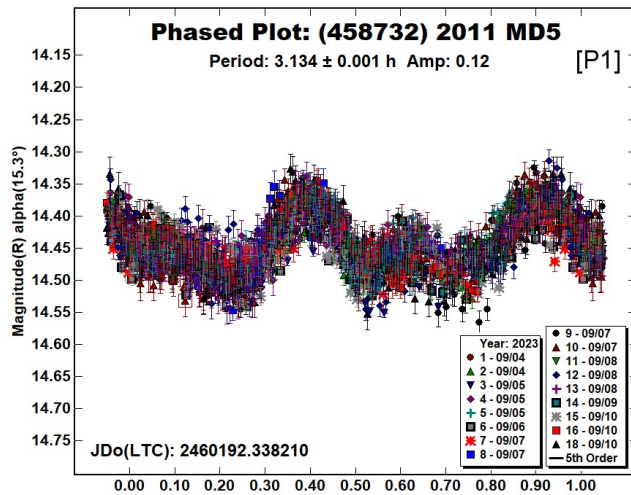
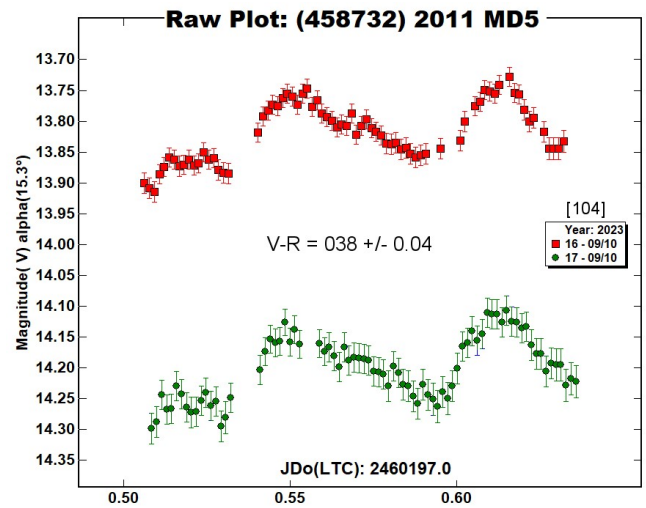
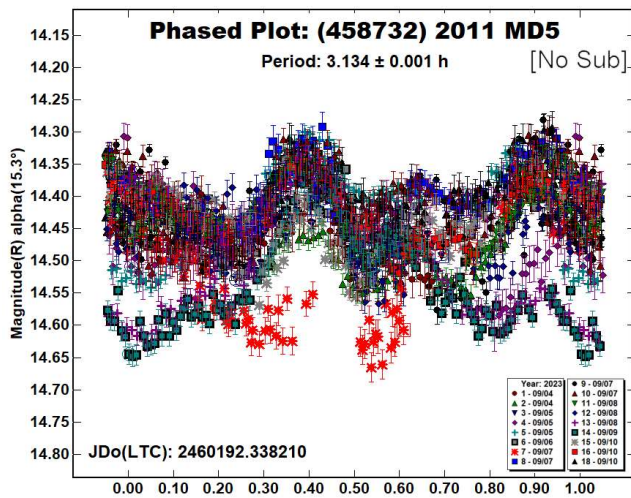
5766 Carmelofalco is a high albedo inner main-belt asteroid. Observations were made over five nights by C. Falco and A. Nastasi (L34). We found a bimodal solution with a synodic period of $P = 2.9726 \pm 0.0002$ h with an amplitude $A = 0.18 \pm 0.06$ mag. For this asteroid, no periods were found in the LCDB.



(458732) 2011 MD5 is an Apollo Near-Earth asteroid. Collaborative observations were made over seven nights, before its close approach to the Earth. The first observed lightcurves showed some anomalous attenuations which let us to hypothesize its binary nature. This hypothesis became certainty when we read the CBET 5287, published on August 24 by P. Pravec et al. (2023).

The analysis was done using the dual-period search function implemented in *MPO Canopus*. We found a primary synodic rotational period of $P_1 = 3.134 \pm 0.001$ h with an amplitude $A_1 = 0.12 \pm 0.06$ mag and an orbital period $P_2 = 15.18 \pm 0.01$ h with an amplitude $A_2 = 0.20 \pm 0.03$. The deep drop of the secondary eclipse, 0.09 ± 0.03 , gives a lower limit to secondary-to-primary mean-diameter ratio of D_s/D_p of 0.29 ± 0.05 . These results are in agreement with those published by Pravec et al. (2023) and confirm the binary nature of this asteroid.

Multiband photometry was made by P. Bacci and M. Maestripietri (104) on 2023 September 10, deriving a color index $V-R = 0.38 \pm 0.04$, which is consistent with a C-type asteroid (Shevchenko and Lupishko, 1998).



References

Bus S.J.; Binzel R.P. (2002), "Phase II of the Small Main-Belt Asteroid Spectroscopic Survey - A Feature-Based Taxonomy." *Icarus* **158**, 146-177.

Harris, A.W.; Young, J.W.; Scaltriti, F.; Zappala, V. (1984). "Lightcurves and phase relations of the asteroids 82 Alkmene and 444 Gytis." *Icarus* **57**, 251-258.

Pravec, P.; Harris, A.W.; Kušnirák, P.; Galád, A.; Hornoch, K. (2012). "Absolute magnitudes of asteroids and a revision of asteroid albedo estimates from WISE thermal observations." *Icarus* **221**, 365-387.

Pravec, P.; Hornoch, K.; Kucakova, H.; Fatka, P.; Ergashev, K.; Burkhonov, P. (2023). "(458732) 2011 MD_5." CBET 5287.

Shevchenko V.G.; Lupishko D.F. (1998). "Optical properties of Asteroids from Photometric Data." *Solar System Research*, **32**, 220-232.

Tholen, D.J. (1984). "Asteroid taxonomy from cluster analysis of Photometry." Doctoral Thesis. University Arizona, Tucson.

UAI (2023). "Unione Astrofili Italiani" web site.
<https://www.uai.it>

Warner, B.D.; Harris, A.W.; Pravec, P. (2009) "The asteroid lightcurve database." *Icarus* **202**, 134-146. Updated 2023 Sep. 27.
<https://minplanobs.org/alcdef/index.php>

Warner, B.D. (2021). MPO Software, MPO Canopus v10.8.5.0. Bdw Publishing. <http://minorplanetobserver.com>

Number	Name	2023 mm/dd	Phase	L _{PAB}	B _{PAB}	Period(h)	P.E.	Amp	A.E.	Grp
81	Terpsichore	08/22-09/05	7.8, 1.9	345	-3	10.946	0.002	0.06	0.01	MB-O
238	Hypatia	08/21-09/26	*12.7, 2.1	358	3	8.873	0.001	0.16	0.03	MB-O
773	Irmintraud	08/17-08/22	0.3, 2.5	323	0	6.745	0.005	0.17	0.03	MB-O
862	Franzia	08/12-09/24	16.7, 7.1	0	15	7.524	0.001	0.14	0.03	MB-M
894	Erda	07/23-08/21	13.8, 12.1	216	4	4.6898	0.0002	0.07	0.02	MB-O
914	Palisana	07/23-08/25	20.4, 22.7	313	32	8.681	0.001	0.17	0.03	MB-I
2763	Jeans	08/23-09/03	2.1, 8.5	328	2					MB-I
5766	Carmelofalco	2021/08/13-09/02	17.8, 8.8	354	-4	2.9726	0.0002	0.18	0.06	MB-I
458732	2011 MD5	09/04-09/10	9.2, 8.2	206	6	3.134	0.001	0.12	0.06	NEA
						15.18	0.01	0.20	0.03	

Table I. Observing circumstances and results. The first line gives the results for the primary of a binary system. The second line gives the orbital period of the satellite and the maximum attenuation. The phase angle is given for the first and last date. If preceded by an asterisk, the phase angle reached an extrema during the period. L_{PAB} and B_{PAB} are the approximate phase angle bisector longitude/latitude at mid-date range (see Harris et al., 1984). Grp is the asteroid family/group (Warner et al., 2009).

Observatory (MPC code)	Telescope	CCD	Filter	Observed Asteroids (#Sessions)
Iota Scorpii (K78)	0.40-m RCT f/8.0	SBIG STXL-6303e (bin 2x2)	C, Rc	894 (2), 914 (1), 862 (3), 238 (3), 458732 (3)
M57 (K38)	0.35-m RCT f/5.5	SBIG STT1603ME	C, B, V, Rc	894 (2), 914 (1), 862 (3), 238 (2), 458732 (3)
HOB Astronomical Observatory (L63)	0.20-m SCT f/6.0	ATIK 383L+	C, B, V, Rc	894 (3), 914 (3), 2763 (1), 81 (1), 458732 (2)
Zen Observatory (M26)	0.30-m RCT f/7.4	ATIK 383L+	C, Rc	914 (2), 862 (1), 238 (1), 458732 (2)
Astronomical Observatory, University of Siena (K54)	0.30-m MCT f/5.6	SBIG STL-6303e (bin 2x2)	C, Rc	81 (5), 458732 (1)
GAL Hassin Robotic Telescope 2 (L34)	0.40-m RCT f/8.0	Andor Aspen CG16M	C	5766 (5)
Blessed Hermann Observatory (L73)	0.30-m SCT f/6.0	QHY 174MGPS (bin 2x2)	V, Rc	773 (4)
GAMP (104)	0.60-m NRT f/4.0	Apogee Alta	C, V, Rc	458732 (4)
Osservatorio Astronomico Margherita Hack (A57)	0.35-m SCT f/8.3	SBIG ST10XME (bin 2x2)	B, V, Rc	894 (1), 862 (1), 238 (1)
Osservatorio Serafino Zani (130)	0.40-m RCT f/5.8	SBIG ST8 XME (bin 2x2)	C	894 (1), 914 (2)
Iris Versari (Felizzano)	0.20-m SCT f/6.3	Moraviann KAF 8300	V, Rc	773 (2), 2763 (1)
GiaGa Observatory (203)	0.36-m SCT f/5.8	Moravian G2-3200	C, Rc	862 (1), 458732 (2)
Osservatorio Astronomico Nastro Verde (C82)	0.35-m SCT f/6.3	SBIG ST10XME (bin 2x2)	C	458732 (1)
GAV	0.20-m SCT f/7.0	SXV-H9	Rc	862 (1)

Table II. Observing Instrumentations. MCT: Maksutov-Cassegrain, NRT: Newtonian Reflector, RCT: Ritchey-Chretien, SCT: Schmidt-Cassegrain.

LIGHTCURVE ANALYSIS OF ASTEROIDS 6108 GLEBOV, 6991 CHICHIBU AND 10039 KEET SEEL

Alessandro Marchini, Riccardo Papini
Astronomical Observatory, University of Siena (K54)
Via Roma 56, 53100 - Siena, ITALY
marchini@unisi.it

(Received: 2023 October 12)

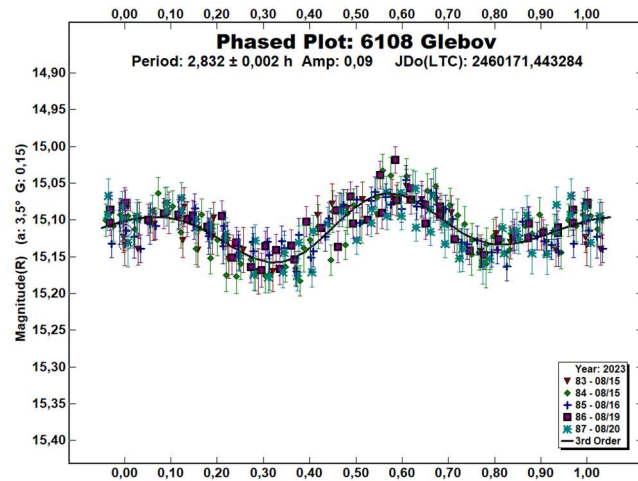
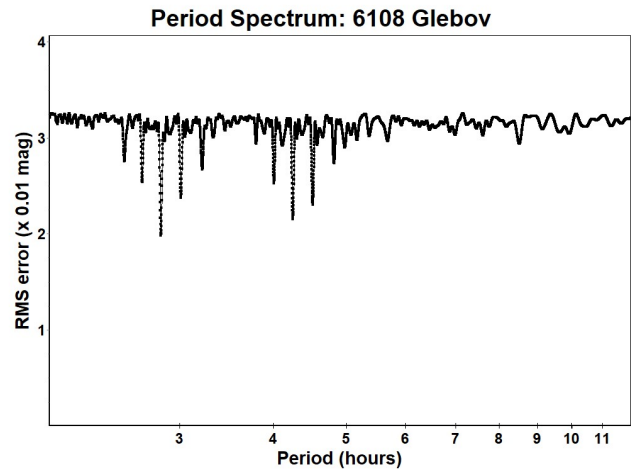
Photometric observations of three main-belt asteroids were conducted to determine their synodic rotation periods. We found: for 6108 Glebov, $P = 2.832 \pm 0.002$ h with $A = 0.09 \pm 0.03$ mag; for 6991 Chichibu, $P = 9.492 \pm 0.001$ h with $A = 0.18 \pm 0.03$ mag; for 10039 Keet Seel, $P = 36.99 \pm 0.02$ h with $A = 0.16 \pm 0.03$ mag.

CCD photometric observations of three main-belt asteroids were carried out in July-September 2023 at the Astronomical Observatory of the University of Siena (K54). We used a 0.30-m $f/5.6$ Maksutov-Cassegrain telescope, SBIG STL-6303E NABG CCD camera, and clear filter; the pixel scale was 2.30 arcsec when binned at 2×2 pixels and all exposures were 300 seconds.

Data processing and analysis were done with *MPO Canopus* (Warner, 2018). All images were calibrated with dark and flat-field frames and the instrumental magnitudes converted to R magnitudes using solar-colored field stars from a version of the CMC-15 catalogue distributed with *MPO Canopus*. Table I shows the observing circumstances and results.

6108 Glebov (1971 QN) was discovered on 1971 August 18 by T.M. Smirnova at the Crimean Astrophysical Observatory and named in honor of academician Igor' Alekseevich Glebov, outstanding scientist in the field of electrical engineering and power engineering. It is an inner main-belt asteroid with a semi-major axis of 2.194 AU, eccentricity 0.203, inclination 2.881° , and an orbital period of 3.25 years. Its absolute magnitude is $H = 14.42$ (JPL, 2023). The NEOWISE satellite infrared radiometry survey (Mainzer et al., 2019) found a diameter $D = 3.385 \pm 0.040$ km using an absolute magnitude $H = 13.9$.

Observations were conducted over five nights and collected 260 data points. The period analysis shows a rotational period of $P = 2.832 \pm 0.002$ h with an amplitude $A = 0.09 \pm 0.03$ mag, in good agreement with the previously published results in the LCDB.



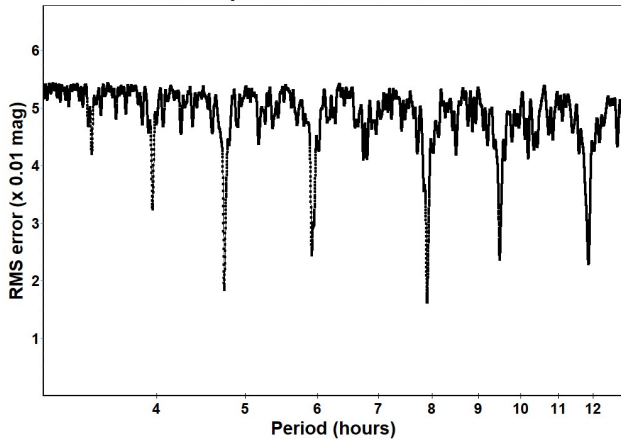
6991 Chichibu (1995 AX) was discovered on 1995 January 6 by T. Kobayashi at Oizumi and named after the western part of the Saitama prefecture. It is an inner main-belt asteroid with a semi-major axis of 2.401 AU, eccentricity 0.203, inclination 5.762° , and an orbital period of 3.72 years. Its absolute magnitude is $H = 12.93$ (JPL, 2023). The NEOWISE satellite infrared radiometry survey (Mainzer et al., 2019) found a diameter $D = 4.464 \pm 0.863$ km using an absolute magnitude $H = 12.6$.

Observations were conducted over six nights and collected 290 data points. Despite the period spectrum shows a peak at 7.901 hours, we prefer the result for the rotational period of $P = 9.492 \pm 0.001$ h with an amplitude $A = 0.18 \pm 0.03$ mag, which is more symmetrical and in excellent agreement with the one just published on LCDB by Behrend (2023web).

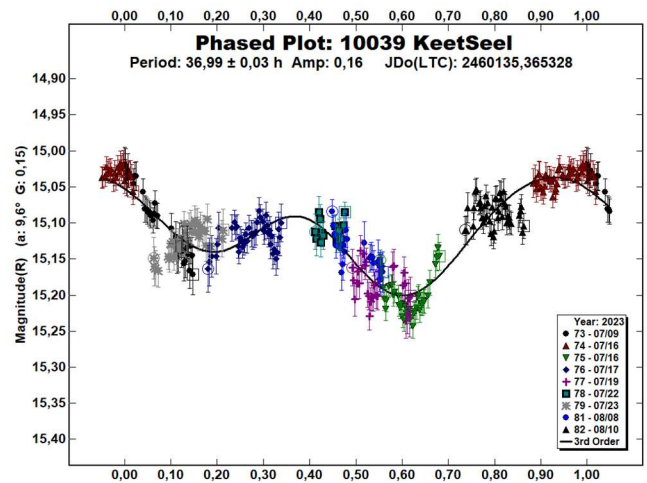
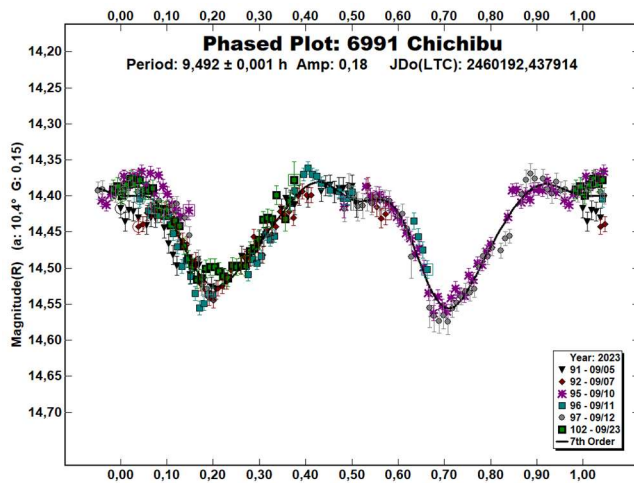
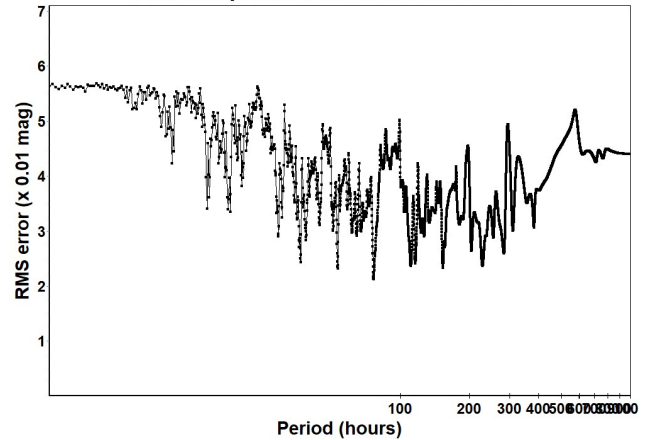
Number	Name	2023/mm/dd	Phase	L_{PAB}	B_{PAB}	Period(h)	P.E.	Amp	A.E.	Grp
6108	Glebov	08/14-08/21	*3.5, 4.7	323	4	2.832	0.002	0.09	0.03	MB-I
6991	Chichibu	09/04-09/23	*10.5, 5.0	357	-6	9.492	0.001	0.18	0.03	MB-I
10039	Keet Seel	07/09-08/10	*9.7, 11.4	301	9	36.99	0.02	0.16	0.03	MB-O

Table I. Observing circumstances and results. The phase angle is given for the first and last date. If preceded by an asterisk, the phase angle reached an extremum during the period. L_{PAB} and B_{PAB} are the approximate phase angle bisector longitude/latitude at mid-date range (see Harris et al., 1984). Grp is the asteroid family/group (Warner et al., 2009).

Period Spectrum: 6991 Chichibu



Period Spectrum: 10039 KeetSeel



10039 Keet Seel (1984 LK) was discovered on 1984 June 2 by B.A. Skiff at the Anderson Mesa Station of the Lowell Observatory and named after a well-preserved prehistoric cliff-dwelling, occupied by ancestors of the modern Hopi people. The site is in what is now the Navajo National Monument in northern Arizona. It is an outer main-belt asteroid with a semi-major axis of 3.148 AU, eccentricity 0.369, inclination 6.491° , and an orbital period of 5.59 years. Its absolute magnitude is $H = 13.23$ (JPL, 2023). The WISE/NEOWISE satellite infrared radiometry survey (Masiero et al., 2011) found a diameter $D = 11.316 \pm 0.351$ km using an absolute magnitude $H = 12.7$.

Observations during the period of visibility, conducted over nine nights collecting 311 data points, do not cover the entire rotation and do not allow us to identify an unambiguous solution. Although the period spectrum shows a few possible alternative solutions, we have excluded those with stronger peaks that provide non-bimodal curves. We suggest that the most likely value of the synodic rotational period is associated with the bi-modal light curve phased to $P = 36.99 \pm 0.02$ hours with an amplitude of $A = 0.16 \pm 0.03$ mag. Further observations will be necessary to nail down the actual period of this slow rotating asteroid.

References

- Behrend, R. (2023web). Observatoire de Geneve web site. http://obswww.unige.ch/~behrend/page_cou.html
- Harris, A.W.; Young, J.W.; Scaltriti, F.; Zappala, V. (1984). "Lightcurves and phase relations of the asteroids 82 Alkmene and 444 Gyptis." *Icarus* **57**, 251-258.
- JPL (2023). Small Body Database Search Engine. <https://ssd.jpl.nasa.gov>
- Mainzer, A.K.; Bauer, J.M.; Cutri, R.M.; Grav, T.; Kramer, E.A.; Masiero, J.R.; Sonnett, S.; Wright, E.L. (2019). "NEOWISE Diameters and Albedos V2.0." NASA Planetary Data System, <https://doi.org/10.26033/18S3-2Z54>.
- Masiero, J.R.; Mainzer, A.K.; Grav, T.; Bauer, J.M.; Cutri, R.M.; Dailey, J.; Eisenhardt, P.R.M.; McMillan, R.S.; Spahr, T.B.; Skrutskie, M.F.; Tholen, D.; Walker, R.G.; Wright, E.L.; DeBaun, E.; Elsbury, D.; Gautier, T. IV; Gomillion, S.; Wilkins, A. (2011). "Main Belt Asteroids with WISE/NEOWISE. I. Preliminary Albedos and Diameters." *Astrophys. J.* **741**, A68.
- Warner, B.D.; Harris, A.W.; Pravec, P. (2009). "The Asteroid Lightcurve Database." *Icarus* **202**, 134-146. Updated 2021 December 21. <https://minplanobs.org/mpinfo/php/lcdb.php>
- Warner, B.D. (2018). MPO Software, MPO Canopus v10.7.7.0. Bdw Publishing. <http://bdwpublishing.com/>

**LIGHTCURVE AND ROTATION PERIOD
FOR MINOR PLANETS 2090 MIZUHO (1978 EA)
AND 4164 SHILOV (1969 UR)**

Mike Foylan
Cherryvalley Observatory, I83,
Cherryvalley, Rathmolyon, Co. Meath, Ireland
mfoylan@yahoo.co.uk

(Received: 2023 October 15 Revised: 2023 October 24)

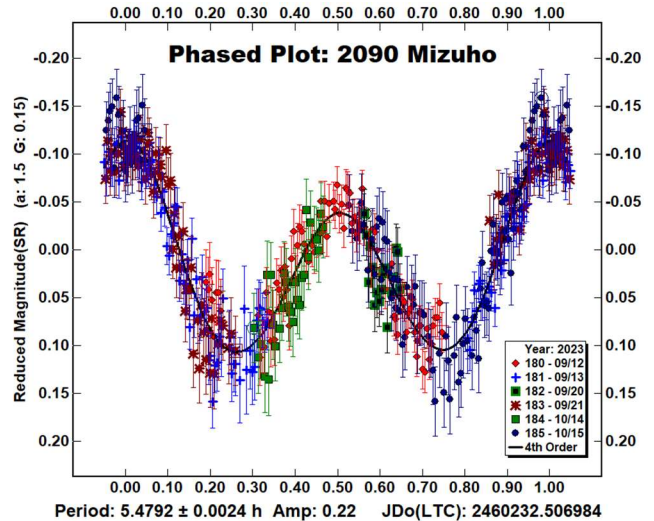
CCD photometric observations of main-belt asteroids 2090 Mizuho (1978 EA) and 4164 Shilov (1969 UR) were acquired during 2023 September and October and 2016 October and November, respectively. A synodic rotation period of 5.4792 ± 0.0024 h and amplitude of $A = 0.22 \pm 0.03$ mag were determined for 2090 Mizuho and 74.500 ± 0.072 h and amplitude of $A = 0.84 \pm 0.05$ mag were determined for 4164 Shilov.

2090 Mizuho is an S-type (Tholen, 1984) asteroid and was discovered 1978 March 12 by T. Urata at Yakiimo Station. Its orbital period is approximately 5.38 years. The absolute magnitude $H = 10.90$ and assumed geometric albedo of 0.219 (JPL, 2023) give an estimated diameter of 17.99 km. 4164 Shilov, is a member of the Eunomia orbital group. It was Discovered 1969 October 16 by L.I. Chernykh at Nauchnyj. Its orbital period is approximately 4.28 years. The absolute magnitude $H = 12.30$ and geometric albedo of 0.234 (JPL, 2023) give an estimated diameter of 10.49 km.

Cherryvalley Observatory (MPC Code I83) is an amateur observatory located in eastern rural Ireland. Observations with R-band and I-band Bessel photometric filters were conducted with a 0.2-m Schmidt-Cassegrain Telescope (SCT) operating at $f/7.6$ using an SBIG STL-1301E CCD camera with a 1280×1024 array of 16-micron pixels. The resulting image scale was 2.19 arcsecond per pixel. Image acquisition was undertaken with Software Bisque's *TheSky6* Professional and *CCDSofit v5*. All images were calibrated with dark and flat-frames using *CCDSofit v5* with mid-exposure time's light-time corrected.

The period analyses were undertaken using *MPO Canopus* (Warner, 2023) using the *MPO Canopus* Fourier-type FALC fitting method (cf. Harris et al., 1989). The Comp Star Selector utility in *MPO Canopus* found up to five comparison stars of near solar-color for differential photometry. To reduce the number of adjusted nightly zero points and their amounts, the analysis of observations acquired using Bessel photometric R and I filters the data were reduced to Sloan r' (SR) passband using the ATLAS catalog r' (SR) Sloan magnitudes (Tonry et al., 2018).

2090 Mizuho was reported as a lightcurve opportunity in the Minor Planet Bulletin (Warner et al., 2023). Opposition occurred on 2023 September 8. A total of 409 useful data points were used in the calculations, which were obtained over three nights during the period 2023 September 12 to October 15 with a Bessel R-band filter. The period solution of 5.4792 ± 0.0024 h as determined by Cherryvalley Observatory using an order-4 fit is in excellent agreement with earlier work by Brinsfield (2010) Via Capote Observatory in which a synodic rotation period of 5.47 ± 0.01 h was determined. Behrend (2021web) reported a period of 5.4792 ± 0.0003 h. Ďurech and Hanuš (2018) determined a period of 5.4793 ± 0.0002 h based on photometric data from Gaia Data Release 2.



Observations of 4164 Shilov were originally taken in 2016 by Cherryvalley Observatory but only recently processed. A total of 840 useful data points were used in the calculations, which were obtained over six nights during the period 2016 October 18 to November 7 with a Bessel I-band filter. During observations, 4164 Shilov reached opposition on October 29. The period solution of 74.500 ± 0.072 h as determined by Cherryvalley Observatory using an order-4 fit is approximately four times greater than previously reported. Angeli and Barucci (1996) reported a single night's observation with a period solution of 18.35 h and amplitude of 0.24 mag. Carbo et al., (2009) reported insufficient data to determine a period but the 64 data points obtained did not fit the period of 18.35 h found previously by Angeli and Barucci (1996). Warner (2017) reported a period solution of 18.5 h and amplitude of 0.29 mag using 58 data points from observations during the period 2016 August 10 to August 11. Cherryvalley Observatory's

Number	Name	yyyy mm/dd	Phase	L_{PAB}	B_{PAB}	Period(h)	P.E.	Amp	A.E.	Grp
2090	Mizuho	2023 09/12-10/15	1.5, 13.7	346.3	2.8	5.4792	0.0024	0.22	0.03	MBA
4164	Shilov	2016 10/18-11/07	*6.3, 4.3	36.8	0.6	74.500	0.072	0.84	0.05	MBA-V

Table I. Observing circumstances and results. The phase angle is given for the first and last date. If preceded by an asterisk, the phase angle reached an extrema during the period. LPAB and BPAB are the approximate phase angle bisector longitude/latitude at mid-date range (see Harris et al., 1984). Grp is the asteroid family/group (Warner et al., 2009).

data did not fit the 18.5 h period solution as previously reported and were in poor agreement. Various period solution aliases were explored but were also of poor fit, however a period solution of 74.5 h was found which indicates a likely solution with the lowest RMS value and demonstrating a typical bimodal shape and a relatively large amplitude of 0.84 mag. Future observations of 4164 Shilov are encouraged to help improve 4164 Shilov current quality U-rating of 1.

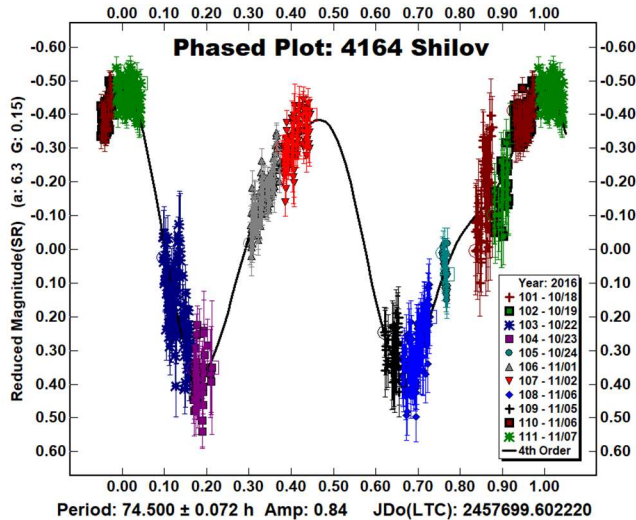


Table I gives the observing circumstances and results.

References

- Angeli, C.A.; Barucci, M.A. (1996). "Rotational properties of 13 small asteroids." *Planet. Space Sci.* **44**, 181-186.
- Behrend, R. (2021web). Observatoire de Geneve web site. http://obswww.unige.ch/~behrend/page_cou.html
- Brinsfield, J.W. (2010). "Asteroid Lightcurve Analysis at the Via Capote Observatory: 2010 February-May." *Minor Planet Bulletin* **37**, 146-147.
- Carbo, L.; Green, D.; Kragh, K.; Krotz, J.; Meiers, A.; Patino, B.; Pligge, Z.; Shaffer, N.; Ditteon, R. (2009). "Asteroid Lightcurve Analysis at the Oakley Southern Sky Observatory: 2008 October thru 2009 March." *Minor Planet Bulletin* **36**, 152-157.
- Đurech, J.; Hanuš, J. (2018b). "Reconstruction of asteroid spin states from Gaia DR2 photometry." *Astron. Astrophys.* **620**, A91.
- Harris, A.W.; Young, J.W.; Scaltriti, F.; Zappala, V. (1984). "Lightcurves and phase relations of the asteroids 82 Alkmene and 444 Gypsis." *Icarus* **57**(2), 251-258.
- Harris, A.W.; Young, J.W.; Bowell, E.; Martin, L.J.; Millis, R.L.; Poutanen, M.; Scaltriti, F.; Zappala, V.; Schober, H.J.; Debehogne, H.; Zeigler, K.W. (1989). "Photoelectric Observations of Asteroids 3, 24, 60, 261, and 863." *Icarus* **77**, 171-186.
- JPL (2023). Small-Body Database Browser - JPL Solar System Dynamics web site. <http://ssd.jpl.nasa.gov/sbdb.cgi>
- Tholen, D.J. (1984). "Asteroid taxonomy from cluster analysis of Photometry." Doctoral Thesis. University Arizona, Tucson.
- Tonry, J.L.; Denneau, L.; Flewelling, H.; Heinze, A.N.; Onken, C.A.; Smartt, S.J.; Stalder, B.; Weiland, H.J.; Wolf, C. (2018). "The ATLAS All-Sky Stellar Reference Catalog." *Astrophys. J.* **867**, A105.
- Warner, B.D.; Harris, A.W.; Pravec, P. (2009). "The Asteroid Lightcurve Database." *Icarus* **202**, 134-146. Updated 2023 Oct. 1. <https://minplanobs.org/MPInfo/php/lcdb.php>
- Warner, B.D. (2017). "Asteroid lightcurve analysis at CS3-Palmer Divide Station: 2016 July - September." *Minor Planet Bull.* **44**, 12-19.
- Warner, B.D. (2023). MPO Canopus Software, version 10.8.6.20. BDW Publishing. <http://www.bdwpublishing.com>
- Warner, B.D.; Harris, A.W.; Durech, J.; Benner, L.A.M. (2023). "Lightcurve Photometry Opportunities: 2023 July - September." *Minor Planet Bulletin* **50**, 240-244.

LIGHTCURVE ANALYSIS FOR SIX NEAR-EARTH ASTEROIDS OBSERVED IN 2009, 2017 AND 2023

Peter Birtwhistle
Great Shefford Observatory
Phlox Cottage, Wantage Road
Great Shefford, Berkshire, RG17 7DA
United Kingdom
peter@birtwhistle.org.uk

(Received: 2023 October 7)

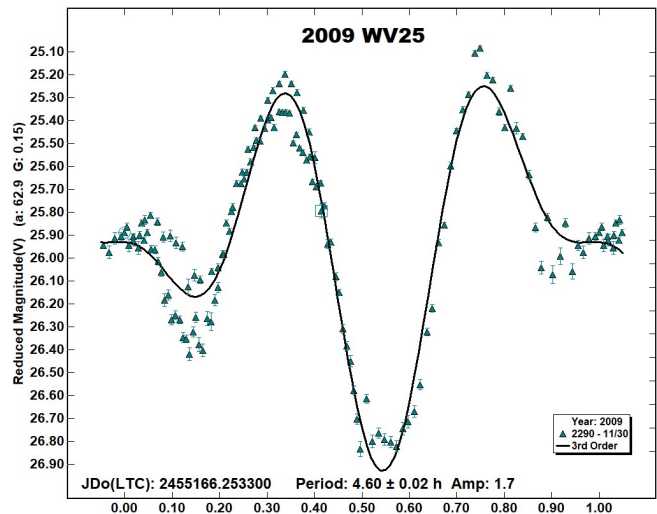
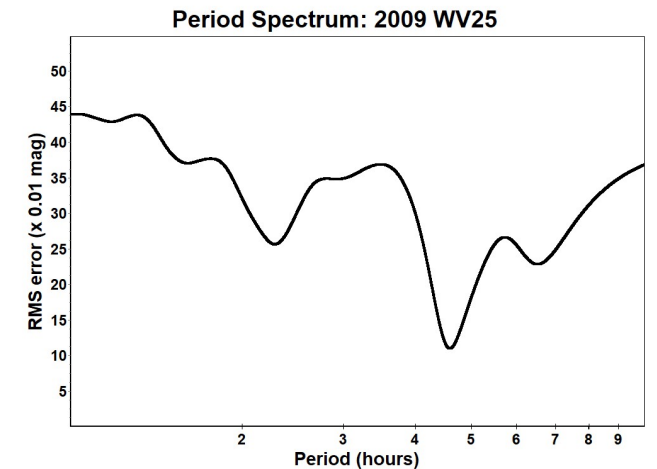
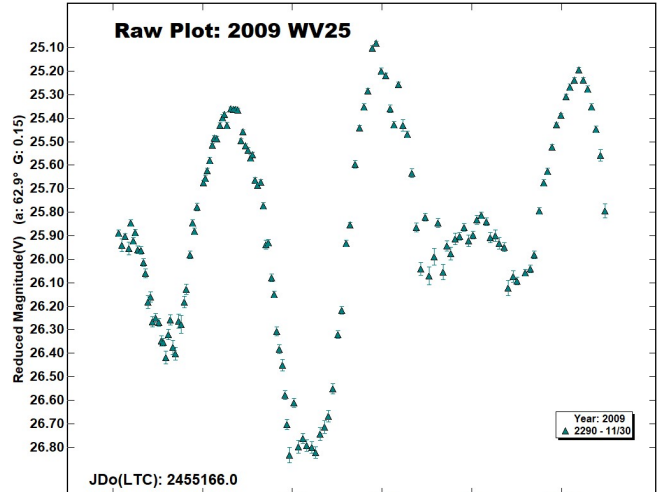
Lightcurves and amplitudes for six small near-Earth asteroids observed from Great Shefford Observatory during close approaches in 2009, 2017, and August to October 2023 are reported. Five have rotation periods less than 20 minutes, two are reliably detected tumblers and another is a possible tumbler.

Photometric observations of near-Earth asteroids during close approaches to Earth in 2009, 2017, and 2023 were made at Great Shefford Observatory using a 0.40-m Schmidt-Cassegrain and Apogee Alta U47+ CCD camera. All observations were made unfiltered and with the telescope operating with a focal reducer at $f/6$. The $1K \times 1K$, 13-micron CCD was binned 2×2 resulting in an image scale of 2.16 arc seconds/pixel. All the images were calibrated with dark and flat frames and *Astrometrica* (Raab, 2018) was used to measure photometry using APASS Johnson V band data from the UCAC4 catalogue (Zacharias et al., 2013). *MPO Canopus* (Warner, 2022), incorporating the Fourier algorithm developed by Harris (Harris et al., 1989) was used for lightcurve analysis.

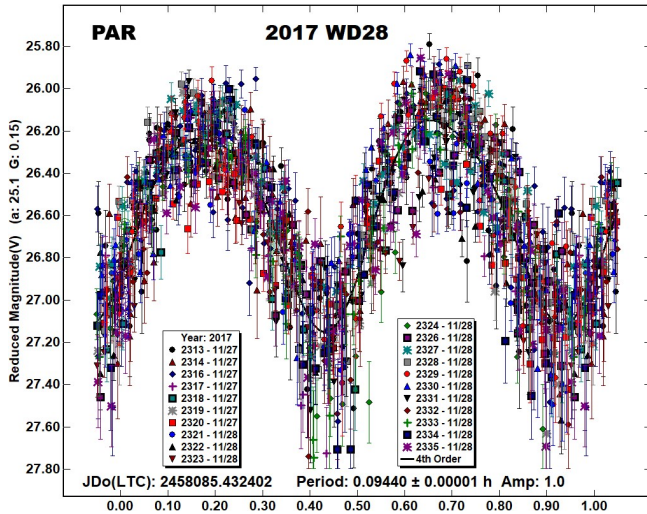
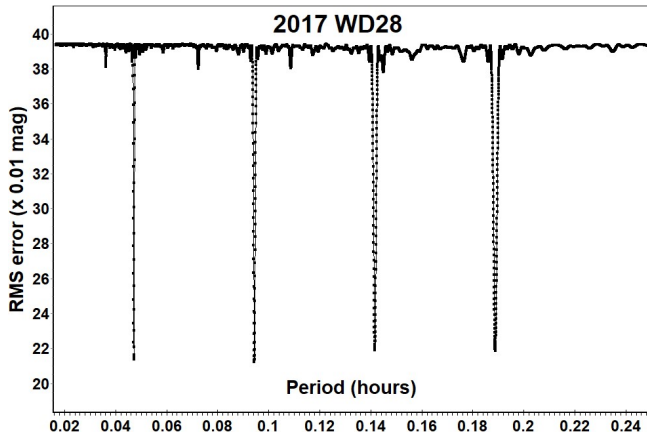
No previously reported results have been found in the Asteroid Lightcurve Database (LCDB) (Warner et al., 2009), from searches via the Astrophysics Data System (ADS, 2023) or from wider searches unless otherwise noted. All size estimates are calculated using H values from the Small-Body Database Lookup (JPL, 2023b), using an assumed albedo for NEAs of 0.2 (LCDB readme.pdf file) and are therefore uncertain and offered for relative comparison only.

2009 WV25. This was a Catalina Sky Survey discovery from 22 Nov 2009 that made an approach to 2.9 Lunar Distances (LD) nine days later on Dec 1.6 UTC (McGaha et al., 2009). The LCDB lists a result by Ryan (2011web) indicating a period of about 5 h, amplitude 1.24 mag and possibly tumbling. The original reference is now unavailable, but the lightcurve also appears in Ryan and Ryan (2010web) and indicates that over a span of ~ 8.6 h on 2009 Nov 25.2 UTC tumbling rotation was detected. Skiff et al. (2023) provides a lightcurve from a 3-h span of observations from the same night as Ryan, at a phase angle of 13° and determines a period of 2.92 ± 0.07 h and amplitude 0.92 mags, but considers that result as suspect. 2009 WV25 was observed from Great Shefford starting on 2009 Nov 30.75 UTC when it was at 3.5 LD and moving at 85 arcsec/min. Exposures were maintained at 2 seconds throughout and 2516 measurable images were obtained, the telescope being repositioned 53 times during the 6.4 h of observation. No very short period variation was evident and for further analysis, the images were combined in *Astrometrica* into 137 stacked images, on average containing 18 images per stack, with the longest span of exposures in a stack being 2.8 minutes. A raw plot of the lightcurve is suggestive of tumbling rotation and a period spectrum shows minima around 2.4 and 4.6 h but the 6.4 h span of observations is not long enough to satisfactorily resolve non-principal axis rotation

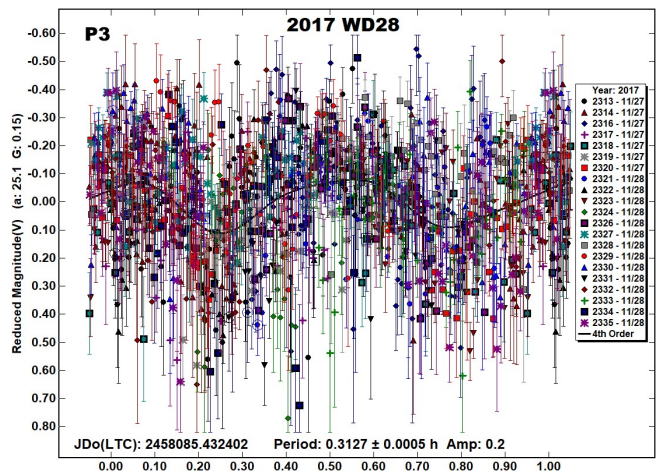
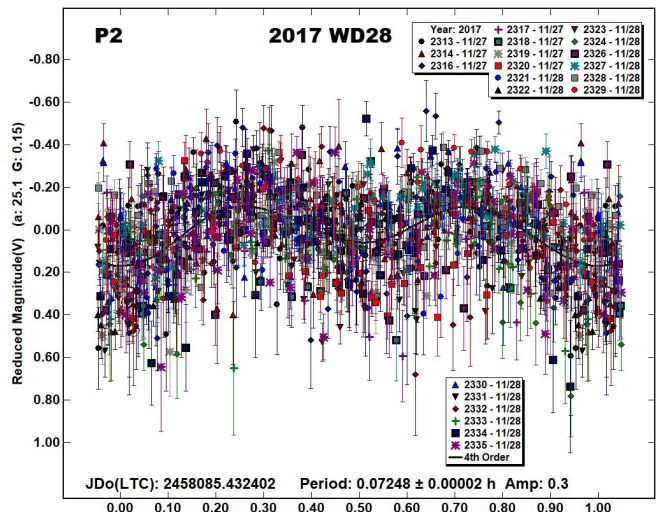
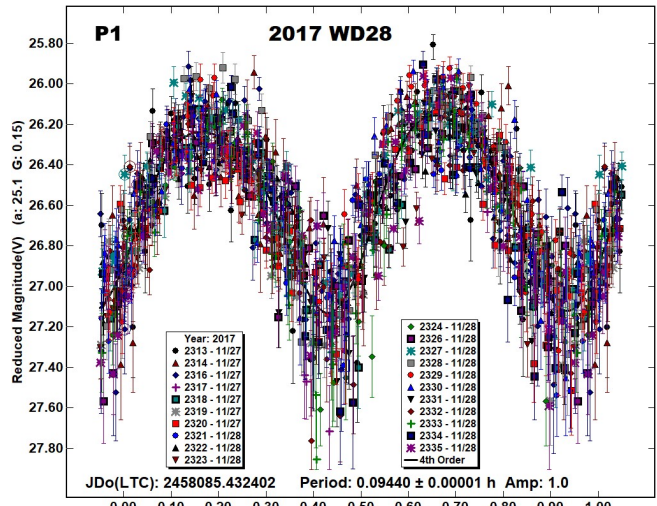
(NPAR) periods. The best fit phased lightcurve is given, indicating a period of 4.60 ± 0.02 h with amplitude 1.7 mags. From this result it is likely that 2009 WV25 is tumbling, with periods in the range 2-5 h, in agreement with both previously published results. A rating of PAR = -2, possibly -1 on the scale defined in Pravec et al. (2005) may be appropriate. As would be expected from the phase angle of 63° , the amplitude of 1.7 mags reported here is significantly larger than the other two results, both obtained at phase angle $\sim 13^\circ$.



2017 WD28. The Catalina Sky Survey discovered this Aten ($H = 25.7$, estimated size 22 m) on 2017 Nov 26.35 UTC ahead of a close approach to within 4.4 LD of Earth on 2017 Nov 28.88 UTC (Bacci et al., 2017). It was observed for 4 hours starting on 2017 Nov 27.93 UTC when it was at a distance of 5 LD and moving at 70+ arcsec/min. Exposures were initially 4 s and after peak-to-peak magnitude variations were obvious within a few minutes, exposure lengths were then doubled to 8 s for the majority of the session and a total of 1240 measurable images were obtained. Initial analysis showed a strong bimodal lightcurve with period of 0.09440 ± 0.00001 h (5.7 min) and 1 mag amplitude, labelled ‘PAR’. The period spectrum also shows a series of four distinct but weaker minima at multiples of 0.036 h.

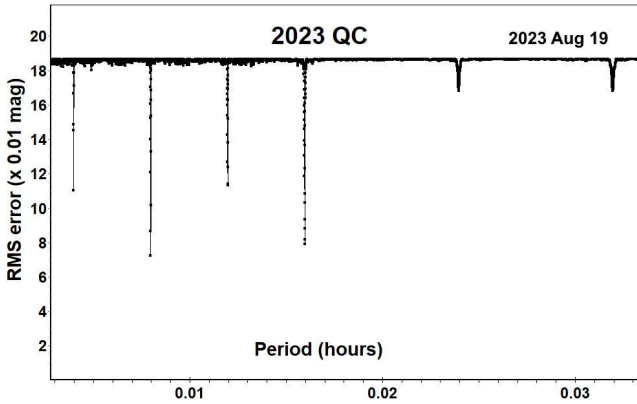


two main frequencies. On the scale defined in Pravec et al. (2005) it is expected to be rated as PAR = -3, i.e., NPA rotation reliably detected with the two periods resolved. There may be some ambiguities in one or both periods (Petr Pravec, personal communication). The full amplitude suggested by the NPAR solutions is ~ 1.3 magnitudes.



The dual period search function in *MPO Canopus* was used to check if these weak minima were evidence of tumbling rotation and this initially revealed the same dominant primary period, labelled P1 and a lower amplitude secondary period of 0.07248 ± 0.00002 h, labelled P2, corresponding to one of the weaker minima in the period spectrum. Further analysis showed that the data also supported another possible NPAR solution, again with the same P1 period, but with a less well-defined secondary period of 0.3127 ± 0.0005 h, labelled as P3. The dominant P1 period is well determined, however, the periods P1, P2 and P3 are related such that $1/P3 \sim 1/P2 - 1/P1$ and it is not clear which of P2 or P3 is the real second period of the tumbler and which is a beat between the

2023 QC. Discovered at magnitude +17 by the Atlas-HKO team on 2023 Aug 17.31 UTC, this is an Apollo and with $H = 24.7$ has an estimated diameter of ~ 34 m (Melnikov et al., 2023a). It approached Earth to 3.6 Lunar Distances (LD) on 2023 Aug 18.53 UTC and was 17th magnitude or brighter for a week following discovery. It was first observed from Great Shefford on 2023 Aug 17.87 UTC to obtain astrometry. With apparent motion of 65 arcsec/min exposures were limited to 3 s to minimise image trailing. Large changes in magnitude were obvious between consecutive exposures taken with a cadence of 4.4 s and the time from maximum to maximum was estimated to be ~ 15 s. A short set of exposures with 8 s duration were also taken but variation was less obvious. Assuming a bimodal lightcurve, the period was therefore expected to be ~ 30 s, indicating that an optimum exposure length to maximise S/Nr with minimal lightcurve smoothing would be $\sim 0.185 \times 30 = 5.5$ s (Pravec et al., 2000). All subsequent exposures were consequently limited to 5 s and a total of 202 measurable exposures were obtained over a period of 76 min. 2023 QC was observed again starting on 2023 Aug 19.87 UTC for 107 min (656 exposures) and again starting on 2023 Aug 20.88 UTC for 94 min (787 exposures). Viewing aspects changed significantly over the three dates, the object moved 69° across the sky, it brightened by 0.7 magnitudes by the second date, and had faded by 0.2 magnitudes by the third date. The apparent speed reduced from 65 to 25 arcsec/min but its altitude also reduced from 50° to 20°, these factors affecting the degree of scatter in the measurements. Analysis of the images confirmed the short rotation period, independently derived period spectra from all three dates are very similar, a representative diagram is given for 2023 Aug 19 and covers rotation periods from 10 to 120 s on a linear scale.

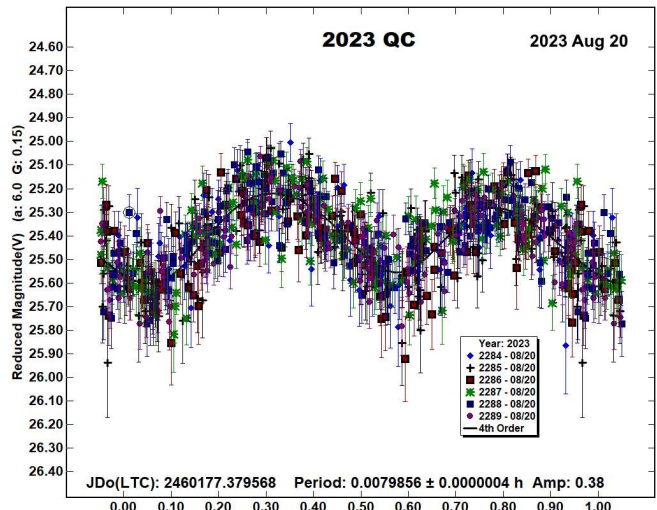
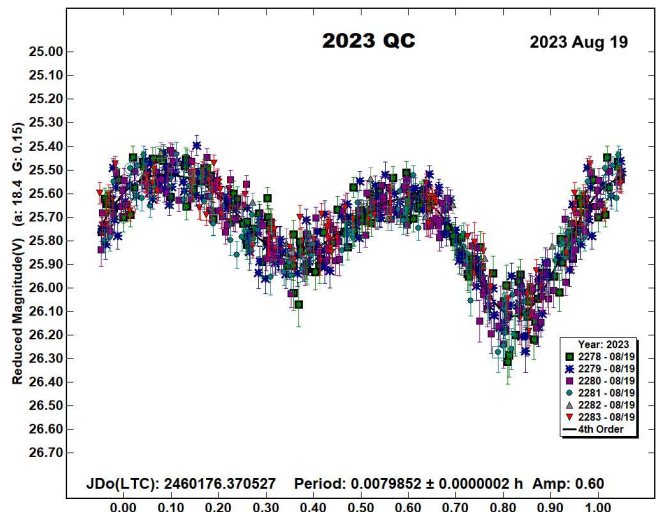
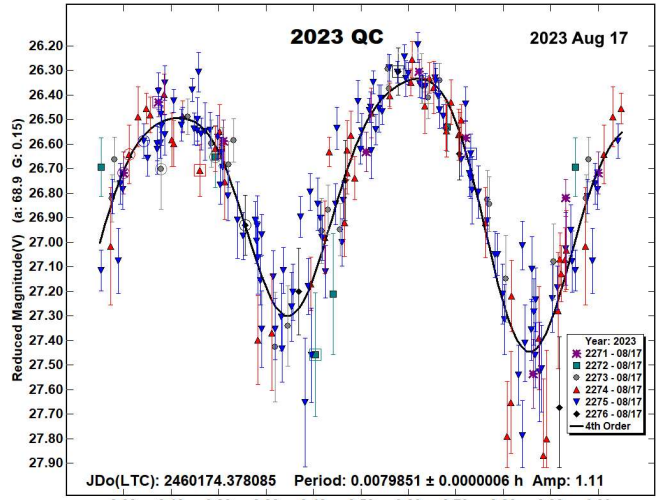


Similarly, independent lightcurve analyses from the three dates, given in diagrams marked as ‘2023 Aug 17’, ‘2023 Aug 19’ and ‘2023 Aug 20’ result in very similar periods and all show a well-defined asymmetric bimodal lightcurve. The degree of asymmetry, calculated as the ratio between the larger and smaller amplitudes within the bimodal curves, was greatest on the second date with the values being 1.4, 2.4, and 1.4 respectively. Note that the lightcurve diagrams have all been plotted with the same range in the Y-axis to aid comparison.

As expected, the amplitude decreased across the three dates as the phase angle reduced. The phase angle, period (s) with formal error, amplitude and amplitude error (calculated as $\sqrt{2} \times$ lightcurve RMS residual) for the three dates are listed here:

Date	Phase°	Period (s)	Amplitude
2023 08 17	68	28.746 ± 0.002	1.11 ± 0.21
2023 08 19	17	28.747 ± 0.001	0.60 ± 0.10
2023 08 20	6	28.748 ± 0.001	0.38 ± 0.16

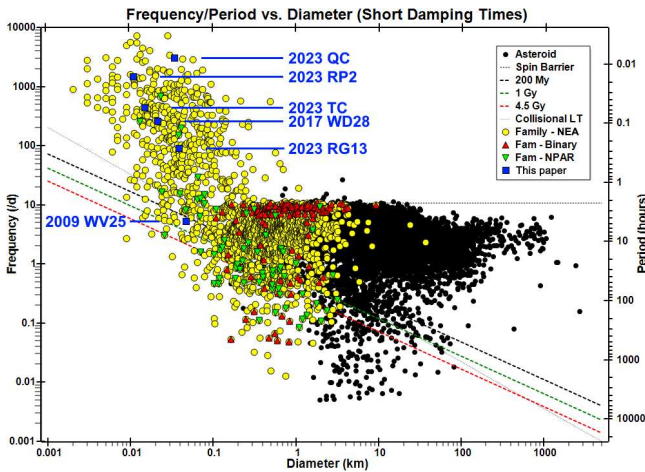
The value of Min a/b (calculated minimum elongation of the asteroid) in Table I is derived from data on 2023 Aug 20 when it was closest to opposition and therefore with the smallest phase angle. The analysis indicates that observations spanned 158 rotations on the first night, 223 on the second and 197 on the third night.



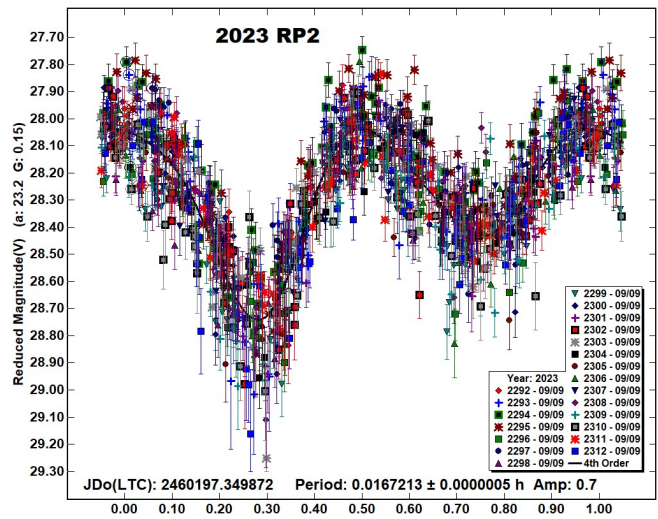
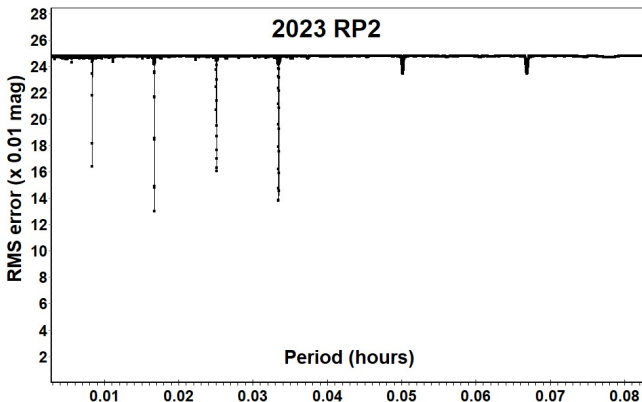
Number	Name	Integration times	Max intg/Pd	Min a/b	Pts	Flds
2009	WV25	170 ²	0.010	1.7*	137	53
2017	WD28	4, 8	0.031	1.9	1240	21
2023	QC	5-5.1	0.177	1.3	1645	18
2023	RP2	5.2-7.6	0.126	1.5	1203	21
2023	RG13	120 ²	0.125	1.6	66	4
2023	TC	2-6.3	0.043	1.9	586	9

Table I. Ancillary information, listing the integration times used (seconds), the fraction of the period represented by the longest integration time (Pravec et al., 2000), the calculated minimum elongation of the asteroid (Zappala et al., 1990), the number of data points used in the analysis and the number of times the telescope was repositioned to different fields. Notes: * = Value uncertain, based on phase angle > 40°, Σ = Longest elapsed integration time for stacked images (start of first to end of last exposure used).

With an estimated diameter of 34 m, 2023 QC is relatively large for a sub-minute rotator. Together with the other NEAs reported in this paper, its position on the LCDB NEA basic Frequency/Period vs. Diameter diagram is plotted here as a blue square.

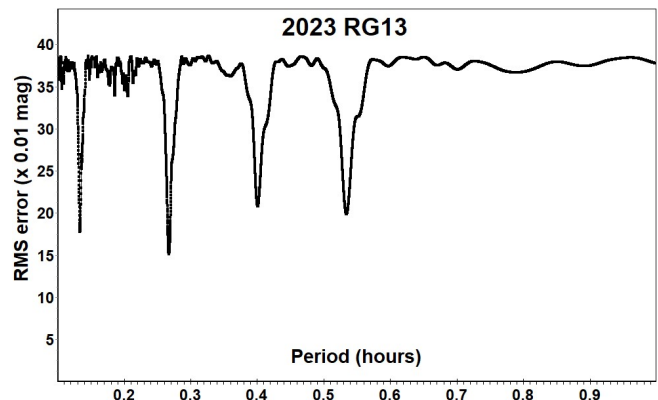


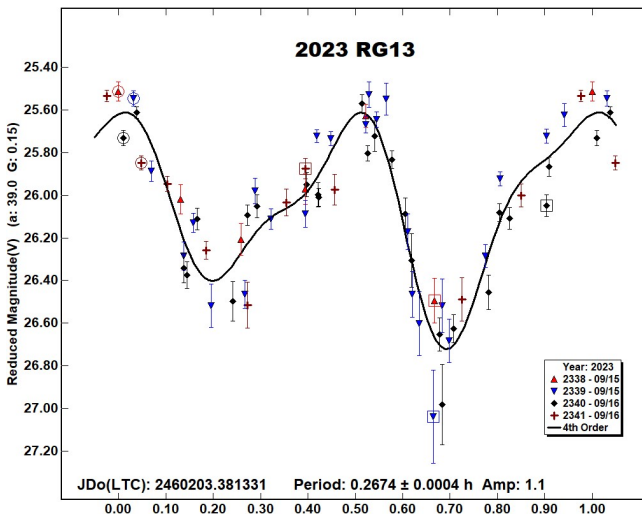
2023 RP2. This Apollo with $H = 27.2$ (est. dia. 11 m) is listed as a virtual impactor with a single low probability, 1 in 83 million, of impact predicted for 2094 Sept 11 (JPL, 2023a). It was discovered by the Catalina Sky Survey on 2023 Sep 9.25 UTC and passed Earth at 1.3 LD on 2023 Sep 10.55 UTC (Melnikov et al., 2023b). 2023 RP2 was under observation for 3.5 h starting at 2023 Sep 9.84 UTC, when it was 16th mag, at a distance of 1.9 LD and moving at 100 arcsec/min. Initial exposure length was set at 2 s and 2023 RP2 could be seen to reach a maximum in brightness approximately every 30 s.



As with 2023 QC, assuming the lightcurve to be bimodal, the period was estimated to be ~60 s and an optimum exposure length calculated to be $\sim 0.185 \times 60 = 11$ s. However, this exposure length would result in too much image trailing for the 12.8 arcsec diameter annulus being used in *Astrometrica* and so subsequent exposure lengths were restricted to 7.6 s, reducing to 5.2 s as the apparent sky motion increased to 123 arcsec/min. The 2 s exposures were not used in the final analysis due to poor SNr, but a total of 1203 images were measured and the resulting lightcurve confirmed the best fit period to be 60.197 ± 0.002 s with amplitude 0.7 mags, indicating that 201 full rotations were observed. The period spectrum ranges from 10 s to 5 minutes on a linear scale.

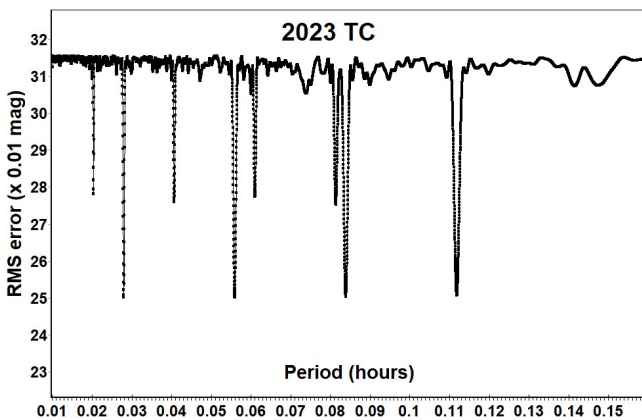
2023 RG13. Discovered at 18th mag by G. Borisov at the MARGO observatory in Nauchnyi on 2023 Sep 15.09 UTC, this Aten with $H = 24.4$ and diameter ~39 m maintained a similar apparent magnitude for the following week, approaching to 13 LD on 2023 Sep 16.87 UTC (Melnikov et al., 2023c). It was observed over a 10-minute period starting on 2023 Sep 15.88 UTC to collect astrometry using 8 s exposures and was seen to vary about 1 magnitude within minutes. Two hours later it was observed for a further 1.9 hours using 16 s exposures. As 2023 RG13 was relatively weakly recorded on the individual images, these were stacked using *Astrometrica* into batches of 13 or fewer images for the 8 s exposures and batches of 7 or fewer for the 16 s exposures, arranged so that the maximum span of exposure times in any one stack was 120 seconds or less. This resulted in the original 434 exposures being reduced to 66 stacked images for measurement. A period spectrum from analysis with *MPO Canopus* is given.





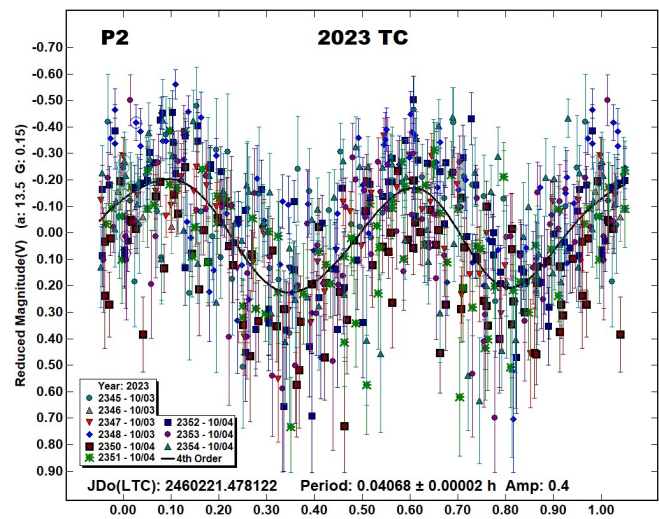
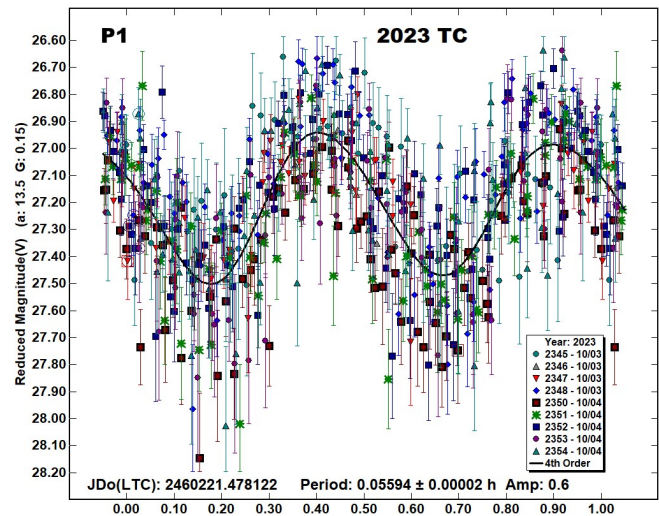
The phased lightcurve is for the best-fit period of 16.05 ± 0.2 minutes, with an amplitude of 1.1 mags, and indicates that the adopted 2-minute effective exposure lengths would not have caused appreciable lightcurve smoothing (Pravec et al., 2000). A 4th order Fourier fit has been used in the reduction, giving residuals 20% smaller than a 3rd order fit. Seven rotations were observed during the longer of the two observing periods.

2023 TC. A Catalina Sky Survey discovery on 2023 Oct 3.34 UTC, this Apollo ($H = 26.5$, est. dia. ~ 15 m) passed Earth at 2.2 LD on 2023 Oct 4.74 UTC (Bacci et al., 2023). It was observed over a period of 105 min starting on 2023 Oct 3.98 UTC and 586 measurable images were obtained. A linearly scaled period spectrum reveals two sets of regularly spaced minima, the strongest in multiples of 0.028 h and the weaker in multiples of 0.020 h.



Suspecting NPA rotation, analysis using the dual period search function in *MPO Canopus* confirmed that 2023 TC is a tumbler with periods $P1 = 0.05594 \pm 0.00002$ h and $P2 = 0.04068 \pm 0.00002$ h.

On the scale defined in Pravec et al. (2005) it is expected to be rated as $PAR = -3$, NPA rotation reliably detected with the two periods resolved (Petr Pravec, personal communication). The full amplitude suggested by the NPAR solution is ~ 1.0 magnitude and the observations of 2023 TC span 31 revolutions of the $P1$ period.



Acknowledgements

The author is indebted to Petr Pravec for his continued help reviewing analyses of tumbling asteroids. The author also gratefully acknowledges a Gene Shoemaker NEO Grant from the Planetary Society (2005) and a Ridley Grant from the British Astronomical Association (2005), both of which facilitated upgrades to observatory equipment used in this study.

References

ADS (2023). Astrophysics Data System.
<https://ui.adsabs.harvard.edu/>

Bacci, P.; Maestripieri, M.; Tesi, L.; Fagioli, G.; Jaeger, M.; Prosperi, E.; Prosperi, S.; Vollmann, W.; Foglia, S.; Galli, G.; Fumagalli, A.; Proserpio, I.; Testa, A.; Bressan, F.; Pettarin, E. and 29 colleagues (2017). "2017 WD28." *MPEC* 2017-W209.
<https://minorplanetcenter.net/mpec/K17/K17WK9.html>

Bacci, P.; Maestripieri, M.; Tesi, L.; Fagioli, G.; Foglia, S.; Galli, G.; Montanar, U.; Pettarin, E.; Rankin, D.; Christensen, E.J.; Fay, D.; Fazekas, J.B.; Fuls, D.C.; Gibbs, A.R.; Grauer, A.D. and 30 colleagues (2023). “2023 TC.” *MPEC* 2023-T11.
<https://minorplanetcenter.net/mpec/K23/K23T11.html>

Harris, A.W.; Young, J.W.; Scaltriti, F.; Zappala, V. (1984). “Lightcurves and phase relations of the asteroids 82 Alkmene and 444 Gypsis.” *Icarus* **57**, 251-258.

Harris, A.W.; Young, J.W.; Bowell, E.; Martin, L.J.; Millis, R.L.; Poutanen, M.; Scaltriti, F.; Zappala, V.; Schober, H.J.; Debehogne, H.; Zeigler, K. (1989). “Photoelectric Observations of Asteroids 3, 24, 60, 261, and 863.” *Icarus* **77**, 171-186.

JPL (2023a). Sentry: Earth Impact Monitoring.
<https://cneos.jpl.nasa.gov/sentry/>

JPL (2023b). Small-Body Database Lookup.
https://ssd.jpl.nasa.gov/tools/sbdb_lookup.html

McGaha, J.E.; Boattini, A.; Beshore, E.C.; Garradd, G.J.; Gibbs, A.R.; Grauer, A.D.; Hill, R.E.; Kowalski, R.A.; Larson, S.M.; McNaught, R.H.; Bezpalko, M.; Torres, D.; Kracke, R.; Spitz, G.; Blythe, M. and 6 colleagues (2009). “2009 WV25” *MPEC* 2009-W71. <https://minorplanetcenter.net/mpec/K09/K09W71.html>

Melnikov, S.; Hoegner, C.; Ludwig, F.; Hartmann, M.; Stecklum, B.; Bacci, P.; Maestripieri, M.; Zoltowski, F.B.; Ikari, Y.; Koch, B.; Ivanov, A.; Barcov, A.; Ivanov, V.; Lysenko, V.; Yakovenko, N. and 46 colleagues (2023a). “2023 QC.” *MPEC* 2023-Q12.
<https://minorplanetcenter.net/mpec/K23/K23Q12.html>

Melnikov, S.; Hoegner, C.; Ludwig, F.; Hartmann, M.; Stecklum, B.; Sonka, A.; Nedelcu, A.; Bacci, P.; Maestripieri, M.; Tesi, L.; Fagioli, G.; Skvarc, J.; Mikuz, H.; Lehmann, G.; Foglia, S. and 58 colleagues (2023b). “2023 RP2.” *MPEC* 2023-R89.
<https://minorplanetcenter.net/mpec/K23/K23R89.html>

Melnikov, S.; Hoegner, C.; Ludwig, F.; Hartmann, M.; Stecklum, B.; Bacci, P.; Maestripieri, M.; Tesi, L.; Fagioli, G.; Mikuz, H.; Lehmann, G.; Tichy, M.; Ticha, J.; Janda, M.; Honkova, M. and 65 colleagues (2023c). “2023 RG13.” *MPEC* 2023-S13.
<https://minorplanetcenter.net/mpec/K23/K23S13.html>

Pravec, P.; Hergenrother, C.; Whiteley, R.; Sarounova, L.; Kusnirak, P.; Wolf, M. (2000). “Fast Rotating Asteroids 1999 TY2, 1999 SF10, and 1998 WB2.” *Icarus* **147**, 477-486.

Pravec, P.; Harris, A.W.; Scheirich, P.; Kušnirák, P.; Šarounová, L.; Hergenrother, C.W.; Mottola, S.; Hicks, M.D.; Masi, G.; Krugly, Yu.N.; Shevchenko, V.G.; Nolan, M.C.; Howell, E.S.; Kaasalainen, M.; Galád, A. and 5 colleagues. (2005). “Tumbling Asteroids.” *Icarus* **173**, 108-131.

Raab, H. (2018). Astrometrica software, version 4.12.0.448.
<http://www.astrometrica.at/>

Ryan, E.V.; Ryan, W.H. (2010web). “Threat Assessment of Small Near-Earth Objects.” Proceedings of the Advanced Maui Optical and Space Surveillance Technologies Conference 2010.
<https://amostech.com/TechnicalPapers/2010/Posters/Ryan.pdf>

Ryan, W.H. (2011web).
http://infohost.nmt.edu/~bryan/research/work/mro_images/BillRyan-k09w25v_091125.jpg

Skiff, B.A.; McLelland, K.P.; Sanborn, J.J.; Koehn, B.W.; Bowell, E. (2023). “Lowell Observatory Near-Earth Asteroid Photometric Survey (NEAPS): Paper 5.” *Minor Planet Bulletin* **50**, 74-101.

Warner, B.D.; Harris, A.W.; Pravec, P. (2009). “The Asteroid Lightcurve Database.” *Icarus* **202**, 134-146. Updated 2023 June.
<https://www.minorplanet.info/php/lcdb.php>

Warner, B.D. (2022). MPO Software, Canopus version 10.8.6.12. Bdw Publishing, Eaton, CO.

Zacharias, N.; Finch, C.T.; Girard, T.M.; Henden, A.; Bartlett, J.L.; Monet, D.G.; Zacharias, M.I. (2013). “The Fourth US Naval Observatory CCD Astrograph Catalog (UCAC4).” *Astronomical Journal* **145**, 44-57.

Zappala, V.; Cellini, A.; Barucci, A.M.; Fulchignoni, M.; Lupishko, D.E. (1990). “An analysis of the amplitude-phase relationship among asteroids.” *Astron. Astrophys.* **231**, 548-560.

Number	Name	yyyy mm/ dd	Phase	L _{PAB}	B _{PAB}	Period(h)	P.E.	Amp	A.E.	PAR	H
2009	WV25	2009 11/30–12/01	58.8–68.8	54	29	4.60	0.02	1.7	0.1	-2?	24.0
2017	WD28	2017 11/27–11/28	25.0–30.5	56	10	0.09440	0.00001	1.0	0.3	-3	25.7
						0.07248	0.00002	0.3	0.3		
						0.3127	0.0005	0.2	0.3		
2023	QC	2023 08/17–08/17	68.8–67.7	300	25	0.0079851	0.0000006	1.1	0.2		24.7
2023	QC	2023 08/19–08/19	18.4–16.6	319	5	0.0079852	0.0000002	0.6	0.1		
2023	QC	2023 08/20–08/20	6.0–5.8	324	-1	0.0079856	0.0000004	0.4	0.2		
2023	RP2	2023 09/09–09/09	22.9–21.8	344	11	0.0167213	0.0000005	0.7	0.2		27.2
2023	RG13	2023 09/15–09/16	39.0–38.2	11	9	0.2674	0.0004	1.1	0.2		24.4
2023	TC	2023 10/03–10/04	13.8–13.1	4	-2	0.05594	0.00002	0.6	0.3	-3	26.5
						0.04068	0.00002	0.4	0.3		

Table II. Observing circumstances and results. The phase angle is given for the first and last date. If preceded by an asterisk, the phase angle reached an extrema during the period. L_{PAB} and B_{PAB} are the approximate phase angle bisector longitude/latitude at mid-date range (see Harris et al., 1984). Amplitude error (A.E.) is calculated as $\sqrt{2} \times$ (lightcurve RMS residual). PAR is the expected Principal Axis Rotation quality detection code (Pravec et al., 2005) and H is the absolute magnitude at 1 au from Sun and Earth taken from the Small-Body Database Lookup (JPL, 2023b).

PHOTOMETRY AND LIGHTCURVE ANALYSIS OF EIGHT NEAR-EARTH ASTEROIDS

Wesley Pereira, Plácida Arcoverde, Marçal Evangelista-Santana,
Jonatan Michimani, Eduardo Rondón, Filipe Monteiro,
Wesley Mesquita, Tatiane Côrrea, Roberto Souza,
Teresinha Rodrigues, Daniela Lazzaro
Observatório Nacional, COAST,
Rua Gal. José Cristino 77, 20921-400
Rio de Janeiro, Brazil
josesilva@on.br

(Received: 2023 August 16)

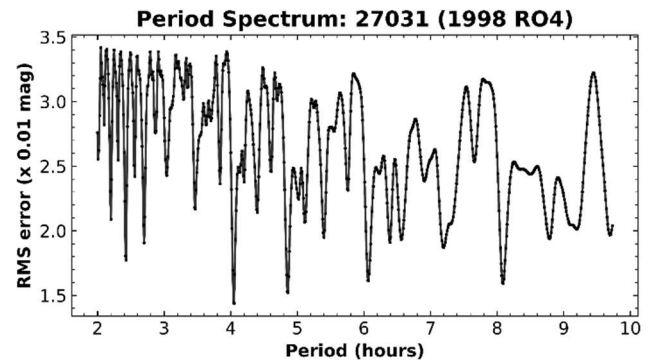
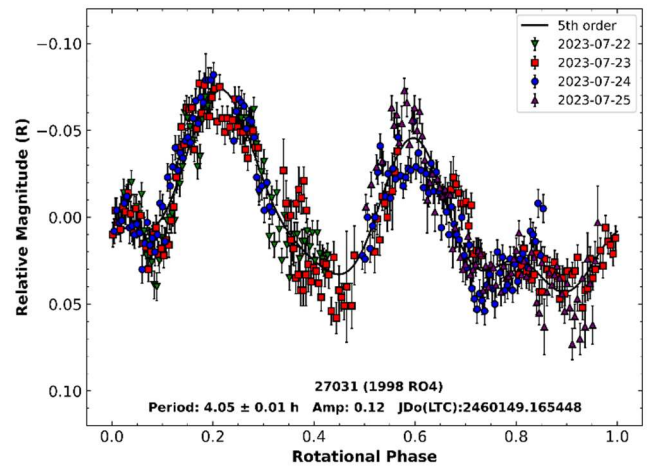
Rotational periods of eight near-Earth asteroids (NEAs) were determined from the lightcurve analysis of photometric observations acquired at the Observatório Astronômico do Sertão de Itaparica (MPC Y28, OASI) from 2021 January to 2023 July.

CCD photometric observations of eight near-Earth asteroids (NEAs) were carried out at the Observatório Astronômico do Sertão de Itaparica (MPC code Y28) between January 2021 and July 2023. We used the 1.0-m $f/8$ telescope of the IMPACTON project, a FLI PL424 CCD camera (2048 \times 2048 pixels), set to 2×2 binning, and a Johnson-Cousins R filter, details on the available instrumentation at OASI are given in Rondón et al. (2020).

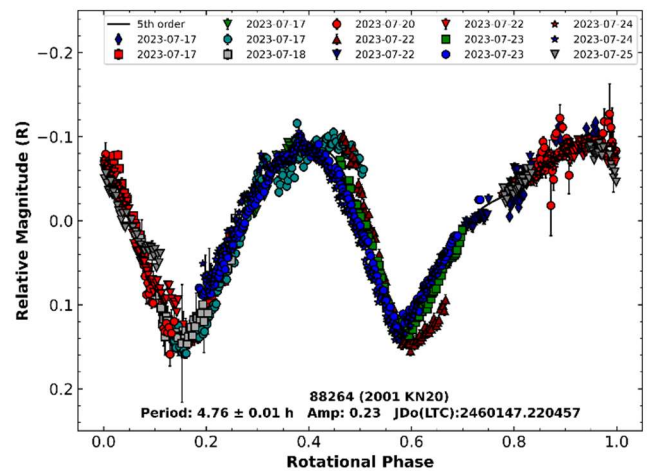
All the images were calibrated using *dark* and *flat field* frames, following standard procedures with IRAF. Lightcurve analysis was performed using the *MPO Canopus* software (Warner, 2018) and the method of differential photometry. To minimize the potential influence of color dependency, particularly at high air masses, comparison stars were selected among those more closely resembling solar colors. The resulting lightcurves yield the synodic rotation period. It is important to note that the given peak-to-peak amplitude was obtained through a Fourier fit (Harris et al., 1989) and may not necessarily represent the true amplitude.

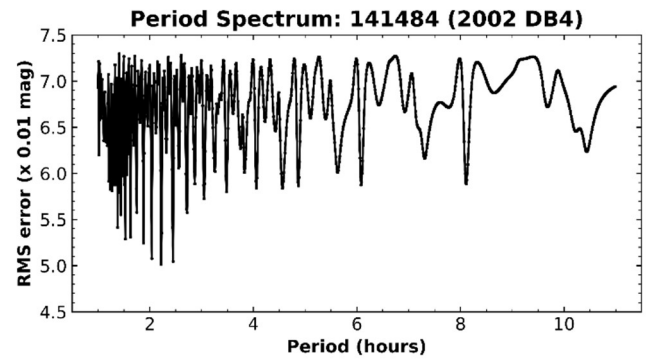
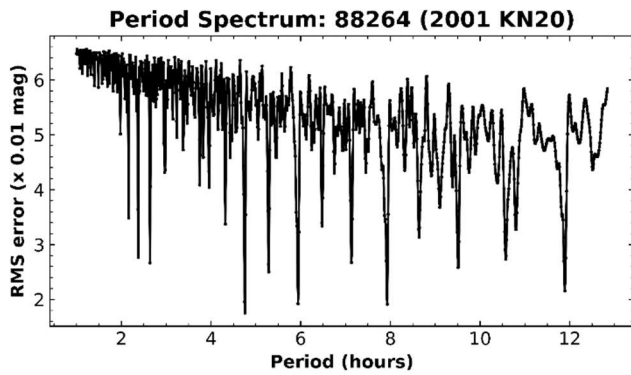
Table I gives for each object the observation dates, and circumstances, along with the computed rotation period and the lightcurve amplitude. Below we discuss the results obtained for each observed NEA and give its phased rotational lightcurve and periodogram.

(27031) 1998 RO4. This near-Earth asteroid was discovered on 14 September 1998 by LINEAR at Socorro, and belongs to the Amor group. A search in the Asteroid Lightcurve Database (LCDB; Warner et al., 2009) yielded no previously reported period for this NEA. Observations of this object were performed between 22 and 25 July, 2023. The period spectrum generated from four measurement groups, covering all data, exhibits a notable RMS minimum at 4.05 ± 0.01 hours and an amplitude of the rotational lightcurve of 0.12 mag. It is important to note that the composite light curve of 27031 (1998 RO4) shows brightness attenuations, as seen in the July 23rd and 24th dataset, which may be caused by possible mutual events. Therefore, more data are needed to investigate the binary nature of this asteroid.



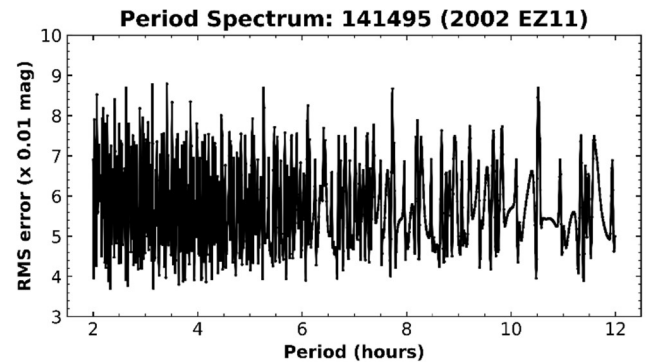
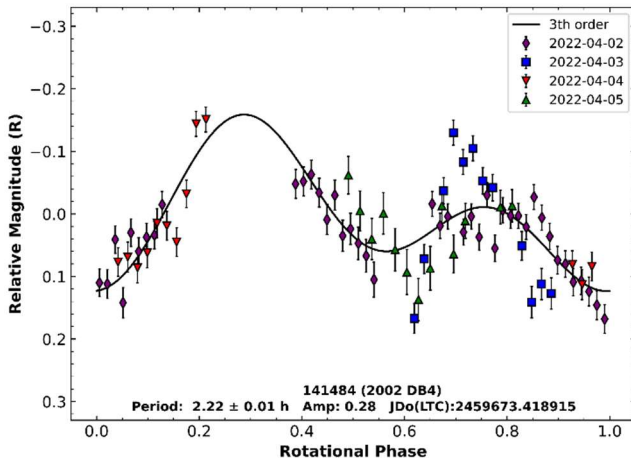
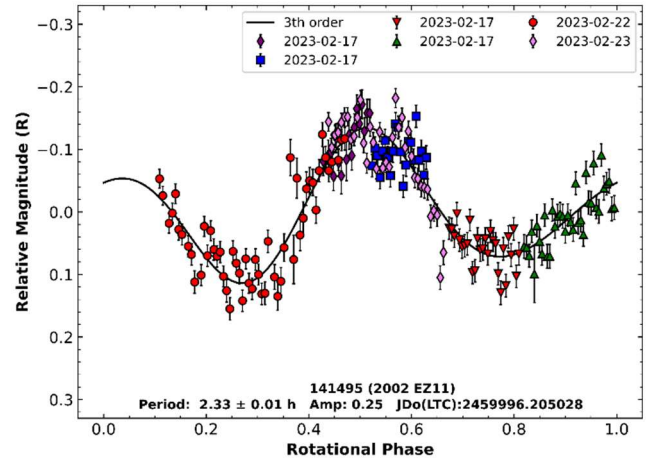
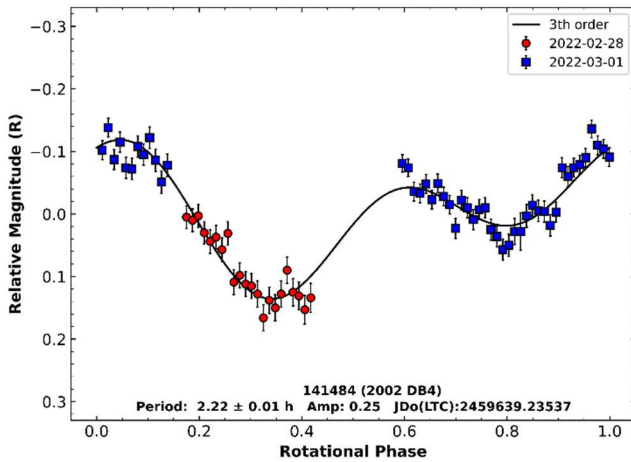
(88264) 2001 KN20. This Amor asteroid has a semimajor axis of 2.148 AU, an eccentricity of 0.451, an inclination of 12.067° , and an orbital period of 3.15 years. Its absolute magnitude is $H = 17.07$ (JPL, 2023), and it was discovered on 22 May, 2001, by LINEAR at Socorro. In the Asteroid Lightcurve Database (LCDB; Warner et al., 2009) we found a diameter $D = 1.3$ km using an absolute magnitude $H = 17.00$ and albedo $p = 0.166 \pm 0.161$ (Masiero et al., 2021). In six nights, from 17 to 25 July, 2023, we obtained over 1300 images of this asteroid. These images yielded a well-matched lightcurve with a rotation period of 4.76 ± 0.01 hours, and an amplitude of 0.25 ± 0.01 mag.



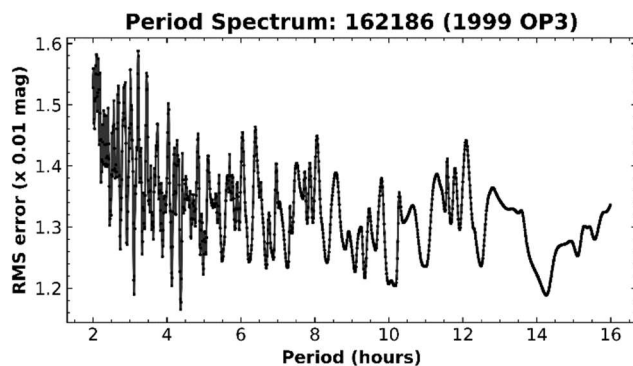
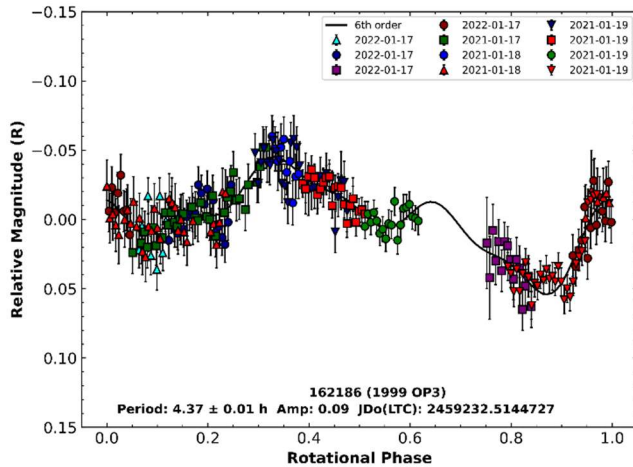


(141484) 2002 DB4. This NEA was discovered on 26 February, 2002 by LONEOS at Anderson Mesa and it belongs to the Aten group. This object was initially classified as Q-type by Lin et al. (2018), and subsequently reclassified as S-type by Binzel et al. (2019), as given in the Asteroid Lightcurve Database (LCDB; Warner et al., 2009). For this NEA it is also reported an estimated diameter of 1.235 ± 0.292 km and an albedo of 0.294 ± 0.182 (Masiero et al., 2020) but no period. Through observations spanning three nights between February and April 2022, we identified a rotation period of 2.22 ± 0.01 hours. The phased lightcurve from data obtained in February and March show an amplitude of 0.25 ± 0.01 mag while the April one an amplitude of 0.28 ± 0.01 mag. The solar phase angle changed slightly between the two set of observations, from 56.6° to 59.7° .

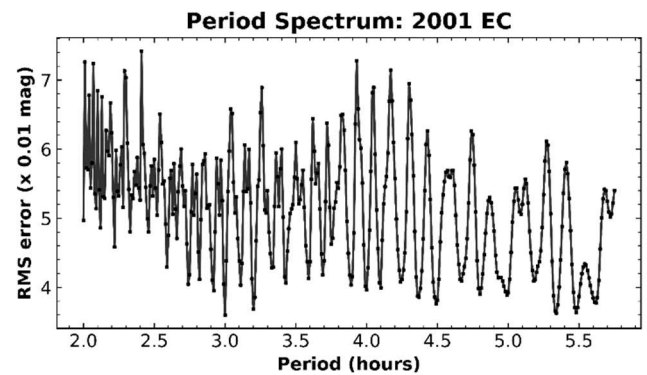
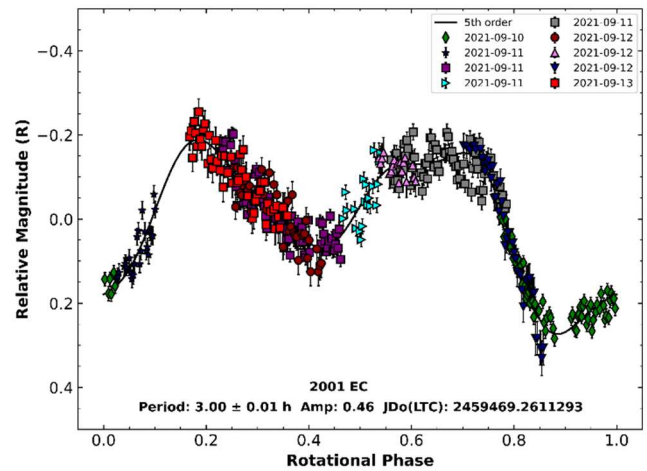
(141495) 2002 EZ11. This NEA, belonging to the Apollo group, classified as a potentially hazardous asteroid (PHA) and discovered by NEAT at Palomar in 2002, has an estimated diameter of 0.476 ± 0.135 km and an albedo of 0.245 ± 0.157 (Masiero et al., 2020). Two published rotation periods are given in the Asteroid Lightcurve Database (LCDB; Warner et al., 2009): Ries et al. (2004), report a period of 2.32 hours with an amplitude of 0.15 magnitudes, and Polishook (2012), a period of 2.327 ± 0.006 hours with an amplitude of 0.06 ± 0.02 mag. From observations over three nights in February 2022, we derived a rotation period of approximately 2.33 ± 0.01 hours, closely mirroring the previous findings. The associated lightcurve amplitude is 0.25 ± 0.01 mag, greater than those previously determined.



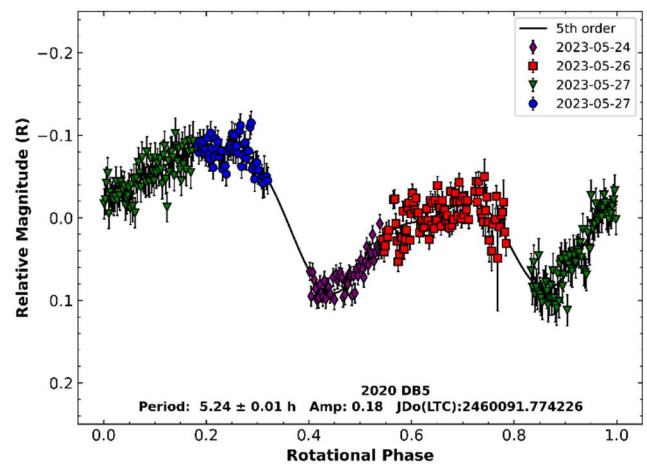
(162186) 1999 OP3. This NEA, of the Amor group, has an estimated diameter of around 3.8 km and an orbit with semi-major axis of 2.71 AU, eccentricity of 0.61 and inclination of 27.54 degrees (JPL, 2023). Observations of this object were obtained during three nights in January 2021, covering a total interval of 11.51 hours. The fit of the obtained data provides a period of 4.37 ± 0.01 hours and a lightcurve amplitude of 0.09 mag. A search in the Asteroid Lightcurve Database (LCDB; Warner et al., 2009) revealed a solution by Warner and Stephens (2021), with a period of 8.36 ± 0.03 hours and an amplitude of 0.04. However, the authors highlight the subtle amplitude of their lightcurve and skepticism regarding the result's reliability. The lightcurve here presented is quite well covered, besides the relatively small observation interval and the small amplitude, and we deem our solution to be reliable.



2001 EC. This NEA is classified as PHA and belongs to the Apollo group. The object has been classified as Sq-type by Binzel et al. (2004), having an absolute magnitude of $H = 18.65$ and an orbit with semimajor axis of 2.599 AU, eccentricity of 0.765 and inclination of 0.605° (JPL, 2023). No reported period is given in the Asteroid Lightcurve Database (LCDB; Warner et al., 2009). We observed this NEA over three nights in September 2021, and determined a rotation period of 3.00 ± 0.01 hours and a lightcurve amplitude of 0.46 mag.

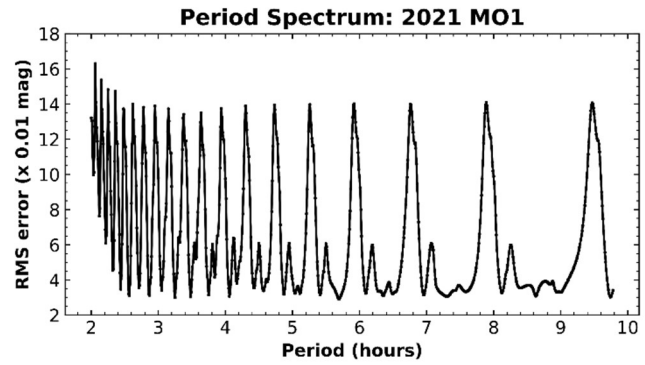
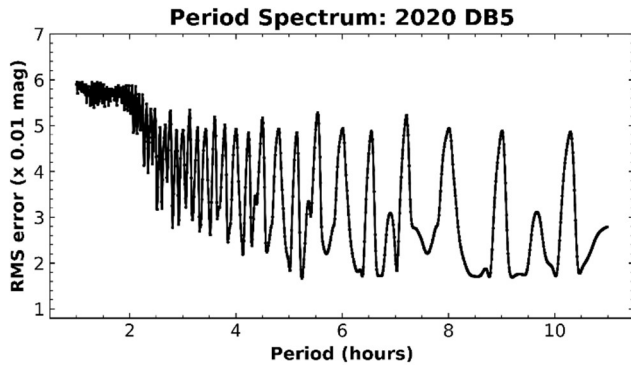


2020 DB5. This NEA, classified as a potentially hazardous asteroid, belongs to the Apollo group, exhibiting an absolute magnitude of $H = 19.23$ and a minimum orbit intersection distance (MOID) of 0.016 AU from Earth (JPL, 2023). This target was observed during three nights, from 24 to 27 May, 2023. The data fit indicates a rotation period of 5.24 ± 0.01 hours, and a lightcurve amplitude of 0.18 mag. An investigation in the Asteroid Lightcurve Database (LCDB; Warner et al., 2009), found no information regarding this object, being this its first determination for the rotation period.

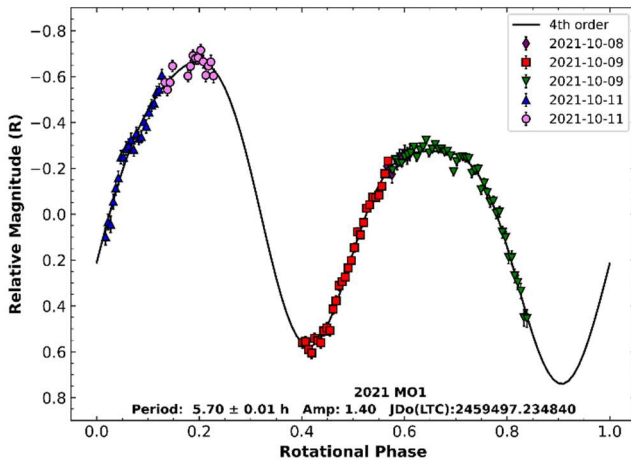


Number	Name	yyyy mm/dd	Phase	L _{PAB}	B _{PAB}	Period(h)	P.E.	Amp	A.E.	U
27031	1998 RO4	2023 07/22-07/25	29.2, 28.3	315	15	4.05	0.01	0.12	0.01	2
88264	2001 KN20	2023 07/17-07/25	11.9, 20.9	293	-10	4.76	0.01	0.23	0.01	3
141484	2002 DB4	2022 02/28-04/02	56.6, 59.7	116	-33	2.22	0.01	0.28	0.01	2-
141495	2002 EZ11	2023 02/17-02/28	37.7, 8.2	162	7	2.33	0.01	0.25	0.01	2-
162186	1999 OP3	2021 01/17-01/19	8.8, 7.5	128	5	4.37	0.01	0.09	0.01	2-
	2001 EC	2021 09/10-09/13	53.2, 74.3	314	2	3.00	0.01	0.46	0.01	3
	2020 DB5	2023 05/24-05/27	28.9, 28.7	179	3	5.24	0.01	0.18	0.01	2
	2021 MO1	2021 10/08-10/11	23.4	359	-7	5.70	0.01	1.40	0.01	2-

Table I. Observing circumstances and results. The phase angle is given for the first and last date. If preceded by an asterisk, the phase angle reached an extrema during the period. L_{PAB} and B_{PAB} are the approximate phase angle bisector longitude/latitude at mid-date range (see Harris et al., 1984).



2021 MO1. We observed this Amor asteroid during three nights in October of 2021 and determined a rotation period of 5.70 ± 0.01 hours. The very high amplitude of the phased lightcurve, $A = 1.40$ mag., suggests an object highly elongated. The light curve shows a limited coverage, since the object was observed for just 3.95 hours over the three nights. This resulted in a periodogram displaying several minimal peaks, which indicates that multiple periods are possible within this dataset. We are considering the presented solution because it has the minimum RMS. No previously published period for this NEA has been found in the literature.



Acknowledgements

The authors acknowledge CAPES, CNPq and FAPERJ for supporting this work through diverse fellowships and grants, and are grateful to the IMPACTON team, in particular, A. Santiago and J. dos Santos for the technical support at OASI.

References

Binzel, R.P.; Rivkin, A.S.; Stuart, J.S.; Harris, A.W.; Bus, S.J.; Burbine, T.H. (2004). "Observed spectral properties of near-Earth objects: results for population distribution, source regions, and space weathering processes." *Icarus* **170**(2), 259-294.

Binzel, R.P.; DeMeo, F.E.; Turtelboom, E.V.; Bus, S.J.; Tokunaga, A.; Burbine, T.H.; Lantz, C.; Polishook, D.; Carry, B.; Morbidelli, A.; Birlan, M.; Vernazza, P.; Burt, B.J.; Moskovitz, N.; Slivan, S.M.; Thomas, C.A.; Rivkin, A.S.; Hicks, M.D.; Dunn, T.; Reddy, V.; Sanchez, J.A.; Granvik, M.; Kohout, T. (2019). "Compositional distributions and evolutionary processes for the near-Earth object population: Results from the MIT-Hawaii Near-Earth Object Spectroscopic Survey (MITHNEOS)." *Icarus* **324**, 41-76.

Harris, A.W.; Young, J.W.; Scaltriti, F.; Zappala, V. (1984). "Lightcurves and phase relations of asteroids 82 Alkmene and 444 Gytis." *Icarus* **57**, 251-258.

Harris, A.W.; Young, J.W.; Bowell, E.; Martin, L.J.; Millis, R.L.; Poutanen, M.; Scaltriti, F.; Zappala, V.; Schober, H.J.; Debehogne, H.; Zeigler, K.W. (1989). "Photoelectric Observations of Asteroids 3, 24, 60, 261, and 863." *Icarus* **77**, 171-186.

JPL (2023). Small Body Database Search Engine. <https://ssd.jpl.nasa.gov>

Lin, C.-H.; Ip, W.-H.; Lin, Z.-Y.; Cheng, Y.-C.; Lin, H.-W.; Chang, C.-K. (2018). "Photometric survey and taxonomic identifications of 92 near-Earth asteroids." *Planetary and Space Science* **152**, 116-135.

Masiero, J.R.; Smith, P.; Teodoro, L.D.; Mainzer, A.K.; Cutri, R.M.; Grav, T.; Wright, E.L. (2020). "Physical Properties of 299 Near-Earth Objects Manually Recovered in Over Five Years of NEOWISE Survey Data." *Planetary Science Journal* **1**(1), 9.

Masiero, J.R.; Mainzer, A.K.; Bauer, J.M.; Cutri, R.M.; Grav, T.; Kramer, E.; Pittichová, J.; Wright, E.L. (2021). "Asteroid Diameters and Albedos from NEOWISE Reactivation Mission Years Six and Seven." *Planetary Science Journal* **2**(4), 162.

Polishook, D. (2012). "Lightcurves and Spin Periods of Near-Earth Asteroids, The Wise Observatory, 2005 - 2010." *Minor Planet Bulletin* **39**(3), 187-192.

Ries, J.G.; Barker, E.S.; Varadi, F.; Shelus, P.J. (2004). "R-Band Photometry of Potentially Hazardous Asteroids at McDonald Observatory." *American Astronomical Society Meeting Abstracts* **204**, 64.02.

Rondón, E.; Lazzaro, D.; Rodrigues, T.; Carvano, J.M.; Roig, F.; Monteiro, F.; Arcoverde, P.; Medeiros, H.; Silva, J.; Jasmim, F.; de Prá, M.; Hasselmann, P.; Ribeiro, A.; Dávalos, J.; Souza, R. (2020). "OASI: A Brazilian Observatory Dedicated to the Study of Small Solar System Bodies - Some Results of NEOs Physical Properties". *PASP* **132**, 065001.

Warner, B.D. (2018). MPO Canopus Software, v.10.8.6.3. Bdw publishing. <http://www.bdwpublishing.com>

Warner, B.D.; Harris, A.W.; Pravec, P. (2009). "The Asteroid Lightcurve Database." *Icarus* **202**, 134-146. Updated 2016 Sep. <http://www.minorplanet.info/lightcurvedatabase.html>

Warner, B.D.; Stephens, R.D. (2021). "Near-Earth Asteroid Lightcurve Analysis at the Center for Solar System Studies: January - March 2021." *Minor Planet Bulletin* **48**(3), 294-302.

**ROTATION PERIODS OF FIVE NEAR-EARTH
ASTEROIDS WITH THE TRAPPIST TELESCOPES:
(17188) 1999 WC2, (242450) 2004 QY2, (503871) 2000 SL,
2023 DZ2 AND 2023 CM**

Mohamed Amine Miftah
Faculté des Sciences Semlalia
Université Cadi Ayyad
Av. Prince My Abdellah, BP 2390, 40000 Marrakech, Morocco
mohamedamine.miftah@edu.uca.ma

Marin Ferrais
Arecibo Observatory, University of Central Florida,
Arecibo, PR 00612, USA

Youssef Moulane
Physics Department, Auburn University, AL 36832, USA

Emmanuël Jehin
Space sciences, Technologies &
Astrophysics Research (STAR) Institute
Université de Liège
Liège, Belgium

Abdelhadi Jabiri, Zouhair Benkhaldoun
Oukaïmeden Observatory,
Cadi Ayyad University, Marrakech, Morocco

(Received: 2023 August 29)

Lightcurves of five near-Earth asteroids were obtained with TRAPPIST-North and TRAPPIST-South from December 2022 to May 2023. For all of them the synodic rotation period and amplitude were found to be: (17188) 1999 WC2, (5.064 ± 0.002 h) and (0.35 ± 0.02 mag); (242450) 2004 QY2, (7.072 h ± 0.001 h) and (0.30 ± 0.01 mag); (503871) 2000 SL, (10.6504 h ± 0.0020 h) and (0.32 ± 0.04 mag); 2023 DZ2, (0.104587 ± 0.000083 h) and (0.58 ± 0.02 mag); 2023 CM, (3.6244 ± 0.0004 h) and (0.24 ± 0.02 mag). All data have been submitted to ALCDEF database.

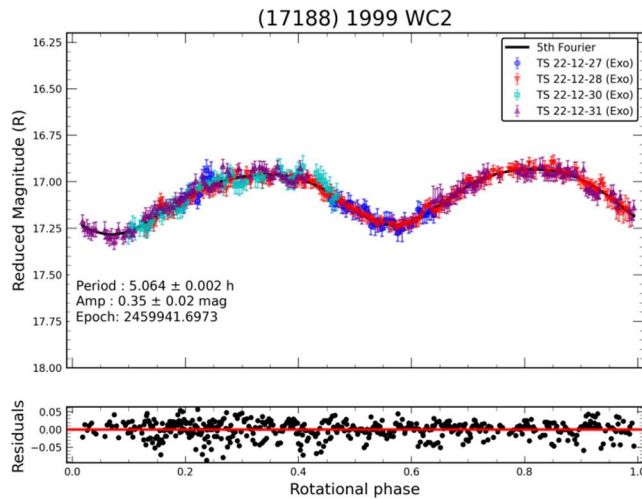
CCD photometric observations of five near-Earth asteroids (NEAs) (17188) 1999 WC2, (242450) 2004 QY2, (503871) 2000 SL, 2023 DZ2 and 2023 CM were made with the telescopes TRAPPIST-North (TN; IAU code Z53) and TRAPPIST-South (TS; IAU code I40) (Jehin et al., 2011), installed at the Oukaïmeden observatory in Morocco and the ESO La Silla observatory in Chile, respectively. Both are 0.6-m Ritchey-Chrétien telescopes operating at $f/8$ on German Equatorial mounts. The TN camera is an Andor IKONL BEX2 DD (0.60 arcsec/pixel), and the TS camera is an FLI ProLine 3041-BB (0.64 arcsec/pixel).

The calibration of the raw images using standard flat fields, dark and bias frames was obtained using the python framework Prose (Garcia et al., 2022). The aperture photometry and lightcurves were obtained with Photometry Pipeline developed by Mommert (2017). This pipeline allows zero-point calibration by matching field stars with online catalogs. The calibrated magnitudes found were corrected to heliocentric and geocentric distances using python script. The rotation periods were then determined using the software Peranso (Paunzen and Vanmunster, 2016), in which we used the FALC (Harris et al., 1989) and the ANOVA (Schwarzenberg-Czerny, 1996) methods. The amplitudes reported are from the Fourier series model curves.

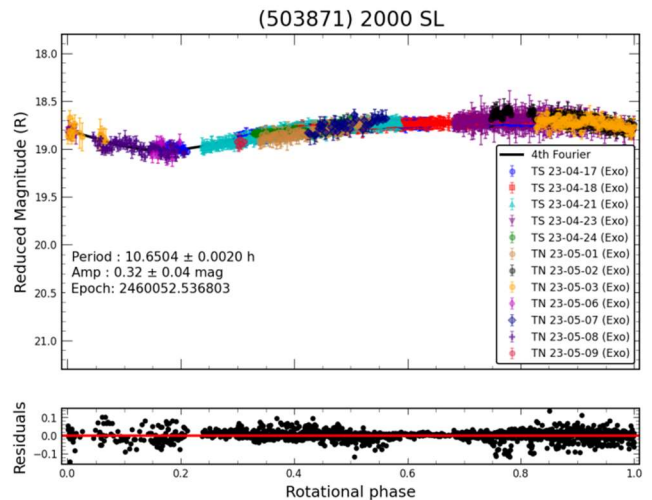
Number	Name	Pts	yyyy	mm/dd	Phase	L_{PAB}	B_{PAB}	Period(h)	P.E.	Amp	A.E.
17188	1999 WC2	563	2022	12/27-12/31	17.9, 19.6	106	-13	5.064	0.002	0.35	0.02
242450	2004 QY2	708	2023	02/05-03/06	76.3, 53.6	165	-56	7.072	0.001	0.30	0.01
503871	2000 SL	1909	2023	04/17-05/09	2.7, 76.6	201	39	10.6504	0.0020	0.32	0.04
	2023 DZ2	633	2023	03/22	60.7, 60.6	150	-0.5	0.104587	0.000083	0.58	0.02
	2023 CM	694	2023	03/07-03/09	22.0, 29.9	165	-12	3.6244	0.0004	0.24	0.02

Table I. Observing circumstances and results. Pts is the number of data points. The phase angle is given for the first and last date. If preceded by an asterisk, the phase angle reached an extrema during the period. L_{PAB} and B_{PAB} are the approximate phase angle bisector longitude/latitude at mid-date range (see Harris et al., 1984).

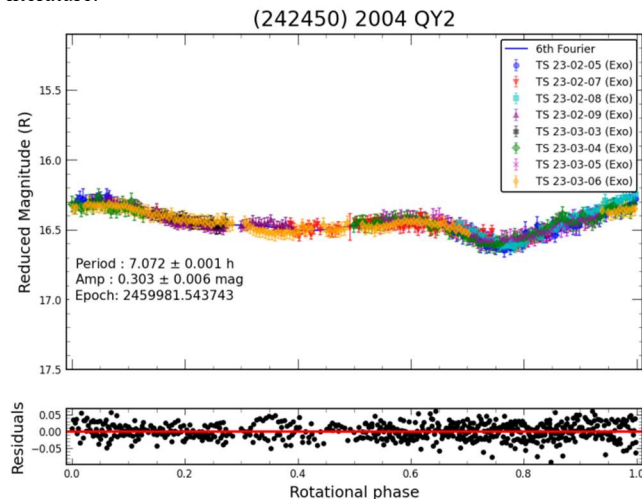
(17188) 1999 WC2 is an S-type NEA (Lin et al., 2018) that belongs to the Apollo family. It was observed for four nights with TS in December 2022 with a total duration of 11.37 h that corresponds roughly to twice its rotation period. All the observations were made using the Exo filter (a broad blue-cutting filter). The best fitting period found is (5.064 ± 0.002) h, which is in agreement with the values reported in ALCDEF (Warner, 2021). An approximate ratio of the a and b axis of 1999 WC2 calculated from the amplitude was found to be 1.38, which with the common bimodal form of the lightcurve suggest an elongated shape.



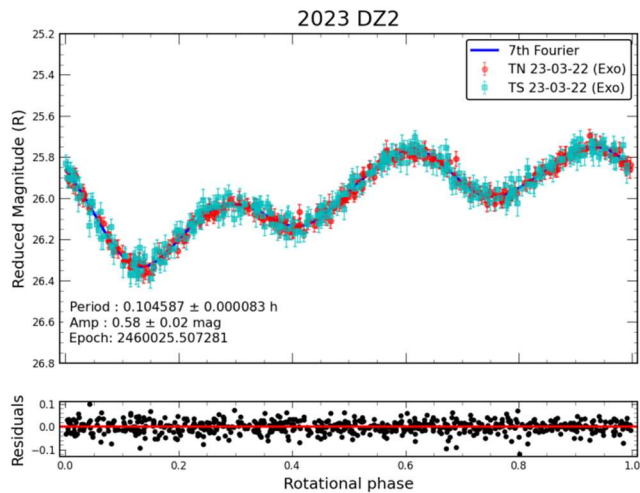
(503871) 2000 SL. This NEA was observed extensively for 12 nights in April and May 2023. Five nights with TS in late April and seven nights with TN in early May with a total duration of 36.41 h. All the observations were made using the Exo filter. The best fitting period found is (10.6504 ± 0.0020) h. We did not find a rotation period reported in the literature. In addition, BVRI sequences were acquired with TS on April 27, 2023, yielding $B-V = 0.86 \pm 0.01$, $V-R = 0.49 \pm 0.01$, $V-I = 0.89 \pm 0.03$. These color indices indicate an S-type classification, as already reported by others (e.g., Binzel et al., 2019).



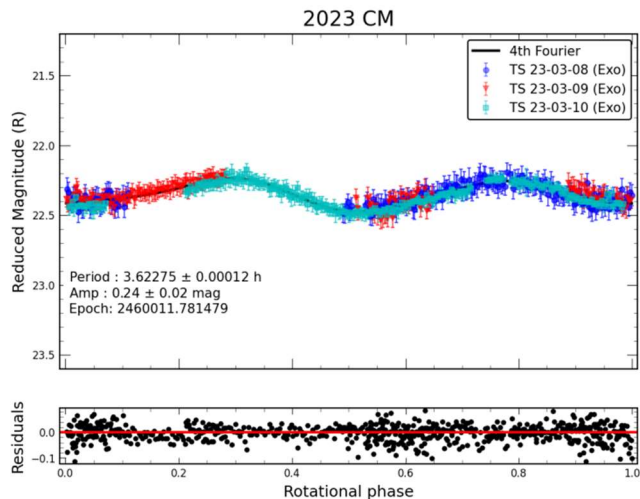
(242450) 2004 QY2 is a potentially hazardous asteroid. A close approach for this asteroid at a distance of 0.047 au to the Earth is expected in July 2029. We have observed it extensively using the Exo filter for eight nights with TS, four nights in early February and four nights in early March. The best fitting period found is (7.072 ± 0.001) h. We did not find a rotation period reported in the literature.



2023 DZ2 is a NEA that approached the Earth at a distance of 0.00117 au in March 2023. During this event, the radar images from Goldstone showed an elongated shape (<https://echo.jpl.nasa.gov/asteroids/2023DZ2/2023DZ2.2023.goldstone.planning.html>). It was observed for one night with both TN and TS at the same time which provided an observing run of 7.82 h. The best period found is (0.104587 ± 0.000083) h (~6 min), which is in agreement with the values reported in ALCDEF (Warner, 2021). We found a large amplitude equals to 0.58 mag. The corresponding axis ratio is 1.70, which suggests an elongated shape, but we note that the phase angle was over 60 degrees.



2023 CM is a potentially hazardous asteroid that approached the Earth at a distance of 0.026 au in March 2023. It was observed for three nights in March 2023 with TS using the Exo filter. The best fitting period found is (3.6244 ± 0.0004) h, which is in agreement with the values reported in ALCDEF (Warner, 2021). We also measured the colors of 2023 CM during the last night of observation and found colors indices $B - V = 0.83 \pm 0.04$, $V - R = 0.45 \pm 0.04$, $V - I = 0.79 \pm 0.06$, which suggest a Q-type classification.



Acknowledgements

TRAPPIST is a project funded by the Belgian Fonds (National) de la Recherche Scientifique (F.R.S.-FNRS) under grant PDR T.0.120.21. TRAPPIST-North is a project funded by the University of Liege, in collaboration with Cadi Ayyad University in Marrakech (Morocco). E. Jehin is FNRS senior Research Associate. The TRAPPIST project can be visited at the website <https://www.trappist.uliege.be>.

References

- Binzel, R.P.; DeMeo, F.; Turtelboom, E.V.; Bus, S.J.; Tokunaga, A.; Burbine, T.H.; Lantz, C.; Polishook, D.; Carry, B.; Morbidelli, A.; Birlan, M.; Vernazza, P.; Burt, B.J.; Moskovitz, N.; Slivan, S.M.; Thomas, C.A.; Rivikin, A.S.; Hicks, M.D.; Dunn, T.; Reddy, V.; Sanchez, J.A.; Granvik, M.; Kohout, T. (2019). "Compositional distributions and evolutionary processes for the near-Earth object population: Results from the MIT-Hawaii Near-Earth Object Spectroscopic Survey (MITHNEOS)." *Icarus* **324**, 41-76.
- Garcia, L.J.; Timmermans, M.; Pozuelos, F.J.; Ducrot, E.; Gillon, M.; Delrez, L.; Wells, R.D.; Jehin, E. (2022). "Prose: A Python framework for modular astronomical images processing." *Monthly Notices of the Royal Astronomical Society* **509(4)**, 4817-4828.
- Harris, A.W.; Young, J.W.; Scaltriti, F.; Zappala, V. (1984). "Lightcurves and phase relations of the asteroids 82 Alkmene and 444 Gyptis." *Icarus* **57(2)**, 251-258.
- Harris, A.W.; Young, J.W.; Bowell, E.; Martin, L.J.; Millis, R.L.; Poutanen, M.; Scaltriti, F.; Zappala, V.; Schoberm H.J.; Debehogne, H.; Zeigler, K.W. (1989). "Photoelectric observations of asteroids 3, 24, 60, 261, and 863." *Icarus* **77(1)**, 171-186.
- Jehin, E.; Gillon, M.; Queloz, D.; Magain, P.; Manfroid, J.; Chantry, V.; Lendl, M.; Hutsemékers, D.; Udry, S. (2011). "TRAPPIST: TRANSiting planets and Planetesimals small telescope." *The Messenger* **145**, 2-6.
- Lin, C.H.; Ip, W.H.; Lin, Z.Y.; Cheng, Y.C.; Lin, H.W.; Chang, C.K. (2018). "Photometric survey and taxonomic identifications of 92 near-Earth asteroids." *Planetary and Space Science* **152**, 116-135.
- Mommert, M. (2017). "PHOTOMETRYPIPELINE: An automated pipeline for calibrated photometry." *Astronomy and Computing* **18**, 47-53.
- Paunzen, E., Vanmunster, T. (2016). "Peranso - light curve and period analysis software." *Astronomische Nachrichten* **337(3)**, 239-245.
- Schwarzenberg-Czerny, A. (1996). "Fast and statistically optimal period search in uneven sampled observations." *The Astrophysical Journal* **460(2)**, L107.
- Warner, B.D.; Harris, A.W.; Pravec, P. (2009). "The Asteroid Lightcurve Database." *Icarus* **202**, 134-146. Updated 2023 Jun. <http://www.minorplanet.info/php/lcdb.php>
- Warner, B.D. (2021). Asteroid Lightcurve Data Exchange Format (ALCDEF) Database V1.0. *NASA Planetary Data System*, 9.

MINOR PLANETS AT UNUSUALLY FAVORABLE ELONGATIONS IN 2024

Frederick Pilcher
4438 Organ Mesa Loop
Las Cruces, NM 88011 USA
fpilcher35@gmail.com

(Received: 2023 September 18)

A list is presented of minor planets which are much brighter than usual at their 2024 apparitions.

The minor planets in the lists which follow will be much brighter at their 2024 apparitions than at their average distances at maximum elongation. Many years may pass before these planets will be again as bright as in 2024. Observers are encouraged to give special attention to those which lie near the limit of their equipment.

These lists have been prepared by an examination of the maximum elongation circumstances of minor planets computed by the author for all years through 2060 with a full perturbation program written by Dr. John Reed, and to whom he expresses his thanks. Elements are from EMP 1992, except that for all planets for which new or improved elements have been published subsequently in the Minor Planet Circulars or in electronic form, the newer elements have been used. Planetary positions are from the JPL DE-200 ephemeris, courtesy of Dr. E. Myles Standish.

Any planets whose brightest magnitudes near the time of maximum elongation vary by at least 2.0 in this interval and in 2024 will be within 0.3 of the brightest occurring, or vary by at least 3.0 and in 2024 will be within 0.5 of the brightest occurring; and which are visual magnitude 14.5 or brighter, are included. For planets brighter than visual magnitude 13.5, which are within the range of a large number of observers, these standards have been relaxed somewhat to include a larger number of planets. Magnitudes have been computed from the updated magnitude parameters published in MPC28104-28116, on 1996 Nov. 25, or more recently in the Minor Planet Circulars.

Oppositions may be in right ascension or in celestial longitude. Here we use still a third representation, maximum elongation from the Sun, instead of opposition. Though unconventional, it has the advantage that many close approaches do not involve actual opposition to the Sun near the time of minimum distance and greatest brightness and are missed by an opposition-based program. Other data are also provided according to the following tabular listings: Minor planet number, date of maximum elongation from the Sun in format yyyy/mm/dd, maximum elongation in degrees, right ascension on date of maximum elongation, declination on date of maximum elongation, both in J2000 coordinates, date of brightest magnitude in format yyyy/mm/dd, brightest magnitude, date of minimum distance in format yyyy/mm/dd, and minimum distance in AU.

Users should note that when the maximum elongation is about 177° or greater, the brightest magnitude is sharply peaked due to enhanced brightening near zero phase angle. Even as near as 10 days before or after minimum magnitude the magnitude is generally about 0.4 magnitudes greater. This effect takes place in greater time interval for smaller maximum elongations. There is some interest in very small minimum phase angles. For maximum elongations E near 180° at Earth distance Δ, an approximate formula for the minimum phase angle φ is

$$\phi=(180^\circ-E)/(\Delta+1)$$

A special list of asteroids approaching the Earth more closely than 0.4 AU is provided following the list of temporal sequence of favorable elongations. This list includes 1036 Ganymed, which with a diameter of 37 kilometers is the largest of the Mars Crossers, will be at magnitude 9.0 on Oct. 17 and brighter than at any time in the next 100 years.

Table I. Numerical Sequence of Favorable Elongations

Planet	Max	Elon	D	Max	E	RA	Dec	Br	Mag	D	Br	Mag	Min	Dist	D	Min	Dist
13	2024/12/01	166.9°	4h30m	+34°	2024/12/02	9.9	2024/12/03	1.457									
15	2024/12/14	169.4°	5h23m	+33°	2024/12/13	8.0	2024/12/08	1.299									
19	2024/10/17	179.6°	1h29m	+9°	2024/10/17	8.9	2024/10/17	1.065									
38	2024/02/07	175.5°	9h15m	+11°	2024/02/07	11.1	2024/02/04	1.392									
42	2024/06/28	176.2°	18h30m	-27°	2024/06/28	9.2	2024/07/05	0.983									
43	2024/06/03	178.3°	16h43m	-23°	2024/06/03	9.1	2024/06/08	0.847									
69	2024/12/12	166.5°	5h21m	+9°	2024/12/12	10.4	2024/12/15	1.563									
78	2024/01/30	173.4°	8h55m	+24°	2024/01/30	10.3	2024/01/30	1.108									
86	2024/10/15	172.7°	1h30m	+1°	2024/10/15	11.6	2024/10/15	1.451									
109	2024/10/07	176.7°	0h49m	+8°	2024/10/08	10.6	2024/10/16	1.017									
126	2024/08/26	175.8°	22h26m	-14°	2024/08/26	11.6	2024/08/26	1.184									
137	2024/09/20	170.6°	23h33m	+7°	2024/09/19	11.5	2024/09/13	1.605									
194	2024/09/02	179.1°	22h49m	-8°	2024/09/02	9.3	2024/08/29	1.004									
281	2024/11/16	175.6°	3h24m	+23°	2024/11/16	13.4	2024/11/14	0.912									
289	2024/09/05	176.2°	22h50m	-3°	2024/09/05	12.2	2024/09/08	1.339									
335	2024/08/03	177.0°	20h50m	-14°	2024/08/03	10.9	2024/07/30	1.058									
350	2024/12/11	171.7°	5h12m	+14°	2024/12/11	11.8	2024/12/10	1.637									
354	2024/01/20	168.6°	7h51m	+9°	2024/01/20	9.7	2024/01/22	1.550									
361	2024/12/03	165.4°	4h31m	+36°	2024/12/03	12.8	2024/12/04	2.192									
372	2024/02/17	179.4°	9h58m	+12°	2024/02/17	10.5	2024/02/10	1.679									
376	2024/06/11	172.2°	17h14m	-30°	2024/06/11	11.0	2024/06/11	0.882									
396	2024/05/29	179.7°	16h24m	-21°	2024/05/29	12.4	2024/06/01	1.316									
445	2024/08/31	154.1°	22h10m	+16°	2024/09/02	13.2	2024/09/04	1.682									
470	2024/04/06	174.6°	13h11m	-1°	2024/04/06	12.4	2024/04/09	1.191									
501	2024/09/16	177.7°	23h39m	-4°	2024/09/16	12.4	2024/09/15	1.708									
518	2024/10/04	177.1°	0h35m	+6°	2024/10/03	13.0	2024/09/25	1.083									
519	2024/10/02	168.6°	0h50m	-7°	2024/10/01	12.0	2024/09/28	1.312									
532	2024/04/08	151.7°	13h53m	+18°	2024/04/07	9.0	2024/04/07	1.352									
547	2024/10/12	176.3°	1h18m	+4°	2024/10/12	11.6	2024/10/12	1.128									
549	2024/01/29	177.6°	8h44m	+15°	2024/01/29	13.0	2024/01/23	1.109									
550	2024/07/13	172.7°	19h30m	-14°	2024/07/14	11.3	2024/07/17	1.031									
569	2024/02/05	179.4°	9h12m	+15°	2024/02/05	12.6	2024/01/31	1.328									
572	2024/09/24	175.4°	23h58m	+4°	2024/09/25	12.9	2024/09/26	1.049									
646	2024/09/26	167.0°	23h53m	+13°	2024/09/25	14.0	2024/09/20	0.862									
679	2024/12/25	163.1°	5h59m	+6°	2024/12/21	11.5	2024/12/12	1.140									
688	2024/08/02	168.0°	20h33m	-6°	2024/08/02	13.5	2024/08/01	1.323									
737	2024/08/09	160.9°	20h47m	+1°	2024/08/09	10.8	2024/08/09	0.973									
749	2024/05/05	169.4°	15h 0m	-5°	2024/05/05	13.3	2024/05/08	0.859									
784	2024/06/07	161.0°	16h55m	-41°	2024/06/06	12.1	2024/06/06	1.371									
787	2024/08/27	165.9°	21h57m	+2°	2024/08/26	12.6	2024/08/23	1.236									
789	2024/06/11	170.8°	17h22m	-13°	2024/06/11	13.6	2024/06/13	1.293									
822	2024/01/04	178.5°	6h59m	+21°	2024/01/04	13.5	2024/01/04	0.925									
883	2024/08/13	173.7°	21h26m	-8°	2024/08/13	13.7	2024/08/13	0.786									
886	2024/11/08	173.1°	2h57m	+9°	2024/11/07	11.8	2024/10/31	1.456									
888	2024/12/31	169.7°	6h37m	+12°	2024/12/30	12.2	2024/12/27	1.276									
901	2024/07/15	176.3°	19h37m	-17°	2024/07/15	12.4	2024/07/23	0.790									
915	2024/09/21	178.0°	23h59m	-2°	2024/09/21	13.4	2024/09/25	1.000									
926	2024/05/26	171.7°	16h10m	-29°	2024/05/26	13.4	2024/05/24	1.465									
953	2024/07/26	164.4°	20h41m	-34°	2024/07/26	13.1	2024/07/24	1.269									
959	2024/11/10	178.5°	3h 2m	+15°	2024/11/09	13.2	2024/11/06	1.493									
1013	2024/12/14	162.3°	5h31m	+40°	2024/12/16	12.9	2024/12/20	1.263									
1035	2024/08/31	167.1°	22h52m	-21°	2024/08/30	13.7	2024/08/29	1.565									
1036	2024/10/27	138.9°	23h18m	+16°	2024/10/17	9.0	2024/10/13	0.374									
1040	2024/01/14	173.3°	7h40m	+14°	2024/01/14	13.8	2024/01/11	1.634									
1057	2024/11/26	178.5°	4h10m	+22°	2024/11/26	13.6	2024/11/18	1.360									
1059	2024/09/06	169.1°	22h39m	+3°	2024/09/04	13.5	2024/08/29	1.295									
1065	2024/09/19	171.0°	23h36m	+7°	2024/09/17	14.1	2024/09/08	0.714									
1074	2024/10/09	179.4°	0h59m	+5°	2024/10/09	13.4	2024/10/12	1.697									
1099	2024/09/07	167.2°	23h21m	-17°	2024/09/08	13.3	2024/09/11	1.348									
1139	2024/10/02	164.5°	23h58m	+16°	2024/10/06	12.9	2024/10/14	0.572									
1188	2024/10/10	177.8°	0h59m	+8°	2024/10/10	12.7	2024/10/08	0.798									
1242	2024/10/11	171.1°	0h55m	+15°	2024/10/11	12.7	2024/10/13	1.254									
1275	2024/11/01	167.7°	2h48m	+3°	2024/11/01	13.4	2024/10/30	1.260									
1284	2024/12/07	165.3°	4h41m	+36°	2024/12/06	12.9	2024/12/04	1.232									
1427	2024/07/26	167.6°	20h38m	-31°	2024/07/26	13.2	2024/07/28	1.184									
1479	2024/11/03	174.8°	2h31m	+20°	2024/11/04	14.1	2024/11/09	1.324									
1539	2024/11/15	177.2°	3h27m	+15°	2024/11/15	13.8	2024/11/12	1.574									
1585	2024/02/05	167.9°	8h53m	+4°	2024/02/03	14.0	2024/01/26	1.515									
1613	2024/01/15	173.1°	7h47m	+28°	2024/01/14	13.5	2024/01/10	1.086									
1626	2024/12/28	176.5°	6h25m	+26°	2024/12/28	11.4	2024/12/23	0.772									
1666	2024/10/21	175.3°	1h38m	+15°	2024/10/21	14.0	2024/10/14	0.860									
1685	2024/02/23	123.2°	6h41m	-2°	2024/01/28	12.6	2024/01/20	0.133									
1693	2024/05/21	176.4°	15h54m	-16°	2024/05/21	13.6	2024/06/01	1.294									
1709	2024/08/06	176.0°	21h 3m	-12°	2024/08/06	14.2	2024/08/11	0.896									
1730	2024/09/12	179.4°	23h24m	-3°	2024/09/13	13.9	2024/09/18	1.288									

Planet	Max Elon	D	Max E	RA	Dec	Br Mag	D	Br Mag	Min Dist	D	Min Dist	Planet	Max Elon	D	Max E	RA	Dec	Br Mag	D	Br Mag	Min Dist	D	Min Dist			
1752	2024/10/10	175.2°	0h57m	+11°	2024/10/10	14.5	2024/10/02	0.865	549	2024/01/29	177.6°	8h44m	+15°	2024/01/29	13.0	2024/01/23	1.109	78	2024/01/30	173.4°	8h55m	+24°	2024/01/30	10.3	2024/01/30	1.108
1759	2024/09/28	175.4°	0h27m	-2°	2024/09/28	14.3	2024/09/26	0.820	569	2024/02/05	179.4°	9h12m	+15°	2024/02/05	12.6	2024/01/31	1.328	1585	2024/02/05	167.9°	8h53m	+4°	2024/02/03	14.0	2024/01/26	1.515
1763	2024/08/05	178.5°	21h 0m	-15°	2024/08/05	13.3	2024/08/08	0.747	38	2024/02/07	175.5°	9h15m	+11°	2024/02/07	11.1	2024/02/04	1.392	372	2024/02/17	179.4°	9h58m	+12°	2024/02/17	10.5	2024/02/10	1.679
1808	2024/11/05	178.1°	2h39m	+17°	2024/11/05	14.5	2024/11/06	1.276	187026	2024/02/19	176.6°	9h56m	+13°	2024/02/19	12.8	2024/02/20	0.097	3125	2024/02/20	172.7°	10h27m	+17°	2024/02/20	14.5	2024/02/18	1.122
1945	2024/08/13	179.6°	21h31m	-14°	2024/08/13	14.1	2024/08/14	1.094	1685	2024/02/23	123.2°	6h41m	-2°	2024/01/28	12.6	2024/01/20	1.133	4744	2024/03/20	176.2°	11h54m	-3°	2024/03/20	13.6	2024/03/20	1.274
1982	2024/09/21	169.2°	0h 7m	-10°	2024/09/19	13.8	2024/09/11	0.798	470	2024/04/06	174.6°	13h11m	-1°	2024/04/06	12.4	2024/04/09	1.191	532	2024/04/08	151.7°	13h53m	+18°	2024/04/07	9.0	2024/04/07	1.352
2021	2024/09/09	177.4°	23h17m	-7°	2024/09/09	14.4	2024/09/03	0.832	2063	2024/04/23	179.4°	14h 2m	-12°	2024/04/23	13.8	2024/03/31	1.120	2637	2024/04/23	179.4°	14h 2m	-12°	2024/04/23	13.8	2024/03/31	1.120
2021	2024/09/09	177.4°	23h17m	-7°	2024/09/09	14.4	2024/09/03	0.832	2830	2024/04/24	163.0°	14h12m	+3°	2024/04/23	14.5	2024/04/22	0.922	2554	2024/06/16	174.7°	17h38m	-28°	2024/05/02	14.2	2024/05/07	1.011
2063	2024/04/23	179.4°	14h 2m	-12°	2024/04/23	13.8	2024/03/01	0.120	4844	2024/05/02	174.8°	14h31m	-20°	2024/05/02	14.2	2024/05/07	1.011	2571	2024/09/09	173.6°	23h24m	-10°	2024/09/09	14.1	2024/09/09	0.792
2262	2024/10/20	167.3°	1h25m	+22°	2024/10/18	14.5	2024/10/11	0.959	749	2024/05/05	169.4°	15h 0m	-5°	2024/05/05	13.3	2024/05/08	0.859	40729	2024/05/12	179.3°	15h20m	-18°	2024/05/12	14.2	2024/05/22	0.910
2266	2024/11/28	174.0°	4h21m	+15°	2024/11/28	14.5	2024/11/28	1.801	21374	2024/05/20	172.5°	15h20m	-17°	2024/05/20	13.3	2024/05/21	1.110	2637	2024/09/26	177.5°	0h11m	+3°	2024/09/27	13.8	2024/09/27	0.727
2308	2024/06/12	159.6°	17h26m	-43°	2024/06/12	14.3	2024/06/13	1.130	1693	2024/05/21	176.4°	15h54m	-16°	2024/05/21	13.6	2024/06/01	1.294	2637	2024/09/26	177.5°	0h11m	+3°	2024/09/27	13.8	2024/09/27	0.727
2393	2024/10/11	172.7°	0h53m	+13°	2024/10/10	14.1	2024/10/05	1.703	926	2024/05/26	171.7°	16h10m	-29°	2024/05/26	13.4	2024/05/24	1.465	2637	2024/09/26	177.5°	0h11m	+3°	2024/09/27	13.8	2024/09/27	0.727
2505	2024/06/01	179.3°	16h37m	-22°	2024/06/01	14.5	2024/06/03	1.603	3089	2024/05/26	168.5°	16h19m	-9°	2024/05/27	14.1	2024/05/31	1.428	396	2024/05/29	179.7°	16h24m	-21°	2024/05/29	12.4	2024/06/01	1.316
2543	2024/07/29	153.3°	21h13m	-44°	2024/07/31	14.0	2024/08/02	1.299	396	2024/05/29	179.7°	16h24m	-21°	2024/05/29	12.4	2024/06/01	1.316	2505	2024/06/01	179.3°	16h37m	-22°	2024/06/01	14.5	2024/06/03	1.603
2554	2024/06/16	174.7°	17h38m	-28°	2024/06/16	14.5	2024/06/17	0.921	43	2024/06/03	178.3°	16h43m	-23°	2024/06/03	9.1	2024/06/08	0.847	10422	2024/06/03	176.7°	16h48m	-25°	2024/06/03	14.4	2024/06/06	1.267
2571	2024/09/09	173.6°	23h24m	-10°	2024/09/09	14.1	2024/09/09	0.792	10422	2024/06/03	176.7°	16h48m	-25°	2024/06/03	14.4	2024/06/06	1.267	2829	2024/08/16	170.8°	21h36m	-4°	2024/08/17	14.5	2024/08/21	0.698
2623	2024/09/26	177.5°	0h11m	+3°	2024/09/26	13.8	2024/09/27	0.727	784	2024/06/07	161.0°	16h55m	-41°	2024/06/06	12.1	2024/06/06	1.371	396	2024/05/29	179.7°	16h24m	-21°	2024/05/29	12.4	2024/06/01	1.316
2637	2024/09/26	178.5°	0h11m	+2°	2024/09/26	13.9	2024/09/19	0.748	4428	2024/06/10	179.0°	17h14m	-22°	2024/06/10	14.4	2024/06/18	0.859	2505	2024/06/01	179.3°	16h37m	-22°	2024/06/01	14.5	2024/06/03	1.603
2648	2024/11/16	172.6°	3h16m	+25°	2024/11/16	14.3	2024/11/14	0.873	376	2024/06/11	172.2°	17h14m	-30°	2024/06/11	11.0	2024/06/11	0.882	43	2024/06/03	178.3°	16h43m	-23°	2024/06/03	9.1	2024/06/08	0.847
2693	2024/11/07	176.0°	2h55m	+12°	2024/11/07	14.5	2024/11/06	0.845	789	2024/06/11	170.8°	17h22m	-13°	2024/06/11	13.6	2024/06/13	1.293	10422	2024/06/03	176.7°	16h48m	-25°	2024/06/03	14.4	2024/06/06	1.267
2829	2024/08/14	179.1°	21h37m	-15°	2024/08/14	13.3	2024/08/11	1.519	2308	2024/06/12	159.6°	17h26m	-43°	2024/06/12	14.3	2024/06/13	1.130	3125	2024/02/20	172.7°	10h27m	+17°	2024/02/20	14.5	2024/02/18	1.122
2830	2024/04/24	163.0°	2h42m	+3°	2024/04/23	14.5	2024/04/22	0.922	2554	2024/06/16	174.7°	17h38m	-28°	2024/06/16	14.5	2024/06/17	0.921	3220	2024/11/08	175.2°	4h52m	+17°	2024/11/08	14.2	2024/11/08	0.852
3089	2024/05/26	168.5°	16h19m	-9°	2024/05/27	14.1	2024/05/31	1.428	42	2024/06/28	176.2°	18h30m	-27°	2024/06/28	9.2	2024/07/05	0.983	3248	2024/09/28	177.9°	0h21m	+0°	2024/09/28	14.4	2024/09/24	1.782
3093	2024/10/05	156.9°	0h 4m	+25°	2024/10/02	14.3	2024/09/28	1.227	10487	2024/06/28	177.9°	18h25m	-21°	2024/06/28	14.5	2024/07/01	0.930	3280	2024/08/05	179.5°	21h 4m	-17°	2024/08/05	14.4	2024/08/05	1.109
3106	2024/11/21	157.6°	4h 1m	-2°	2024/11/20	14.1	2024/11/19	1.445	3973	2024/07/04	177.9°	18h55m	-24°	2024/07/04	14.5	2024/07/10	0.903	3722	2024/11/14	179.8°	3h18m	+18°	2024/11/14	14.0	2024/11/06	0.878
3125	2024/02/20	172.7°	10h27m	+17°	2024/02/20	14.5	2024/02/18	1.122	550	2024/07/13	172.7°	19h30m	-14°	2024/07/14	11.3	2024/07/17	1.031	3737	2024/07/15	176.3°	19h37m	-17°	2024/07/15	12.4	2024/07/23	0.790
3220	2024/11/08	175.2°	4h52m	+17°	2024/11/08	14.2	2024/11/08	0.852	901	2024/07/15	176.3°	19h37m	-17°	2024/07/15	12.4	2024/07/23	0.790	3737	2024/07/17	173.6°	19h50m	-14°	2024/07/19	14.3	2024/08/06	0.809
3248	2024/09/28	177.9°	0h21m	+0°	2024/09/28	14.4	2024/09/24	1.782	17512	2024/07/18	167.5°	19h57m	-33°	2024/07/17	14.5	2024/07/14	0.805	3831	2024/08/06	176.8°	21h 2m	-13°	2024/08/06	14.3	2024/08/02	0.738
3280	2024/08/05	179.5°	21h 4m	-17°	2024/08/05	14.4	2024/08/05	1.109	3300	2024/07/24	149.6°	20h55m	-49°	2024/07/23	14.2	2024/07/22	1.608	737	2024/08/09	160.9°	20h47m	+1°	2024/08/09	10.8	2024/08/09	0.973
3300	2024/07/24	149.6°	20h55m	-49°	2024/07/23	14.2	2024/07/22	1.608	953	2024/07/26	164.4°	20h41m	-34°	2024/07/26	13.1	2024/07/24	1.269	4511	2024/08/10	142.1°	21h33m	-53°	2024/08/08	14.2	2024/08/06	0.891
3330	2024/09/21	176.7°	23h59m	-2°	2024/09/21	14.5	2024/09/15	1.626	1427	2024/07/26	167.6°	20h38m	-31°	2024/07/26	13.2	2024/07/28	1.184	4066	2024/09/27	170.1°	23h58m	+10°	2024/09/27	13.8	2024/09/27	0.727
3682	2024/10/17	157.2°	0h38m	+3°	2024/10/15	13.4	2024/10/12	0.929	5330	2024/07/27	175.6°	20h27m	-23°	2024/07/27	14.5	2024/07/29	1.349	4150	2024/08/17	177.4°	21h49m	-15°	2024/08/16	14.1	2024/08/15	0.851
3698	2024/08/06	179.7°	21h 7m	-16°	2024/08/06	14.3	2024/08/05	0.802	2543	2024/07/29	153.3°	21h13m	-44°	2024/07/31	14.0	2024/08/02	1.299	4428	2024/06/10	179.0°	17h14m	-22°	2024/06/10	14.4	2024/06/18	0.859
3722	2024/11/14	179.8°	3h18m	+18°	2024/11/14	14.0	2024/11/06	0.878	688	2024/08/02	168.0°	20h33m	-6°	2024/08/02	13.5	2024/08/01	1.323	4511	2024/08/10	142.1°	21h33m	-53°	2024/08/02	13.5	2024/08/01	1.323
3737	2024/07/17	173.6°	19h50m	-14°	2024/07/19	14.3	2024/08/06	0.809	335	2024/08/03	177.0°	20h50m	-14°	2024/08/03	10.9											

Planet	Max	Elon	D	Max	E	RA	Dec	Br	Mag	D	Br	Mag	Min	Dist	D	Min	Dist
1759	2024/09/28	175.4°		0h27m	- 2°	2024/09/28	14.3	2024/09/26		0.820							
3248	2024/09/28	177.9°		0h21m	+ 0°	2024/09/28	14.4	2024/09/24		1.782							
7898	2024/09/28	163.7°		0h44m	-12°	2024/09/26	14.3	2024/09/22		0.760							
519	2024/10/02	168.6°		0h50m	- 7°	2024/10/01	12.0	2024/09/28		1.312							
1139	2024/10/02	164.5°		23h58m	+16°	2024/10/06	12.9	2024/10/14		0.572							
518	2024/10/04	177.1°		0h35m	+ 6°	2024/10/03	13.0	2024/09/25		1.083							
3093	2024/10/05	156.9°		0h 4m	+25°	2024/10/02	14.3	2024/09/28		1.227							
109	2024/10/07	176.7°		0h49m	+ 8°	2024/10/08	10.6	2024/10/16		1.017							
1074	2024/10/09	179.4°		0h59m	+ 5°	2024/10/09	13.4	2024/10/12		1.697							
1188	2024/10/10	177.8°		0h59m	+ 8°	2024/10/10	12.7	2024/10/08		0.798							
1752	2024/10/10	175.2°		0h57m	+11°	2024/10/10	14.5	2024/10/02		0.865							
1242	2024/10/11	171.1°		0h55m	+15°	2024/10/11	12.7	2024/10/13		1.254							
2393	2024/10/11	172.7°		0h53m	+13°	2024/10/10	14.1	2024/10/05		1.703							
547	2024/10/12	176.3°		1h18m	+ 4°	2024/10/12	11.6	2024/10/12		1.128							
13441	2024/10/13	176.2°		1h23m	+ 4°	2024/10/13	14.2	2024/10/06		0.999							
86	2024/10/15	172.7°		1h30m	+ 1°	2024/10/15	11.6	2024/10/15		1.451							
19	2024/10/17	179.6°		1h29m	+ 9°	2024/10/17	8.9	2024/10/17		1.065							
3682	2024/10/17	157.2°		0h38m	+28°	2024/10/15	13.4	2024/10/12		0.929							
6153	2024/10/19	174.6°		1h50m	+ 5°	2024/10/20	14.1	2024/10/19		1.050							
66146	2024/10/19	127.2°		4h30m	-21°	2024/10/30	11.9	2024/11/05		0.089							
2262	2024/10/20	167.3°		1h25m	+22°	2024/10/18	14.5	2024/10/11		0.959							
1666	2024/10/21	175.3°		1h38m	+15°	2024/10/21	14.0	2024/10/14		0.860							
1036	2024/10/27	138.9°		23h18m	+16°	2024/10/17	9.0	2024/10/13		0.374							
1275	2024/11/01	167.7°		2h48m	+ 3°	2024/11/01	13.4	2024/10/30		1.260							
1479	2024/11/03	174.8°		2h31m	+20°	2024/11/04	14.1	2024/11/09		1.324							
1808	2024/11/05	178.1°		2h39m	+17°	2024/11/05	14.5	2024/11/06		1.276							
2693	2024/11/07	176.0°		2h55m	+12°	2024/11/07	14.5	2024/11/06		0.845							
886	2024/11/08	173.1°		2h57m	+ 9°	2024/11/07	11.8	2024/10/31		1.456							
3220	2024/11/08	175.2°		2h48m	+21°	2024/11/08	14.2	2024/11/08		0.852							
959	2024/11/10	178.5°		3h 2m	+15°	2024/11/09	13.2	2024/11/06		1.493							
3722	2024/11/14	179.8°		3h18m	+18°	2024/11/14	14.0	2024/11/06		0.878							
1539	2024/11/15	177.2°		3h27m	+15°	2024/11/15	13.8	2024/11/12		1.574							
7870	2024/11/15	178.9°		3h21m	+19°	2024/11/15	13.6	2024/11/09		0.652							
281	2024/11/16	175.6°		3h24m	+23°	2024/11/16	13.4	2024/11/14		0.912							
2648	2024/11/16	172.6°		3h16m	+25°	2024/11/16	14.3	2024/11/14		0.873							
36183	2024/11/17	175.1°		3h11m	+18°	2024/11/16	9.9	2024/11/13		0.135							
3106	2024/11/21	157.6°		4h 1m	- 2°	2024/11/20	14.1	2024/11/19		1.445							
14162	2024/11/23	176.0°		3h56m	+24°	2024/11/23	14.5	2024/11/17		0.847							
1057	2024/11/26	178.5°		4h10m	+22°	2024/11/26	13.6	2024/11/18		1.360							
3951	2024/11/27	175.3°		4h 7m	+25°	2024/11/27	14.4	2024/11/26		0.948							
2266	2024/11/28	174.0°		4h21m	+15°	2024/11/28	14.5	2024/11/28		1.801							
163899	2024/11/29	96.9°		21h32m	+45°	2024/12/01	14.3	2024/12/02		0.088							
13	2024/12/01	166.9°		4h30m	+34°	2024/12/02	9.9	2024/12/03		1.457							
361	2024/12/03	165.4°		4h31m	+36°	2024/12/03	12.8	2024/12/04		2.192							
3935	2024/12/04	167.0°		4h29m	+34°	2024/12/02	14.1	2024/11/28		1.012							
1284	2024/12/07	165.3°		4h41m	+36°	2024/12/06	12.9	2024/12/04		1.232							
3824	2024/12/08	173.7°		4h59m	+28°	2024/12/08	14.1	2024/12/08		0.739							
4558	2024/12/09	177.5°		5h 8m	+20°	2024/12/08	13.6	2024/11/22		0.872							
6821	2024/12/10	179.3°		5h10m	+22°	2024/12/10	14.3	2024/12/11		1.211							
350	2024/12/11	171.7°		5h12m	+14°	2024/12/11	11.8	2024/12/10		1.637							
69	2024/12/12	166.5°		5h21m	+ 9°	2024/12/12	10.4	2024/12/15		1.563							
15	2024/12/14	169.4°		5h23m	+33°	2024/12/13	8.0	2024/12/08		1.299							
1013	2024/12/14	162.3°		5h31m	+40°	2024/12/16	12.9	2024/12/20		1.263							
679	2024/12/25	163.1°		5h59m	+ 6°	2024/12/21	11.5	2024/12/12		1.140							
1626	2024/12/28	176.5°		6h25m	+26°	2024/12/28	11.4	2024/12/23		0.772							
888	2024/12/31	169.7°		6h37m	+12°	2024/12/30	12.2	2024/12/27		1.276							

Table III. Numerical list of approaches closer than 0.3 AU

Planet	Max	Elon	D	Max	E	RA	Dec	Br	Mag	D	Br	Mag	Min	Dist	D	Min	Dist
1036	2024/10/27	138.9°		23h18m	+16°	2024/10/17	9.0	2024/10/13		0.374							
1685	2024/02/23	123.2°		6h41m	- 2°	2024/01/28	12.6	2024/01/20		0.133							
2063	2024/04/23	179.4°		14h 2m	-12°	2024/04/23	13.8	2024/03/31		0.120							
4954	2024/09/14	167.7°		23h24m	-15°	2024/09/24	11.1	2024/10/11		0.243							
36183	2024/11/17	175.1°		3h11m	+18°	2024/11/16	9.9	2024/11/13		0.135							
66146	2024/10/19	127.2°		4h30m	-21°	2024/10/30	11.9	2024/11/05		0.089							
163899	2024/11/29	96.9°		21h32m	+45°	2024/12/01	14.3	2024/12/02		0.088							
187026	2024/02/19	176.6°		9h56m	+13°	2024/02/19	12.8	2024/02/20		0.097							

ASTEROID-DEEPSKY APPULSES IN 2024

Brian D. Warner
Center for Solar System Studies
446 Sycamore Ave.
Eaton, CO 80615
brian@MinorPlanetObserver.com

(Received: 2023 October 15)

The following list is a *very small* subset of the results of a search for asteroid-deepsky appulses for 2024, presenting only the highlights for the year based on close approaches of brighter asteroids to brighter DSOs. For the complete set visit

<https://www.minorplanet.info/php/dsoappulses.php>

For any event not covered, the Minor Planet Center's web site at <https://www.minorplanetcenter.net/cgi-bin/checkmp.cgi> allows you to enter the location of a suspected asteroid or supernova and check if there are any known targets in the area.

The table gives the following data:

Date/Time	Universal Date (MM DD) and Time of closest approach.
#/Name	The number and name of the asteroid.
RA/Dec	The J2000 position of the asteroid.
AM	The approximate visual magnitude of the asteroid.
Sep/PA	The separation in arcseconds and the position angle from the DSO to the asteroid.
DSO	The DSO name or catalog designation.
DM	The approximate total magnitude of the DSO.
DT	DSO Type: OC = Open Cluster; GC = Globular Cluster; G = Galaxy.
SE/ME	The elongation in degrees from the sun and moon, respectively.
MP	The phase of the moon: 0 = New, 1.0 = Full. Positive = waxing; Negative = waning.

Date	UT	#	Name	RA	Dec	AM	Sep	PA	DSO	DM	DT	SE	ME	MP
01 06 16:43		404	Arsinoe	12:38.41	+13:05.13	13.4	112	93	NGC 4584	12.9	G	102	45	-0.25
01 10 15:58		404	Arsinoe	12:43.04	+13:12.59	13.3	207	100	NGC 4639	11.5	G	104	80	-0.05
02 04 16:07		1685	Toro	05:02.17	-08:11.80	12.9	135	282	NGC 1752	12.4	G	114	145	-0.32
02 07 13:02		124	Alkeste	09:25.89	+11:25.24	11.6	47	74	NGC 2874	12.5	G	176	154	-0.04
02 07 15:24		124	Alkeste	09:25.80	+11:25.73	11.6	16	76	NGC 2872	11.9	G	176	164	-0.02
02 12 06:42		175	Andromache	09:53.12	+16:41.69	13.9	44	247	NGC 3041	11.5	G	176	138	0.14
02 12 18:42		653	Berenike	09:16.17	+17:39.31	13.5	98	232	NGC 2795	12.8	G	172	126	0.16
03 05 15:40		451	Patientia	09:19.75	+33:48.95	11.6	181	255	NGC 2832	11.9	G	142	155	-0.23
03 08 11:05		1113	Katja	09:02.31	+16:49.62	13.8	23	102	NGC 2730	13.0	G	145	170	-0.05
03 08 21:29		117	Lomia	11:24.40	+03:18.96	12.2	62	90	NGC 3664	12.8	G	179	173	-0.01
03 09 14:01		83	Beatrix	10:48.90	+14:12.99	11.6	1	56	NGC 3391	12.9	G	167	176	-0.01
03 11 08:35		38	Leda	08:51.38	+11:45.77	12.8	195	84	NGC 2682	6.9	OC	119	153	-0.46
03 15 16:45		779	Nina	14:01.31	-33:06.28	12.9	160	126	NGC 5398	12.3	G	131	158	0.25
04 03 13:36		770	Bali	12:45.20	-00:26.80	13.9	12	265	NGC 4666	10.7	G	174	126	-0.24
04 04 19:27		477	Italia	13:05.70	-08:00.73	13.6	16	260	NGC 4958	10.7	G	177	129	-0.17
04 05 13:09		375	Ursula	13:18.13	-26:48.01	12.3	240	264	NGC 5061	10.4	G	160	140	-0.04
04 10 01:50		57	Nemosyne	09:53.28	+00:41.77	12.4	110	7	NGC 3042	12.9	G	126	71	0.23
04 10 05:24		484	Pittsburghia	14:53.96	+03:32.26	13.8	59	49	NGC 5775	11.4	G	152	156	0.01
04 10 12:24		484	Pittsburghia	14:53.77	+03:34.21	13.7	54	60	NGC 5774	12.1	G	154	150	0.11
04 12 06:40		390	Alma	13:24.81	-30:18.75	13.8	16	245	NGC 5124	12.1	G	159	136	0.18
05 01 17:39		980	Anacostia	11:53.96	-23:10.38	13.1	42	31	NGC 3955	11.9	G	141	125	-0.44
05 03 17:21		784	Pickeringia	17:22.25	-38:28.74	12.9	37	340	NGC 6337	12.3	PN	140	110	-0.08
05 07 12:33		683	Lanzia	18:03.17	-24:22.17	13.8	74	219	NGC 6523	5.0	CNB	139	160	0.04
06 09 10:21		784	Pickeringia	16:53.96	-41:45.30	12.5	164	282	NGC 6231	2.6	OC	161	130	0.15
07 02 23:51		151	Abundantia	18:34.37	-32:19.35	12.8	101	284	NGC 6637	7.7	GC	171	133	-0.17
07 09 14:19		27	Euterpe	14:25.03	-13:09.86	11.9	72	250	NGC 5605	12.3	G	108	37	0.34
08 02 15:04		39	Laetitia	01:19.60	+03:24.75	10.4	15	90	NGC 470	12.4	G	110	73	-0.10
08 02 22:07		39	Laetitia	01:19.78	+03:24.22	10.4	48	73	NGC 470	11.8	G	111	98	-0.01
08 03 09:22		39	Laetitia	01:20.07	+03:23.35	10.4	101	76	NGC 474	11.5	G	112	110	-0.00
08 30 14:28		511	Dauida	03:09.07	-02:55.36	11.4	119	236	NGC 1222	12.5	G	113	93	-0.04
09 02 03:22		246	Asporina	02:38.08	+02:05.96	13.6	206	18	NGC 1016	11.6	G	119	90	-0.07
09 03 09:38		137	Meliboea	23:44.41	+09:55.79	12.1	16	130	NGC 7743	11.5	G	158	156	0.00
09 24 20:24		376	Geometria	18:07.25	-23:24.05	13.6	246	100	NGC 6546	8.0	OC	90	172	-0.44
09 30 03:56		423	Diotima	22:09.16	-27:46.86	12.4	136	249	NGC 7214	12.7	G	133	141	-0.00
10 01 13:56		519	Sylvania	00:50.98	-06:59.84	12.0	250	273	NGC 275	12.5	G	169	168	-0.00
10 01 23:15		66146	1998 TU3	04:36.25	-03:08.78	13.6	44	196	NGC 1618	12.7	G	119	117	-0.00
10 10 12:24		500	Selinur	02:29.40	+31:39.52	12.8	31	266	NGC 940	12.4	G	148	128	0.42
10 20 09:40		178	Belisana	06:08.96	+24:16.67	13.8	207	106	NGC 2168	5.1	OC	130	166	0.09
11 01 06:42		734	Benda	02:34.15	+20:55.66	13.9	204	103	NGC 976	12.9	G	174	174	0.00
11 08 07:29		36183	1999 TX16	04:42.36	-20:25.46	14.0	57	213	NGC 1640	11.7	G	134	109	0.39
11 24 01:41		336	Lacadiera	01:59.45	+13:59.71	13.5	90	122	NGC 774	13.0	G	152	121	-0.47
12 01 21:20		886	Washingtonia	02:36.54	+11:42.36	13.1	235	238	NGC 990	12.4	G	151	153	-0.00
12 03 16:41		193	Ambrosia	22:50.62	-01:29.28	13.9	126	306	NGC 7391	12.0	G	91	50	0.12
12 06 10:05		679	Pax	06:21.83	+02:24.79	11.8	204	235	Cr 91	6.4	OC	149	145	0.16
12 23 13:41		54	Alexandra	03:47.50	+35:03.05	12.7	3	301	IC 351	12.4	PN	146	136	-0.35
12 23 19:59		332	Siri	06:43.11	+26:58.52	13.7	82	340	NGC 2266	9.5	OC	173	110	-0.28
12 31 07:59		189	Phthia	02:39.11	+10:51.61	13.4	97	265	NGC 1024	12.1	G	129	147	-0.44

LIGHTCURVE PHOTOMETRY OPPORTUNITIES: 2024 JANUARY-MARCH

Brian D. Warner
Center for Solar System Studies (CS3)
446 Sycamore Ave.
Eaton, CO 80615 USA
brian@MinPlanObs.org

Alan W. Harris
Center for Solar System Studies (CS3)
La Cañada, CA 91011-3364 USA

Josef Ďurech
Astronomical Institute
Charles University
18000 Prague, CZECH REPUBLIC
durech@sirrah.troja.mff.cuni.cz

Lance A.M. Benner
Jet Propulsion Laboratory
Pasadena, CA 91109-8099 USA
lance.benner@jpl.nasa.gov

We present lists of asteroid photometry opportunities for objects reaching a favorable apparition and have no or poorly-defined lightcurve parameters. Additional data on these objects will help with shape and spin axis modeling using lightcurve inversion. The “Radar-Optical Opportunities” section includes a list of potential radar targets as well as some that might be in critical need of astrometric data.

We present several lists of asteroids that are prime targets for photometry and/or astrometry during the period 2024 January-March. The “Radar-Optical Opportunities” section provides an expanded list of potential NEA targets, many of which are planned or good candidates for radar observations.

In the first three sets of tables, “Dec” is the declination and “U” is the quality code of the lightcurve. See the latest asteroid lightcurve data base (LCDB from here on; Warner et al., 2009) documentation for an explanation of the U code:

<http://www.minorplanet.info/lightcurvedatabase.html>

The ephemeris generator on the MinorPlanet.info web site allows creating custom lists for objects reaching $V \leq 18.0$ during any month in the current year and up to five years in the future, e.g., limiting the results by magnitude and declination, family, and more.

<https://www.minorplanet.info/php/callopplcdbquery.php>

We refer you to past articles, e.g., Warner et al. (2021a; 2021b) for more detailed discussions about the individual lists and points of advice regarding observations for objects in each list.

Once you’ve obtained and analyzed your data, it’s important to publish your results. Papers appearing in the *Minor Planet Bulletin* are indexed in the Astrophysical Data System (ADS) and so can be referenced by others in subsequent papers. It’s also important to make the data available at least on a personal website or upon request. We urge you to consider submitting your raw data to the ALCDEF database. This can be accessed for uploading and downloading data at

<http://www.alcdef.org>

The database contains more than 10.4 million observations for 24,202 objects (as of 2023 April 6), making it one of the more useful sources for raw data of *dense* time-series asteroid photometry.

Lightcurve/Photometry Opportunities

Objects with $U = 3-$ or 3 are excluded from this list since they will likely appear in the list for shape and spin axis modeling. Those asteroids rated $U = 1$ or have only a lower limit on the period, should be given higher priority over those rated $U = 2$ or $2+$. On the other hand, do not overlook asteroids with $U = 2/2+$ on the assumption that the period is sufficiently established. Regardless, do not let the existing period influence your analysis since even highly-rated result have been proven wrong at times. Note that the lightcurve amplitude in the tables could be more or less than what’s given. Use the listing only as a guide.

All objects are reaching one of their five brightest apparitions from 1995-2050. Bold text, if any, indicates a near-Earth asteroid (NEA).

Number	Name	Brightest			Period	LCDB Data		U
		Date	Mag	Dec		Amp		
5824	Inagaki	01	02.6	15.3	30			
4766	Malin	01	03.0	15.3	25	32.22	0.03	2
2444	Lederle	01	03.2	14.8	25	17.85	0.18-0.45	2+
85804	1998 WQ5#	01	05.3	15.5	28	2.676	0.05-0.10	2
2733	Hamina	01	07.2	14.9	17	93.23	0.36-0.48	2
4735	Gary	01	07.5	15.1	27			
29515	1997 YL7	01	07.7	15.3	32	12.231	0.65-0.67	2+
5356	Neagari	01	09.7	15.5	+0			
41074	1999 VL40	01	10.0	15.4	+2			
2240	Tsai	01	12.4	15.5	23	4.416		2
1040	Klumpkea	01	14.3	13.8	15	59.2	0.25-0.77	2
1613	Smiley	01	14.7	13.8	28	80.61	0.29-0.30	2+
4931	Tomsk	01	15.0	15.0	-9	9.27	0.40-0.46	3-
69971	Tanzi	01	20.2	15.4	20	32.54	0.44	2+
6460	Bassano	01	22.0	15.5	20	2.914	0.29-0.38	2
93040	2000 SG	01	25.4	15.3	42	16.015	0.09	2-
5785	Fulton	01	28.5	15.5	20			
2137	Priscilla	01	31.6	15.4	20	7.85	0.19-0.21	2
2879	Shimizu	02	12.8	14.9	12	18.72	0.08-0.17	2
417264	2006 AT2#	02	16.4	14.7	18			
1532	Inari	02	19.0	14.5	12	25	0.09	1+
187026	2005 EK70#	02	19.2	12.8	15			
3808	Tempel	02	21.0	15.5	11	7.451		2
1698	Christophe	02	21.3	15.1	13			
3999	Aristarchus	02	23.0	15.1	+8	12.609	0.18-0.30	2+
56116	1999 CZ7	03	08.6	15.5	+3	3.12	0.27	2+
8602	Oedicnemus	03	14.1	15.5	+3			
5008	Miyazawakenji	03	15.6	15.0	+7	17.4	0.18-0.34	2
2410	Morrison	03	21.2	14.8	+3			
19260	1995 GT	03	29.3	15.3	+2	21.919	0.73	2
19818	Shotwell	03	31.8	15.4	-8	2368	0.83	2+

Low Phase Angle Opportunities

The Low Phase Angle list includes asteroids that reach very low phase angles ($\alpha < 1^\circ$). The “ α ” column is the minimum solar phase angle for the asteroid. Getting accurate, calibrated measurements (usually V band) at or very near the day of opposition can provide important information for those studying the “opposition effect.” Use the on-line query form for the LCDB to get more details about a specific asteroid.

<https://www.minorplanet.info/php/callopplcdbquery.php>

The best chance of success comes with covering at least half a cycle a night, meaning periods generally < 16 h, when working objects with low amplitude. Objects with large amplitudes and/or long periods are much more difficult for phase angle studies since, for proper analysis, the data must be reduced to the average magnitude of the asteroid for each night. Refer to Harris et al. (1989) for the details of the analysis procedure.

As an aside, it is arguably better for physical interpretation (e.g., G value versus albedo) to use the maximum light rather than mean level to find the phase slope parameter (G), which better models the behavior of a spherical object of the same albedo, but it can produce significantly different values for both H and G versus using average light, which is the method used for values listed by the Minor Planet Center. Using and reporting the results of both methods can provide additional insights into the physical properties of an asteroid.

The International Astronomical Union (IAU) has adopted a new system, H-G₁₂, introduced by Muinonen et al. (2010). It will be some years before H-G₁₂ becomes widely used, and hopefully not until a discontinuity flaw in the G₁₂ function has been fixed. This discontinuity results in false “clusters” or “holes” in the solution density and makes it impossible to draw accurate conclusions.

We strongly encourage obtaining data as close to 0° as possible, then every 1-2° out to 7°, below which the curve tends to be non-linear due to the opposition effect. From 7° out to about 30°, observations at 3-6° intervals should be sufficient. Coverage beyond 50° or so is not generally helpful since the H-G system is best defined with data from 0-30°.

It’s important to emphasize that all observations should (must) be made using high-quality catalogs to set the comparison star magnitudes. These include ATLAS, Pan-STARRS, SkyMapper, and Gaia2/3. Catalogs such as CMC-15, APASS, or the MPOSC from *MPO Canopus* have too high systematic errors.

Also important is that there are sufficient data from each observing run such that their location can be found on a combined, phased lightcurve derived from two or more nights obtained *near the same phase angle*. If necessary, the magnitudes for a given run should be adjusted so that they correspond to mid-light of the combined lightcurve. This goes back to the H-G system being based on average, not maximum or minimum light.

The asteroid magnitudes are brighter than in others lists because higher precision is required and the asteroid may be a full magnitude or fainter when it reaches phase angles out to 20-30°. Even so, starting now, the list will include objects that reach $V \leq 15.0$ at opposition. The list of objects using the previous limit of $V \leq 14.0$ was becoming very short.

Num Name	Date	α	V	Dec	Period	Amp	U
2444 Lederle	01 03.2	0.77	14.8	+25	17.85	0.18-0.45	2+
1553 Bauersfelda	01 03.3	0.30	14.9	+22	51.191	0.26	2
822 Lalage	01 05.0	0.73	13.5	+21	3.345	0.47-0.67	3
476 Hedwig	01 05.7	0.22	12.4	+23	27.33	0.13-0.21	3
92 Undina	01 08.7	0.45	11.4	+24	15.941	0.15-0.20	3
277 Elvira	01 14.2	0.52	13.9	+20	29.69	0.34-0.59	3
847 Agnia	01 20.4	0.68	13.7	+18	14.827	0.05-0.51	3
588 Achilles	01 20.8	0.84	14.4	+24	7.306	0.10-0.31	3
1457 Ankara	01 22.3	0.33	14.5	+19	35.54	0.21-0.31	2
279 Thule	01 23.4	0.57	14.2	+22	23.896	0.02-0.10	3
2345 Fucik	01 29.4	0.44	14.7	+17	17.12	0.10-0.39	2
229 Adelinda	02 01.1	0.70	14.6	+20	6.60	0.04-0.30	3
1245 Calvinia	02 03.1	0.43	14.1	+15	4.852	0.28-	0.7 3
2271 Kiso	02 04.6	0.15	15.0	+16	17.14	0.14	3-
569 Misa	02 05.4	0.28	12.7	+16	11.595	0.09-0.25	3
653 Berenike	02 06.9	0.46	13.2	+17	12.489	0.03-0.11	3
1113 Katja	02 08.2	0.74	13.1	+17	18.465	0.08-0.17	3
462 Eriphyla	02 09.5	0.86	13.6	+17	8.659	0.11-0.39	3
3031 Houston	02 10.1	0.19	15.0	+14	11.218	0.11-0.17	3
658 Asteria	02 10.7	0.41	14.3	+16	21.034	0.22-0.28	3
558 Carmen	02 11.6	0.20	12.8	+14	11.387	0.2-0.31	3
1282 Utopia	02 11.8	0.33	14.5	+15	13.623	0.28-0.36	3
2879 Shimizu	02 12.7	0.80	14.9	+12	18.72	0.08-0.17	2
1437 Diomedes	02 13.2	0.71	15.0	+10	24.49	0.34-0.70	3-
175 Andromache	02 14.0	0.92	14.0	+17	8.324	0.28-0.30	3

Num Name	Date	α	V	Dec	Period	Amp	U
372 Palma	02 17.0	0.09	10.7	+12	8.567	0.06-0.17	3
63 Ausonia	02 17.5	0.63	10.6	+14	9.298	0.27-0.47	3
112 Iphigenia	02 18.9	0.16	13.3	+11	31.466	0.30	3
1532 Inari	02 19.0	0.09	14.6	+12	25.	0.09	1+
100 Hekate	02 19.8	0.97	12.7	+15	27.066	0.11-0.23	3
46 Hestia	02 20.5	0.62	12.4	+9	21.040	0.09-0.12	3
474 Prudentia	02 24.9	0.50	14.9	+8	8.572	0.47-0.90	3
1338 Duponta	02 25.3	0.72	14.9	+8	3.855	0.23-0.26	3
208 Lacrimosa	02 26.2	0.43	13.0	+10	14.085	0.15-0.33	3
58 Concordia	03 01.0	0.04	12.2	+8	9.895	0.01-0.15	3
468 Lina	03 01.8	0.12	14.9	+8	16.33	0.13-0.18	3
1157 Arabia	03 03.4	0.49	14.7	+5	11.55	0.37-0.42	3
3 Juno	03 03.9	0.88	8.5	+4	7.210	0.11-0.22	3
260 Huberta	03 04.2	0.09	14.4	+6	8.29	0.21-0.34	3
577 Rhea	03 09.3	0.77	14.0	+2	12.249	0.19-0.24	3-
117 Lomia	03 10.6	0.23	12.1	+3	9.127	0.10-0.35	3
316 Goberta	03 11.6	0.80	14.4	+6	8.605	0.20-0.27	3
1938 Lausanna	03 11.9	0.11	14.3	+3	2.748	0.12-0.17	3
490 Veritas	03 13.0	0.37	13.3	+2	7.930	0.21-0.58	3
805 Hormuthia	03 13.1	0.73	14.7	+5	9.510	0.05-0.10	3-
632 Pyrrha	03 14.4	0.19	14.3	+2	4.117	0.40	3
1046 Edwin	03 17.1	0.92	14.9	+4	5.291	0.14-0.33	3
1908 Pobeda	03 18.0	0.74	15.0	+3			
645 Agrippina	03 19.2	0.10	14.1	+1	32.6	0.11-0.18	2
604 Tekmessa	03 20.4	0.36	14.4	+1	5.560	0.43-0.60	3
167 Urda	03 24.4	0.37	13.1	-1	13.07	0.24-0.39	3
1848 Delvaux	03 27.4	0.45	14.9	-4	3.637	0.57-0.69	3
1790 Volkov	03 27.5	0.46	14.3	-4	10.742	0.09-0.14	3

Shape/Spin Modeling Opportunities

Those doing work for modeling should contact Josef Ďurech at the email address above. If looking to add lightcurves for objects with existing models, visit the Database of Asteroid Models from Inversion Techniques (DAMIT) web site.

<https://astro.troja.mff.cuni.cz/projects/damit/>

Additional lightcurves could lead to the asteroid being added to or improving one in DAMIT, thus increasing the total number of asteroids with spin axis and shape models.

Included in the list below are objects that:

1. Are rated U = 3- or 3 in the LCDB.
2. Do not have reported pole in the LCDB Summary table.
3. Have at least three entries in the Details table of the LCDB where the lightcurve is rated U \geq 2.

The caveat for condition #3 is that no check was made to see if the lightcurves are from the same apparition or if the phase angle bisector longitudes differ significantly from the upcoming apparition. The last check is often not possible because the LCDB does not list the approximate date of observations for all details records. Including that information is an on-going project.

With the wide use of sparse data from the surveys for modeling that produces hundreds of statistically valid poles and shapes, the need for data for main-belt objects is not what it used to be. The best use of observing time might be to concentrate on near-Earth asteroids, or on asteroids where the only period was derived from sparse data, which can help eliminate alias periods.

The latter targets are usually flagged with an ‘S’ on the LCDB summary line. Regardless, it’s a good idea to visit the DAMIT site and see what it has, if anything, on the target(s) you’ve picked for observations.

All objects are at a favorable apparition. If any, those in italic text are near-Earth objects.

About YORP Acceleration

Num	Name	Brightest			LCDB Data		U
		Date	Mag	Dec	Period	Amp	
4833	Meges	01 02.2	15.7	+22	14.25	0.13-0.44	3
5264	Telephus	01 05.5	16.0	+8	9.525	0.20-0.58	3
1749	Telamon	01 05.8	15.8	+29	11.413	0.06-0.11	3-
2797	Teucer	01 11.8	15.4	+41	10.145	0.20-0.25	3
4931	Tomsik	01 15.0	15.0	-9	9.27	0.40-0.46	3-
4175	Billbaum	01 16.4	15.2	+3	2.73	0.08-0.15	3-
3063	Makhaon	01 16.6	15.1	+19	8.637	0.06-0.15	3
69406	Martz-Kohl	01 21.1	15.8	+19	4.49	0.10-0.19	3
4673	Bortle	01 21.3	14.9	+28	2.64	0.09-0.17	3
12559	1998 QB69	01 26.1	16.0	+17	6.21	0.15-0.19	3
2000	Herschel	01 27.0	13.2	+2	133.6	0.17-1.16	3
78	Diana	01 30.7	10.5	+24	7.299	0.02-0.30	3
653	Berenike	02 07.0	13.2	+17	12.489	0.03-0.15	3
3223	Forsius	02 17.9	14.2	+6	2.343	0.20-0.28	3
58	Concordia	03 01.0	12.2	+8	9.895	0.01-0.15	3
10041	Parkinson	03 24.7	15.2	+1	2.564	0.12-0.30	3

Radar-Optical Opportunities

Table I below gives a list of near-Earth asteroids reaching maximum brightness for the current quarter-year based on calculations by Warner. We switched to this presentation in lieu of ephemerides for reasons outlined in the 2021 October-December opportunities paper (Warner et al., 2021b), which centered on the potential problems with ephemerides generated several months before publication.

The initial list of targets started using the planning tool at

<https://www.minorplanet.info/php/callopplcdbquery.php>

where the search was limited to near-Earth asteroids only that were $V \leq 17$ for at least part of the quarter.

The final step was to cross-reference our list with that found on the Goldstone planned targets schedule at

http://echo.jpl.nasa.gov/asteroids/goldstone_asteroid_schedule.html

In Table I, objects in bold text are on the Goldstone proposed observing list as of 2023 July.

It's important to note that the final list in Table I is based on *known* targets and orbital elements when it was prepared. It is common for newly discovered objects to move in or out of the list. We recommend that you keep up with the latest discoveries by using the Minor Planet Center observing tools.

In particular, monitor NEAs and be flexible with your observing program. In some cases, you may have only 1-3 days when the asteroid is within reach of your equipment. Be sure to keep in touch with the radar team (through Benner's email or their Facebook or Twitter accounts) if you get data. The team may not always be observing the target but your initial results may change their plans. In all cases, your efforts are greatly appreciated.

For observation planning, use these two sites

MPC: <http://www.minorplanetcenter.net/iau/MPEph/MPEph.html>

JPL: <http://ssd.jpl.nasa.gov/?horizons>

Cross-check the ephemerides from the two sites just in case there is discrepancy that might have you imaging an empty sky.

Near-Earth asteroids are particularly sensitive to YORP acceleration. YORP (Yarkovsky-O'Keefe-Radzievskii-Paddack; (Rubincam, 2000)) is the asymmetric thermal re-radiation of sunlight that can cause an asteroid's rotation period to increase or decrease. High precision lightcurves at multiple apparitions can be used to model the asteroid's *sidereal* rotation period and see if it's changing.

It usually takes four apparitions to have sufficient data to determine if the asteroid rotation rate is changing under the influence of YORP. This is why observing an asteroid that already has a well-known period remains a valuable use of telescope time. It is even more so when considering the BYORP (binary-YORP) effect among binary asteroids that has stabilized the spin so that acceleration of the primary body is not the same as if it would be if there were no satellite.

The Quarterly Target List Table

The Table I columns are

Num	Asteroid number, if any.
Name	Name assigned by the MPC.
H	Absolute magnitude from MPCOrb.
Dkm	Diameter (km) assuming $p_V = 0.2$.
Date	Date (mm dd.d) of brightest magnitude.
V	Approximate V magnitude at brightest.
Dec	Approximate declination at brightest.
Period	Synodic rotation period from summary line in the LCDB summary table.
Amp	Amplitude range (or single value) of reported lightcurves.
U	LCDB U (solution quality) from 1 (probably wrong) to 3 (secure).
A	Approximate SNR for Arecibo (if operational and at full power).
G	Approximate SNR for Goldstone radar at full power.
Notes	Comments about the object.

"PHA" is a potentially hazardous asteroid. NHATS is for "Near-Earth Object Human Space Flight Accessible Targets Study." Presume that that astrometry and photometry have been requested to support Goldstone observations. The sources for the rotation period are given in the Notes column. If none are qualified with a specific period, then the periods from multiple sources were in general agreement. Higher priority should be given to those where the current apparition is the last one $V \leq 18$ through 2050 or several years to come.

References

Behrend, R. (2007web). Observatoire de Geneve web site. http://obswww.unige.ch/~behrend/page_cou.html

Harris, A.W.; Young, J.W.; Bowell, E.; Martin, L.J.; Millis, R.L.; Poutanen, M.; Scaltriti, F.; Zappala, V.; Schober, H.J.; Debehogne, H.; Zeigler, K.W. (1989). "Photoelectric Observations of Asteroids 3, 24, 60, 261, and 863." *Icarus* 77, 171-186.

Num	Name	H	Diam	BDate	BMag	BDec	Period	AMn	AMx	U	Notes
96590	1998 XB	16.32	1.62	01 02.0	15.0	51	520		1.	3	Pravec et al. (2005web)
430804	2005 AD13	17.91	0.778	01 19.7	16.4	26					
68350	2001 MK3	16.18	1.730	01 21.7	16.2	-12	3.21082	0.17	0.20	3	Skiff et al. (2019)
1685	Toro	14.32	4.06	01 28.5	12.7	-11	10.1995	0.47	1.80	3	Higgins 2008
613986	2008 JG	20.86	0.200	01 30.6	17.1	19					
152563	1992 BF	19.81	0.324	01 31.4	16.3	23	32	0.60	0.60	1	Pravec et al. (2018web)
4544	Xanthus	17.40	0.984	02 14.1	17.0	60	37.65	0.27	0.27	2	Behrend (2007web)
417264	2006 AT2	17.14	1.11	02 16.4	14.7	18					
163693	Atria	16.39	1.57	02 18.7	17.0	57	3.398	0.22	0.68	3	Binary Rivera-Valentin et al.(2017) Vaduvescu et al. (2017)
187026	2005 EK70	17.40	0.984	02 19.2	12.8	15					
163243	2002 FB3	16.52	1.48	02 27.4	16.3	-50	6.231		0.19	2	Monteiro et al. (2017)
264993	2003 DX10	20.41	0.246	03 19.6	16.8	26					
30825	1990 TG1	14.78	3.29	03 19.6	15.1	5	2.62428		0.11	3	Higgins et al. (2006)
152787	1999 TB10	18.70	0.541	03 20.3	16.4	35					
1864	Daedalus	14.88	3.14	03 30.2	15.7	-6	8.572	0.72	1.04	3	Pravec et al. (1995)

Table 1. A list of near-Earth asteroids reaching brightest in 2023 January-March. PHA: potentially hazardous asteroid. NHATS: Near-Earth Object Human Space Flight Accessible Targets Study. Diameters are based on $p_V = 0.20$. The Date, V, and Dec columns are the mm/dd.d, approximate magnitude, and declination when at brightest. Amp is the single or range of amplitudes. The references in the Notes column are those for the adopted period.

Higgins, D.; Pravec, P.; Kusnirak, P.; Masi, G.; Galad, A.; Gajdos, S.; Kornos, L.; Vilagi, J.; Pray, D. (2006). "Asteriod lightcurve analysis at Hunters Hill Observatory and collaborating stations - autumn/winter 2005." *Minor Planet Bull.* **33**, 8-10.

Higgins, D. (2008). "Asteroid Lightcurve Analysis at Hunters Hill Observatory and Collaborating Stations: April 2007 - June 2007." *Minor Planet Bull.* **35**, 30-32.

Monteiro, F.; Silva, J.S.; Lazzaro, D.; Arcoverde, P.; Medeiros, H.; Souza, R.; Rodriggues, T. (2017). "Lightcurve Analysis for Ten Near-Earth Asteroids." *Minor Planet Bull.* **44**, 20-22.

Muironen, K.; Belskaya, I.N.; Cellino, A.; Delbò, M.; Lvasseur-Regourd, A.-C.; Penttilä, A.; Tedesco, E.F. (2010). "A three-parameter magnitude phase function for asteroids." *Icarus* **209**, 542-555.

Pravec, P.; Wolf, M.; Sarounova, L. (-2005web; -2018web). <http://www.asu.cas.cz/~ppravec/neo.htm>

Pravec, P.; Wolf, M.; Varady, M.; Barta, P. (1995). "CCD Photometry of 6 Near-Earth Asteroids." *Earth, Moon, and Planets* **71**, 177-187.

Rivera-Valentin, E.G.; Tayloer, P.A.; Virkki, A.; Aponte-Hernandez, B. (2017). "(163693) Atira." *CBET* **4347**.

Rubincam, D.P. (2000). "Radiative Spin-up and Spin-down of Small Asteroids." *Icarus* **148**, 2-11.

Skiff, B.A.; McLelland, K.P.; Sanborn, J.; Pravec, P.; Koehn, B.W. (2019). "Lowell Observatory Near-Earth Asteroid Photometric Survey (NEAPS): Paper 4." *Minor Planet Bull.* **46**, 458-503.

Vaduvescu, O.; Aznar, A.M.; Tudor, V.; Predatu, M.; and 23 colleagues (2017). "The EURONEAR Lightcurve Survey of Near Earth Asteroids." *Earth, Moon, and Planets* **120**, 41-100.

Warner, B.D.; Harris, A.W.; Pravec, P. (2009). "The Asteroid Lightcurve Database." *Icarus* **202**, 134-146. Updated 2021 Dec. <http://www.minorplanet.info/lightcurvedatabase.html>

Warner, B.D.; Harris, A.W.; Ďurech, J.; Benner, L.A.M. (2021a). "Lightcurve Photometry Opportunities" 2021 January-March." *Minor Planet Bull.* **48**, 89-97.

Warner, B.D.; Harris, A.W.; Ďurech, J.; Benner, L.A.M. (2021b). "Lightcurve Photometry Opportunities" 2021 October-December." *Minor Planet Bull.* **48**, 406-410.

IN THIS ISSUE

This list gives those asteroids in this issue for which physical observations (excluding astrometric only) were made. This includes lightcurves, color index, and H-G determinations, etc. In some cases, no specific results are reported due to a lack of or poor-quality data. The page number is for the first page of the paper mentioning the asteroid. EP is the "go to page" value in the electronic version.

Number	Name	EP	Page	Number	Name	EP	Page
81	Terpsichore	56	56	1937	Locarno	39	39
238	Hypatia	56	56	2068	Dangreen	1	1
354	Eleonora	1	1	2090	Mizuho	49	49
489	Comacina	33	33	2090	Mizuho	64	64
600	Musa	33	33	2376	Martynov	49	49
716	Berkeley	33	33	2427	Kobzar	1	1
773	Irmtraud	56	56	2466	Golson	42	42
784	Pickeringia	16	16	2483	Guinevere	22	22
830	Petropolitana	39	39	2588	Flavia	22	22
862	Franzia	56	56	2591	Dworetzky	12	12
894	Erda	56	56	2697	Albina	42	42
903	Nealley	19	19	2738	Viracocha	3	3
907	Rhoda	33	33	2763	Jeans	56	56
914	Palisana	56	56	2841	Puijo	3	3
931	Whitemora	39	39	3015	Candy	31	31
953	Painleva	39	39	3022	Dobermann	22	22
1010	Marlene	49	49	3042	Zelinsky	42	42
1051	Merope	19	19	3127	Bagration	42	42
1051	Merope	42	42	3127	Bagration	49	49
1051	Merope	49	49	3210	Lupishko	33	33
1064	Aethusa	39	39	3286	Anatoliya	33	33
1109	Tata	49	49	3379	Oishi	33	33
1187	Afra	19	19	3811	Karma	42	42
1195	Orangia	42	42	3819	Robinson	42	42
1199	Geldonia	39	39	4164	Shilov	64	64
1292	Luce	3	3	4226	Damiaan	49	49
1337	Gerarda	42	42	4226	Damiaan	54	54
1340	Yvette	3	3	4288	Tokiyotech	49	49
1354	Botha	33	33	4362	Carlisle	3	3
1400	Tirela	12	12	4482	Frèrebassile	1	1
1465	Autonoma	16	16	4490	Bamberg	22	22
1465	Autonoma	39	39	4569	Baerbel	39	39
1525	Savonlinna	42	42	4727	Ravel	22	22
1525	Savonlinna	49	49	4729	Mikhailmil'	49	49
1796	Riga	42	42	5139	Rumoi	6	6
1850	Kohoutek	12	12	5163	Vollmayr-Lee	12	12
1887	Virton	42	42	5468	Hamatonbetsu	42	42
				5606	Muramatsu	12	12
				5708	Melancholia	16	16
				5766	Carmelofalco	56	56
				5780	Lafontaine	10	10
				5806	Archieroy	22	22
				5871	Bobbell	22	22
				6108	Glebov	62	62
				6147	Straub	42	42
				6493	Cathybenett	22	22
				6991	Chichibu	62	62
				7102	Neilbone	42	42
				7187	Isobe	22	22
				7560	Spudis	22	22
				8548	Sumizihara	16	16
				9628	Sendaiotsuna	42	42
				9911	Quantz	3	3
				10039	Keet Seel	62	62
				10423	Dajcic	31	31
				11736	Viktorfischl	33	33
				13186	1996 UM	22	22
				13653	Priscus	33	33
				14815	Rutberg	42	42
				14835	Holdridge	42	42
				15304	Wikberg	1	1
				16556	1991 VQ1	1	1
				17399	Andysanto	22	22
				17408	McAdams	22	22
				17428	Charleroi	22	22
				20037	Duke	22	22
				21149	Kenmitchell	22	22
				23080	1999 XH100	12	12
				23552	1994 NB	33	33
				23715	1998 FK2	22	22
				25242	1998 UH15	54	54
				27031	1998 RO4	72	72
				37638	1993 VB	33	33
				37855	1998 EE12	31	31
				47141	1999 HB3	22	22
				49669	1999 RZ30	22	22
				53453	1999 XX135	22	22
				56451	2000 GN81	31	31
				66875	1999 VY52	12	12
				76644	2000 HY24	33	33
				86192	1999 SV1	22	22
				88264	2001 KN20	72	72
				99676	2002 JR12	31	31
				100584	1997 JJ14	31	31
				141484	2002 DB4	72	72
				141495	2002 EZ11	72	72
				162186	1999 OP3	72	72
				242450	2004 QY2	76	76
				458732	2011 MD5	56	56
				503871	2000 SL	76	76
					2001 EC 2021	72	72
					2009 WV25	66	66
					2011 ED78	22	22
					2017 WD28	66	66
					2020 DB5	72	72
					2021 MO1	72	72
					2023 CM	76	76
					2023 DZ2 633	76	76
					2023 QC	66	66
					2023 RG13	66	66
					2023 RP2	66	66
					2023 TC	66	66

THE MINOR PLANET BULLETIN (ISSN 1052-8091) is the quarterly journal of the Minor Planets Section of the Association of Lunar and Planetary Observers (ALPO, <http://www.alpo-astronomy.org>). Current and most recent issues of the *MPB* are available on line, free of charge from:

<https://mpbulletin.org/>

The Minor Planets Section is directed by its Coordinator, Prof. Frederick Pilcher, 4438 Organ Mesa Loop, Las Cruces, NM 88011 USA (fpilcher35@gmail.com). Robert Stephens (rstephens@foxandstephens.com) serves as Associate Coordinator. Dr. Alan W. Harris (MoreData! Inc.; harrisaw@colorado.edu), and Dr. Petr Pravec (Ondrejov Observatory; ppravec@asu.cas.cz) serve as Scientific Advisors. The Asteroid Photometry Coordinator is Brian D. Warner (Center for Solar System Studies), Palmer Divide Observatory, 446 Sycamore Ave., Eaton, CO 80615 USA (brian@MinorPlanetObserver.com).

The *Minor Planet Bulletin* is edited by Professor Richard P. Binzel, MIT 54-410, 77 Massachusetts Ave, Cambridge, MA 02139 USA (rpb@mit.edu). Brian D. Warner (address above) is Associate Editor. Assistant Editors are Dr. David Polishook, Department of Earth and Planetary Sciences, Weizmann Institute of Science (david.polishook@weizmann.ac.il) and Dr. Melissa Hayes-Gehrke,

Department of Astronomy, University of Maryland (mhayesge@umd.edu). The *MPB* is produced by Dr. Pedro A. Valdés Sada (psada2@ix.netcom.com).

Effective with Volume 50, the *Minor Planet Bulletin* is an electronic-only journal; print subscriptions are no longer available. In addition to the free electronic download of the *MPB* as noted above, electronic retrieval of all *Minor Planet Bulletin* articles (back to Volume 1, Issue Number 1) is available through the Astrophysical Data System:

<http://www.adsabs.harvard.edu/>

Authors should submit their manuscripts by electronic mail (rpb@mit.edu). Author instructions and a Microsoft Word template document are available at the web page given above. All materials must arrive by the deadline for each issue. Visual photometry observations, positional observations, any type of observation not covered above, and general information requests should be sent to the Coordinator.

* * * * *

The deadline for the next issue (51-2) is January 15, 2024. The deadline for issue 51-3 is April 15, 2024.

THIS PAGE INTENTIONALLY LEFT BLANK